UiT
THE ARCTIC
UNIVERSITY
OF NORWAY

Faculty of Health Sciences
Department of Medical Biology

Breast cancer-associated *NEAT1* in cellular stress response pathways

Seyed Mohammad Lellahi

A dissertation for the degree of Philosophiae Doctor – April 2019

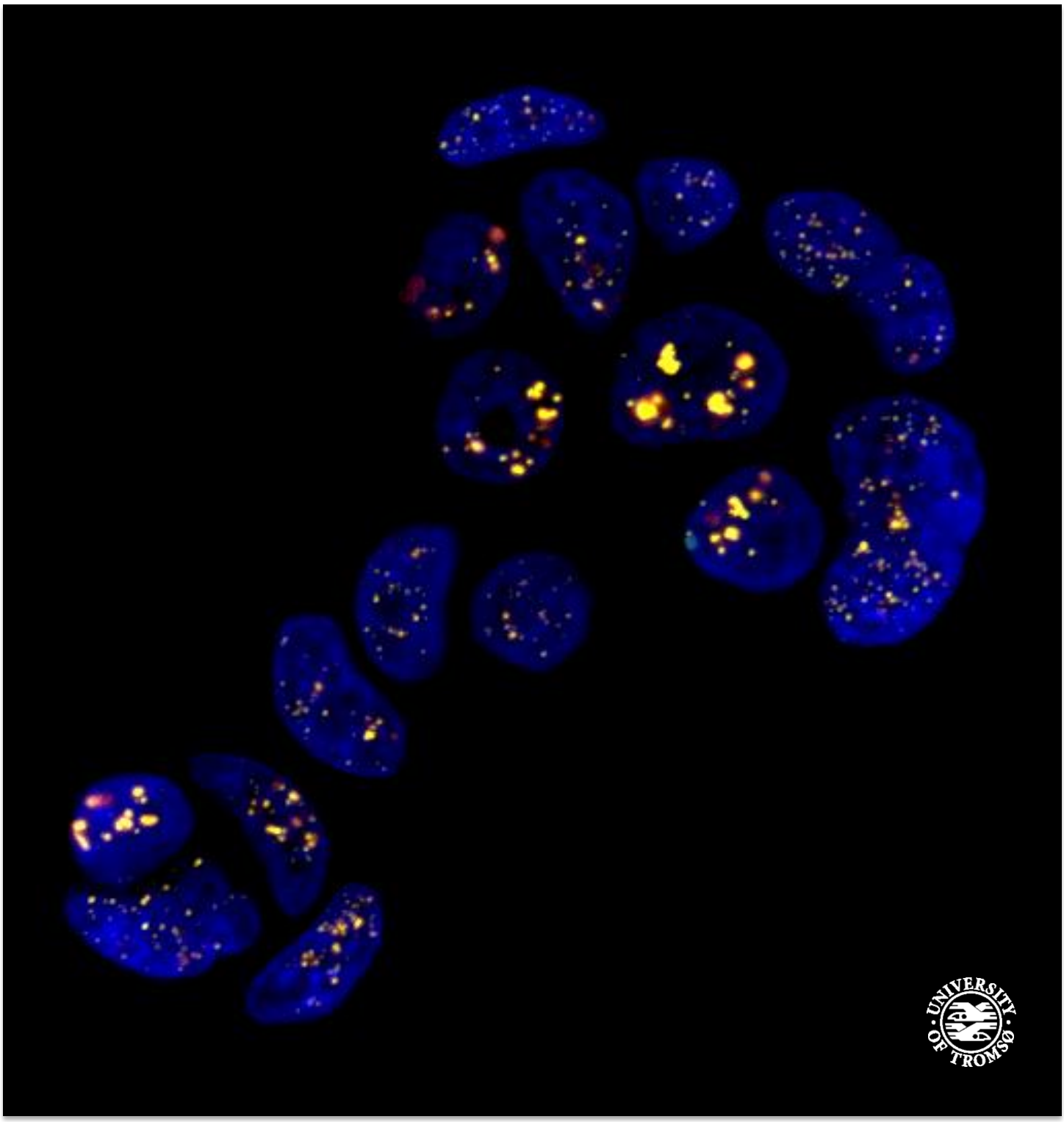

Breast cancer-associated *NEAT1* in cellular stress response pathways

By

Seyed Mohammad Lellahi

A dissertation for the degree of Philosophiae Doctor

UiT – The arctic university of Norway

Faculty of Health Sciences

Department of Medical Biology

April 2019

Acknowledgements

The work presented in this thesis was carried out in the laboratory of Maria Perander, RNA and Molecular Pathology Research Group (RAMP), Institute of Medical Biology, Faculty of Health Science, UiT-The Arctic University of Norway in the period from March 2015-May 2019. The financial support was provided by UiT- The Arctic Univerity of Norway.

First and foremost, I would like to express my utmost and sincere gratitude to my main supervisor, Maria Perander, who gave me this great opportunity to be a part of this amazing group. Thank you for inspired guidance, valuable suggestions, insightful criticism, encouragement and support throughout my PhD. Thank you Maria for always being open to discussion. I really appreciate for giving me the freedom to develop and follow own research idea especially during the fourth year.

Many thanks go to my friends and colleagues: Annica Hedberg, Erik Knutsen, Ingrid Arctander, Anita Ursvik, Hanne Britt Brenne, Kenneth Bowitz Larsen, Hallvard Lauritz Olsvik, Yakubu Princely Abudu, Aud-Malin Karlsson Hovd, Marta Tellez Gabriel, you guys provided such a friendly and helpful working environment that enabled me to finish this PhD work. Special thanks go to Annica and Erik for many insightful scientific discussions and endless technical and moral support to pass all big and small problem during these years.

I would like to thank Elin Synnøve Mortensen for her scientific support, and also for creating a positive, interactive and cordial environment in our group. I gratefully acknowledge the contributions of Ingvild Mikkola for her scientific support.

My appreciations further go to previous and current members of the RAMP that have contributed to a stimulating working environment and co-authors for their contributions to the scientific part of this thesis.

I wish to thank my beautiful wife, Niloufar, who has stood by me through all my travails, my absences, my fits of pique and impatience. Dearest Niloufar thank you for all of the support you have given through all of these years.

I would like to thanks my family, Dad, Mom, and little sister and brother, for your continuous and unparalleled love, help and support; I could not have done it without you. Lovely Mam, at

least both of us know that this journey would not have been possible without your love and inspiration.

Tromsø, April 2019
Seyed Mohammad Lellahi

Table of Contents

List of papers

I. The long noncoding RNA *NEAT1* and nuclear paraspeckles are up-regulated by the transcription factor HSF1 in the heat shock response.

S. Mohammad Lellahi, Ingrid Arctander Rosenlund, Annica Hedberg, Liv Torill Kiær, Ingvild Mikkola, Erik Knutsen, Maria Perander.
Journal of Biological Chemistry 293.49 (2018): 18965–18976.

II. The expression of the long *NEAT1_2* isoform is associated with human epidermal growth factor receptor 2-positive breast cancers.

Erik Knutsen, Mohammad Seyed Lellahi, Silje Nord, Silje Fismen, Kenneth Bowitz Larsen, Marta Tellez Gabriel, Annica Hedberg, Anna Bofin, Therese Sørlie, Elin Synnøve Mortensen, Maria Perander**.**
Manuscript

III. Knockdown of the long non-coding RNA *NEAT1* induces basal autophagy in breast cancer cell lines.

Mohammad Seyed Lellahi, Annica Hedberg, Hallvard Olsvik, Erik Knutsen, Maria Perander.
Manuscript

Preface

In this thesis, we investigated the role of *NEAT1* in stress, cancer, and autophagy in breast cancer. In paper I, we studied *NEAT1* in oxidative stress and heat shock. In the heat shock response, HSF1 translocates into the nucleus in order to activate its target gene, and we discovered a novel binding site for HSF1 in the promoter of *NEAT1*. The expression of *NEAT1*, as well as paraspeckle formation, were induced by both SFN and heat shock. The study further displayed that the proliferation of breast cancer cells is highly dependent on *NEAT1* expression, in line with what previous studies have shown. In paper II, we have continued to study *NEAT1* in breast cancer tumors and also breast cancer cell lines. From analyses of four different breast cancer cohorts, we found that *NEAT1_2* expression was positively correlated with HER2-positive breast cancer tumor, whereas, it was negatively associated with ER-positive luminal A breast cancer. Interestingly, high levels of *NEAT1_2* was observed in lactating tissue as well as in breast tissue of a pregnant female. As repeatedly reported, *NEAT1* expression resulted in chemoresistance, and we also showed that *NEAT1_2*-depletion increased apoptosis in HER2-positive breast cancer cells, when treated with the dual HER2 and EGFR inhibitor lapatinib. Finally, according to the results in paper I, we hypothesized that *NEAT1* might affect the autophagy in breast cancer cell line. Therefore, we decided to investigate the role of this lncRNA in autophagy in paper III. Interestingly, our data revealed that *NEAT1*-depletion induce basal autophagy in breast cancer cell lines. Further, the results suggesting a role for *NEAT1* in normal functionality of lysosome in cancer cells. Finally, we illustrated that the induction of autophagy was regulated by AMPK, but not mTOR. Activated AMPK bypasses mTOR and activates Ulk1 in our model.

The introduction is divided into three main sections focused on present knowledge on *NEAT1*, heat shock response, and autophagy. A short description of breast cancer will be given, also providing an overview of the different subtypes. In the methodology section, we will discuss the logic behind the chosen method as well as their limitations and advantages. Finally, the main conclusions from the thesis will be further discussed according to the current knowledge within the field in the discussion section.

Abbreviations

AD	Activation domains
ADARB2	Adenosine Deaminase, RNA Specific B2
AKT	Protein kinase B
Ambra1	Activating molecule in Beclin-1-regulated autophagy
AMPK	AMP-activated protein kinase
AR	Androgen receptor
ASO	Antisence oligo
ATF2	Activating transcription factor 2
ATG	AuTophaGy-related genes
ATP7A	ATPase Copper Transporting Alpha
ATP7B	ATPase Copper Transporting Beta
ATRA	All-trans retinoic acid
Baf A1	Bafilomycin A1
BCL2	Apoptosis Regulator Bcl-2
BECN1	Beclin 1
BRCA1	Breast Cancer Type 1 Susceptibility Protein
CARM1	Coactivator-associated arginine methyltransferase 1
CDK5R1	Cyclin dependent kinase 5 regulatory subunit 1
CFIm	Cleavage factor I_m
CMA	Chaperone-mediated autophagy
CNS	Central nervous system
CRPC	Castrate-resistant prostate cancer
DBD	DNA-binding domain
EMT	Epithelial-mesenchymal transition
ER	Estrogen receptor
FFPE	Formalin-fixed paraffin-embedded
FIP200	Focal adhesion kinase family interacting protein 200 kDa
FOXN3	Forkhead Box N3
FYCO1	FYVE and coiled-coil domain containing 1
GABARAP	Gamma-aminobutyric receptor-associated protein
GATA3	GATA Binding Protein 3
GATE16	Golgi-associated ATPase enhancer of 16 kDa
HER2/ERBB2	Human epidermal growth factor receptor 2
HIF-2α	Hypoxia-Inducible Factor 2 Alpha
HNRNPK	Heterogeneous nuclear ribonucleoprotein K
HOPS	Homotypic fusion and protein sorting
HOPS	Homotypic fusion and protein sorting
HR	Heptad repeat
Hsc70	Heat shock cognate protein of 70kDa
Hsc70	Heat shock cognate 71 kDa protein
HSE	Heat shock elements
HSF	Heat shock transcription factor
HSP	Heat shock protein
HSR	Heat shock response
IL-8	Interleukin 8
IR*Alu*	Inverted repeated *Alu* element
JNK	C-Jun N-terminal kinases

Ki-67	Proliferation-Related Ki-67 Antigen
LAMP-2A	Lysosome-associated membrane protein type 2A
LC3B	Microtubule-associated protein 1 light chain 3
LLPS	Liquid-liquid phase separation
LNA	Locked nucleic acid
lncRNA	Long non-coding RNA
miRNA	Micro RNA
ncRNA	Non-coding RNA
NEAT1	Nuclear paraspeckle assembly transcript 1
NF-κB	Nuclear Factor Kappa B Subunit 1
NONO	POU domain-containing octamer-binding protein
p53	Tumor protein p53
PARP	Poly (ADP-ribose) polymerase
PE	Phosphatidylethanolamine
PI	Phosphatidylinositol
PI3P	Phosphatidylinositol-3-phosphate
PIK3C3/Vps34	Class III PIK3
PLEKHM1	Pleckstrin Homology And RUN Domain Containing M1
PN	Proteostasis network
poly I:C	Polyinosinic:polycytidylic acid
PR	Progesterone receptor
PSP1	Paraspeckle protein 1
PTEN	Phosphatase And Tensin Homolog
PTM	Post-translational modification
Rab7a	Ras-Related Protein Rab-7a
RBP	RNA-binding protein
RD	Regulatory domain
RISC	RNA-induced silencing complex
RNP	Ribonucleoprotein
rRNA	Ribosomal RNA
SFPQ	Splicing factor proline and glutamine-rich
SIN3A	SIN3 Transcription Regulator Family Member A
siRNA	Small interfering RNA
SM	Smooth muscle
SNARE	Soluble N-ethylmaleimide-sensitive fusion (NSF) attachment protein
SRF	Serum response factor
STK11/LKB1	Serine/Threonine Kinase 11
TDP-43	TAR DNA-Binding Protein 43
TLR3	Poll-like receptor 3
TMA	Tissue microarray
TNBC	Triple-negative breast cancers
tRNA	Transfer RNA
ULK1	Unc-51 like kinase 1
UVRAG	UV irradiation resistance-associated gene
VMP1	Vacuole membrane protein-1
VPS	Vacuolar protein sorting
VSMC	Vascular smooth muscle cells
WDR5	Transcriptional co-activator WD repeat domain 5
WIPI2	WD repeat domain phosphoinositide-interacting proteins-2

Introduction

NON-CODING RNA

The human genome project and ENCyclopedia of DNA Elements (ENCODE) have provided a tremendous amount of information about the human genome and its complexity[1]. It is now well known that more than 85% of the human genome is transcribed, even though only 2% of the human genome encodes for proteins[2]. These comprehensive studies have shown that the number of protein-coding genes is very similar from nematodes to humans[3], and that there is a direct correlation between the percentage of intron and non-coding RNAs (ncRNAs) with developmental complexity of species[4]. Accordingly, there is strong evidence that development in higher eukaryotes is under the control of RNAs signals[4]. Intergenic sequences are a large part of the human genome and for many years they were thought of as "junk DNA" as no functions had been discovered for these regions. However, today it is now clear that intergenic regions contain important functional elements, as well as ncRNA genes[2].

NcRNAs are RNA transcripts that do not code for proteins[5], and they are implicated in a variety of biological functions. These RNA species have been found to control gene expression by regulating transcription, mRNA stability, and translation. Moreover, ncRNAs are involved in DNA synthesis and repair, genome rearrangement, and cellular architecture and protein complexes[6–8]. NcRNAs are divided into two groups; small (20-200 nucleotides long) and long ncRNAs (longer than 200 nucleotides). Small ncRNAs include ribosomal RNA (rRNA), transfer RNA (tRNA), microRNAs (miRNAs), small interfering RNAs (siRNAs), small nuclear RNAs (snRNA), small nucleolar RNAs (snoRNA), and Piwi-interacting RNAs (piRNAs)[5].

LONG NON-CODING RNA

Long non-coding RNAs (LncRNAs) have little or no coding potential[9]. They are mostly transcribed by RNA polymerase II and processed by 5´capping, polyadenylation, and splicing[9]. LncRNAs loci are often in close association with protein-coding genes, where they can be located intronic or exonic in either the sense or antisense orientation[10]. However, some of the lncRNAs are transcribed from intergenic regions[2]. Most lncRNAs are expressed at a lower levels than protein-coding genes, and many of them have a tissue-specific expression pattern[11]. LncRNAs have slightly longer exons than protein-coding genes, but they generally contain

fewer exons. For this reason, most of them are shorter in length in comparison to protein-coding genes[12,13].

LncRNAs are less conserved in evolution than the protein-coding gens[14]. The lesser conserved sequence may reflect that lncRNAs function are more dependent on higher-order structures than specific nucleotide sequences. Complementary base pairing or secondary structure of lncRNAs enable them to associate with DNA, RNA, and proteins to exert their functions[15,16]. Furthermore, lncRNAs can be localized in both the nucleus and the cytosol, where they can regulate gene expression at different levels[17,18].

LncRNAs are commonly classified according to their genomic location relative to protein-coding genes and DNA regulatory elements[19]. The method is commonly used by GENCODE/Ensembl portal for annotation of new transcripts. Based on location, lncRNAs can be mainly divided into (Fig.1)[13,20]:

1. **Intergenic lncRNA/lincRNA:** A ncRNA transcribed from a genomic region that does not cross any annotated genes.
2. **Exonic sense lncRNA:** A ncRNA transcribed from in the sense direction of a protein-coding gene and overlaps with one or more exons.
3. **Exonic antisense lncRNA:** A ncRNA transcribed in the antisense direction of protein-coding genes and overlaps with one or more exons.
4. **Intronic lncRNA:** A ncRNA that resides inside an intron of a protein-coding gene, either in the sense or antisense direction, and terminates without overlapping any of the exons.
5. **Bidirectional transcript:** A ncRNA that shares the same promoter as a protein-coding gene, but is transcribed in the opposite direction. The distance between the transcription start site of the ncRNA and the start site of the protein-coding gene should be less than 1kb.

LncRNAs can also be classified based on their function. According to this, lncRNAs can behave as a[16,19]:

1) Scaffolding RNA that helps the assembly of a ribonucleoprotein (RNP) complex at a specific site[21].

2) Guide RNA that physically binds to specific chromatin-regulatory complexes and guides them to specific chromatin loci.
3) Ribo-activator that enhances protein activity.
4) Ribo-repressor and RNA decoy that inhibits/minimizes protein activity by induction of allosteric modifications, inhibition of catalytic activity, and/or blocking protein binding sites.
5) Competing endogenous RNA/RNA sponge that can remove miRNAs from their original targets. These lncRNAs are commonly pseudogenes or circular RNAs containing the complementary sequences for specific miRNAs.

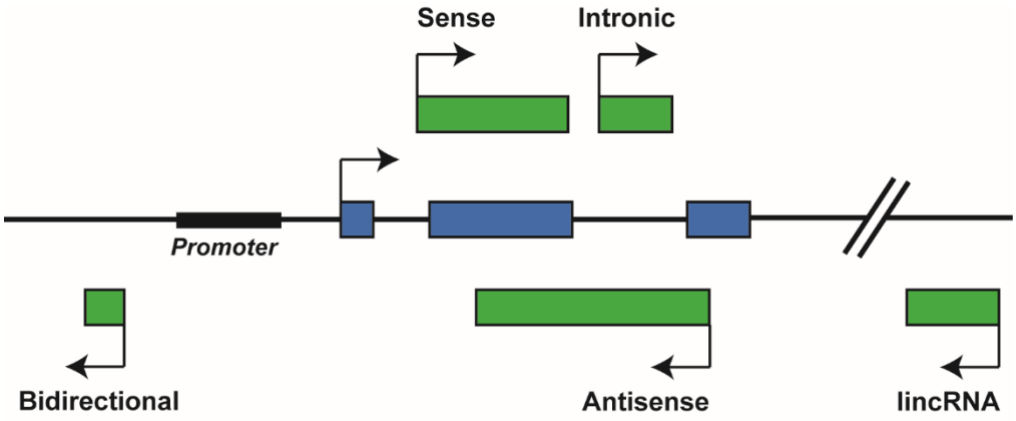

FIGURE 1. Classification of long non-coding RNAs. LncRNAs are classified into five groups: Sense, antisense, intronic, bidirectional, and intergenic. LncRNAs are shown as green boxes and protein-coding gene are illustrated as blue boxes.

Nuclear enriched abundant transcript 1/Nuclear paraspeckle assembly transcript 1 (*NEAT1*)

Nuclear Enriched Abundant Transcript 1 (*NEAT1*), now more commonly referred to as nuclear paraspeckle assembly transcript 1, was discovered by Hutchinson et al. in 2007[22]. *NEAT1* is located on chromosome 11q13.1 and transcribed from the familial tumor syndrome multiple endocrine neoplasia (MEN) type 1 loci. The *NEAT1* gene encodes two transcripts: *NEAT1_1* (3.7kb) and *NEAT1_2* (22.3kb). Both isoforms share the same promoter and *NEAT1_1* overlaps

with the 5´ end of *NEAT1_2*[23]. The *NEAT1_1* isoform becomes polyadenylated, while a tRNA-like structure forms at the 3´ end of *NEAT1_2* that is subsequently cleaved by RNase P and stabilized through the formation of a triple helix structure[24,25] (Fig. 2). The *NEAT1_2* isoform forms when the polyadenylation signal in *NEAT1_1* is suppressed. Heterogeneous nuclear ribonucleoprotein K (HNRNPK) has been shown to play a key role in this process by binding to Cleavage factor I_m (CFIm) in a manner that outcompetes its binding to 3´ processing factors, and thereby inhibits cleavage and polyadenylation of *NEAT1_1* allowing production of *NEAT1_2* in cells[26,27].

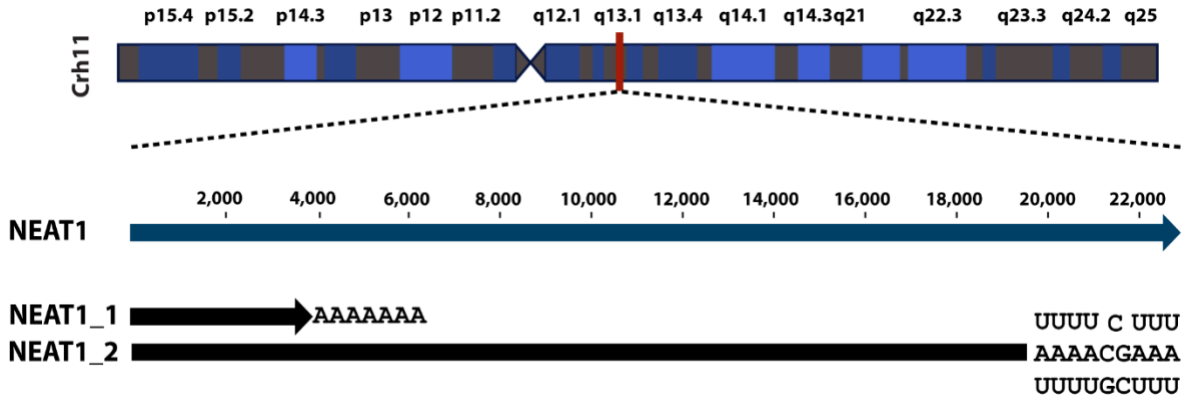

FIGURE 2. Schematic illustration of the *NEAT1* locus. *NEAT1* gene locus is located on chromosome 11q13.1. The *NEAT1* locus encodes two overlapping isoforms: *NEAT1_1* of 3.7 kb and *NEAT1_2* of 22.3 kb. *NEAT1_1* is polyadenylated, whereas *NEAT1_2* is stabilized by a triple helical structure.

NEAT1 is the fundamental RNA component of paraspeckles

NEAT1_2 is essential for the formation of punctuated sub-nuclear structures called paraspeckles[27,28]. Paraspeckles are found in interchromosomal regions in the proximity of nuclear speckles, and they are nuclear RNA-protein complexes with the potential to regulate gene expression. Architectural *NEAT1_2* associates with more than forty proteins to form paraspeckles[29,30] (Table 1). Some of these proteins associate with each other in RNA-dependent manners such as Non-POU domain-containing octamer-binding protein (P54nrb/NONO), paraspeckle protein 1 (PSP1), and splicing factor proline and glutamine-rich (SFPQ)[31]. Paraspeckles have a core-shell spheroidal structure and are highly dynamic. A subset

of paraspeckle proteins (PSP) can fuse to/diffuse from paraspeckles dependent on cellular circumstances[32]. Many paraspeckle proteins contain prion-like domains, low complexity domains, intrinsically disordered regions, and coiled-coil domains (Table 1). Due to these features, they drive liquid-liquid phase separation (LLPS) to form paraspeckles as a liquid drop-like membraneless organelle[32,33]. Two of the essential PSPs, fused in sarcoma (FUS) and RNA binding protein 14 (RBM14) seem to have a particular important role in phase separation as they readily form so-called hydrogels *in vitro*[34,35]. Depletion of *NEAT1_2* showed that *NEAT1_1* could form numerous non-paraspeckle structures in the vicinity of nuclear speckle, termed "microspeckles", which may serve as a platform for a paraspeckle-independent function of *NEAT1_1*[36]. Paraspeckles are seen in mammalian nuclei and most cultured cells, and also in some mammalian tissues like the tip of gut epithelium in mice[28]. Paraspeckles are absent in embryonic stem cells, but appear upon differentiation[28,37]. The number and the size of paraspeckles are cell-dependent; for example, HeLa cells have 13-17 paraspeckles per nucleus, while the number of paraspeckles in NIH3T3 is between 5-10 per nucleus[23].

The presence of some proteins is essential for the structure of paraspeckles such as NONO, SFPQ, HNRNPH3, HNRNPK, DAZAP1, FUS, RBM14, and HNRNPH3[27]. NONO, SFPQ, and PSPC1 are the most studied paraspeckle proteins containing a common domain structure which has two RNA recognition motifs. Paraspeckles have an organized structure in which proteins and RNAs are arranged at specific sites. Immunohistochemistry analysis has shown that NONO, SFPQ, FUS, and PSPC1 are located in the core of the paraspeckle and RBM14 and BRG1 form small patches found both in the core and in the outer shell area. The 5´ and 3´ ends of *NEAT1_2* are localized close to each other in the outer shell of the paraspeckles, whereas the middle part of *NEAT1_2* is located in the core of the paraspeckle[38]. Paraspeckle proteins and some of their characteristics are listed in Table 1.

Table 1. Paraspeckle proteins

	Protein	Function	Prion like domain	Liquid–liquid phase separation link	Paraspeckle zone	Reference
1	HNRNPK	Essential				27
2	NONO	Essential	+		Core	29,31,8
3	RBM14	Essential	+	+	Patch	29,39
4	SFPQ	Essential	+		Core	31,8,40,39,41
5	DAZAP1	Essential	+			27
6	FUS	Essential	+	+	Core	27
7	HNRNPH3	Essential	+			27
8	BRG1	Essential	NO		Patch	42
9	CPSF7	Important for paraspeckle integrity	NO			27
10	FAM98A	Important for paraspeckle integrity	+			27
11	FAM113A	Important for paraspeckle integrity				27
12	FIGN	Important for paraspeckle integrity	+			27
13	HNRNPA1	Important for paraspeckle integrity	+	+		27
14	HNRNPR	Important for paraspeckle integrity	+			27
15	HNRNPUL1	Important for paraspeckle integrity	+			27
16	RBM12	Important for paraspeckle integrity	+			27
17	TAF15	Important for paraspeckle integrity	+			27
18	SRSF10	Important for paraspeckle integrity	NO			27
19	ENOX1	Involved in paraspeckle formation				43
20	FAM53B	Involved in paraspeckle formation				43
21	HECTD3	Involved in paraspeckle formation				43
22	ZNF24	Involved in paraspeckle formation				43
23	RNA POLYMERASE-II	Inhibition of RNA polymerase II causes redistribution of paraspeckle components				44
24	ANNEXIN A10	Overexpression reduces paraspeckle				45
25	CPSF6	Dispensable	NO			46
26	NUDT21/CPSF5	Dispensable				27
27	UBAP2L	Dispensable	+			27
28	AHDC1	Dispensable	NO			27
29	AKAP8L	Dispensable	+			27
30	CIRBP	Dispensable	NO			27
31	EWSR1	Dispensable	+			27
32	PSPC1	Dispensable	+		Core	29,39
33	RBM3	Dispensable	+			27
34	RBM7	Dispensable	NO			27
35	RBMX	Dispensable				27
36	RUNX3	Dispensable	+			27
37	ZC3H6	Dispensable				27
38	ZNF335	Dispensable				27
39	CYBA	Dispensable				43
40	FAM53A	Dispensable				43
41	GATA1	Dispensable				43
42	KIAA1683	Dispensable				43
43	KLF4	Dispensable				43
44	LMNB2	Dispensable				43
45	SCYL1	Dispensable				43
46	SH2B1	Dispensable				43
47	SRSF11	Dispensable				43
48	XIAP	Dispensable				43
49	ZNF444	Dispensable				43
50	RBM4B	Dispensable	NO			27
51	TDP-43	n.d	+		Shell	27

52	BCL6	n.d		47
53	BCL11A	n.d		47
54	CELF6	n.d	NO	27
55	CHMP6	n.d		43
56	DLX3	n.d	+	27
57	HNRNPA1L2	n.d	+	27
58	HNRNPF	n.d		27
59	HNRNPH1	n.d	+	27,39,41
60	HNRNPM	n.d		48
61	KIAA1530	n.d		43
62	MEX3C	n.d		27
63	SOX9	n.d		49
64	SS18L1	n.d	+	27
65	v-FOS	n.d		43
66	WTX	n.d		50
67	WT1 (+KTS)	n.d		51
68	MEX3A	n.d	NO	27

Abbreviations: n.d, not determined[27,30,354].

NEAT1 expression and paraspeckle formation are induced by cellular stress

Increased expression of *NEAT1* and elevated paraspeckle formation have been observed in many stress-induced situations like viral infection, hypoxia, proteasome inhibition, and oncogene-induced replication stress (Fig. 3)[52–59]. Emerging evidence suggests that *NEAT1* has a cytoprotective role in cells since *NEAT1*-depleted cells are more sensitive to stress-induced cell death than wild type cells[55].

One of the first reports on *NEAT1* being upregulated by cellular stress came in 2014 by Tetsuro Hirose et al[55]. They showed that *NEAT1* levels increased in cells treated with the proteasome inhibitor MG-132. This was accompanied by a change in the morphology of the paraspeckles to become more elongated. The authors presented evidence that this upregulation was due to increased transcription of the *NEAT1* gene[55]. This study was followed by a study by Choudry et al.[59] showing that *NEAT1* and paraspeckle formation were induced in breast cancer cells upon hypoxia. This was indeed shown to be due to transcriptional upregulation of the *NEAT1* by Hypoxia-Inducible Factor 2 Alpha (HIF-2α). In these papers, *NEAT1*-depleted cells were shown to be more sensitive to proteasome inhibition and hypoxia, respectively, than wild type cells. Recently, *NEAT1* was shown to be a transcriptional target of tumor protein p53 (p53), the key guardian of the genome in mammalian cells which is activated by a variety of cellular stressors known to induce the DNA damage response (DDR)[60,61]. Importantly, *NEAT1*-depleted cells accumulated DNA damage and displayed replication stress and were more sensitive to

chemotherapy. A very recent study uncovered a cross-talk between mitochondria and *NEAT1*/paraspeckles[62]. Mitochondria generally sense internal and external stressors and sustain cell homeostasis by regulating energy production and intracellular signaling[62]. Mitochondrial stress induced *NEAT1* transcription and the formation of elongated paraspeckles in a mechanism that was dependent on activating transcription factor 2 (ATF2) binding to the *NEAT1* promoter. Furthermore, the presence of *NEAT1* was vital for the normal function of mitochondria, as knockout of *NEAT1* in HeLa cells resulted in a reduction in mitochondrial DNA content, impaired mitochondrial respiration, and reduced ATP production[63]. Finally, *NEAT1* has also been shown to be transcriptionally activated by Nuclear Factor Kappa B Subunit 1 (NF-κB) as in response to lipopolysaccharide stimulation of lung adenocarcinoma cells[64]. Taken together, all these reports show that *NEAT1* is upregulated upon cellular stress by transcriptional activation mediated by key stress-induced transcription factors including HIF-2α, p53, ATF2, and NF-κB. (Fig. 3).

NEAT1 expression is induced in cells in response to infections by a series of viruses and several lines of evidence suggests that *NEAT1* plays a critical role in the innate immune response against viral infection[52,54,57,58,65–69]. Stimulation of cells by polyinosinic:polycytidylic acid (poly I:C) that mimics a dsRNA virus infection, induced *NEAT1* expression through the toll-like receptor 3 (TLR3)[52]. Microarray analysis showed that *NEAT1* is involved in the regulation of antiviral genes since depletion of *NEAT1* reduced the expression of more than 250 poly I:C-inducible genes in HeLa cells[52].

NEAT1 and paraspeckles regulate gene expression at different levels

Even though the functions of *NEAT1* and paraspeckles are not fully understood, several studies have shown that they can regulate the expression of specific genes at both transcriptional and post-transcriptional levels.

Transcriptional regulation of gene expression by *NEAT1*

Paraspeckles are dynamic structures, and elevated *NEAT1* expression is associated with enhanced recruitment of proteins into paraspeckles[52,55]. Many of the paraspeckle-associated proteins have diverse functions in the nucleus. One such protein is SFPQ that also works as a transcriptional regulator. When *NEAT1* levels increase, more SFPQ is recruited to the paraspeckles and thus the levels in the nucleoplasm decrease. This sequestration removes SFPQ

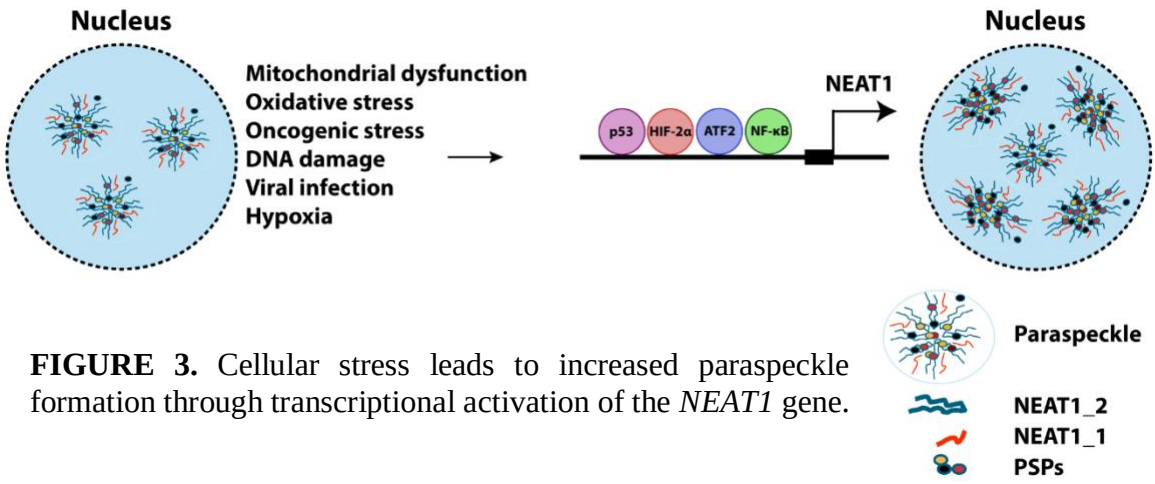

FIGURE 3. Cellular stress leads to increased paraspeckle formation through transcriptional activation of the *NEAT1* gene.

from the promoters of its target genes. This is exemplified by the interleukin 8 (IL-8) gene[52]. In normal conditions, SFPQ binds to the promoter region and represses the transcription of *IL-8*. Stimulation of cells with poly I:C increases *NEAT1* expression and paraspeckle formation that subsequently relocates SFPQ from the *IL-8* promoter allowing transcription of the *IL-8* gene[52]. SFPQ can also work as a transcriptional activator[55]. This has been demonstrated for the gene encoding the RNA-editing enzyme adenosine deaminase, RNA specific B2 (ADARB2). The elongation of paraspeckles upon proteasome inhibition sequesters SFPQ away from ADARB2 promoter, and thereby represses ADARB2 expression[55]. Enhanced *NEAT1* expression during neointima in vascular smooth muscle cells has also been shown to sequester the transcriptional co-activator WD repeat domain 5 (WDR5) away from its target genes[70] (see below).

The above-mentioned examples demonstrate an indirect role of *NEAT1* in gene regulation through SFPQ or WDR5. It has, however, been reported that *NEAT1* also binds directly close to the transcriptional start sites of active genes and influence their transcriptional activity[71]. Chakravarty et al. showed that *NEAT1_1* can interact with chromatin via histone H3 and that this interaction is associated with the formation of active chromatin as measured by increased levels of H3K4Me3 and H3AcK9. This suggests that *NEAT1_1* can change the epigenetic landscape of target gene promoter to regulate gene expression[72].

Post-transcriptional regulation of gene expression by *NEAT1*

Several reports have shown that *NEAT1* and paraspeckles have an important role in the regulation of cytoplasmic export of certain mRNAs[37,40]. This was first described for mRNAs containing inverted repeated *Alu* elements (IR*Alu*s) in their 3´ untranslated regions. The presence of IR*Alu*s leads to the formation of double-stranded RNA regions subjected to adenosine to inosine editing. IR*ALus*-containing mRNAs are recruited to paraspeckles upon specific cellular circumstances through direct interaction with NONO. This prevents their export to the cytoplasm and thus their translation into proteins[37,40]. Interestingly, upon mitochondrial stress and dysfunction, many nuclear-encoded mitochondrial mRNAs are retained in paraspeckles. This indicates that *NEAT1* and paraspeckles play a regulatory role in mitochondrial biogenensis[63]. The formation of paraspeckles has been shown to follow a circadian rhythm in pituitary cells, leading to rhythmical retention of a range of mRNAs[73]. The retention of mRNAs in the nucleus is opposed by coactivator-associated arginine methyltransferase 1 (CARM1). CARM1 methylates NONO that decreases its ability to bind to mRNAs containing 3´UTR IR*Alu*s. CARM1 also reduces paraspeckle formation by suppressing *NEAT1* at the transcriptional level[74,75].

Recently, it has been suggested that *NEAT1* and paraspeckles facilitate the maturation of miRNAs. The NONO-SFPQ heterodimer was found to bind to a large group of pri-miRNAs and accelerate their processing into pre-miRNA in the nucleus. Furthermore, an interaction between *NEAT1* and the Drosha–DGCR8 microprocessor was demonstrated. The authors proposed a "bird nest model" in which *NEAT1* provides the cells with a platform to facilitate the processing of the pri-miRNAs to pre-miRNAs, eventually generally increasing the overall number of mature miRNAs in the cells[76]. *NEAT1* has also been suggested to act as a so-called competing endogenous RNA sponging a whole series of miRNAs (reviewed in Klec et al)[77]. However, how a nuclear RNA sponges miRNAs is not well described, and therefore further experiments should be undertaken to prove that this is a true regulatory mechanism of *NEAT1 in vivo*.

Biological functions of *NEAT1* and paraspeckles

As mentioned above, increased *NEAT1* expression and paraspeckles formation are induced by a variety of cellular stressors. Several lines of evidence also suggest that *NEAT1* can regulate gene expression at different levels. Soon after its discovery, it became clear that *NEAT1* is not

vital for the development of mammalians since *Neat1*-knockout mice can survive under normal conditions[28]. In line with this, human embryonic stem cells in culture do not express *NEAT1*[37]. This suggests that *NEAT1* has specific functions at certain biological circumstances. It has now been demonstrated that *NEAT1* has a critical role in the development of the mammary gland[78]. Virgin *Neat1*-knockout mice display defect ductal outgrowth and branching during puberty. Furthermore, during pregnancy, lactation was severely compromised in *NEAT1*-depleted mice due to reduced proliferation of milk-producing luminal alveolar epithelial cells[78]. A subset of *Neat1*-knockout female mice developed impaired corpus luteum, the transient secretory gland in female ovaries[79]. Corpus luteum development is one of the critical steps in gestation and secretion of progesterone. The formation of corpus luteum is essential for the establishment and maintenance of pregnancy. Consequently, *Neat1*-knockout mice become pregnant less frequently than wild-type mice[79].

Recently, *Neat1* and NONO were found to be vital for the establishment of embryonic and extra-embryonic lineages at a very early stage of mouse embryonic development. Microinjection of *Neat1* antisense oligos at the 2-cell stage resulted in a developmental arrest at either the 16- (52.46% of embryos) or 32 cells (26.3% of embryos) stage. This is partially caused by lack of paraspeckle recruitment of CARM1, which critically interfered with its ability to methylate histone H3 at arginine 26 (H3R26me2), causing an imbalance between cells destined to develop into embryonic and extra-embryonic tissue.

It has recently been shown that *NEAT1* is upregulated when vascular smooth muscle cells (VSMCs) switch from a contractile to a proliferative phenotype upon vascular injury, a process referred to as neointima[70]. This switch is associated with a profound change in the gene expression pattern where smooth muscle (SM)-specific genes are downregulated. The authors showed that knockdown of *NEAT1* enhanced the expression of SM-specific genes by a mechanism involving the transcriptional co-activator WD repeat domain 5 (WDR5). WDR5 stimulates the transcription of SM-genes by creating an active chromatin state that allows serum response factor (SRF) to bind to their promoters. The authors demonstrated that upon neointima, WDR5 is sequestered in nuclear structures believed to be paraspeckles, preventing its association with promoters of SM-specific genes. Importantly, in response to carotid artery ligation, neointima was severely compromised in *Neat1*-knockout mice[70]. Finally, it has been shown that *NEAT1* has a pivotal role in myeloid differentiation, as knockdown of *NEAT1* inhibits all-trans retinoic acid (ATRA)-induce differentiation[80]. Taken together, many lines of

evidence suggest that *NEAT1* has specific functions at certain developmental stages, cell differentiation, and under cellular stress, and it orchestrates changes in gene expression patterns both at the transcriptional and post-transcriptional levels.

NEAT1 is abnormally expressed in cancer

As described above, *NEAT1* is believed to have an important role in cell survival upon cellular stress, including genotoxic stress and hypoxia that are prominent in cancer cells. In 2014, Chakravarty et al. reported that *NEAT1* is upregulated and associated with poor prognosis in prostate cancer. This was followed by a study by Choudhry et al. showing that *NEAT1* is overexpressed in hypoxic regions of breast cancer cell line xenografts and associated with poor clinical outcome of breast cancer. Now, *NEAT1* has been found to be upregulated in tumor cells compared to normal cells in a series of human cancers including lung cancer, hepatocellular carcinoma, ovarian cancer, nasopharyngeal carcinoma, gastric cancer, osteosarcoma, glioblastoma, oral and esophageal carcinoma, clear cell renal carcinoma, and cervical carcinoma[81–90]. In most cases, high *NEAT1* expression is associated with aggressive disease. Moreover, a large number of mutations in the *NEAT1* sequence are frequently observed in hepatocellular carcinoma, prostate cancer, stomach cancer, lung adenocarcinoma, breast cancer, and B cell lymphoma[91,92]. A deep sequencing study of the promoter and regulatory elements in 360 breast cancer samples identified mutational hotspots in the core promoter of *NEAT1*[93]. Interestingly, the majority of these mutations are associated with decreased expression *in vitro*. In the same study, *NEAT1* was found to be focally deleted in 8% of the samples[93]. *NEAT1* expression was also reduced in peripheral blood samples from patients suffering from acute promyelotic leukemia compared to samples from healthy donors[94]. Taken together, although enhanced *NEAT1* expression is mostly associated with tumor cells and aggressive disease, it might also have a protective role depending on the type of cancer and cancer stage. This already has been demonstrated in two different cancer models in mice. *Neat1* knockout mice are less prone to develop squamous cell carcinoma in a two-stage DMBA-TPA skin carcinogenesis model[56]. On the other hand, knockout of *Neat1* in Ras^{G12D} genetic model, promoted the development of premalignant pancreatic intraepithelial neoplasia. This suggests that *NEAT1* can also act as a tumor suppressor, preventing the development of pancreatic cancer[95].

NEAT1 expression is associated with resistance to cancer therapy

Aforementioned, high level of *NEAT1* is associated with tumor progression and poor survival, just as its role in chemoresistance has been shown in several studies[56,72,96–106]. The expression level of *NEAT1_2* correlates with response to chemotherapy, as higher expression of *NEAT1_2* conversely associates with progression-free survival in ovarian cancer patients who underwent platinum-based chemotherapy[56]. Targeting *NEAT1_2* has also been shown to sensitize cancer cells to chemotherapy reagent such as poly (ADP-ribose) polymerase (PARP) inhibitors, ABT-888[56]. Moreover, it has been shown that *NEAT1* knockdown suppressed P-glycoprotein (cell membrane protein that pumps drugs out of the cell) and GST-π (involved in drug metabolism) level in paclitaxel-resistant ovarian cancer cells resulting in higher sensitivity to paclitaxel[107]. Furthermore, *NEAT1* expression result in drug resistance in breast cancer. The breast cancer cell lines MCF7 and MDA-MB-231 became sensitized to Fluorouracil (5-FU) upon downregulation of *NEAT1*[108]. The analysis of triple negative breast cancer cell line illustrated that *NEAT1* expression increased in cisplatin/taxol treated cancer cells, and targeting *NEAT1* in combination with cisplatin/taxol treatment had a synergistic effect to inhibit cell growth[97]. Moreover, RT-qPCR data revealed that drug transporter, ATP7A and ATP7B were downregulated in *NEAT1* knockdown cell[97]. The role of *NEAT1* in the reduction of cisplatin-sensitivity was also showed in osteosarcoma[105].

ERα-*NEAT1* signaling promotes prostate cancer progression both in the androgen receptor (AR)-positive and AR-negative cell lines[72]. Although both ERα and AR antagonists (4-hydroxy tamoxifen and Enzalutamide, respectively) constrained *NEAT1*, longer treatment of prostate cancer cells by these drugs resulted in *NEAT1* induction. Consistently, *NEAT1* and ERα were higher in castrate-resistant prostate cancer (CRPC) suggesting a role for *NEAT1* in therapeutic resistance in prostate cancer[72]. Furthermore, targeting *NEAT1* in docetaxel-resistant prostate cancer cell line increased the sensitivity of these cells to docetaxel[98].

NEAT1 in breast cancer

Neat1 knockout mice are viable. However as mentioned above, they display impaired mammary gland development both in puberty and in pregnancy/lactation. Given this, it is reasonable to assume that *NEAT1* could have a role in breast cancer. Indeed, the expression of *NEAT1* is critical for proliferation and survival of breast cancer cell lines[59,79,109–111]. *NEAT1* is also upregulated in breast tumor samples compared to adjacent normal tissue, and is associated

with poor clinical outcome[59,109,112,113]. *NEAT1* is regulated by estrogen both in prostate and breast cancer cell lines[72,114]. In estrogen receptor positive (ER+) breast cancer cell line, *NEAT1* is responsible for the interaction between FOXN3 and SIN3A[114]. The FOXN3-*NEAT1*-SIN3A complex promotes epithelial-mesenchymal transition (EMT) by repressing the expression of GATA binding protein 3 (GATA3). This promotes metastasis *in vivo*[114]. Another study showed that BRCA1 represses *NEAT1* transcription[115]. *BRCA1* mutations are well-known genetic causes of hereditary breast cancer and plays a pivotal role in the development of the mammary gland[115]. Deficiency of BRCA1 increases expression of *NEAT1* and promotes tumorigenicity both *in vivo* and *in vitro*[96].

NEAT1 in neurodegenerative diseases

Neurodegenerative disease is a general term for a wide range of diseases which affect neurons in the central nervous system (CNS). Specific subsets of neurons in specific functional anatomic systems can be affected resulting in hundreds of different neurodegenerative disorders such as amyotrophic lateral sclerosis (ALS), Parkinson's disease (PD), Huntington's disease (HD), frontotemporal dementia (FTD), and Alzheimer disease (AD)[116]. Interestingly, *NEAT1* is abnormally expressed in several of these diseases. Furthermore, genes encoding the paraspeckle associated proteins TAR DNA-Binding Protein 43 (TDP-43) and fused in sarcoma FUS are frequently mutated in ALS.

Amyotrophic lateral sclerosis: ALS is a fatal motor neuron disorder in the spinal cord and motor cortex[117]. Mutations in genes encoding RNA-binding proteins (RBPs) or their regulators are frequent in ALS. As showed by Nakagawa et al. *NEAT1_2* expression is low in adult CNS[28], but the paraspeckle formation was detected in sporadic ALS (sALS) in two separate experiments[118,119]. Formation of paraspeckle is not only seen in sALS, but also detected in familial ALS (fALS)[120]. Approximately 25 proteins have a high association with ALS[121]. Interestingly, eight of these proteins have also been found in paraspeckles, including FUS, TDP-43, EWS, TAF15, SFPQ, MATR3, CREST, and hnRNPA1, suggesting the importance of *NEAT1*/paraspeckle in ALS pathogenesis[121]. Moreover, the aggregation of these proteins can affect paraspeckle indirectly since aggregated protein can recruit more paraspeckle proteins. For instance, aggregation of FUS and TDP-43 in ALS can sequester other paraspeckle components from the nucleus[120].

Huntington's disease: HD is a progressive, fatal inherited autosomal dominant neurodegenerative disorder. The extension of CAG repeats in the *HTT* gene, which encodes a polyglutamine stretch in the huntingtin protein is the cause of HD[122,123]. Two separate studies have shown that *NEAT1* level is elevated in the caudate of affected individuals[124], and RT-qPCR analysis showed higher expression of *NEAT1_2* in HD patients' brain. *In vitro* studies on HD cell model revealed that overexpression of *NEAT1_1* protected the cell against oxidative stress, whereas *NEAT1_2* knockdown decreased cell survival[125,126].

Parkinson's disease: PD is a chronic, progressive neurodegenerative disorder characterized by both motor and non-motor features which affect 1% of individuals over 60 years old. Meta-analysis of the microarray from public dataset showed that *NEAT1* is upregulated almost 1.5-fold (gene expression ratio of value in HD patient/healthy group) in the substantia nigra of PD patients compared to healthy control[127]. Also, a high level of *NEAT1* in the midbrain of Parkinson mouse model was reported. It has been shown that knockdown of *NEAT1* increases survival of dopaminergic neurons in PD mouse model[128,129].

***NEAT1* in Alzheimer's disease (AD):** AD is the most prevalent neurodegenerative disorder in individuals older than 65 years old. More than 95% of AD cases are sporadic by late onset (80-90 years) in the patient. There are two clinical features which are typically associated with AD neuropathological process, namely, disability of cells to clear the amyloid-β (Aβ) peptide from the neurons and accumulation of hyperphosphorylated tau-protein intracellularly as neurofibrillary tangles. Symptoms of AD are started with slow progression of dementia, as well as gross atrophy in the cerebral cortical of the brain. A massive number of genetic risk factors have been reported for sporadic AD, however, less than 1% of patients have a mutation in genes involved in regulation of amyloid-β (Aβ) peptide; Individuals who carry the mutation develop the disease much earlier, at an average age of 45 years[130,131,132]. Microarray analysis revealed a high level of *NEAT1* in five regions of the brain, namely, entorhinal cortex, hippocampus, middle temporal gyrus, posterior cingulate cortex, and the superior frontal gyrus[133]. Furthermore, two independent studies have reported overexpression of *NEAT1* both in the hippocampus and temporal cortex in AD patients[134,135]. Interestingly, expression of cyclin-dependent kinase 5 regulatory subunit 1 (*CDK5R1)*, which has a pivotal role in the development of the brain, is positively correlated with *NEAT1* expression, suggesting a neuroprotective role for *NEAT1* in AD patients to compensate for increased CDK5R1 levels[135].

Heat shock response

Cells are frequently exposed to external and internal stressors that can affect important cellular processes leading to cell death. To counteract stressors and retain homeostasis, cells have developed a range of cytoprotective stress response mechanisms. One such stress response pathway is the heat shock response (HSR) pathway. The heat shock response pathway is conserved in evolution and activated by factors causing protein misfolding. Misfolded proteins often mislocalize and form aggregates within the cell and lose their original function. Efficient function of proteins is pivotal for the health of the organism, and the functional state of each protein is precisely monitored by a dynamic network called the proteostasis network (PN)[136]. To keep the proteostasis, cells need to coordinate the triangle of protein synthesis and folding, conformation change, and degradation.

Protein aggregation is associated with serious pathological disorders. It reduces the number of active proteins from the cell's protein pool[137–139]. Aggregated proteins may result in toxicity regardless of their biological function. Protein aggregates can damage membranes and interact abnormally with macromolecules[137–139]. In response to protein aggregation, a series of molecular chaperones, under the control of HSR, become activated[140]. During the HSR, a group of proteins termed the Heat Shock Proteins (HSPs) are upregulated. Most HSPs act as molecular chaperones. Chaperones are proteins that mediate correct assembly of other proteins[141]. They facilitate *de novo* folding during translation, refolding of protein after stress trafficking, translocation, ubiquitination, and degradation of proteins, and in this way, HSPs monitor quality of the proteome to ensure proteostasis[142,143]. Most of the chaperones are classified as stress proteins, while they also have essential roles in normal cell physiology[141]. Chaperones can be classified based on different parameters such as size, cellular localization, chaperone's action, and their specificity. They are usually divided into different classes based on their molecular weight including HSP40, HSP60, HSP70, HSP90, HSP100, and the small HSPs[143,144].

Heat shock transcription factors (HSFs) are a family of DNA-binding proteins that mainly regulate the HSR in proteotoxic stress[145]. They are highly conserved from fungi to mammals[145]. In human, six HSFs have been discovered, which include HSF1, HSF2, HSF4, HSF5, HSFX, and HSFY[146] . HSF1 is a master regulator of the HSR since mammalian cells lacking the expression of the HSF1 are unable to induce a stress response[147,148]. In contrast, deficient cells for *HSF2* and *HSF4* are still able to induce the stress response[149,150]. HSF2 is mostly studied in the development of the brain and reproductive organ[151,152], and it can form heterotrimers with

HSF1 to bind to promoters of genes encoding HSPs like the HSPA1A (HSP70) promoter. HSF3 has not been discovered in humans, but it has a crucial role in the induction of HSR in avian cells. It also controls non-*HSPs* heat shock genes in mice[153]. HSF4 has a pivotal role in growth and differentiation of the eye during lens development, and mutation in *HSF4* leads to cataracts[149,154]. The functions of HSF5, HSFX, and HSFY remain to be explored; however, it has been shown that deletion of HSFY leads to male infertility[153,155,156].

The HSF1 protein consists of four conserved functional domains including N-terminal DNA-binding domain (DBD), the heptad repeat (HR)-A/B/C, a regulatory domain (RD), and two activation domains (AD1, AD2) (Fig. 4A)[145,157]. The DBD is the best-conserved domain within the HSF family and contains a looped helix-turn-helix structure. Unlike many other transcription factors that form dimers, HSFs form a trimer to bind to the target sequence. This is mediated by the HR-A/B/C domains. Trimerization enables HSF1 to correctly recognize specific DNA sequences called Heat Shock Elements (HSE). HSEs are located in the upstream region of HSF1 target genes and consist of pentameric sequence nGAAn, where "n" can be any nucleotide. The arrangement of HSE in a regulatory region can be varied, and three continuous inverted repeats of nGAAn are the best fit to be detected by HSF1[145,157,158]. While DBD in N-terminal is responsible for DNA binding, ADs in C-terminal regulates transcriptional activation of target genes[145,157].

In normal physiological conditions, HSF1 is kept in the cytoplasm as a monomer by forming a complex with HSP70, HSP90, and HSP40[159–162]. Upon stress and presence of misfolded proteins, monomeric HSF1 is released from its inhibitory complex and undergoes trimerization (Fig. 4B)[163,164]. Activated HSF1 promotes the transcription of its target genes including those that encode HSP70 and HSP90. These proteins inactivate HSF1 by a negative feedback loop. In this model, activation and inactivation of HSF1 are dependent on the concentration of HSP40, HSP70, and HSP90 in cells. After trimerization, HSF1 translocate to the nucleus and binds to consensus sequence[163,165,166]. HSF1 binds to its target through the DBD recognition helix containing conserved Ser-Phe-Val-Arg-Gln amino sequence. The sequence inserts into the major groove of the HSE and binds guanine of nGAAn sequence via conserved Arg[167]. Crystallographic studies have illustrated that DNA is surrounded by a carboxy-terminal helix of DBD and connect LZ1-3 to the other side of DNA. Acetylation of Lys80 neutralize positive charge on Lys and disrupts HSF1-DNA interaction[168].

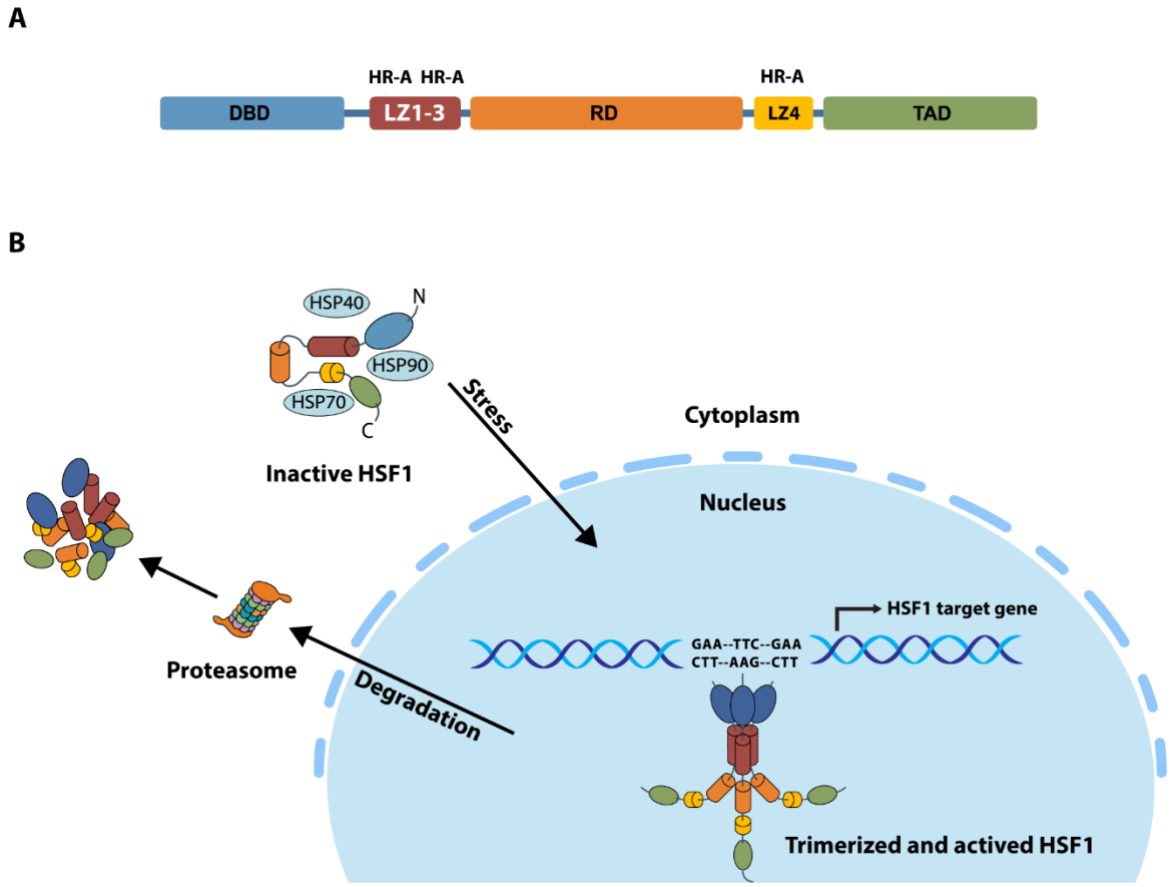

FIGURE 4. HSF1 activation cycle. **A.** Domain structure of the human HSF1 protein. **B.** HSF1 activation. Upon oxidative stress, heat shock, and accumulation of unfolded proteins, HSF1 is released from an inhibitory complex consisting of HSP70, HSP90, and HSP40, and undergoes a multistep activation process in which HSF1 translocates into nucleus and trimerized. Trimerized and activated HSF1 binds to its HSE regions in the promoters of its target genes, including *HSP40*, *HSP70*, and *HSP90*, to activate their expression. When the HSR is attenuated, HSF1 is inhibited and either degraded by the 26S proteasome or recruited to the inhibitory complex[157,166].

HSF1 also undergoes a variety of post-translational modifications (PTMs) such as phosphorylation, sumoylation, and acetylation in which phosphorylation is the most studied. PMTs influence HSF1 function and stability both positively and negatively[166]. For instance, phosphorylation of Ser121, Ser303, and Ser306 associates with repression of HSF1 transcriptional activity in normal condition, whereas phosphorylation of HSF1 on Ser230, Ser320, and Ser326 is induced by stress. The acetyltransferase p300 control the turnover of HSF1 by acetylation of Lys208, and Lys298 which prevent proteasomal degradation. As mentioned above, p300 inhibits HSF1-DNA interaction by acetylation of Lys80 in HSF1[169].

Activation of HSF1 can protect cells against environmental stressors such as heat, ischemia, inflammation, oxidative stress, and other noxious conditions[152,170–178]. In most cases, activation of HSF1 is an acute and transient process. The deregulation of HSF1 causes different diseases including neurodegenerative disease and cancer[152,170–178]. The level of HSF1 is reduced in neurodegenerative diseases[171–174]. HSF1-depleteion exacerbates protein misfolding and aggregation as the expression of HSP chaperones are severely reduced. High levels of HSF1 and HSPs has been reported in many cancers correlating with poor prognosis; They can support protein synthesise in cancer cells and also protect them from stress[156,179]. HSF1 helps cancer cells to adapt to hypoxia, acidosis, and nutrient deprivation[175]. Activation and overexpression of HSF1 have been discovered in different kinds of human tumors including breast cancer[154,175–178,180]. In agreement with this, the lack of HSF1 in mice protects them from carcinogen-induced skin tumors[175]. In cancer, a variety of signaling pathways influence HSF1 via PMTs such as RAS, AMPK, GSK3, JNK, and PKA. For instance, MEK can phosphorylate HSF1 on Ser326 resulting in HSF1 activation[181] and, in turn, the high level of HSF1 increases MAPK activity which leads to proliferation and growth. Furthermore, chaperones can activate specific signaling pathways to promote oncogenesis and inhibit apoptosis. For example, HSP70 and HSP90 prevent stress-induced apoptosis through JNK and AKT, respectively. Moreover, chaperones also facilitate folding of abnormal proteins in cancer cells that are encoded by mutated genes[156,182].

Autophagy

Autophagy is a conserved catabolism process through which cytosolic cargo such as long-lived proteins, organelles and pathogens are removed by the lysosomal system to maintain cell homeostasis[183]. The process was for the first time described by Christian De Duve who named the process Autophagy meaning ‘eating of self’[184,185]. In the 1990s, the Yoshinori Ohsumi lab discovered that autophagy mechanisms in yeast are very similar to those in mammalian cells. Using yeast as a model, many AuTophaGy-related genes (*ATG*) were discovered that are conserved in human cells. Up until now, 42 *ATG* genes have been identified among which 16 *ATG* genes are known as core *ATG* genes since they are commonly involved in both non-selective and selective macroautophagy[186]. Other *ATG* genes are associated with specific kinds of selective autophagy[187]. The non-selective autophagy unspecifically engulfs a part of the cytoplasm and containing component upon cellular stress such as starvation to recycle cellular component and ensure cell survival until new resources provided[188]. Furthermore, non-selective autophagy has a basal level activity for the removal of protein aggregates, damaged organelle,

and also an unnecessary substrate in cells[188]. Selective autophagy, on the other hand, targets a cargo by selective autophagy adaptors such as ubiquitin-binding protein p62/Sequestosome-1 (p62/SQSTM1)[189]. Selective autophagy can remove lipid droplets (lipophagy), Mitochondria (Mitophagy), pathogenes (Xenophagy), iron bound ferritin (ferrintinophagy), lysosome (lysophagy), ER (reiculophagy), ribosome (ribophagy), aggregated protein (aggrephagy)[190].

Autophagy is divided into three types: Microautophagy, chaperone-mediated autophagy (CMA), and macroautophagy (Fig. 5)[191]. In microautophagy, part of mammalian cytoplasm is directly sequestered and engulfed by lysosomes (Fig. 5C)[192]. In CMA, a cytosolic chaperone protein, the heat shock cognate protein of 70kDa (Hsc70), recognizes a penta-peptide KFERQ-like motif in the amino acid sequence of targeted cargo and guides the cargo to the surface of the lysosomes. Afterward, the protein-chaperone complex interacts with the cytosolic tail of the lysosome-associated membrane protein type 2A (LAMP-2A), and subsequently, they enter the lysosome after unfolding (Fig. 5B)[193]. Macroautophagy (hereafter called 'autophagy) is a highly conserved multistep process in which a *de novo* double-membrane structure called the phagophore, engulfs a portion of cytosol and/or organelles. The phagophores expand their structure to surround their target completely generating an autophagosome. Finally, the autophagosome fuses with the lysosome creating autolysosome (Fig. 5A)[194]. Alternatively, autophagosomes can fuse with endosomes and generate amphisomes before fusing with lysosomes[194]. Autophagy is generally divided into three main steps: Initiation and nucleation, elongation and closure, and fusion and degradation.

Initiation and nucleation

Under normal physiological conditions, autophagy remains at a basal level to regulate the balance between biosynthesis and turnover of proteins[195–197]. Autophagy has also an important role in removing damaged cellular organelles and intracellular pathogenes. The rate of autophagy dramatically increases upon nutrient starvation to provide the cells with more internal nutrient supplies. A key step in the initiation of autophagy is the inactivation of mammalian target of rapamycin (mTOR). mTOR is a phosphoinositide 3 kinase-related serine/threonine kinase which has an instrumental role in regulating cellular growth and metabolism in response to growth factors, nutrients, energy, amino acids, and stress [195–197]. It is involved in two complexes of mTORC1 and mTORC2. The mTORC1 complex consisting of mTOR, Raptor and mLST8 actively suppresses the initiation of autophagy in the presence of

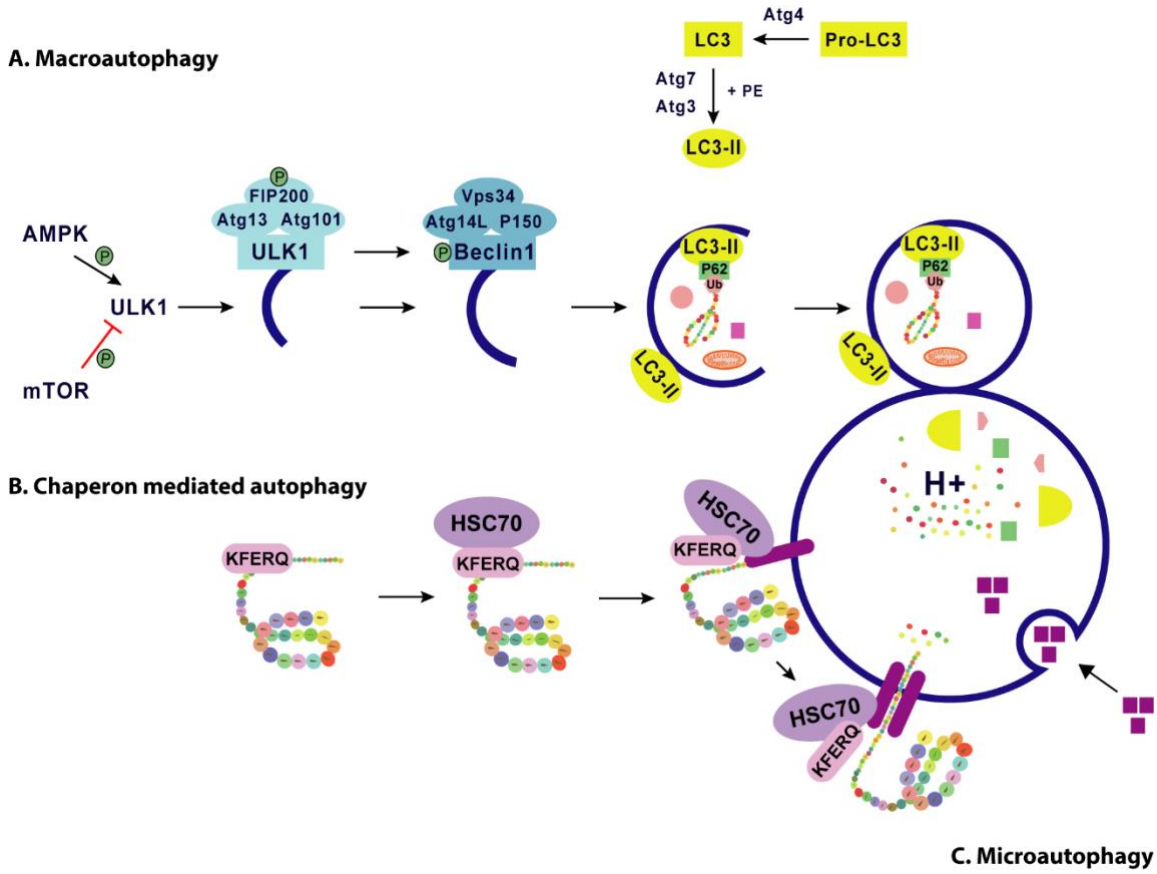

FIGURE 5. Cellular autophagy pathways. A. Macroautophagy. mTOR and AMPK are key regulators of autophagy. When autophagy is induced, cytosolic components are engulfed into double membrane structures called autophagosomes. Autophagy is a multistep process that includes initiation and nucleation, elongation and closure, and fusion and degradation. These processes are regulated by several protein complexes. Initiation of the process is started by activation of Ulk1 protein leading to recruitment and activation FIP200, Atg13, and Atg101 into a complex. Next, the membrane becomes elongated by activation of a second complex containing Beclin1, PI3K/Vps34, ATG14L, and p150. LC3B binds to targeted cargo via p62, and autophagosomes then fuse with lysosomes for degradation of the cargo. **B.** Chaperone-mediated autophagy (CMA). In CMA, Hsc70 recognizes cargo that contains a recognition motif, KFERQ, and subsequently introduces it to lysosomal-associated membrane protein 2A (LAMP-2A). The cargo becomes unfolded and enters lysosomes for degradation. **C.** Microautophagy. In microautophagy, lysosomes directly engulf part of cytoplasm with/without organelle.

nutrients by phosphorylating and inactivating the Unc-51 like kinase 1 (Ulk1) complex. The Ulk1 complex consists of Ulk1, FIP200, Atg13, and Atg101 and, when activated, it initiates autophagy. Upon nutrient deprivation, mTOR1 is inactivated which leads to dephosphorylation of Ulk1, Ulk2, and Atg13. After dephosphorylation, Atg13 mediates the interaction of Ulk1 and Ulk2 with focal adhesion kinase family interacting protein 200 kDa (FIP200)[198,199]. Forming of the Ulk1 protein complex stabilizes and promotes the kinase activity of Ulk1, resulting in the phosphorylation of FIP200 which is crucial for autophagy initiation[200]. Ulk1 is also under the control of AMP-activated protein kinase (AMPK). When the ratio of ATP decreases relative to AMP/ADP (a drop of energy level in the cell), AMPK directly phosphorylates Ulk1 to induce autophagy[201].

Initiation of autophagy also requires the activity of class III PIK3 (PIK3C3)/Vps34 complex (hereafter referred to as the Vps34 complex). In mammals, there are three types of PI3K which are classified based on lipid substrate specificity: Class I, - II, and- III. The Vps34 converts phosphatidylinositol (PI) to phosphatidylinositol-3-phosphate (PI3P), and this phosphorylation is critical to driving autophagy[202,203]. In mammals, there are two types of Vps34 complexes. Complex-I consists of Vps34-P150-Atg14L/Barkor-Beclin-1, and complex-II consists of Vps34-p150-Beclin-1-UVRAG (UV irradiation resistance-associated gene)[204]. The Vps34 complexes are mainly regulated by the Ulk1 complex through phosphorylation of Beclin-1[205,206]. In normal conditions, Beclin-1 interacts with the apoptotic protein Bcl-2 (B-Cell CLL/lymphoma 2), which prevents it from taking part in the Vps34 complex to initiate autophagy. Due to lack of nutrients, Ulk1-mediated phosphorylation of Beclin-1 leads to its dissociation from Bcl-2, It is now free to interact with Vps34 and another pro-autophagy protein, Atg14L[207,208]. Vps34 is activated upon interaction with Beclin-1 and generates PI3P, which is essential for phagophore formation[206,209]. Ulk1 binds to PIP3 and thus stabilizes and supports the Vps34 complex in the level of phagophore[210]. Finally, Ambra1 (activating molecule in Beclin-1-regulated autophagy) and VMP1 (Vacuole membrane protein-1) interact with Beclin-1 to govern the autophagosome formation[211,212].

Elongation and closure

Elongation of the phagophore to eventually form the mature autophagosome is mediated by two ubiquitin-like conjugation systems involving the ubiquitin-like proteins Atg12 and Atg8 [213]. Atg12 is conjugated to Atg5 via E1-like enzyme Atg7 and E2-like enzyme Atg10. Atg12–Atg5 then interacts with Atg16L1 and associates with the phagophore. The Atg12–Atg5-

Atg16L1 complex is then involved in targeting of Atg8 to the phagophore. In mammals, six homologs of yeast Atg8 have been reported and are divided into three groups: 1) microtubule-associated protein 1 light chain 3 (MAP1LC3)-A, B, C, 2) gamma-aminobutyric receptor-associated protein (GABARAP), and 3) Golgi-associated ATPase enhancer of 16 kDa (GATE16)[214–216]. The MAP1LC3s, often referred to as LC3, are the most studied Atg8 members in autophagy in mammalian cells[217]. The conjugation of LC3 to phosphatidylethanolamine (PE) is crucial for the expansion of the phagophore. This lipidation of LC3 requires the activity of Atg4, Atg7, and Atg3. First, Atg4 cleaves at the C-terminus of LC3, generating LC3-I that exposes a C-terminal glycine [218]. Second, Atg7 activates LC3-I. Activated LC3-I is then conjugated to PE by Atg3, generating the lipidated LC3-II form of LC3[219,220]. For binding of LC3-II to the phagophore, LC3-II needs the E3-like enzymatic activity of Atg12–Atg5-tg16L1 complex[219,221]. The WD repeat domain phosphoinositide-interacting proteins-2 (WIPI2) binds to PI3P in the surface of phagophore and recruits Atg12–Atg5-tg16L1 complex through Atg16L1 and facilitate lipidation of LC3/GABARAP[222]. The process of phagophore closure has not been fully understood. It seems that later stages of phagophore formation are regulated by Atg2A and Atg2B, since depletion of both Atg2A and Atg2B results in accumulation of unclosed phagophore[223].

Fusion and degradation

The fusion between autophagosome and lysosome has to take place after closure of the autophagosome. Autophagosomes are spread all over the cytoplasm. Their location seems to be random[224], whereas endosomes and lysosomes are mostly located in perinuclear region[225]. Therefore, autophagosome and lysosome have to move towards each other for the fusion step[226,227,228]. In the process of maturation, autophagosomes gradually lose Atgs from the outer membrane and recruit the machinery responsible for lysosomal delivery and also the machinery mediating lysosome and autophagosome fusion[229,230]. In this process, autophagosomes move along microtubules to reach in the proximity of nuclear before the fusion to lysosome[224]. Both dynein (a minus-end-directed microtubule motor) and kinesins (plus-end-directed microtubule) are involved in the movement of lysosome and autophagosome, as a number of autophagosome-lysosome fusions decreases in cells which have dysfunction in dynein and kinesins[231,232]. Also, LC3 are vital for efficient movement of autophagosome[224].

Fusion step is dependent on three sets of protein families: Rab GTPase, membrane-tethering complexes, and soluble SNAREs [226,227,228]. Ras-related protein Rab-7a (Rab7) has several roles

in the maturation of the autophagosome. Rab7 binds to late endosomes and lysosomes, and coordinates their motility and fusion to autophagosomes by interaction with dynein motor through its protein effector called RILP (RAB-interacting lysosomal protein)[233]. Furthermore, Rab7 on autophagosome also recruits kinesin motors via binding to FYCO1 (FYVE and coiled-coil domain containing 1)[234]; and FYCO1 can also bind to LC3 and PI3P. Taken together, Rab7, PI3P, and LC3-binding protein FYCO1 are necessary for the movement of autophagosome towards nuclear region[234,235].

The HOPS (homotypic fusion and protein sorting) complex has a key role in tethering vacuoles and lysosomes for fusion in mammals[236–238]. HOPS consists of six subunits including vacuolar protein sorting (Vps)11, Vps16, Vps18, Vps33A, Vps39, and Vps41[236–238]. The HOPS complex interacts with lysosomes via Rab7 and with autophagosomes via the SNARE protein STX17[230]. HOPS also facilitates autophagosome-lysosome fusion by binding to pleckstrin homology and RUN domain containing M1 (PLEKHM1) that also interacts with LC3 on the autophagosome membranes[239].

SNAREs are membrane-anchored proteins and are the core components of the fusion machinery in mammalian cells. SNAREs form four-helix bundles to fuse autophagosome and lysosome namely QSNAREs (Qa-SNARE, Qb-SNARE, Qc-SNARE), and R-SNARE. To fuse membrane vesicles in the cell, R-SNARE on donor membranes and Q-SNAREs on the acceptor membranes form a complex called trans-SNARE[240]. In autophagy, STX17 on autophagosomes acts as a Q-SNARE and binds to the R-SNARE VAMP8 on lysosomes[229,230]. After fusion, autophagosome and the inner membrane of the autolysosome degrade by lysosome resulting in additional resources for cells such as amino acids, nucleotides, sugars, and free fatty acids[241,242].

Autophagy in cancer

Dysregulation of the autophagy process has been reported in different diseases. Knockout studies of *ATG* genes have shown that autophagy has a pivotal role in adaptive responses to stress, homeostasis, as well as cellular differentiation and development[241–245]. Parallel with this, systemic and tissue-specific knockdown studies of *ATG* genes have demonstrated the connection between autophagy and different disease including neurodegenerative disease, cancer, metabolic diseases, and infectious disease[242–244,246–249]. In cancer, autophagy has been referred to as a "double-edged sword" meaning that autophagy can behave as an inhibitor or an inducer of tumorigenesis[250,251]. This paradoxical role of autophagy suggests that autophagy has

distinct roles depending on the context and stages of carcinogenesis. It is believed that autophagy can prevent tumor initiation, whereas in advanced cancer stages, it may have pro-metastatic roles. Autophagy assists metastatic cells in surviving and colonizing at a secondary site, and in case of failing to establish a new colony, it helps metastatic cells to stay in a dormant stage. Loss of autophagy can cause genotoxic stress due to the accumulation of reactive oxygen species. In this scenario, normal autophagy can be seen as a tumor suppressor mechanism that protects the genome[252–254,77]. Consistence with this, the deletion of *BECN1* (encoding a necessary component for formation of phagophore) is observed in many cancers including breast cancer, ovarian cancer, and prostate cancers[252,255,256]. This leads to autophagy inhibition and induction of cell proliferation[252,255,256]. The knockout of other *ATGs* genes have also showed that autophagy can have a tumor suppressor role in cancer. This is exemplified by knockout of *BIF-1* (Endophilin-B1), *Atg7*, and *Atg5* in mice that promote tumor progression[257,258]. Some of the active signaling pathways in cancer such as RAS are dependent on autophagy for cancer development[259,260]. Upregulation of baseline autophagy levels has been reported in RAS-activated tumors such as pancreatic cancer. The inhibition of autophagy in these tumors results in a reduction in cellular proliferation and tumor regression both in cell lines and in a mouse model. The same role for autophagy has been reported in RAS-activated non-small cell lung cancer[259–262]. Oxidative stress in cancer cells and surrounding tissues leads to upregulation of autophagy, which can fuel cancer development[263–267]. Increased mitophagy in tumor stromal fibroblasts makes them dependent on aerobic glycolysis, leading to the production of produce lactate and ketones are taken up and used in metabolism by neighboring cancer cells[263–267]. Although autophagy process is a double-edged sword in cancer, manipulation of autophagy may help us to control cancer. Since it is not clear when autophagy should be on or off, deep knowledge of the autophagy process is critical for autophagy-based treatment[250].

The mammary gland and breast cancer

Human female breast development starts from week 4-6 of gestation and continues to develop into adulthood. The branching of the breasts stays at a modest level until women are influenced by sex hormones during puberty, and this development continues during and after pregnancy[268]. The human female mammary gland consists of an extensive tree-like network of branched ducts that starts from the nipple and terminates in an alveolar structure called lobules. Both lobules and ducts are embedded in a collagen-rich stroma containing blood vessels, lymphatic vessels,

adipocytes, connective tissue, and macrophages[269]. The normal mammary epithelium is a bilayer structure consisting of an outer "basal" layer and inner "luminal" layer which have different features and functions. The outer basal/myoepithelial layer is in direct connection with the basement membrane, whereas the inner luminal layer contains polarized epithelial cells that can produce and secrete milk upon hormonal exposure[268,269]. The mammary glands are dynamic organs that experience extensive morphogenesis from a very early stage of development followed by puberty, pregnancy, lactation, and involution[270]. Thus, the mammary glands undergo proliferation, differentiation, cell death, and also tissue remodeling, all of which are dependent on a renewable stem cell population situated between the luminal and myoepithelial cells[270,271].

Breast cancer is the most common cancer among women worldwide; 3589 new cases were registered in Norway in 2017, and 629 persons died from breast cancer in 2017, which makes it the second highest cause of cancer-related deaths among women after lung cancer[272]. Statistics show that the number of registered breast cancer cases in Norway is increasing as 9.7% more cases were detected in 2013-2017 than in 2008-2012[272]. The mortality rate has been stable since the 1990s when it began declining[272]. The decline in mortality in mid-90s is attributed to early detection by mammography screening and adjuvant therapy[273,274]. Although metastasis is not common in breast cancer patients at the time of the diagnosis, metastasis to liver, bone, lungs, and central nervous system is common at later time points (30%)[275,276]. While 90% of breast cancer cases are due to the accumulation of somatic mutations, 10% are caused by hereditary mutations received from the previous generation[277]. The most common inherited genetic changes in breast cancer are mutations in tumor suppressors *BRCA1,* and *BRCA2*[278,279], followed by germ-line mutation in the gene encoding p53 (Li-Fraumeni syndrome), *PTEN* germ-line mutation (Cowden syndrome), and *STK11/LKB1* mutation (Peutz-Jegher syndrome)[280,281].

Prognosis, diagnosis, and treatment strategy of breast cancer are dependent on expression of biomarker including estrogen receptor (ER), progesterone receptor (PR), human epidermal growth factor receptor 2 (HER2), cytokeratins, and Ki-67[282,283]. The molecular subtypes of breast cancer can be determined by both immunohistochemistry (IHC) and gene expression patterns[283]. According to IHC staining of ER, PR, HER2+ receptors, and Ki-67 proliferative index, the subtypes of breast cancer in the clinic are classified as luminal A, luminal B, HER2-enriched and basal-like breast cancers[284]. According to high throughput gene expression analysis, breast cancer is classified into five intrinsic subtypes: luminal A, luminal B, HER2-

enriched, basal-like, and normal-like[285]. Both luminal A and luminal B subtypes are ER-positive, but the expression of HER2, Ki-67, and PR expression are different in these subtypes. Luminal A cancers are HER2-negative with low expression of Ki-67 and high level of PR. Moreover, luminal A is characterized by expressing ER-related genes[283,285]. Luminal B breast cancers also express ER, but show worse prognosis due to the expression of proliferation-associated genes such as Ki-67 and HER2 growth factor[285–287]. Luminal B is either ER+, PR+, HER-, Ki-67 (high expression) or ER+, PR+, HER2+, Ki-67 (high/low expression)[287]. The HER2-enriched subtypes of breast cancer are characterized by high expression of the *ERBB2* (HER2) and *GRB7* genes.[283,288,289]. Triple-negative breast cancers (TNBC) are defined as ER-, PR-, HER2- and have the worst prognosis among the breast cancer subtypes. TNBC classification is faced with some ambiguity as a variety of subgroups have been identified by different research groups. Three important subgroups of TNBC are basal-like, normal-like, and claudin-low[283].

Aims of this study

NEAT1 is the essential structural RNA component of nuclear paraspeckles. Several reports have shown that *NEAT1* expression and paraspeckle formation are upregulated by a variety of cellular stressors, and at specific stages in development. *NEAT1* and paraspeckles regulate the expression of specific genes at both transcriptional and post-transcriptional levels. It has for some time now been clear that *NEAT1* is abnormally expressed in serious human diseases including cancer and neurological disorders. The aim of this study was to further add knowledge about the function of *NEAT1* in cellular stress response pathways including autophagy and to further dissect the role of *NEAT1* in breast cancer by analysing the expression in different breast cancer subtypes.

The objectives of the study are:

i) To contribute to a better understanding of the role of *NEAT1* in cellular stress conditions that are prominent in cancer cells
ii) To determine the expression pattern of *NEAT1* in different subtypes of breast cancer.
iii) To elucidate the role of *NEAT1* in autophagy.

Summary of papers

Paper I: The long non-coding RNA *NEAT1* and nuclear paraspeckles are upregulated by the transcription factor HSF1 in the heat shock response.

NEAT1 is a highly abundant lncRNA that is critical for the formation of paraspeckles. *NEAT1* expression is induced upon intrinsic and extrinsic stress such as viral infections, proteasome inhibition, oncogene-induced replication stress, and hypoxia. In this paper, we show that the isothiocyanate sulforaphane (SFN) induces *NEAT1* expression at the transcriptional level and elevates paraspeckle formation. SFN-mediated *NEAT1* induction is not dependent on NRF2, whereas depletion of HSF1 severely compromises SFN-induced *NEAT1* expression and paraspeckle formation. HSF1 binds to a novel conserved heat shock element (HSE) in *NEAT1* promoter. *NEAT1* is also induced upon heat shock, suggesting that *NEAT1* upregulation is a universal mechanism in the heat shock response. Finally, we show that *NEAT1*-depletion results in amplified and prolonged expression of HSP27, HSP70, and HSP90 mRNAs during heat shock.

Paper II: The expression of the long *NEAT1_2* isoform is associated with human epidermal growth factor receptor 2-positive breast cancers

The *NEAT1* locus in transcribed into two overlapping isoforms, *NEAT1_1* and *NEAT1_2*. *NEAT1_2*, but not total *NEAT1*, has recently been shown to predict progression-free survival of ovarian cancer treated with platinum-based chemotherapy. Therefore, the expression of *NEAT1_2* was investigated in breast cancer. We have performed *NEAT1_2*-specific RNA-FISH analyzes on 74 needle biopsies taken from females at the time of diagnosis of breast cancer. *NEAT1_2* expression correlates with HER2-positive cancers, and independently, with high-grade disease. This was verified in a microarray-based expression cohort and in breast cancer cell lines. Moreover, *NEAT1_2* expression associates with HER2-enriched and luminal B PAM50 subtypes of breast cancer in 3 cohorts. Total *NEAT1* shows a distinct expression distribution between PAM50 subtypes compared to *NEAT1_2*, being highest in ER-positive luminal A cancers. This indicates that the relative expression between *NEAT1_1* and *NEAT1_2* varies in different breast cancer subtypes. Finally, for the first time, we show that *NEAT1_2*

expression and paraspeckle formation increase in human breast tissue upon lactation, confirming what has previously been observed in mice.

Paper III: Knockdown of the long non-coding RNA *NEAT1* induces basal autophagy in breast cancer cell lines

NEAT1 expression is induced by a variety of cellular stressors that are known to enhance autophagy, including hypoxia, heat shock, genotoxic and mitochondrial stress. We recently showed that *NEAT1* is induced at the transcriptional level by SFN, a compound that is known to induce autophagy in cells. Here, we show that *NEAT1* knockdown in breast cancer cell lines leads to the accumulation of lipidated LC3B, which is a marker of autophagy. The lipidated LC3B-II form continues to accumulate after inhibiting lysosomal activity with bafilomycin A1, indicating that the on-rate of autophagy is increased in *NEAT1*-depleted cells. In line with this, AMPK is activated in *NEAT1*-deficient cells. This is accompanied by increased phosphorylation of Ser317 and Ser555 of Ulk1, which is required for initiation of autophagy. We also report that *NEAT1*-depletion leads to a slight accumulation of the p62 protein. This might indicate that lysosomal functions are affected in *NEAT1* knockdown cells. We speculate that *NEAT1* deficiency leads to accumulation of damaged macromolcules and mitochondria, which eventually will trigger autophagy.

Methodological consideration

Generation of *NEAT1*-depleted cells

To study the cellular function of *NEAT1*, generation of an efficient knockout or knockdown strategy is instrumental. During the course of this study, several attempts were made to make stable *NEAT1* knockdown cell lines. These experiments never succeeded (see below for further description and comments). Therefore, transient knockdown of *NEAT1* with small oligonucleotides was done in papers I - III. Generally, there are two main technologies that are used for knocking down the expression of a gene: Small interfering RNAs (siRNAs) and antisense oligos (ASOs)[290,291]. siRNAs are double-stranded RNA molecules that are incorporated into the RNA-induced silencing complex (RISC) where the guide strand binds to and degrades the targeted mRNA. ASOs are single-stranded RNA, DNA or RNA/DNA hybrid oligonucleotides that bind to their RNA targets by complementary base pairing. The RNA duplex is then recognized and degraded by RNase H1[290,291]. *NEAT1* is a highly abundant nuclear transcript. This has to be taken into consideration when trying to deplete *NEAT1* expression in cell lines. As the RISC machinery operates in the cytoplasm where it targets mature mRNAs, we envisioned that the siRNA technology was not optimal for silencing *NEAT1* expression. ASOs, on the other hand, can enter the nucleus and there are nuclear forms of RNase H1[290,291]. Therefore, we decided to use GapmeRs which are chimeric ASOs of 16 nucleotides, to transiently knockdown *NEAT1* expression (Exiqon, QIAGEN). In this technology, a specific central sequence consisting of DNA nucleotides is flanked by blocks of modified Locked Nucleic Acid (LNA) ribonucleotides that protect it from degradation. In LNAs, the ribose ring is locked by a methylene bridge connecting the 2´-O atom and the 4´-C atom (Fig. 6). This modification makes the nucleotides ideal for Watson-Crick binding[292,293]. This increases the affinity and thus the specificity for the targeted RNA molecule. Off-target activities and toxicity are always an issue when using ASOs (or siRNAs). Therefore, ideally, different ASOs targeting the same RNA molecules should be used in functional assays. In our studies, *NEAT1* expression was inhibited by two GapmeRs: One recognizing the overlapping region between *NEAT1_1* and *NEAT1_2* (referred to as *NEAT1*-specific) and one that solely silences the expression of the long *NEAT1_2* isoform (Fig. 7)[294–297].

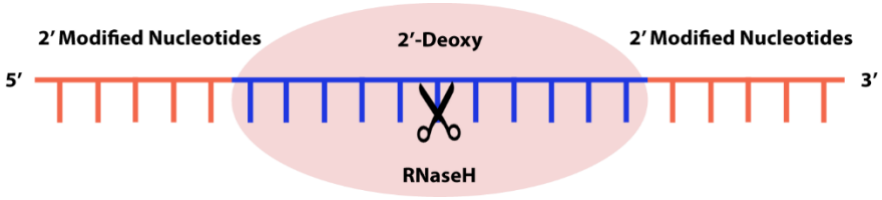

FIGURE 6. GapmeR structure. Typically, GapmeR is 8-12 base single strand antisense DNA that flanked by 2-5 chemically modified nucleotides. RNase H1 recognizes and cleaves the hybrid targeted RNA.

In the paper I - III, Lipofectamine 2000 (Thermo Fisher Scientific) reagent was used for delivery of the GapmeRs and siRNAs to the cells. Lipofectamine 2000 is a cationic liposome which surrounds nucleic acid molecules and facilitates their entrance to cells. They have positive charge head group by which they interact with negatively charged sugar-phosphate backbone of nucleic acid strand so lipid bilayers encapsulate nucleic acid molecules and help them overcome electrostatic repulsion of cellular membrane[298,299]. Lipofectamine containing siRNA or GapmeR are taken up with endocytosis. However, the efficiency of lipid-based transfection can be affected by different biological barriers such as cellular uptake, intracellular trafficking, endosomal escape, and lysosomal degradation. Therefore, achieving consistent transfection efficiency can be challenging in lipid-based transfection[300,301]. According to the optimization result, a so-called reverse transfection protocol where the oligonucleotides and transfection reagent were mixed with trypsinized cells upon seeding, were used which gave consistent transfection efficiencies in almost all of the experiments. As suggested by the manufacturers, GapmeR stocks were aliquoted, and repeated thaw-freeze cycles were avoided (5 times at the max). Knockdown efficiencies were always analysed by RT-qPCR before further functional analyses were conducted.

As mentioned above, our group has made several attempts to try to establish stable *NEAT1* knockout or knockdown cell lines using the CRISPR-Cas9 technology or short hairpin RNAs (shRNA). In the case of the shRNA, colonies expressing the shRNA were obtained, but *NEAT1* expression was not inhibited by this mechanism (Dr. Erik Knutsen, personal communication). *NEAT1* is an abundant long non-coding RNA in the nucleus, whereas the shRNAs are processed by Dicer and loaded into RISC in the cytoplasm. We, therefore, postulate that the *NEAT1*-

shRNA never got access to nuclear *NEAT1*. The CRISPR-Cas9 technology was also used to specifically deplete *NEAT1_2* in MCF7, but single colonies did not survive (Dr. Erik Knutsen, personal communication). Since cell confluence is significantly compromised in *NEAT1*-depleted cells (see paper I), it is likely that the survival of MCF7 cells is dependent on *NEAT1*. In the future, an inducible CRISPR-Cas9-mediated knockdown strategy can be an alternative.

Methods for studying the role of *NEAT1* in autophagy

Autophagy is a dynamic multistep catabolic mechanism regulated by a variety of signaling pathways. A key step in autophagy is the formation of the phagosomes where the Atg8/LC3 protein (hereafter just referred to as LC3) has a critical role. During maturation of the phagosomes, LC3 is conjugated onto phosphatidylethanolamine (PE) and thereby becomes lipidated forming the so-called LC3-II form. Measuring the lipidation of LC3 by western blott analyses looking for the faster migrating LC3-II form, or analysing the incorporation of LC3 into punctuated phagosomes by fluorescence microscopy, are common methods for studying autophagy. However, as these are intermediate steps in a highly dynamic process, accumulation of either LC3-punctas or LC3-II might be the result of either increased induction of autophagy, or decreased autophagic flux. Inhibition of lysosomal functions, low acidity of the lysosome, deficiency in fusion of phagosome to the lysosome, or dysregulation of the transport machinery results in accumulation of both LC3-II and LC3-puncta. Consequently, analyses of LC3-puncta/LC3-II must be accompanied by other assays to avoid misinterpretation. In regard to the dynamic nature of autophagy, the analysis of a phenomenon at a specific time point cannot be conclusive. Thus analysis of autophagic flux from the beginning of the process to degradation in lysosome provides us with better understanding[217]. P62/SQSTM1 is one of the frequent autophagy markers which is usually used in parallel with LC3 in autophagy analyses. The p62 proteins binds to ubiquitinated substrates and acts as a link between LC3-II and the autophagic cargo. As parts of LC3-II are reused in new autophagosomes, p62 is completely degraded in the autolysosome together with the cargo. Thus, the cargo degradation rate in autophagy can be estimated by p62 analyses. To sum up, the accumulation of both LC3-II and p62 usually indicate inhibition of autophagy in later steps, whereas the accumulation of LC3-II and degradation of p62 are an index for autophagy induction[217]. In this study, the amount of LC3-II and LC3-puncta were detected by immunoblotting and immunocytochemistry, respectively in the presence and absence of lysosomal inhibitor (Bafilomycin A1)[217]. The activation of AMPK, mTOR and Ulk1 were monitored by immunoblotting with phosphospecific antibodies.

The ribosomal protein S6K is one of the first mTOR substrates, meaning the activation of S6k requires mTOR-mediated phosphorylation[302]. Therefore, phosphorylation of S6K on The389 was monitored to check the activation of mTOR. As the activation of AMPK is dependent on phosphorylation of Thr172, phospho-Thr172 antibody was used to detect activated AMPK. Finally, the activation of Ulk1 was checked by phosphorylation of Ser317 and-Ser555 which are direct targets of activated AMPK.

Reverse transcription quantitative polymerase chain reaction (RT-qPCR)

Fluorescence-based reverse transcription quantitative PCR (RT-qPCR) was used for gene expression analyses in papers I - III using the SYBR Green method. Here, cDNA is made from total RNA, and specific primers were used to amplify the expressed gene of interest. SYBR green binds to the minor groove of double-stranded DNA generated in the PCR reaction, and releases energy as fluorescence when bound to DNA. It can thus be used in real-time measurements of the amount of produced DNA. There are many factors that influence the expression of a gene in a sample, and RNA molecules are generally unstable. RT-qPCR is a very sensitive method and prone to technical variations. To compensate for different inputs of samples, the expression of the gene of interest is often normalized to a so-called reference housekeeping gene. Ideally, as good reference gene should be stably expressed independently of experimental conditions, and also between different populations of cells and individuals[303]. Although the mRNA levels of such housekeeping genes are supposed to stay constant in an experimental treatment, the expression of these genes have been reported to be changed under some experimental conditions[304–307]. Even very small changes in the housekeeping gene result in more significant noise or erroneous result, therefore, verification of internal control is vital

FIGURE 7. The location of qPCR primers and GapmeR are shown in schematic picture of short and long isoform of *NEAT1*.

for the validity of the experiment[308]. We generally use glyceraldehyde-3-phosphate-dehydrogenase (*GAPDH*) as a reference gene when analysing samples from experiments using only one cell line. In the paper II, *NEAT1_2* expression in 9 different cell lines is compared. Here, we decided to use the average expression of 3 housekeeping genes, *GAPDH*, *B2M*, and *RPLP0* for normalization. We analysed gene expression using the delta-delta Ct method. In the first step, delta Cq was calculated by subtracting the Cq value of the reference gene from the Cq value of the gene of interest. To calculate fold change, the treated groups were compared to a control sample using the $2^{-\text{delta deltaCq}}$ formula, $2^{-(\Delta Cq \text{ treated}) - (\Delta Cq \text{ control})}$[309].

RNA-FISH (Fluorescent *In-Situ* hybridization)

The Stellaris™ RNA-fluorescent in-situ hybridization (RNA-FISH) technology was used (in papers I and II) for detection of *NEAT1* in cells. The Stellaris™ RNA FISH are multiple singly labeled oligonucleotides, which are able to detect individual molecules of mRNA. As the binding of at least 10 probes are necessary for detection, the possibility of false positive is very low. Therefore, even if one off-target probe produces a weak signal, they have a significantly lower intensity compared to the main signal[310]. Two probe sets were used to detect *NEAT1*-one detected a region that is common in *NEAT1_1* and *NEAT1_2*, while the other recognized only *NEAT1_2* (paper I and II). RNA-FISH can be combined with immunocytohistohemistry/immunocytochemistry to simultaneously investigate the expression and localization of an RNA molecule and a protein[311]. Tissue handling and technical procedures are two important steps as RNA has to be preserved during the whole process. The tissue handling, including fixation and storage, is vital for preserving RNA in the cell.

For FISH, the fixation method should be efficient enough to preserve the RNA, and also tissue morphology. In two separate experiments, formalin-fixed paraffin-embedded (FFPE) samples were produced from the patient. The first patient samples came from needle biopsy (paper II), while the other one was tissue microarrays (TMA) prepared from lumpectomy (data not shown). In needle biopsy samples, more than 40% of samples were positive for *NEAT1*, whereas, in the TMA samples, less than 3% of samples were positive. It means, the fixation step may take more time in bigger tissues which gives time to endogenous ribonuclease to degrade the RNAs, whereas needle biopsies became fixed significantly faster due to their thickness. To avoid degradation of RNA during the staining process, only nuclease free materials were used, and all the surfaces including slides, incubator, tweezers, and laboratory hood were wiped with RNAase removal solution. To check the specificity of the probes, *NEAT1*

was knocked down with specific GapmeR transfections. This considerably decreased *NEAT1* signals, therefore verify that the probes are specific for *NEAT1*.

Patent cohort and ethics

Breast cancer samples and complete follow-up data from a total of 74 patients were collected from the time period 2012-2018 (REK: 2014/371). As a control, 27 non-cancerous samples were also collected including 23 fibroadenomas, 3 mammary reduction, and 1 BRCA1 prophylactic mastectomy. Needle biopsies were performed at UNN hospital in Tromsø, and samples were prepared by pathologists. The study was approved by regional committees for medical and health research ethics (REK) and all the procedure were performed according to approved principles. To further investigate the association between *NEAT1_2* expression and breast cancer subtypes, microarray gene expression data from three public breast cancer patient cohorts, METABRIC (PMID: 22522925), The Cancer Genome Atlas (TCGA - PMID: 23000897), and Oslo2, were analysed. As the *NEAT1_2* isoform is not poly-adenylated, standard sequencing methods which include a poly(A) purification step could not be used in our analyses. As total RNA is used as input for microarray gene expression analyses, cohorts which used this technology was included in the analysis (Fig. 8).

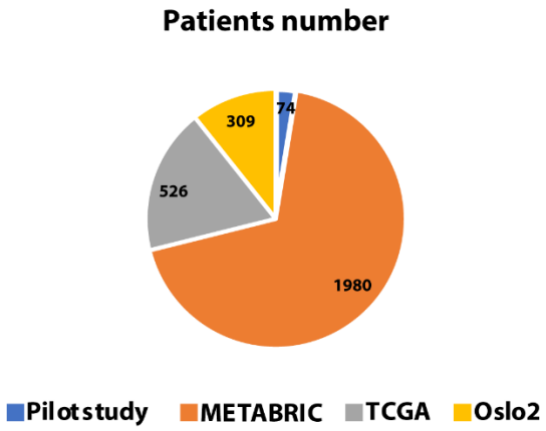

FIGURE 8. A pie chart showing number of patients in each cohort

Discussion

Mammalian cells are constantly exposed to intrinsic and extrinsic stressors. Cells have acquired a variety of mechanisms to preserve cellular homeostasis during stress. Such mechanisms involve the activation of one or several stress response pathways. DNA-damaging reagents activate DNA repair pathways, proteotoxic stress activates the heat shock response or the unfolded protein response pathways, mitochondrial dynamics and functions change upon hypoxia, and nutrient deprivation results in activation of autophagy[312]. Initially, cells will try to preserve homeostasis by inducing cell repair mechanism. If the cells do not manage to re-establish the balance, they will go through apoptosis, necrosis, and/or cell death caused by extensive autophagy[312–314]. The aim of this study was to add knowledge to the role of the long non-coding RNA *NEAT1* in stress response pathways and breast cancer. We have found that *NEAT1* expression and paraspeckle formation are induced during the heat shock response through HSF1-mediated transcriptional activation of the *NEAT1* promoter. We further show that *NEAT1_2* expression associates with HER2-positive cancers and hypothesize that *NEAT1_1* and *NEAT1_2* have distinct distribution and functions in different breast cancer subtypes. Finally, we present evidence that autophagy is induced upon depletion of *NEAT1* in breast cancer cell lines.

SFN activates NEAT1 transcription through the heat shock response

From the very beginning of this project, we hypothesized that *NEAT1* could have a role in cellular autophagy. That made us analyse *NEAT1* expression after exposing cells to a variety of agents known to induce autophagy (data not shown). One such agent is sulforaphane (SFN). As demonstrated in the paper I, SFN potently induces *NEAT1* expression and paraspeckle formation. SFN is a well-known activator of the transcription factor NRF2[315]. The basal activity of NRF2 under non-stressed conditions is low due to its ubiquitination and rapid degradation by the 26 S proteasome. The turnover is tightly regulated by the redox sensitive protein Kelch-like ECH-associated protein 1 (KEAP1) that binds to NRF2 in the cytoplasm and functions as an adaptor for the Cul3 ubiquitin ligase complex. SFN binds directly to and modifies cysteine 151 of KEAP1 that leads to a conformational change that abolishes the interaction with NRF2. As this function of SFN is so established, we initially hypothesized that SFN-mediated activation of *NEAT1* was dependent on NRF2 and a part of a cellular oxidative stress pathway. However, knockdown of NRF2 in MCF7 cells did not have any effect on SFN-induced *NEAT1* expression, indicating that the compound upregulated *NEAT1* through another mechanism. We

then switched our attention to the heat shock response as heat shock factor 1 (HSF1) is also known to be activated by SFN[316] transcription factor HSF1, within expression is not dependent on NRF2. In the paper I, we indeed demonstrate that HSF1 is responsible for transcriptionally upregulation of the *NEAT1* gene via binding to a heat shock element (HSE) in the promoter. We show that this site is highly conserved in *NEAT1* promoters among mammalian species, clearly supporting that activation of *NEAT1* transcription is a universal and important mechanism in the heat shock response. Studies in mice indicate that *Neat1* knockout mice and HSF1 knockout mice share some common features that supports that HSF1 is an important regulator of *NEAT1*. Both *Neat1* and HSF1 knockout mice are viable suggesting that they are not required for normal development of the mouse embryo[317,318]. Both *Neat1* and HSF1 are important for female fertility[317]. Interestingly, HSF1 is critical for mammary gland morphogenesis, as HSF1-knockout mice showed a severe defect in ductal branching and alveolar branching similar to what is observed in *Neat1* knockout mice[78,319,320]. Finally, both *Neat1* knockout mice and HSF1 knockout mice are less susceptible to develop a tumor in a two-step DMBA-TPA carcinogenesis model; and their depletion is associated with lesser proliferation, growth, invasion, and metastasis in a wide range of cancer cells[56,77,156,175].

The role of *NEAT1* in the heat shock response is still unclear. In paper I, we show that *NEAT1* knockdown enhances and prolongs the upregulation of HSP70, HSP27, and HSP90 mRNAs during heat shock. This might indicate that *NEAT1* has a regularly role in the turnover of the HSF1 protein. Alternatively, *NEAT1* depletion might lead to accumulation of misfolded proteins that will activate HSF1, and thus give an additive effect during heat shock. In line with this, we do see a slight increase in the background expression of HSP70, HSP27, and HSP90 upon *NEAT1* deficiency. We hypothesize that *NEAT1* has a protective role counteracting the accumulation of misfolded proteins, but further experiments should be undertaken to add proof to this hypothesis. The mechanism for this is obscure, but one might assume that increased *NEAT1* expression and formation of paraspeckles during the heat shock response can lead to the sequestration of specific gene regulatory proteins or mRNAs, and thereby change the expression of specific genes.

Findings of paper I endorse the importance of *NEAT1* in stress response pathways. A general concept is emerging where *NEAT1* expression is upregulated by key stress-activated transcription factors including HIF-2α, NF-κB, p53, ATF2, and now HSF1, to protect cells cellular functions and preserve homeostasis. Most established cell lines grown in culture are

highly dependent on *NEAT1* expression. It is important to acknowledge that the majority of the cell lines are transformed and constantly exposed to oncogenic stress.

NEAT1_2 expression is associated with HER2-postive breast

The two isoforms of *NEAT1*, *NEAT1_1* and *NEAT1_2*, are overlapping and transcribed from the same promoter. Recent reports suggest that they may have distinct function in gene regulation[36,321,322]. *NEAT1_2* is essential for the assembly of paraspeckles and exerts it gene regulatory function by sequestering specific mRNAs and proteins into these structures[28,37,55,323]. *NEAT1_1*, on the other hand, has also been suggested to interact directly with chromatin[72,322]. Given this, it is logical to hypothesize that they can have distinct functions in cancer. Importantly, *NEAT1_2*, but not *NEAT1_1* expression, has recently been shown to predict progression-free survival of ovarian cancer that had been treated with platinum-based chemotherapy[56]. This prompted us to specifically investigate the expression of *NEAT1_2* and paraspeckle formation in breast cancer subtypes. We chose a strategy where we first analysed a cohort of 74 breast cancer samples by *NEAT1_2*–specific RNA-FISH analyses. The samples were selected to represent ER-positive, HER2-positive and triple negative breast cancers. We then inspected microarray data from 2 publically available cohorts, as well as from a cohort generated by collaborators. Microarray data was preferred over RNA-Seq data, as the microarray technology use total RNA as input while RNA-Seq often includes an enrichment step for polyadenylated transcripts. As *NEAT1_2* is not polyadenylated, RNA-Seq experiments including a poly(A) enrichment step will not be able to sequence the long isoform. We found that *NEAT1_2* expression associates with high tumor grade and HER2-positive breast cancer. Moreover, we found a negative correlation between *NEAT1_2* expression and ER-positive tumors. A similar expression pattern was also observed in breast cancer cell lines, where the highest expression of *NEAT1_2* was detected in HER2-positive cell lines. Furthermore, in the 3 different breast cancer cohorts *NEAT1_2* expression was highest in cancers subclassified as HER2 enriched or luminal B, using to the PAM50 expression signature. Luminal A breast cancers showed the lowest expression of *NEAT1_2* in all three cohorts. The association between HER2 and *NEAT1_2* expression, suggests that *NEAT1_2* is upregulated by a HER2-driven signalling pathway. As we in paper I showed that HSF1 activates *NEAT1* transcription, it is reasonable to assume that HSF1 also had an important role in *NEAT1* activation in HER2-positive cancers. Indeed, it has been shown that HSF1 is required for HER2-mediated transformation in breast cancer cell lines[324]. Nuclear HSF1 staining and expression of HSF1-target genes correlate with high-grade breast cancers, and with worse prognosis[170,324,325]. This

is however, independent of HER2 expression[170]. In contrast, it was recently shown that MCF7 cells engineered to overexpress HER2, displayed increased levels of HIF-2α, but not HIF1α, both in normoxia and hypoxia[326]. In line with this, the *HIF2A* gene was highly expressed in HER2-enriched cancers. The expression of both *HIF2A* and HIF-2α target genes correlated with poor clinical outcome in HER2-positive cancers. It has been shown that HIF-2α, but not HIF-1α, can upregulate *NEAT1* expression in breast cancer cells upon hypoxia[59]. As we can't rule out that HSF1 is involved in upregulation of *NEAT1_2* expression in HER2-positive cancers, it is logical to assume that this at least partially, can be a result of increased HIF-2α expression. We are currently generating tissue micro arrays of our *NEAT1* pilot cohort described in paper II, and will analyse the expression of the HSF1 protein by immunohistochemistry. Of note, we have found that HCC1569 that expresses high levels of *NEAT1_2*, display constitutive nuclear localization of activated HSF1 (Data not shown).

An important observation described in paper II is that the distribution of total *NEAT1* and *NEAT1_2* expression is different among different breast cancer subtypes. *NEAT1* expression in the TCGA microarray is measured by 5 different probes in total, of which one probe specifically binds to *NEAT1_2* and the remaining 4 to the region that is common in both *NEAT1_1* and *NEAT1_2*. By analysing data generated from the 4 overlapping probes, we found that total *NEAT1* expression was highest in luminal A cancers that are ER-positive. This made us hypothesize that *NEAT1_1* is highly expressed in ER-positive cancers. As discussed in paper II, this is in line with a recent publication by Li et al showing that *NEAT1* is engaged in a repressor complex with FOXN3 and SIN3A that inhibits the expression of GATA3 specifically in ER-positive cancers[322]. The authors suggest that it is indeed the *NEAT1_1* isoform that participates in this complex. Generally, in future studies, it is important to acknowledge that the two different isoforms of *NEAT1* might have distinct expression patterns and functions, and care should be taken when choosing an experimental strategy. The overlapping nature of the two transcripts, will obviously hamper *NEAT1_1* specific analysis by hybridization-based assays like RT-qPCR.

As *NEAT1_1* and *NEAT1_2* are transcribed from the same promoter, it is not likely that transcriptional upregulation accounts for the isotype-specific expression in different breast cancer subtypes. Proteins that are specifically expressed in HER2-postive cancers might stabilize the *NEAT1_2* transcript in paraspeckles. The production of *NEAT1_1* might also be specifically inhibited in HER2-positive cancers. In the future, experiments should be

undertaken to further elucidate the mechanism behind isoform-specific expression of the *NEAT1* in breast cancer.

We report that *NEAT1_2* is upregulated in human breast tissue during lactation and pregnancy confirming what has previously been reported in *Neat1* knockout mice. This strongly suggests that *NEAT1* expression is regulated by hormones or growth factors that orchestrate proliferation and/or differentiation of the mammary gland. A better understanding of this mechanism will be important to further understand the role of abnormal *NEAT1* expression in breast cancer. Relevant to this, initial experiments in our lab failed to show any connections between prolactin treatment and *NEAT1* levels in breast cancer cell lines.

NEAT1 has role in basal autophagy

NEAT1 expression is induced by a variety of stressors, and several lines of evidence suggest that it plays a role in cytoprotection and cell survival[55,59]. Cells depleted of *NEAT1* have been shown to accumulate DNA damages and have dysfunctional mitochondria[56,63]. As we have shown that *NEAT1* is activated upon the heat shock response, it is tempting to speculate that *NEAT1* can counteract accumulation of misfolded proteins. Taken together, all these observations might indicate that *NEAT1* plays a role in the regulation of cellular autophagy. In paper I, we indeed show that SFN that is known to induce autophagy, upregulates *NEAT1* expression. This led us to further investigate the impact of *NEAT1* in autophagy. We started up by measuring the formation of lipidated LC3B, referred to as LC3B-II, in *NEAT1* knockdown cells by western blot analyses. As lipidated LC3B is localized in the membranes of autophagosomes and autolysosomes, it is a marker of autophagic activity in cells. *NEAT1*-depletion not only enhanced SFN-induced LC3B-II accumulation, but was sufficient to alter basic autophagy in 2 different breast cancer cell lines. Immunofluorescence analyses showed increased punctuated staining of endogenous LC3B in the cells. These punctas continued to accumulate after inhibition of lysosomal acidification by bafilomycin A. This led us to hypothesize that autophagy is induced upon *NEAT1* deficiency. mTOR is a master regulator of autophagy that actively suppresses the process under normal physiological conditions[198,199]. Our results show that the mTOR activity is not affected upon *NEAT1* depletion. In contrast, we found AMPK activity to be enhanced in *NEAT1* knockdown cells. This was accompanied by increased phosphorylation of Ulk1 at Ser317 and Ser555, which is essential for autophagy induction[201,327].

Recently, it was reported that *NEAT1*-depletion impaired mitochondrial dynamics and function, as paraspeckle disassembly affected the sequestration of mitochondrial mRNAs in the nucleus[63]. The same study showed that mitochondrial dysfunction was associated with lower mitochondrial respiration, lower ATP production, and reduction in mitochondrial DNA[63]. Therefore, it is very likely that a change in the ATP/AMP ratio activates AMPK that subsequently will initiate autophagy. A relevant question is whether *NEAT1* is actively participating in one of the steps in autophagy, or if induction of autophagy is merely a consequence of accumulation of damaged macromolecules and organelles upon *NEAT1* deficiency. Based on recent reports, the latter is highly likely. Mitochondrial dysfunction upon *NEAT1*-depletion might induce mitophagy. Moreover, it is easy to envision that the severe effect on mitochondria will lead to the accumulation of reactive oxygen species (ROS)[328–330]. ROS can induce double stranded DNA breaks that can trigger autophagy via p53-dependent and independent mechanisms[331]. *NEAT1*-depletion will also lead to the disassembly of paraspeckles and potentially mislocalization of paraspeckle-associated proteins that again can elicit autophagy. Here, the potential mislocalization of the disease-associated proteins TAR DNA-binding protein 43 (TDP-43) and fused in sarcoma (FUS) is particularly interesting as they can influence autophagy[332,333]. Interstingly, TDP-43 can regulate autophagy by stabilization of the *ATG7* mRNA[332]. One might envision that this ability can be repressed by sequestering TDP-43 into paraspeckles, and that *NEAT1*-depletion would relieve this repression. Finally, we have demonstrated that *NEAT1* is activated by the heat shock response. Even though further mechanistic studies are required, it is tempting to speculate that *NEAT1* might function to counteract the accumulation of misfolded proteins that normally occurs when cells are exposed to agents that activate the heat shock response pathway. Thus *NEAT1*-depletion might lead to the accumulation of misfolded proteins that will activate autophagy along with the ubiquitin-proteasome pathway (UPS)[334]. We can't rule out that *NEAT1* more specifically negatively regulates autophagy by repressing the expression of key autophagy genes at either transcriptional or post-transcriptional levels. This should be a subject for future research.

In paper III, we suggest that *NEAT1*-depletion leads to the induction of autophagy. This would normally lead to reduced levels of the selective autophagy receptor p62 as it is degraded with its cargo in autolysosome[217]. However, we repeatedly observed an accumulation of the p62 protein in *NEAT1* knockdown cells. This might indicate that *NEAT1* expression is required for normal lysosomal activity. It has been shown that loss of mitochondrial functions severely

affects the structure and function of the lysosomes[335–337]. Therefore, experiments aimed at analysing lysosomal activity should be undertaken in *NEAT1*-depleterd cells in the future. As discussed in paper III, ROS can also activate the expression of the *SQSTM1* gene that encodes p62 via the transcription factor NRF2. Initial experiments in our lab suggest that this indeed can be the case, but further studies are required to confirm this.

NEAT1 in human diseases

In this doctoral thesis, we have shown that *NEAT1* expression and paraspeckle formation are activated during the heat shock response and provided evidence suggesting that *NEAT1*-depletion leas to induction of autophagy. Interestingly, defects in both these processes are associated with neurodegenerative diseases. The heat shock response has a critical role in repairing or degrading misfolded proteins[338]. Misfolded proteins generally tend to form aggregates that disturb ordinary functions within a cell. Formation of protein aggregates or inclusions are known to destroy neurons and is the direct cause of neurodegenerative diseases including amyotrophic lateral sclerosis (ALS), Huntington's disease, Parkinson's disease, and Alzheimer[339]. Loss of HSF1 expression or activity is frequently observed in these diseases[174,340–342]. Autophagy has also a critical role in clearance of protein aggregates, and autophagy is severely abrogated in most neurological diseases[249].On the other hand, excessive autophagy can have an adverse effect on neuronal cells[343]. As our results suggest that *NEAT1* has a role in both in the heat shock pathway and autophagy, it is no surprise that also *NEAT1* has been found to be abnormally expressed in neurodegenerative disorders. Several reports have shown that *NEAT1* is abnormally expressed in ALS and Huntington's disease[118,120,126]. Emerging evidence suggests that *NEAT1* expression and paraspeckle formation might have a protective role in neuronal cells in early stages of ALS and Huntington's disease. As mentioned above, two paraspeckle proteins, FUS and TDP-43, are associated with ALS[344]. Paraspeckles are highly dynamic structures[119,120,126]. It is natural to assume that loss of paraspeckles might lead to mislocalization and aggregation of TDP-43 and FUS. Importantly, both proteins have also been shown to regulate the morphology and function of paraspeckles[120]. One might envision that HSF1 induces *NEAT1* expression at an early stage in the disease in order to protect neuronal cells from misfolded proteins. HSF1 can also induce autophagy through transcriptional activation of the *ATG7* gene[345]. However, the very intricate interconnection between *NEAT1*, paraspeckle formation, the heat shock response and autophagy in neurological disorders needs to be further explored.

NEAT1 is abnormally expressed in many cancers. Cancer cells are constantly exposed to intrinsic and extrinsic stressors[346–348]. Consequently, many stress response pathways, including the heat shock pathway, are constitutively activated in malignant cells[156]. Emerging evidence suggests that *NEAT1* has a role in protecting organelles and macromolecules form stress-induced damages[55,59]. Therefore, it is likely that *NEAT1* has an important cell survival function in cancer cells. This is potentially a serious obstacle in cancer therapy. Chemotherapeutic agents and radiation therapy act by increasing the stress burden in cancer cells. Importantly, elevated *NEAT1* expression is associated with drug resistance. In paper II we show that *NEAT1_2* is specifically expressed in breast cancer tissue, but not in normal surrounding tissue. This is indicating that *NEAT1* can be a promising target for therapeutic intervention. Cancer drugs based on antisense oligos have indeed attracted attention as they are highly specific[349]. We present evidence that *NEAT1* can repress autophagy. Loss of autophagy is associated with initiation of cancer[252,350,351]. However, at later stages of cancer development, enhanced autophagy is associated with drug resistance. Thus, *NEAT1* targeting in cancer cells should be accompanied by agents that inhibit autophagy.

Future perspective

Mammalian cells express a plethora of non-coding RNA molecules[352,353]. The function of the vast majority of them is still enigmatic, and many of them might by seen as transcriptional by-products. In this regard, *NEAT1* is clearly an exception. Although viable, mice lacking Neat1 expression display developmental defects with compromised mammary gland formation being the most pronounced[78]. Since its discovery in 2007, several studies have shown that *NEAT1* is activated upon cellular stress, and several lines of evidence suggest that it confers cell protection and survival upon such conditions. The *NEAT1* locus is transcribed into two overlapping isoforms, *NEAT1_1* and *NEAT1_2*. *NEAT1_2* is critical for the assembly of paraspeckles[23]. Although both isoforms of *NEAT1* are implicated in gene expression regulation, recent research suggests that they have distinct subcellular localization and functions[36]. *NEAT1* is abnormally expressed in cancer and in neurons upon neurodegenerative diseases. During the last few years, a large number of papers have suggested *NEAT1* as a biomarker in a variety of cancers, and many researchers have suggested it works as a competing endogenous RNA sponging miRNAs[77]. However, proper mechanistic studies aimed at clearly elucidating the role of *NEAT1* in physiology and pathophysiology, are still scarce. This is probably partially due to technical difficulties, and isoform-specific studies are hampered by the overlapping nature of the two transcripts. More than 40 proteins have been shown to be associated with paraspeckles.

Paraspeckles are highly dynamic structures that change in morphology and probably functions depending on *NEAT1_2* expression and the presence and recruitment of specific proteins[27,30,354]. Many of the RNA binding proteins in the paraspeckles have features that lead to liquid-liquid phase separation in the nucleus, and paraspeckles can be regarded as liquid drop-like membraneless organelles[32,33]. This dynamic feature is probably instrumental for their roles in widely regulating gene expression. As the number of proteins associated with paraspeckles are high, and they retain a wide variety of mRNAs, we still probably only see the top of the iceberg when it comes to the number of gene regulatory incidences they participate in. Thus, the gene regulatory functions of both isoforms of *NEAT1* should be a topic for further research. Recently it was reported that *NEAT1* paraspeckles actively crosstalk with mitochondria[63]. This is a particularly interesting feature as it might account for many of the functions of *NEAT1* upon stress and pathological conditions. These interactions need to be further analysed in the future.

As mentioned above, *NEAT1* is abnormally expressed in many human diseases including cancer and neurological disorders. These are devastating diseases that desperately need increased understanding and identification of new therapeutic targets. This should motivate further studies to understand the role of *NEAT1* in cellular stress and pathogenesis. As mentioned above, RNA molecules are theoretically attractive drug targets. They can be targeted by antisense oligos that are highly specific. And as *NEAT1* is frequently seen specifically overexpressed in cancer cells, probably due to malignancy-associated stress, a therapeutic window should exist.

In the future it is important to address whether *NEAT1_1* and *NEAT1_2* have different expression and functions in diseases. It has been shown that *NEAT1_2*, but not *NEAT1_1*, can predict the disease free survival of cervical cancer after treatment[56]. We have also suggested that the relative expression of the two isoforms differs in different breast cancer subtypes. This may contribute to the different gene expression pattern we see in different breast cancer subtypes, and potentially also predict the outcome of specific treatment. Furthermore, we observed a positive correlation between the level of *NEAT1_2* and subtypes of breast cancers. As each subclass of breast cancer have an exclusive genetic signature and specific phenotype, the mechanism that breast cancer cell gain capability to generate longer isoform can suggest a therapeutic strategy. Luminal A breast cancer with the highest level of *NEAT1_1* has the best survival among other subtypes, whereas, Her2-positive breast cancer with the highest level of *NEAT1_2* had worse prognosis suggest that different isoform of *NEAT1* can play different roles

in breast cancer, as it also showed in colorectal cancer[355]. Therefore, it emphasizes the need for more research on the signalling pathway and function of *NEAT1* in breast cancer. Finally, the majority of the publication confirmed the oncogenic role of *NEAT1* in cancer. Moreover, targeting *NEAT1* has been shown to reduce proliferation and resistance to chemotherapy, as it has been verified in our study[56,72,96–106]. Therefore, it could be a great deal if we can design a therapeutic strategy to specifically inhibit *NEAT1_1* or *NEAT1_2* in breast cancer cells *in vivo* and finally in patients.

Conclusion

In this doctoral thesis, we have showed that *NEAT1* is involved in the heat shock response and autophagy. We have also demonstrated that *NEAT1_2* is highly expressed in HER2-positive breast cancers. We suggest that the two *NEAT1* isoforms might have distinct expression pattern in different cancers. Our work is an important contribution to the understanding of the role of *NEAT1* in human diseases associated with extrinsic and intrinsic cellular stress.

Reference

1. Rinn, J. L. & Chang, H. Y. Genome Regulation by Long Noncoding RNAs. *Annu. Rev. Biochem.* **81,** 145–166 (2012).
2. Hangauer, M. J., Vaughn, I. W. & McManus, M. T. Pervasive Transcription of the Human Genome Produces Thousands of Previously Unidentified Long Intergenic Noncoding RNAs. *PLoS Genet.* **9,** e1003569 (2013).
3. Mattick, J. S. Non-coding RNAs: the architects of eukaryotic complexity. *EMBO Rep.* **2,** 986–991 (2001).
4. Mattick, J. S. & Gagen, M. J. The evolution of controlled multitasked gene networks: the role of introns and other noncoding RNAs in the development of complex organisms. *Mol. Biol. Evol.* **18,** 1611–1630 (2001).
5. Kapranov, P. *et al.* RNA Maps Reveal New RNA Classes and a Possible Function for Pervasive Transcription. *Science (80-.).* **316,** 1484–1488 (2007).
6. d'Adda di Fagagna, F. A direct role for small non-coding RNAs in DNA damage response. *Trends Cell Biol.* **24,** 171–178 (2014).
7. Cech, T. R. & Steitz, J. A. The Noncoding RNA Revolution—Trashing Old Rules to Forge New Ones. *Cell* **157,** 77–94 (2014).
8. Sasaki, Y. T. F., Ideue, T., Sano, M., Mituyama, T. & Hirose, T. MENε/β noncoding RNAs are essential for structural integrity of nuclear paraspeckles. *Proc. Natl. Acad. Sci.* **106,** 2525–2530 (2009).
9. Neguembor, M., Jothi, M. & Gabellini, D. Long noncoding RNAs, emerging players in muscle differentiation and disease. *Skelet. Muscle* **4,** 8 (2014).
10. Kapranov, P. Examples of the complex architecture of the human transcriptome revealed by RACE and high-density tiling arrays. *Genome Res.* **15,** 987–997 (2005).
11. Cabili, M. N. *et al.* Integrative annotation of human large intergenic noncoding RNAs reveals global properties and specific subclasses. *Genes Dev.* **25,** 1915–1927 (2011).
12. Pauli, A. *et al.* Systematic identification of long noncoding RNAs expressed during zebrafish embryogenesis. *Genome Res.* **22,** 577–591 (2012).
13. Derrien, T. *et al.* The GENCODE v7 catalog of human long noncoding RNAs: Analysis of their gene structure, evolution, and expression. *Genome Res.* **22,** 1775–1789 (2012).
14. Hezroni, H. *et al.* Principles of Long Noncoding RNA Evolution Derived from Direct Comparison of Transcriptomes in 17 Species. *Cell Rep.* **11,** 1110–1122 (2015).
15. Hudson, W. H. & Ortlund, E. A. The structure, function and evolution of proteins that bind DNA and RNA. *Nat. Rev. Mol. Cell Biol.* **15,** 749–760 (2014).
16. Guttman, M. & Rinn, J. L. Modular regulatory principles of large non-coding RNAs. *Nature* **482,** 339–346 (2012).
17. Batista, P. J. & Chang, H. Y. Long Noncoding RNAs: Cellular Address Codes in Development and Disease. *Cell* **152,** 1298–1307 (2013).
18. van Heesch, S. *et al.* Extensive localization of long noncoding RNAs to the cytosol and mono- and polyribosomal complexes. *Genome Biol.* **15,** R6 (2014).

19. Rao Editor, M. R. S. *Long Non Coding RNA Biology*. **1008,** (Springer Singapore, 2017).

20. Losko, M., Kotlinowski, J. & Jura, J. Long Noncoding RNAs in Metabolic Syndrome Related Disorders. *Mediators Inflamm.* **2016,** 1–12 (2016).

21. Guo, X. *et al.* Advances in long noncoding RNAs: identification, structure prediction and function annotation. *Brief. Funct. Genomics* **15,** 38–46 (2016).

22. Hutchinson, J. N. *et al.* A screen for nuclear transcripts identifies two linked noncoding RNAs associated with SC35 splicing domains. *BMC Genomics* **8,** 39 (2007).

23. Bond, C. S. & Fox, A. H. Paraspeckles: nuclear bodies built on long noncoding RNA. *J. Cell Biol.* **186,** 637–644 (2009).

24. Sunwoo, H. *et al.* MEN / nuclear-retained non-coding RNAs are up-regulated upon muscle differentiation and are essential components of paraspeckles. *Genome Res.* **19,** 347–359 (2008).

25. Brown, J. A., Valenstein, M. L., Yario, T. A., Tycowski, K. T. & Steitz, J. A. Formation of triple-helical structures by the 3'-end sequences of MALAT1 and MEN noncoding RNAs. *Proc. Natl. Acad. Sci.* **109,** 19202–19207 (2012).

26. Yang, Q., Gilmartin, G. M. & Doublié, S. The structure of human Cleavage Factor I m hints at functions beyond UGUA-specific RNA binding. *RNA Biol.* **8,** 748–753 (2011).

27. Naganuma, T. *et al.* Alternative 3′-end processing of long noncoding RNA initiates construction of nuclear paraspeckles. *EMBO J.* **31,** 4020–4034 (2012).

28. Nakagawa, S., Naganuma, T., Shioi, G. & Hirose, T. Paraspeckles are subpopulation-specific nuclear bodies that are not essential in mice. *J. Cell Biol.* **193,** 31–39 (2011).

29. Fox, A. H. *et al.* Paraspeckles. *Curr. Biol.* **12,** 13–25 (2002).

30. Fox, A. H., Nakagawa, S., Hirose, T. & Bond, C. S. Paraspeckles: Where Long Noncoding RNA Meets Phase Separation. *Trends Biochem. Sci.* **43,** 124–135 (2018).

31. Fox, A. H., Bond, C. S. & Lamond, A. I. P54nrb Forms a Heterodimer with PSP1 That Localizes to Paraspeckles in an RNA-dependent Manner. *Mol. Biol. Cell* **16,** 5304–5315 (2005).

32. Yamazaki, T. *et al.* Functional Domains of NEAT1 Architectural lncRNA Induce Paraspeckle Assembly through Phase Separation. *Mol. Cell* **70,** 1038–1053.e7 (2018).

33. Staněk, D. & Fox, A. H. Nuclear bodies: news insights into structure and function. *Curr. Opin. Cell Biol.* **46,** 94–101 (2017).

34. Hennig, S. *et al.* Prion-like domains in RNA binding proteins are essential for building subnuclear paraspeckles. *J. Cell Biol.* **210,** 529–539 (2015).

35. Kwon, I. *et al.* Phosphorylation-Regulated Binding of RNA Polymerase II to Fibrous Polymers of Low-Complexity Domains. *Cell* **155,** 1049–1060 (2013).

36. Li, R., Harvey, A. R., Hodgetts, S. I. & Fox, A. H. Functional dissection of NEAT1 using genome editing reveals substantial localization of the NEAT1_1 isoform outside paraspeckles. *RNA* **23,** 872–881 (2017).

37. Chen, L.-L. & Carmichael, G. G. Altered Nuclear Retention of mRNAs Containing Inverted Repeats in Human Embryonic Stem Cells: Functional Role of a Nuclear Noncoding RNA. *Mol. Cell* **35,** 467–478 (2009).

38. West, J. A. *et al.* Structural, super-resolution microscopy analysis of paraspeckle nuclear body organization. *J. Cell Biol.* **214,** 817–830 (2016).

39. Li, Y. R., King, O. D., Shorter, J. & Gitler, A. D. Stress granules as crucibles of ALS pathogenesis. *J. Cell Biol.* **201,** 361–372 (2013).

40. Prasanth, K. V. *et al.* Regulating Gene Expression through RNA Nuclear Retention. *Cell* **123,** 249–263 (2005).

41. Chiodi, I. *et al.* Structure and dynamics of hnRNP-labelled nuclear bodies induced by stress treatments. *J Cell Sci* **113 (Pt 2,** 4043–4053 (2000).

42. Kawaguchi, T. *et al.* SWI/SNF chromatin-remodeling complexes function in noncoding RNA-dependent assembly of nuclear bodies. *Proc. Natl. Acad. Sci.* **112,** 4304–4309 (2015).

43. Fong, K. *et al.* Whole-genome screening identifies proteins localized to distinct nuclear bodies. *J. Cell Biol.* **203,** 149–164 (2013).

44. Xie, S. Q., Martin, S., Guillot, P. V, Bentley, D. L. & Pombo, A. Splicing Speckles Are Not Reservoirs of RNA Polymerase II, but Contain an Inactive Form, Phosphorylated on Serine 2 Residues of the C-Terminal Domain. *Mol. Biol. Cell* **17,** 1723–1733 (2006).

45. Quiskamp, N. *et al.* The tumor suppressor annexin A10 is a novel component of nuclear paraspeckles. *Cell. Mol. Life Sci.* **71,** 311–329 (2014).

46. Dettwiler, S., Aringhieri, C., Cardinale, S., Keller, W. & Barabino, S. M. L. Distinct Sequence Motifs within the 68-kDa Subunit of Cleavage Factor I m Mediate RNA Binding, Protein-Protein Interactions, and Subcellular Localization. *J. Biol. Chem.* **279,** 35788–35797 (2004).

47. Liu, H. *et al.* Functional studies of BCL11A: characterization of the conserved BCL11A-XL splice variant and its interaction with BCL6 in nuclear paraspeckles of germinal center B cells. *Mol. Cancer* **5,** 18 (2006).

48. Marko, M., Leichter, M., Patrinou-Georgoula, M. & Guialis, A. hnRNP M interacts with PSF and p54nrb and co-localizes within defined nuclear structures. *Exp. Cell Res.* **316,** 390–400 (2010).

49. Ikeda, F. *et al.* Paraspeckle protein p54nrb links Sox9-mediated transcription with RNA processing during chondrogenesis in mice. *J. Clin. Invest.* **118,** 3098–3108 (2008).

50. Rivera, M. N. *et al.* The tumor suppressor WTX shuttles to the nucleus and modulates WT1 activity. *Proc. Natl. Acad. Sci.* **106,** 8338–8343 (2009).

51. Dutton, J. R., Lahiri, D. & Ward, A. Different isoforms of the Wilms' tumour protein WT1 have distinct patterns of distribution and trafficking within the nucleus. *Cell Prolif.* **39,** 519–535 (2006).

52. Imamura, K. *et al.* Long Noncoding RNA NEAT1-Dependent SFPQ Relocation from Promoter Region to Paraspeckle Mediates IL8 Expression upon Immune Stimuli. *Mol. Cell* **53,** 393–406 (2014).

53. Michelhaugh, S. K. *et al.* Mining Affymetrix microarray data for long non-coding RNAs: altered expression in the nucleus accumbens of heroin abusers. *J. Neurochem.* **116,** 459–466 (2011).

54. Zhang, Q., Chen, C.-Y., Yedavalli, V. S. R. K. & Jeang, K.-T. NEAT1 Long Noncoding

RNA and Paraspeckle Bodies Modulate HIV-1 Posttranscriptional Expression. *MBio* **4,** e00596-12 (2013).

55. Hirose, T. *et al.* NEAT1 long noncoding RNA regulates transcription via protein sequestration within subnuclear bodies. *Mol. Biol. Cell* **25,** 169–183 (2014).

56. Adriaens, C. *et al.* p53 induces formation of NEAT1 lncRNA-containing paraspeckles that modulate replication stress response and chemosensitivity. *Nat. Med.* **22,** 861–868 (2016).

57. Beeharry, Y., Goodrum, G., Imperiale, C. J. & Pelchat, M. The Hepatitis Delta Virus accumulation requires paraspeckle components and affects NEAT1 level and PSP1 localization. *Sci. Rep.* **8,** 6031 (2018).

58. Ma, H. *et al.* The Long Noncoding RNA NEAT1 Exerts Antihantaviral Effects by Acting as Positive Feedback for RIG-I Signaling. *J. Virol.* **91,** 1–20 (2017).

59. Choudhry, H. *et al.* Tumor hypoxia induces nuclear paraspeckle formation through HIF-2α dependent transcriptional activation of NEAT1 leading to cancer cell survival. *Oncogene* **34,** 4482–4490 (2015).

60. Lukas, J., Lukas, C. & Bartek, J. Mammalian cell cycle checkpoints : signalling pathways and their organization in space and time. **3,** 997–1007 (2004).

61. Bert Vogelstein, D. L. and A. J. L. Full-Text. *Nat.* | *doi10.1038/35042675* **408,** 307–310 (2000).

62. Picard, M. & McEwen, B. S. Psychological Stress and Mitochondria. *Psychosom. Med.* **80,** 141–153 (2018).

63. Wang, Y. *et al.* Genome-wide screening of NEAT1 regulators reveals cross-regulation between paraspeckles and mitochondria. *Nat. Cell Biol.* **20,** 1145–1158 (2018).

64. Zhou, W. *et al.* Galectin-3 activates TLR4/NF-κB signaling to promote lung adenocarcinoma cell proliferation through activating lncRNA-NEAT1 expression. *BMC Cancer* **18,** 580 (2018).

65. Cao, S. *et al.* New Noncoding Lytic Transcripts Derived from the Epstein-Barr Virus Latency Origin of Replication, oriP , Are Hyperedited, Bind the Paraspeckle Protein, NONO/p54nrb, and Support Viral Lytic Transcription. *J. Virol.* **89,** 7120–7132 (2015).

66. Morchikh, M. *et al.* HEXIM1 and NEAT1 Long Non-coding RNA Form a Multi-subunit Complex that Regulates DNA-Mediated Innate Immune Response. *Mol. Cell* **67,** 387–399.e5 (2017).

67. Saha, S. Identification and characterization of a virus-inducible non-coding RNA in mouse brain. *J. Gen. Virol.* **87,** 1991–1995 (2006).

68. Budhiraja, S. *et al.* Mining the Human Complexome Database Identifies RBM14 as an XPO1-Associated Protein Involved in HIV-1 Rev Function. *J. Virol.* **89,** 3557–3567 (2015).

69. Wang, Z. *et al.* NEAT1 modulates herpes simplex virus-1 replication by regulating viral gene transcription. *Cell. Mol. Life Sci.* **74,** 1117–1131 (2017).

70. Ahmed, A. S. I. *et al.* Long noncoding RNA NEAT1 (nuclear paraspeckle assembly transcript 1) is critical for phenotypic switching of vascular smooth muscle cells. *Proc. Natl. Acad. Sci.* **115,** E8660–E8667 (2018).

71. West, J. A. *et al.* The Long Noncoding RNAs NEAT1 and MALAT1 Bind Active Chromatin Sites. *Mol. Cell* **55,** 791–802 (2014).

72. Chakravarty, D. *et al.* The oestrogen receptor alpha-regulated lncRNA NEAT1 is a critical modulator of prostate cancer. *Nat. Commun.* **5,** 5383 (2014).

73. Torres, M. *et al.* Circadian RNA expression elicited by 3'-UTR IRAlu-paraspeckle associated elements. *Elife* **5,** 1–23 (2016).

74. Hu, S.-B. *et al.* Protein arginine methyltransferase CARM1 attenuates the paraspeckle-mediated nuclear retention of mRNAs containing IR Alu s. *Genes Dev.* **29,** 630–645 (2015).

75. Hupalowska, A. *et al.* CARM1 and Paraspeckles Regulate Pre-implantation Mouse Embryo Development. *Cell* **175,** 1902–1916.e13 (2018).

76. Jiang, L. *et al.* NEAT1 scaffolds RNA-binding proteins and the Microprocessor to globally enhance pri-miRNA processing. *Nat. Struct. Mol. Biol.* **24,** 816–824 (2017).

77. Klec, C., Prinz, F. & Pichler, M. Involvement of the long noncoding RNA NEAT1 in carcinogenesis. *Mol. Oncol.* **13,** 46–60 (2019).

78. Standaert, L. *et al.* The long noncoding RNA Neat1 is required for mammary gland development and lactation. *RNA* **20,** 1844–1849 (2014).

79. Nakagawa, S. *et al.* The lncRNA Neat1 is required for corpus luteum formation and the establishment of pregnancy in a subpopulation of mice. *Development* **141,** 4618–4627 (2014).

80. Zeng, C. *et al.* Inhibition of long non-coding RNA NEAT1 impairs myeloid differentiation in acute promyelocytic leukemia cells. 1–7 (2014).

81. Guo, S. *et al.* Clinical implication of long non-coding RNA NEAT1 expression in hepatocellular carcinoma patients. *Int. J. Clin. Exp. Pathol.* **8,** 5395–5402 (2015).

82. Liu, L. *et al.* Enhanced expression of long non-coding RNA NEAT1 is associated with the progression of gastric adenocarcinomas. *World J. Surg. Oncol.* **14,** 1–6 (2016).

83. Kim, Y., Hwan Do, J., Bae, S., Bae, D. & Shick Ahn, W. Identification of differentially expressed genes using an annealing control primer system in stage III serous ovarian carcinoma. *BMC Cancer* **10,** 576 (2010).

84. Wang, H., Yu, Y., Fan, S. & Luo, L. Knockdown of long non-coding RNA NEAT1 inhibits proliferation and invasion and induces apoptosis of osteosarcoma by inhibiting miR-194 expression. *Yonsei Med. J.* **58,** 1092–1100 (2017).

85. Han, D., Wang, J. & Cheng, G. LncRNA NEAT1 enhances the radio-resistance of cervical cancer via miR-193b-3p/CCND1 axis. *Oncotarget* **9,** 2395–2409 (2018).

86. Huang, G., He, X. & Wei, X. lncRNA NEAT1 promotes cell proliferation and invasion by regulating miR-365/RGS20 in oral squamous cell carcinoma. *Oncol. Rep.* (2018). doi:10.3892/or.2018.6283

87. Cheng, N. & Guo, Y. Long noncoding NEAT1 promotes nasopharyngeal carcinoma progression through regulation of miR-124/NF-κB pathway. *Onco. Targets. Ther.* **10,** 5843–5853 (2017).

88. Zhen, L., Yun-hui, L., Hong-yu, D., Jun, M. & Yi-long, Y. Long noncoding RNA NEAT1 promotes glioma pathogenesis by regulating miR-449b-5p/c-Met axis. *Tumor*

Biol. **37,** 673–683 (2016).

89. Liu, F. *et al.* The long non-coding RNA NEAT1 enhances epithelial-to-mesenchymal transition and chemoresistance via the miR-34a/c-Met axis in renal cell carcinoma. *Oncotarget* **8,** 62927–62938 (2017).

90. Pan, L. J. *et al.* Upregulation and clinicopathological significance of long non-coding NEAT1 RNA in NSCLC tissues. *Asian Pacific J. Cancer Prev.* **16,** 2851–2855 (2015).

91. Wedge, D. C. *et al.* Sequencing of prostate cancers identifies new cancer genes, routes of progression and drug targets. *Nat. Genet.* **50,** 682–692 (2018).

92. Fujimoto, A. *et al.* Whole-genome mutational landscape and characterization of noncoding and structural mutations in liver cancer. *Nat. Genet.* **48,** 500–509 (2016).

93. Rheinbay, E. *et al.* Recurrent and functional regulatory mutations in breast cancer. *Nature* **547,** 55–60 (2017).

94. Zeng, C. *et al.* Inhibition of long non-coding RNA NEAT1 impairs myeloid differentiation in acute promyelocytic leukemia cells. *BMC Cancer* **14,** 693 (2014).

95. Mello, S. S. *et al.* Neat1 is a p53-inducible lincRNA essential for transformation suppression. *Genes Dev.* **31,** 1095–1108 (2017).

96. Lo, P.-K. *et al.* Dysregulation of the BRCA1/long non-coding RNA NEAT1 signaling axis contributes to breast tumorigenesis. *Oncotarget* **7,** (2016).

97. Shin, V. Y. *et al.* Long non-coding RNA NEAT1 confers oncogenic role in triple-negative breast cancer through modulating chemoresistance and cancer stemness. *Cell Death Dis.* **10,** 270 (2019).

98. Tian, X., Zhang, G., Zhao, H., Li, Y. & Zhu, C. Long non-coding RNA NEAT1 contributes to docetaxel resistance of prostate cancer through inducing RET expression by sponging miR-34a. *RSC Adv.* **7,** 42986–42996 (2017).

99. Zhang, J. *et al.* Silence of Long Noncoding RNA NEAT1 Inhibits Malignant Biological Behaviors and Chemotherapy Resistance in Gastric Cancer. *Pathol. Oncol. Res.* **24,** 109–113 (2018).

100. An, J., Lv, W. & Zhang, Y. LncRNA NEAT1 contributes to paclitaxel resistance of ovarian cancer cells by regulating ZEB1 expression via miR-194. *Onco Targets Ther* **10,** 5377–5390 (2017).

101. Jiang, P. *et al.* NEAT1 acts as an inducer of cancer stem cell-like phenotypes in NSCLC by inhibiting EGCG-upregulated CTR1. *J. Cell. Physiol.* **233,** 4852–4863 (2018).

102. Wu, Y. & Wang, H. LncRNA NEAT1 promotes dexamethasone resistance in multiple myeloma by targeting miR-193a/MCL1 pathway. *J. Biochem. Mol. Toxicol.* **32,** 1–6 (2018).

103. Pouyanrad, S., Rahgozar, S. & Ghodousi, E. S. Dysregulation of miR-335-3p, targeted by NEAT1 and MALAT1 long non-coding RNAs, is associated with poor prognosis in childhood acute lymphoblastic leukemia. *Gene* **692,** 35–43 (2019).

104. Li, B., Gu, W. & Zhu, X. NEAT1 mediates paclitaxel-resistance of non-small cell of lung cancer through activation of Akt/mTOR signaling pathway. *J. Drug Target.* **0,** 1–23 (2019).

105. Hu, Y. *et al.* Knockdown of the oncogene lncRNA NEAT1 restores the availability of

miR-34c and improves the sensitivity to cisplatin in osteosarcoma. *Biosci. Rep.* **38,** BSR20180375 (2018).

106. Gong, W. *et al.* Knockdown of NEAT1 restrained the malignant progression of glioma stem cells by activating microRNA *let-7e*. *Oncotarget* **7,** 62208–62223 (2016).

107. Li, Y. *et al.* Inhibition of long non-coding RNA ROR reverses resistance to Tamoxifen by inducing autophagy in breast cancer. *Tumor Biol.* **39,** (2017).

108. Li, X. *et al.* The lncRNA NEAT1 facilitates cell growth and invasion via the miR-211/HMGA2 axis in breast cancer. *Int. J. Biol. Macromol.* **105,** 346–353 (2017).

109. Qian, K. *et al.* The long non-coding RNA NEAT1 interacted with miR-101 modulates breast cancer growth by targeting EZH2. *Arch. Biochem. Biophys.* **615,** 1–9 (2017).

110. Zhao, D., Zhang, Y., Wang, N. & Yu, N. NEAT1 negatively regulates miR-218 expression and promotes breast cancer progression. *Cancer Biomarkers* **20,** 247–254 (2017).

111. Ke, H. *et al.* NEAT1 is Required for Survival of Breast Cancer Cells through FUS and miR-548. *Gene Regul. Syst. Bio.* **10s1,** GRSB.S29414 (2016).

112. Ling, Z. A. *et al.* LncRNA NEAT1 Promotes Deterioration of Hepatocellular Carcinoma Based on in Vitro Experiments, Data Mining, and RT-qPCR Analysis. *Cell. Physiol. Biochem.* **48,** 540–555 (2018).

113. Li, P. *et al.* Long non-coding RNA NEAT1 promotes proliferation, migration and invasion of human osteosarcoma cells. *Int. J. Med. Sci.* **15,** 1227–1234 (2018).

114. Li, W. *et al.* The FOXN3-NEAT1-SIN3A repressor complex promotes progression of hormonally responsive breast cancer. *J. Clin. Invest.* **127,** 3421–3440 (2017).

115. Foulkes, W. D. BRCA1 functions as a breast stem cell regulator. *J. Med. Genet.* **41,** 1–5 (2004).

116. Przedborski, S., Vila, M. & Jackson-Lewis, V. Series Introduction: Neurodegeneration: What is it and where are we? *J. Clin. Invest.* **111,** 3–10 (2003).

117. An, H., Williams, N. G. & Shelkovnikova, T. A. NEAT1 and paraspeckles in neurodegenerative diseases: A missing lnc found? *Non-coding RNA Res.* **3,** 243–252 (2018).

118. Nishimoto, Y. *et al.* The long non-coding RNA nuclear-enriched abundant transcript 1_2 induces paraspeckle formation in the motor neuron during the early phase of amyotrophic lateral sclerosis. *Mol. Brain* **6,** 31 (2013).

119. Shelkovnikova, T. A. *et al.* Protective paraspeckle hyper-assembly downstream of TDP-43 loss of function in amyotrophic lateral sclerosis. *Mol. Neurodegener.* **13,** 30 (2018).

120. Shelkovnikova, T. A., Robinson, H. K., Troakes, C., Ninkina, N. & Buchman, V. L. Compromised paraspeckle formation as a pathogenic factor in FUSopathies. *Hum. Mol. Genet.* **23,** 2298–2312 (2014).

121. Česnik, A. B. *et al.* Nuclear RNA foci from C9ORF72 expansion mutation form paraspeckle-like bodies. *J. Cell Sci.* jcs.224303 (2019). doi:10.1242/jcs.224303

122. Saudou, F. & Humbert, S. The Biology of Huntingtin. *Neuron* **89,** 910–926 (2016).

123. Ross, C. A. & Tabrizi, S. J. Huntington's disease: from molecular pathogenesis to

clinical treatment. *Lancet Neurol.* **10,** 83–98 (2011).

124. Johnson, R. Long non-coding RNAs in Huntington's disease neurodegeneration. *Neurobiol. Dis.* **46,** 245–254 (2012).

125. Cheng, C. *et al.* The long non-coding RNA NEAT1 is elevated in polyglutamine repeat expansion diseases and protects from disease gene-dependent toxicities. *Hum. Mol. Genet.* **27,** 4303–4314 (2018).

126. Sunwoo, J.-S. *et al.* Altered Expression of the Long Noncoding RNA NEAT1 in Huntington's Disease. *Mol. Neurobiol.* **54,** 1577–1586 (2017).

127. Mariani, E. *et al.* Meta-analysis of Parkinson's disease transcriptome data using TRAM software: Whole substantia nigra tissue and single dopamine neuron differential gene expression. *PLoS One* **11,** 1–21 (2016).

128. Liu, Y. & Lu, Z. Long non-coding RNA NEAT1 mediates the toxic of Parkinson's disease induced by MPTP/MPP+ via regulation of gene expression. *Clin. Exp. Pharmacol. Physiol.* **45,** 841–848 (2018).

129. Yan, W., Chen, Z. Y., Chen, J. Q. & Chen, H. M. LncRNA NEAT1 promotes autophagy in MPTP-induced Parkinson's disease through stabilizing PINK1 protein. *Biochem. Biophys. Res. Commun.* **496,** 1019–1024 (2018).

130. Bekris, L. M., Yu, C.-E., Bird, T. D. & Tsuang, D. W. Review Article: Genetics of Alzheimer Disease. *J. Geriatr. Psychiatry Neurol.* **23,** 213–227 (2010).

131. Masters, C. L. *et al.* Alzheimer's disease. *Nat. Rev. Dis. Prim.* **1,** 15056 (2015).

132. Reitz, C., Brayne, C. & Mayeux, R. Epidemiology of Alzheimer disease. *Nat. Rev. Neurol.* **7,** 137–152 (2011).

133. Puthiyedth, N., Riveros, C., Berretta, R. & Moscato, P. Identification of differentially expressed genes through integrated study of Alzheimer's disease affected brain regions. *PLoS One* **11,** 1–29 (2016).

134. Annese, A. *et al.* Whole transcriptome profiling of Late-Onset Alzheimer's Disease patients provides insights into the molecular changes involved in the disease. *Sci. Rep.* **8,** 4282 (2018).

135. Spreafico, M., Grillo, B., Rusconi, F., Battaglioli, E. & Venturin, M. Multiple Layers of CDK5R1 Regulation in Alzheimer's Disease Implicate Long Non-Coding RNAs. *Int. J. Mol. Sci.* **19,** 2022 (2018).

136. Balch, W. E., Morimoto, R. I., Dillin, A. & Kelly, J. W. Adapting Proteostasis for Disease Intervention. *Science (80-.).* **319,** 916–919 (2008).

137. Lashuel, H. A., Hartley, D., Petre, B. M., Walz, T. & Lansbury, P. T. Amyloid pores from pathogenic mutations. *Nature* **418,** 291–291 (2002).

138. Woerner, A. C. *et al.* Cytoplasmic protein aggregates interfere with nucleocytoplasmic transport of protein and RNA. *Science (80-.).* **351,** 173–176 (2016).

139. Anguiano, M., Nowak, R. J. & Lansbury, P. T. Protofibrillar Islet Amyloid Polypeptide Permeabilizes Synthetic Vesicles by a Pore-like Mechanism that May Be Relevant to Type II Diabetes †. *Biochemistry* **41,** 11338–11343 (2002).

140. Hipp, M. S., Kasturi, P. & Hartl, F. U. The proteostasis network and its decline in ageing. *Nat. Rev. Mol. Cell Biol.* (2019). doi:10.1038/s41580-019-0101-y

141. Hartl, F. U. Molecular chaperones in cellular protein folding. *Nature* **381,** 571–580 (1996).

142. Morimoto, R. I. The Heat Shock Response: Systems Biology of Proteotoxic Stress in Aging and Disease. *Cold Spring Harb. Symp. Quant. Biol.* **76,** 91–99 (2011).

143. Hartl, F. U., Bracher, A. & Hayer-Hartl, M. Molecular chaperones in protein folding and proteostasis. *Nature* **475,** 324–332 (2011).

144. Suss, O. & Reichmann, D. Protein plasticity underlines activation and function of ATP-independent chaperones. *Front. Mol. Biosci.* **2,** 1–10 (2015).

145. Åkerfelt, M., Morimoto, R. I. & Sistonen, L. Heat shock factors: integrators of cell stress, development and lifespan. *Nat. Rev. Mol. Cell Biol.* **11,** 545–555 (2010).

146. Xu, Y.-M., Huang, D.-Y., Chiu, J.-F. & Lau, A. T. Y. Post-Translational Modification of Human Heat Shock Factors and Their Functions: A Recent Update by Proteomic Approach. *J. Proteome Res.* **11,** 2625–2634 (2012).

147. Xiao, X. HSF1 is required for extra-embryonic development, postnatal growth and protection during inflammatory responses in mice. *EMBO J.* **18,** 5943–5952 (1999).

148. Zhang, Y., Huang, L., Zhang, J., Moskophidis, D. & Mivechi, N. F. Targeted disruption ofhsf1 leads to lack of thermotolerance and defines tissue-specific regulation for stress-inducible Hsp molecular chaperones. *J. Cell. Biochem.* **86,** 376–393 (2002).

149. Fujimoto, M. *et al.* Analysis of HSF4 Binding Regions Reveals Its Necessity for Gene Regulation during Development and Heat Shock Response in Mouse Lenses. *J. Biol. Chem.* **283,** 29961–29970 (2008).

150. Paslaru, L., Morange, M. & Mezger, V. Phenotypic characterization of mouse embryonic fibroblasts lacking heat shock factor 2. *J. Cell. Mol. Med.* **7,** 425–435 (2003).

151. Wang, G., Zhang, J., Moskophidis, D. & Mivechi, N. F. Targeted disruption of the heat shock transcription factor (hsf)-2 gene results in increased embryonic lethality, neuronal defects, and reduced spermatogenesis. *genesis* **36,** 48–61 (2003).

152. Kallio, M. Brain abnormalities, defective meiotic chromosome synapsis and female subfertility in HSF2 null mice. *EMBO J.* **21,** 2591–2601 (2002).

153. Fujimoto, M. *et al.* A Novel Mouse HSF3 Has the Potential to Activate Nonclassical Heat-Shock Genes during Heat Shock. *Mol. Biol. Cell* **21,** 106–116 (2010).

154. Fujimoto, M. *et al.* HSF4 is required for normal cell growth and differentiation during mouse lens development. *EMBO J.* **23,** 4297–4306 (2004).

155. Tessari, A. Characterization of HSFY, a novel AZFb gene on the Y chromosome with a possible role in human spermatogenesis. *Mol. Hum. Reprod.* **10,** 253–258 (2004).

156. Dai, C. & Sampson, S. B. HSF1: Guardian of Proteostasis in Cancer. *Trends Cell Biol.* **26,** 17–28 (2016).

157. Anckar, J. & Sistonen, L. Regulation of HSF1 Function in the Heat Stress Response: Implications in Aging and Disease. *Annu. Rev. Biochem.* **80,** 1089–1115 (2011).

158. Verghese, J., Abrams, J., Wang, Y. & Morano, K. A. Biology of the Heat Shock Response and Protein Chaperones: Budding Yeast (Saccharomyces cerevisiae) as a Model System. *Microbiol. Mol. Biol. Rev.* **76,** 115–158 (2012).

159. Morimoto, R. I. Dynamic Remodeling of Transcription Complexes by Molecular Chaperones. *Cell* **110,** 281–284 (2002).

160. Ali, A., Bharadwaj, S., O'Carroll, R. & Ovsenek, N. HSP90 Interacts with and Regulates the Activity of Heat Shock Factor 1 in Xenopus Oocytes. *Mol. Cell. Biol.* **18,** 4949–4960 (1998).

161. Gómez, A. V. *et al.* CoREST Represses the Heat Shock Response Mediated by HSF1. *Mol. Cell* **31,** 222–231 (2008).

162. Shi, Y., Mosser, D. D. & Morimoto, R. I. Molecularchaperones as HSF1-specific transcriptional repressors. *Genes Dev.* **12,** 654–666 (1998).

163. Zou, J., Guo, Y., Guettouche, T., Smith, D. F. & Voellmy, R. Repression of Heat Shock Transcription Factor HSF1 Activation by HSP90 (HSP90 Complex) that Forms a Stress-Sensitive Complex with HSF1. *Cell* **94,** 471–480 (1998).

164. Mercier, P. A., Winegarden, N. A. & Westwood, J. T. Human heat shock factor 1 is predominantly a nuclear protein before and after heat stress. *J. Cell Sci.* **112 (Pt 1,** 2765–74 (1999).

165. Sivéry, A., Courtade, E. & Thommen, Q. A minimal titration model of the mammalian dynamical heat shock response. *Phys. Biol.* **13,** 066008 (2016).

166. Gomez-Pastor, R., Burchfiel, E. T. & Thiele, D. J. Regulation of heat shock transcription factors and their roles in physiology and disease. *Nat. Rev. Mol. Cell Biol.* **19,** 4–19 (2017).

167. Littlefield, O. & Nelson, H. C. M. A new use for the 'wing' of the 'winged' helix-turn-helix motif in the HSF-DNA cocrystal. *Nat. Struct. Biol.* **6,** 464–470 (1999).

168. Jaeger, A. M., Pemble, C. W., Sistonen, L. & Thiele, D. J. Structures of HSF2 reveal mechanisms for differential regulation of human heat-shock factors. *Nat. Struct. Mol. Biol.* **23,** 147–154 (2016).

169. Raychaudhuri, S. *et al.* Interplay of Acetyltransferase EP300 and the Proteasome System in Regulating Heat Shock Transcription Factor 1. *Cell* **156,** 975–985 (2014).

170. Tamimi, R. M. *et al.* High levels of nuclear heat-shock factor 1 (HSF1) are associated with poor prognosis in breast cancer. *Proc. Natl. Acad. Sci.* **108,** 18378–18383 (2011).

171. Maheshwari, M. *et al.* Dexamethasone induces heat shock response and slows down disease progression in mouse and fly models of Huntington's disease. *Hum. Mol. Genet.* **23,** 2737–2751 (2014).

172. Kondo, N. *et al.* Heat shock factor-1 influences pathological lesion distribution of polyglutamine-induced neurodegeneration. *Nat. Commun.* **4,** 1405 (2013).

173. Chafekar, S. M. & Duennwald, M. L. Impaired Heat Shock Response in Cells Expressing Full-Length Polyglutamine-Expanded Huntingtin. *PLoS One* **7,** e37929 (2012).

174. Gomez-Pastor, R. *et al.* Abnormal degradation of the neuronal stress-protective transcription factor HSF1 in Huntington's disease. *Nat. Commun.* **8,** 14405 (2017).

175. Dai, C., Whitesell, L., Rogers, A. B. & Lindquist, S. Heat Shock Factor 1 Is a Powerful Multifaceted Modifier of Carcinogenesis. *Cell* **130,** 1005–1018 (2007).

176. Kasamatsu, A. State of heat shock factor 1 expression as a putative diagnostic marker for oral squamous cell carcinoma. *Int. J. Oncol.* **40,** 47–52 (2011).

177. Zheng, X. *et al.* Dynamic control of Hsf1 during heat shock by a chaperone switch and phosphorylation. *Elife* **5,** 1–26 (2016).

178. Jiang, S. *et al.* Multifaceted roles of HSF1 in cancer. *Tumor Biol.* **36,** 4923–4931 (2015).

179. Anckar, J. & Sistonen, L. Regulation of H <scp>SF</scp> 1 Function in the Heat Stress Response: Implications in Aging and Disease. *Annu. Rev. Biochem.* **80,** 1089–1115 (2011).

180. Santagata, S. *et al.* P5-01-13: High Levels of Nuclear Heat Shock Factor 1 (HSF1) Are Associated with Poor Prognosis in Breast Cancer: Results from the Nurses' Health Study. *Cancer Res.* **71,** P5-01-13-P5-01-13 (2011).

181. Tang, Z. *et al.* MEK Guards Proteome Stability and Inhibits Tumor-Suppressive Amyloidogenesis via HSF1. *Cell* **160,** 729–744 (2015).

182. Whitesell, L. & Lindquist, S. L. HSP90 and the chaperoning of cancer. *Nat. Rev. Cancer* **5,** 761–772 (2005).

183. Dikic, I. & Elazar, Z. Mechanism and medical implications of mammalian autophagy. *Nat. Rev. Mol. Cell Biol.* **19,** 349–364 (2018).

184. DE DUVE, C., PRESSMAN, B. C., GIANETTO, R., WATTIAUX, R. & APPELMANS, F. Tissue fractionation studies. 6. Intracellular distribution patterns of enzymes in rat-liver tissue. *Biochem. J.* **60,** 604–17 (1955).

185. DE DUVE, C. The lysosome. *Sci. Am.* **208,** 64–72 (1963).

186. Parzych, K. R., Ariosa, A., Mari, M. & Klionsky, D. J. A newly characterized vacuolar serine carboxypeptidase, Atg42/Ybr139w, is required for normal vacuole function and the terminal steps of autophagy in the yeast Saccharomyces cerevisiae. *Mol. Biol. Cell* **29,** 1089–1099 (2018).

187. Nakatogawa, H., Suzuki, K., Kamada, Y. & Ohsumi, Y. Dynamics and diversity in autophagy mechanisms: lessons from yeast. *Nat. Rev. Mol. Cell Biol.* **10,** 458–467 (2009).

188. Klionsky, D. J. *et al.* How Shall I Eat Thee? *Autophagy* **3,** 413–416 (2007).

189. Rogov, V., Dötsch, V., Johansen, T. & Kirkin, V. Interactions between Autophagy Receptors and Ubiquitin-like Proteins Form the Molecular Basis for Selective Autophagy. *Mol. Cell* **53,** 167–178 (2014).

190. Anding, A. L. & Baehrecke, E. H. Cleaning House: Selective Autophagy of Organelles. *Dev. Cell* **41,** 10–22 (2017).

191. Boya, P., Reggiori, F. & Codogno, P. Emerging regulation and functions of autophagy. *Nat. Cell Biol.* **15,** 713–720 (2013).

192. Mijaljica, D., Prescott, M. & Devenish, R. J. Microautophagy in mammalian cells: Revisiting a 40-year-old conundrum. *Autophagy* **7,** 673–682 (2011).

193. Chiang, H. L., Terlecky, S. R., Plant, C. P. & Dice, J. F. A role for a 70-kilodalton heat shock protein in lysosomal degradation of intracellular proteins. *Science* **246,** 382–385 (1989).

194. Eskelinen, E.-L. Maturation of Autophagic Vacuoles in Mammalian Cells. *Autophagy* **1,** 1–10 (2005).

195. He, C. & Klionsky, D. J. Regulation Mechanisms and Signaling Pathways of Autophagy. *Annu. Rev. Genet.* **43,** 67–93 (2009).

196. Kamada, Y. *et al.* Tor Directly Controls the Atg1 Kinase Complex To Regulate Autophagy. *Mol. Cell. Biol.* **30,** 1049–1058 (2010).

197. Kamada, Y. *et al.* Tor-Mediated Induction of Autophagy via an Apg1 Protein Kinase Complex. *J. Cell Biol.* **150,** 1507–1513 (2000).

198. Hosokawa, N. *et al.* Nutrient-dependent mTORC1 Association with the ULK1–Atg13–FIP200 Complex Required for Autophagy. *Mol. Biol. Cell* **20,** 1981–1991 (2009).

199. Ganley, I. G. *et al.* ULK1·ATG13·FIP200 Complex Mediates mTOR Signaling and Is Essential for Autophagy. *J. Biol. Chem.* **284,** 12297–12305 (2009).

200. Jung, C. H. *et al.* ULK-Atg13-FIP200 Complexes Mediate mTOR Signaling to the Autophagy Machinery. *Mol. Biol. Cell* **20,** 1992–2003 (2009).

201. Kim, J., Kundu, M., Viollet, B. & Guan, K.-L. AMPK and mTOR regulate autophagy through direct phosphorylation of Ulk1. *Nat. Cell Biol.* **13,** 132–141 (2011).

202. Jean, S. & Kiger, A. A. Classes of phosphoinositide 3-kinases at a glance. *J. Cell Sci.* **127,** 923–928 (2014).

203. Petiot, A., Ogier-Denis, E., Blommaart, E. F. C., Meijer, A. J. & Codogno, P. Distinct Classes of Phosphatidylinositol 3'-Kinases Are Involved in Signaling Pathways That Control Macroautophagy in HT-29 Cells. *J. Biol. Chem.* **275,** 992–998 (2000).

204. Itakura, E., Kishi, C., Inoue, K. & Mizushima, N. Beclin 1 Forms Two Distinct Phosphatidylinositol 3-Kinase Complexes with Mammalian Atg14 and UVRAG. *Mol. Biol. Cell* **19,** 5360–5372 (2008).

205. Park, J.-M. *et al.* The ULK1 complex mediates MTORC1 signaling to the autophagy initiation machinery via binding and phosphorylating ATG14. *Autophagy* **12,** 547–564 (2016).

206. Russell, R. C. *et al.* ULK1 induces autophagy by phosphorylating Beclin-1 and activating VPS34 lipid kinase. *Nat. Cell Biol.* **15,** 741–750 (2013).

207. Fan, W., Nassiri, A. & Zhong, Q. Autophagosome targeting and membrane curvature sensing by Barkor/Atg14(L). *Proc. Natl. Acad. Sci.* **108,** 7769–7774 (2011).

208. Pattingre, S. *et al.* Bcl-2 Antiapoptotic Proteins Inhibit Beclin 1-Dependent Autophagy. *Cell* **122,** 927–939 (2005).

209. Jaber, N. *et al.* Class III PI3K Vps34 plays an essential role in autophagy and in heart and liver function. *Proc. Natl. Acad. Sci.* **109,** 2003–2008 (2012).

210. Karanasios, E. *et al.* Dynamic association of the ULK1 complex with omegasomes during autophagy induction. *J. Cell Sci.* **126,** 5224–5238 (2013).

211. Ropolo, A. *et al.* The Pancreatitis-induced Vacuole Membrane Protein 1 Triggers Autophagy in Mammalian Cells. *J. Biol. Chem.* **282,** 37124–37133 (2007).

212. Maria Fimia, G. *et al.* Ambra1 regulates autophagy and development of the nervous system. *Nature* **447,** 1121–1125 (2007).

213. Shibutani, S. T. & Yoshimori, T. A current perspective of autophagosome biogenesis. *Cell Res.* **24,** 58–68 (2014).

214. Wu, J. *et al.* Molecular cloning and characterization of rat LC3A and LC3B—Two novel markers of autophagosome. *Biochem. Biophys. Res. Commun.* **339,** 437–442 (2006).

215. Shpilka, T., Weidberg, H., Pietrokovski, S. & Elazar, Z. Atg8: an autophagy-related ubiquitin-like protein family. *Genome Biol.* **12,** 226 (2011).

216. Tanida, I., Tanida-Miyake, E., Ueno, T. & Kominami, E. The Human Homolog of Saccharomyces cerevisiae Apg7p Is a Protein-activating Enzyme for Multiple Substrates Including Human Apg12p, GATE-16, GABARAP, and MAP-LC3. *J. Biol. Chem.* **276,** 1701–1706 (2001).

217. Klionsky, D. J. *et al.* Guidelines for the use and interpretation of assays for monitoring autophagy (3rd edition). *Autophagy* **12,** 1–222 (2016).

218. Kabeya, Y. LC3, GABARAP and GATE16 localize to autophagosomal membrane depending on form-II formation. *J. Cell Sci.* **117,** 2805–2812 (2004).

219. Fujita, N. *et al.* An Atg4B Mutant Hampers the Lipidation of LC3 Paralogues and Causes Defects in Autophagosome Closure. *Mol. Biol. Cell* **19,** 4651–4659 (2008).

220. Tanida, I., Ueno, T. & Kominami, E. Human Light Chain 3/MAP1LC3B Is Cleaved at Its Carboxyl-terminal Met 121 to Expose Gly 120 for Lipidation and Targeting to Autophagosomal Membranes. *J. Biol. Chem.* **279,** 47704–47710 (2004).

221. Tanida, I., Ueno, T. & Kominami, E. LC3 conjugation system in mammalian autophagy. *Int. J. Biochem. Cell Biol.* **36,** 2503–2518 (2004).

222. Dooley, H. C. *et al.* WIPI2 Links LC3 Conjugation with PI3P, Autophagosome Formation, and Pathogen Clearance by Recruiting Atg12–5-16L1. *Mol. Cell* **55,** 238–252 (2014).

223. Velikkakath, A. K. G., Nishimura, T., Oita, E., Ishihara, N. & Mizushima, N. Mammalian Atg2 proteins are essential for autophagosome formation and important for regulation of size and distribution of lipid droplets. *Mol. Biol. Cell* **23,** 896–909 (2012).

224. Kimura, S., Noda, T. & Yoshimori, T. Dynein-dependent Movement of Autophagosomes Mediates Efficient Encounters with Lysosomes. *Cell Struct. Funct.* **33,** 109–122 (2008).

225. Jongsma, M. L. M. *et al.* An ER-Associated Pathway Defines Endosomal Architecture for Controlled Cargo Transport. *Cell* **166,** 152–166 (2016).

226. Nakamura, S. & Yoshimori, T. New insights into autophagosome–lysosome fusion. *J. Cell Sci.* **130,** 1209–1216 (2017).

227. Köchl, R., Hu, X. W., Chan, E. Y. W. & Tooze, S. A. Microtubules Facilitate Autophagosome Formation and Fusion of Autophagosomes with Endosomes. *Traffic* **7,** 129–145 (2006).

228. Gutierrez, M. G. Rab7 is required for the normal progression of the autophagic pathway in mammalian cells. *J. Cell Sci.* **117,** 2687–2697 (2004).

229. Diao, J. *et al.* ATG14 promotes membrane tethering and fusion of autophagosomes to endolysosomes. *Nature* **520,** 563–566 (2015).

230. Itakura, E., Kishi-Itakura, C. & Mizushima, N. The Hairpin-type Tail-Anchored SNARE Syntaxin 17 Targets to Autophagosomes for Fusion with Endosomes/Lysosomes. *Cell* **151,** 1256–1269 (2012).

231. Jahreiss, L., Menzies, F. M. & Rubinsztein, D. C. The Itinerary of Autophagosomes: From Peripheral Formation to Kiss-and-Run Fusion with Lysosomes. *Traffic* **9,** 574–587 (2008).

232. Mauvezin, C. *et al.* Coordination of autophagosome–lysosome fusion and transport by a Klp98A–Rab14 complex in Drosophila. *J. Cell Sci.* **129,** 971–982 (2016).

233. Jordens, I. *et al.* The Rab7 effector protein RILP controls lysosomal transport by inducing the recruitment of dynein-dynactin motors. *Curr. Biol.* **11,** 1680–1685 (2001).

234. Pankiv, S. *et al.* FYCO1 is a Rab7 effector that binds to LC3 and PI3P to mediate microtubule plus end–directed vesicle transport. *J. Cell Biol.* **188,** 253–269 (2010).

235. Hyttinen, J. M. T., Niittykoski, M., Salminen, A. & Kaarniranta, K. Maturation of autophagosomes and endosomes: A key role for Rab7. *Biochim. Biophys. Acta - Mol. Cell Res.* **1833,** 503–510 (2013).

236. Rieder, S. E. & Emr, S. D. A Novel RING Finger Protein Complex Essential for a Late Step in Protein Transport to the Yeast Vacuole. *Mol. Biol. Cell* **8,** 2307–2327 (1997).

237. Wurmser, A. E., Sato, T. K. & Emr, S. D. New Component of the Vacuolar Class C-Vps Complex Couples Nucleotide Exchange on the Ypt7 Gtpase to Snare-Dependent Docking and Fusion. *J. Cell Biol.* **151,** 551–562 (2000).

238. Seals, D. F., Eitzen, G., Margolis, N., Wickner, W. T. & Price, A. A Ypt/Rab effector complex containing the Sec1 homolog Vps33p is required for homotypic vacuole fusion. *Proc. Natl. Acad. Sci.* **97,** 9402–9407 (2000).

239. McEwan, D. G. *et al.* PLEKHM1 Regulates Autophagosome-Lysosome Fusion through HOPS Complex and LC3/GABARAP Proteins. *Mol. Cell* **57,** 39–54 (2015).

240. Jahn, R. & Scheller, R. H. SNAREs — engines for membrane fusion. *Nat. Rev. Mol. Cell Biol.* **7,** 631–643 (2006).

241. Rabinowitz, J. D. & White, E. Autophagy and Metabolism. *Science (80-.).* **330,** 1344–1348 (2010).

242. Mizushima, N. & Komatsu, M. Autophagy: Renovation of Cells and Tissues. *Cell* **147,** 728–741 (2011).

243. Choi, A. M. K., Ryter, S. W. & Levine, B. Autophagy in Human Health and Disease. *N. Engl. J. Med.* **368,** 651–662 (2013).

244. Levine, B., Mizushima, N. & Virgin, H. W. Autophagy in immunity and inflammation. *Nature* **469,** 323–335 (2011).

245. Mizushima, N. & Levine, B. Autophagy in mammalian development and differentiation. *Nat. Cell Biol.* **12,** 823–830 (2010).

246. Murrow, L. & Debnath, J. Autophagy as a Stress-Response and Quality-Control Mechanism: Implications for Cell Injury and Human Disease. *Annu. Rev. Pathol. Mech. Dis.* **8,** 105–137 (2013).

247. Rubinsztein, D. C., Mariño, G. & Kroemer, G. Autophagy and Aging. *Cell* **146,** 682–695 (2011).

248. White, E. Deconvoluting the context-dependent role for autophagy in cancer. *Nat. Rev. Cancer* **12,** 401–410 (2012).

249. Nixon, R. A. The role of autophagy in neurodegenerative disease. *Nat. Med.* **19,** 983–997 (2013).

250. Hippert, M. M., O'Toole, P. S. & Thorburn, A. Autophagy in Cancer: Good, Bad, or Both?: Figure 1. *Cancer Res.* **66,** 9349–9351 (2006).

251. Kenific, C. M., Thorburn, A. & Debnath, J. Autophagy and metastasis: another double-edged sword. *Curr. Opin. Cell Biol.* **22,** 241–245 (2010).

252. Qu, X. Promotion of tumorigenesis by heterozygous disruption of the beclin 1 autophagy gene. *J. Clin. Invest.* **112,** 1809–1820 (2003).

253. Liou, G.-Y. & Storz, P. Reactive oxygen species in cancer. *Free Radic. Res.* **44,** 479–496 (2010).

254. Wilde, L., Tanson, K., Curry, J. & Martinez-Outschoorn, U. Autophagy in cancer: a complex relationship. *Biochem. J.* **475,** 1939–1954 (2018).

255. Aita, V. M. *et al.* Cloning and Genomic Organization of Beclin 1, a Candidate Tumor Suppressor Gene on Chromosome 17q21. *Genomics* **59,** 59–65 (1999).

256. Yue, Z., Jin, S., Yang, C., Levine, A. J. & Heintz, N. Beclin 1, an autophagy gene essential for early embryonic development, is a haploinsufficient tumor suppressor. *Proc. Natl. Acad. Sci.* **100,** 15077–15082 (2003).

257. Takamura, A. *et al.* Autophagy-deficient mice develop multiple liver tumors. *Genes Dev.* **25,** 795–800 (2011).

258. Takahashi, Y. *et al.* Bif-1 interacts with Beclin 1 through UVRAG and regulates autophagy and tumorigenesis. *Nat. Cell Biol.* **9,** 1142–1151 (2007).

259. Pattingre, S., Bauvy, C. & Codogno, P. Amino Acids Interfere with the ERK1/2-dependent Control of Macroautophagy by Controlling the Activation of Raf-1 in Human Colon Cancer HT-29 Cells. *J. Biol. Chem.* **278,** 16667–16674 (2003).

260. Schmukler, E., Kloog, Y. & Pinkas-Kramarski, R. Ras and autophagy in cancer development and therapy. *Oncotarget* **5,** (2014).

261. Perera, R. M. *et al.* Transcriptional control of autophagy–lysosome function drives pancreatic cancer metabolism. *Nature* **524,** 361–365 (2015).

262. Yang, S. *et al.* Pancreatic cancers require autophagy for tumor growth. *Genes Dev.* **25,** 717–729 (2011).

263. Wilde, L. *et al.* Metabolic coupling and the Reverse Warburg Effect in cancer: Implications for novel biomarker and anticancer agent development. *Semin. Oncol.* **44,** 198–203 (2017).

264. Martinez-Outschoorn, U. E. *et al.* Stromal–epithelial metabolic coupling in cancer: Integrating autophagy and metabolism in the tumor microenvironment. *Int. J. Biochem. Cell Biol.* **43,** 1045–1051 (2011).

265. Pavlides, S. *et al.* The autophagic tumor stroma model of cancer. *Cell Cycle* **9,** 3485–3505 (2010).

266. Pavlides, S. *et al.* Warburg Meets Autophagy: Cancer-Associated Fibroblasts Accelerate Tumor Growth and Metastasis via Oxidative Stress, Mitophagy, and Aerobic Glycolysis. *Antioxid. Redox Signal.* **16,** 1264–1284 (2012).

267. Valencia, T. *et al.* Metabolic Reprogramming of Stromal Fibroblasts through p62-mTORC1 Signaling Promotes Inflammation and Tumorigenesis. *Cancer Cell* **26,** 121–135 (2014).

268. Javed, A. & Lteif, A. Development of the human breast. *Semin. Plast. Surg.* **27,** 5–12 (2013).

269. Pellacani, D., Tan, S., Lefort, S. & Eaves, C. J. Transcriptional regulation of normal human mammary cell heterogeneity and its perturbation in breast cancer. *EMBO J.* e100330 (2019). doi:10.15252/embj.2018100330

270. Sreekumar, A., Roarty, K. & Rosen, J. M. The mammary stem cell hierarchy: a looking glass into heterogeneous breast cancer landscapes. *Endocr. Relat. Cancer* **22,** T161–T176 (2015).

271. Sharma, N. *et al.* Distinct stem cells contribute to mammary gland development and maintenance. *Nature* **479,** 189–193 (2011).

272. Cancer in Norway 2017: Cancer incidence, mortality, survival and prevalence in Norway. *Cancer Regist. Norw.* (2018).

273. Trewin, C. B., Strand, B. H., Weedon-Fekjær, H. & Ursin, G. Changing patterns of breast cancer incidence and mortality by education level over four decades in Norway, 1971-2009. *Eur. J. Public Health* **27,** 160–166 (2017).

274. Jatoi, I. & Miller, A. B. Why is breast-cancer mortality declining? *Lancet. Oncol.* **4,** 251–254 (2003).

275. Berman, A. T., Thukral, A. D., Hwang, W.-T., Solin, L. J. & Vapiwala, N. Incidence and Patterns of Distant Metastases for Patients With Early-Stage Breast Cancer After Breast Conservation Treatment. *Clin. Breast Cancer* **13,** 88–94 (2013).

276. Gerratana, L. *et al.* Pattern of metastasis and outcome in patients with breast cancer. *Clin. Exp. Metastasis* **32,** 125–133 (2015).

277. Rizzolo, P., Silvestri, V., Falchetti, M. & Ottini, L. Inherited and acquired alterations in development of breast cancer. *Appl. Clin. Genet.* **4,** 145–158 (2011).

278. Hall, J. M. *et al.* Linkage of early-onset familial breast cancer to chromosome 17q21. *Science* **250,** 1684–9 (1990).

279. Easton, D. F., Bishop, D. T., Ford, D. & Crockford, G. P. Genetic linkage analysis in familial breast and ovarian cancer: results from 214 families. The Breast Cancer Linkage Consortium. *Am. J. Hum. Genet.* **52,** 678–701 (1993).

280. Mavaddat, N., Antoniou, A. C., Easton, D. F. & Garcia-Closas, M. Genetic susceptibility to breast cancer. *Molecular Oncology* **4,** 174–191 (2010).

281. Garber, J. E. *et al.* Follow-up study of twenty-four families with Li-Fraumeni syndrome. *Cancer Res.* **51,** 6094–7 (1991).

282. Goldhirsch, A. *et al.* Personalizing the treatment of women with early breast cancer: highlights of the St Gallen International Expert Consensus on the Primary Therapy of Early Breast Cancer 2013. *Ann. Oncol.* **24,** 2206–2223 (2013).

283. Santos, C. *et al.* Intrinsic cancer subtypes-next steps into personalized medicine. *Cell. Oncol.* **38,** 3–16 (2015).

284. Hugh, J. *et al.* Breast Cancer Subtypes and Response to Docetaxel in Node-Positive

Breast Cancer: Use of an Immunohistochemical Definition in the BCIRG 001 Trial. *J. Clin. Oncol.* **27,** 1168–1176 (2009).

285. Perou, C. M. *et al.* Molecular portraits of human breast tumours. *Nature* **406,** 747–752 (2000).

286. Børresen-Dale, A.-L. *et al.* Repeated observation of breast tumor subtypes in independent gene expression data sets. *Proc. Natl. Acad. Sci.* **100,** 8418–8423 (2003).

287. Inic, Z. *et al.* Difference between Luminal A and Luminal B subtypes according to Ki-67, tumor size, and progesterone receptor negativity providing prognostic information. *Clin. Med. Insights Oncol.* **8,** 107–111 (2014).

288. Mullins, M. *et al.* Supervised Risk Predictor of Breast Cancer Based on Intrinsic Subtypes. *J. Clin. Oncol.* **27,** 1160–1167 (2009).

289. Prat, A. & Perou, C. M. Deconstructing the molecular portraits of breast cancer. *Mol. Oncol.* **5,** 5–23 (2011).

290. Kole, R., Krainer, A. R. & Altman, S. RNA therapeutics: beyond RNA interference and antisense oligonucleotides. *Nat. Rev. Drug Discov.* **11,** 125–140 (2012).

291. Kher, G., Trehan, S. & Misra, A. in *Challenges in Delivery of Therapeutic Genomics and Proteomics* 325–386 (Elsevier, 2011). doi:10.1016/B978-0-12-384964-9.00007-4

292. Koshkin, A. A. *et al.* LNA (Locked Nucleic Acids): Synthesis of the adenine, cytosine, guanine, 5-methylcytosine, thymine and uracil bicyclonucleoside monomers, oligomerisation, and unprecedented nucleic acid recognition. *Tetrahedron* **54,** 3607–3630 (1998).

293. Torigoe, H., Hari, Y., Sekiguchi, M., Obika, S. & Imanishi, T. 2′- O ,4′- C -Methylene Bridged Nucleic Acid Modification Promotes Pyrimidine Motif Triplex DNA Formation at Physiological pH. *J. Biol. Chem.* **276,** 2354–2360 (2001).

294. Petersen, M. & Wengel, J. LNA: a versatile tool for therapeutics and genomics. *Trends Biotechnol.* **21,** 74–81 (2003).

295. Kurreck, J. Antisense technologies. Improvement through novel chemical modifications. *Eur. J. Biochem.* **270,** 1628–1644 (2003).

296. Leech, S. H. *et al.* Induction of apoptosis in lung-cancer cells following bclxL anti-sense treatment. *Int. J. Cancer* **86,** 570–576 (2000).

297. Prakash, T. P. An Overview of Sugar-Modified Oligonucleotides for Antisense Therapeutics. *Chem. Biodivers.* **8,** 1616–1641 (2011).

298. Gershon, H., Ghirlando, R., Guttman, S. B. & Minsky, A. Mode of formation and structural features of DNA-cationic liposome complexes used for transfection. *Biochemistry* **32,** 7143–7151 (1993).

299. Miller, A. D. Cationic Liposomes for Gene Therapy. *Angew. Chemie Int. Ed.* **37,** 1768–1785 (1998).

300. Cardarelli, F. *et al.* The intracellular trafficking mechanism of Lipofectamine-based transfection reagents and its implication for gene delivery. *Sci. Rep.* **6,** 25879 (2016).

301. Kim, T. K. & Eberwine, J. H. Mammalian cell transfection: the present and the future. *Anal. Bioanal. Chem.* **397,** 3173–3178 (2010).

302. Magnuson, B., Ekim, B. & Fingar, D. C. Regulation and function of ribosomal protein S6 kinase (S6K) within mTOR signalling networks. *Biochem. J.* **441,** 1–21 (2012).

303. Karge, W. H., Schaefer, E. J. & Ordovas, J. M. in *Lipoprotein Protocols* 43–62 (Humana Press). doi:10.1385/1-59259-582-0:43

304. Thellin, O. *et al.* Housekeeping genes as internal standards: use and limits. *J. Biotechnol.* **75,** 291–295 (1999).

305. Bereta, J. & Bereta, M. Stimulation of Glyceraldehyde-3-Phosphate Dehydrogenase mRNA Levels by Endogenous Nitric Oxide in Cytokine-Activated Endothelium. *Biochem. Biophys. Res. Commun.* **217,** 363–369 (1995).

306. Zhang, J. & Snyder, S. H. Nitric oxide stimulates auto-ADP-ribosylation of glyceraldehyde-3-phosphate dehydrogenase. *Proc. Natl. Acad. Sci.* **89,** 9382–9385 (1992).

307. Bhatia, P., Taylor, W. R., Greenberg, A. H. & Wright, J. A. Comparison of Glyceraldehyde-3-phosphate Dehydrogenase and 28S-Ribosomal RNA Gene Expression as RNA Loading Controls for Northern Blot Analysis of Cell Lines of Varying Malignant Potential. *Anal. Biochem.* **216,** 223–226 (1994).

308. Bustin, S. A. Absolute quantification of mRNA using real-time reverse transcription polymerase chain reaction assays. *J. Mol. Endocrinol.* **25,** 169–193 (2000).

309. Livak, K. J. & Schmittgen, T. D. Analysis of Relative Gene Expression Data Using Real-Time Quantitative PCR and the 2−ΔΔCT Method. *Methods* **25,** 402–408 (2001).

310. Orjalo, A., Johansson, H. E. & Ruth, J. L. Stellaris™ fluorescence in situ hybridization (FISH) probes: a powerful tool for mRNA detection. *Nat. Methods* **8,** i–ii (2011).

311. Orjalo, A. V. & Johansson, H. E. in 119–134 (2016). doi:10.1007/978-1-4939-3378-5_10

312. Galluzzi, L., Yamazaki, T. & Kroemer, G. Linking cellular stress responses to systemic homeostasis. *Nat. Rev. Mol. Cell Biol.* **19,** 731–745 (2018).

313. Fulda, S., Gorman, A. M., Hori, O. & Samali, A. Cellular stress responses: Cell survival and cell death. *Int. J. Cell Biol.* **2010,** (2010).

314. Poljšak, B. & Milisav, I. Clinical implications of cellular stress responses. *Bosn. J. Basic Med. Sci.* **12,** 122–126 (2012).

315. Hu, C., Eggler, A. L., Mesecar, A. D. & van Breemen, R. B. Modification of Keap1 Cysteine Residues by Sulforaphane. *Chem. Res. Toxicol.* **24,** 515–521 (2011).

316. Gan, N. *et al.* Sulforaphane activates heat shock response and enhances proteasome activity through up-regulation of Hsp27. *J. Biol. Chem.* **285,** 35528–35536 (2010).

317. Tanabe, M. *et al.* HSF1 is required for extra-embryonic development, postnatal growth and protection during inflammatory responses in mice. *EMBO J.* **17,** 1750–1758 (1998).

318. Standaert, L. *et al.* The long noncoding RNA Neat1 is required for mammary gland development and lactation. *RNA* **20,** 1844–1849 (2014).

319. Xi, C., Hu, Y., Buckhaults, P., Moskophidis, D. & Mivechi, N. F. Heat Shock Factor Hsf1 Cooperates with ErbB2 (Her2/Neu) Protein to Promote Mammary Tumorigenesis and Metastasis. *J. Biol. Chem.* **287,** 35646–35657 (2012).

320. Kim, G. *et al.* Heat Shock Transcription Factor Hsf1 Is Involved in Tumor Progression via Regulation of Hypoxia-Inducible Factor 1 and RNA-Binding Protein HuR. *Mol. Cell. Biol.* **32,** 929–940 (2012).

321. Chakravarty, D. *et al.* The oestrogen receptor alpha-regulated lncRNA NEAT1 is a critical modulator of prostate cancer. *Nat. Commun.* **5,** 5383 (2014).

322. Li, W. *et al.* The FOXN3-NEAT1-SIN3A repressor complex promotes progression of hormonally responsive breast cancer. *J. Clin. Invest.* **127,** 3421–3440 (2017).

323. Imamura, K. *et al.* Long Noncoding RNA NEAT1-Dependent SFPQ Relocation from Promoter Region to Paraspeckle Mediates IL8 Expression upon Immune Stimuli. *Mol. Cell* **53,** 393–406 (2014).

324. Meng, L., Gabai, V. L. & Sherman, M. Y. Heat-shock transcription factor HSF1 has a critical role in human epidermal growth factor receptor-2-induced cellular transformation and tumorigenesis. *Oncogene* **29,** 5204–5213 (2010).

325. Cheng, Q. *et al.* Amplification and high-level expression of heat shock protein 90 marks aggressive phenotypes of human epidermal growth factor receptor 2 negative breast cancer. *Breast Cancer Res.* **14,** R62 (2012).

326. Jarman, E. J. *et al.* HER2 regulates HIF-2α and drives an increased hypoxic response in breast cancer. *Breast Cancer Res.* **21,** 10 (2019).

327. Tian, W. *et al.* Phosphorylation of ULK1 by AMPK regulates translocation of ULK1 to mitochondria and mitophagy. *FEBS Lett.* **589,** 1847–1854 (2015).

328. Bhat, A. H. *et al.* Oxidative stress, mitochondrial dysfunction and neurodegenerative diseases; a mechanistic insight. *Biomed. Pharmacother.* **74,** 101–110 (2015).

329. Van Houten, B., Woshner, V. & Santos, J. H. Role of mitochondrial DNA in toxic responses to oxidative stress. *DNA Repair (Amst).* **5,** 145–152 (2006).

330. Indo, H. P. *et al.* Evidence of ROS generation by mitochondria in cells with impaired electron transport chain and mitochondrial DNA damage. *Mitochondrion* **7,** 106–118 (2007).

331. Eliopoulos, A. G., Havaki, S. & Gorgoulis, V. G. DNA Damage Response and Autophagy: A Meaningful Partnership. *Front. Genet.* **7,** 1–13 (2016).

332. Bose, J. K., Huang, C.-C. & Shen, C.-K. J. Regulation of Autophagy by Neuropathological Protein TDP-43. *J. Biol. Chem.* **286,** 44441–44448 (2011).

333. Soo, K. Y. *et al.* ALS-associated mutant FUS inhibits macroautophagy which is restored by overexpression of Rab1. *Cell Death Discov.* **1,** 15030 (2015).

334. Høyer-Hansen, M. & Jäättelä, M. Connecting endoplasmic reticulum stress to autophagy by unfolded protein response and calcium. *Cell Death Differ.* **14,** 1576–1582 (2007).

335. Graef, M. & Nunnari, J. Mitochondria regulate autophagy by conserved signalling pathways. *EMBO J.* **30,** 2101–2114 (2011).

336. Demers-Lamarche, J. *et al.* Loss of Mitochondrial Function Impairs Lysosomes. *J. Biol. Chem.* **291,** 10263–10276 (2016).

337. Las, G., Serada, S. B., Wikstrom, J. D., Twig, G. & Shirihai, O. S. Fatty Acids Suppress Autophagic Turnover in β-Cells. *J. Biol. Chem.* **286,** 42534–42544 (2011).

338. Ron, D. & Walter, P. Signal integration in the endoplasmic reticulum unfolded protein response. *Nat. Rev. Mol. Cell Biol.* **8,** 519–529 (2007).

339. Ross, C. A. & Poirier, M. A. Protein aggregation and neurodegenerative disease. *Nat. Med.* **10,** S10–S17 (2004).

340. Wang, P., Wander, C. M., Yuan, C. X., Bereman, M. S. & Cohen, T. J. Acetylation-induced TDP-43 pathology is suppressed by an HSF1-dependent chaperone program. *Nat. Commun.* **8,** 1–15 (2017).

341. Chen, H.-J. *et al.* The heat shock response plays an important role in TDP-43 clearance: evidence for dysfunction in amyotrophic lateral sclerosis. *Brain* **139,** 1417–1432 (2016).

342. Neef, D. W., Jaeger, A. M. & Thiele, D. J. Heat shock transcription factor 1 as a therapeutic target in neurodegenerative diseases. *Nat. Rev. Drug Discov.* **10,** 930–944 (2011).

343. Nah, J., Yuan, J. & Jung, Y.-K. Autophagy in neurodegenerative diseases: from mechanism to therapeutic approach. *Mol. Cells* **38,** 381–9 (2015).

344. Gao, F., Almeida, S. & Lopez-Gonzalez, R. Dysregulated molecular pathways in amyotrophic lateral sclerosis–frontotemporal dementia spectrum disorder. *EMBO J.* **36,** 2931–2950 (2017).

345. Desai, S. *et al.* Heat shock factor 1 (HSF1) controls chemoresistance and autophagy through transcriptional regulation of autophagy-related protein 7 (ATG7). *J. Biol. Chem.* (2013). doi:10.1074/jbc.M112.422071

346. Brahimi-Horn, M. C., Chiche, J. & Pouysségur, J. Hypoxia and cancer. *J. Mol. Med.* **85,** 1301–1307 (2007).

347. Księżakowska-Łakoma, K., Żyła, M. & R. Wilczyński, J. Mitochondrial dysfunction in cancer. *Menopausal Rev.* **2,** 136–144 (2014).

348. Liou, G.-Y. & Storz, P. Reactive oxygen species in cancer. *Free Radic. Res.* **44,** 479–496 (2010).

349. Gleave, M. E. & Monia, B. P. Antisense therapy for cancer. *Nat. Rev. Cancer* **5,** 468–479 (2005).

350. Liang, X. H. *et al.* Induction of autophagy and inhibition of tumorigenesis by beclin 1. *Nature* **402,** 672–676 (1999).

351. Takamura, A. *et al.* Autophagy-deficient mice develop multiple liver tumors. *Genes Dev.* **25,** 795–800 (2011).

352. Hu, W., Alvarez-Dominguez, J. R. & Lodish, H. F. Regulation of mammalian cell differentiation by long non-coding RNAs. *EMBO Rep.* **13,** 971–983 (2012).

353. Wang, K. C. & Chang, H. Y. Molecular mechanisms of long noncoding RNAs. *Mol. Cell* **43,** 904–914 (2011).

354. Yamazaki, T. & Hirose, T. The building process of the functional paraspeckle with long non-coding RNAs. *Front. Biosci. (Elite Ed).* **7,** 1–41 (2015).

355. Wu, Y. *et al.* Nuclear-enriched abundant transcript 1 as a diagnostic and prognostic biomarker in colorectal cancer. *Mol. Cancer* **14,** 191 (2015).

PAPER I

JBC Papers in Press. Published on October 10, 2018 as Manuscript RA118.004473
The latest version is at http://www.jbc.org/cgi/doi/10.1074/jbc.RA118.004473

The long non-coding RNA NEAT1 and nuclear paraspeckles are upregulated by the transcription factor HSF1 in the heat shock response

S. Mohammad Lellahi[1], Ingrid Arctander Rosenlund[1], Annica Hedberg[1], Liv Torill Kiær[1], Ingvild Mikkola[2], Erik Knutsen[1], Maria Perander[1*].

[1]Department of Medical Biology, Faculty of Health Sciences, UiT – The Arctic University of Norway, Tromsø, Norway
[2]Department of Pharmacy, Faculty of Health Sciences, UiT – The Arctic University of Norway, Tromsø, Norway

Running title: *NEAT1 is a novel HSF1 target gene in the heat shock response*

[*]To whom correspondence should be addressed: RNA and molecular pathology research group, Department of Medical Biology, Faculty of Health Sciences, UiT – the Arctic University of Norway, N-9037 Tromsø, Norway. Tel.: +47 77649253; E-mail: maria.perander@uit.no

Keywords: NEAT1, paraspeckle formation, HSF1, Sulforaphane, heat shock response, transcription factor, lncRNA, nuclear paraspeckle, chaperone, stress response

ABSTRACT

The long non-coding RNA (lncRNA) NEAT1 is the architectural component of nuclear paraspeckles, and has recently gained considerable attention as it is abnormally expressed in pathological conditions such as cancer and neurodegenerative diseases. NEAT1 and paraspeckle formation are increased in cells upon exposure to a variety of environmental stressors, and believed to play an important role in cell survival. The present study was undertaken to further investigate the role of NEAT1 in cellular stress response pathways. We show that NEAT1 is a novel target gene of heat shock transcription factor 1 (HSF1), and upregulated when the heat shock response pathway is activated by Sulforaphane (SFN) or elevated temperature. HSF1 binds specifically to a newly identified conserved heat shock element (HSE) in the NEAT1 promoter. In line with this, SFN induced the formation of NEAT1-containing paraspeckles via a HSF1-dependent mechanism. HSF1 plays a key role in the cellular response to proteotoxic stress by promoting the expression of a series of genes, including those encoding molecular chaperones. We have found that the expression of HSP70, HSP90, and HSP27 is amplified and sustained during heat shock in NEAT1-depleted cells compared to control cells, indicating that NEAT1 feeds back via an unknown mechanism to regulate HSF1 activity. This interrelationship is potentially significant in human diseases such as cancer and neurodegenerative disorders.

NEAT1 (Nuclear Enriched Abundant Transcript 1) is a highly abundant long non-coding RNA (lncRNA) that is essential for the formation of specific nuclear bodies called paraspeckles (1-3). There are two overlapping isoforms of NEAT1 transcribed from the same promoter: NEAT1_1 of 3.7 kb and NEAT1_2 of 22.3 kb (2-4). NEAT1_2 is indispensable for paraspeckle formation and is generated when the polyadenylation signal, and thus termination of the NEAT1_1 transcript, is suppressed by an hnRNPK-dependent mechanism (4). Unlike NEAT1_1, the 3' end of NEAT1_2 is not polyadenylated, but processed by RNAse P cleavage and subsequently stabilized through formation of a triple helical structure (3,5,6).

Whereas NEAT1_1 is highly expressed in many tissues in mice, the expression pattern of NEAT1_2, and consequently the presence of paraspeckles, are more restricted (7). Recently, NEAT1 was found to be required for mammary gland development and lactation in mice (8). NEAT1 has also a critical role in corpus luteum formation (9). Even though the function of NEAT1 is still not fully understood, several reports have suggested that increased NEAT1 expression regulates the expression of certain genes by sequestering specific mRNAs and proteins into paraspeckles (10-12). NEAT1 expression is upregulated in response to different cellular stresses including viral infections, proteasome inhibition, oncogene-induced replication stress, and hypoxia (11-17). Emerging evidences suggest that NEAT1 plays a cytoprotective role, as cells deficient of NEAT1 display increased sensitivity towards stress-induced cell death (11,15). In line with this, NEAT1 was found to be transcriptionally activated by HIF2α in response to hypoxia in cancer cells, and more recently, reported as a p53 target gene that prevents replication stress and DNA damage induced by mutagenic agents and oncogenes (13,15,18,19). Interestingly, high levels of NEAT1 are associated with tumorigenic characteristics and poor clinical outcome in several human cancers (13,15,20).

Cells are constantly subjected to extrinsic and intrinsic stressors that might have detrimental effects unless neutralized by specific cytoprotective mechanisms. The heat shock response is a universal cellular defense mechanism towards agents causing proteotoxic stress (21,22) . Elevated temperatures, as well as wide range of oxidative and electrophilic agents, cause misfolding and damage of cellular proteins that will lead to cellular dysfunction or death unless repaired and/or removed. The heat shock transcription factor 1 (HSF1) plays a key role in this response mechanism (21-24). Under normal conditions, HSF1 is kept in an inactive form in the cytoplasm by a multichaperone complex consisting of Hsp90, Hsp70, Hsp40, and TriC (23,25-29). Upon activation, HSF1 is released from the repressive complex, undergoes a series of posttranslational modifications, and forms homotrimers that accumulates in the nucleus (21,23,30). Here, HSF1 stimulates the transcription of genes encoding proteins involved in repair and clearance of damaged proteins (21,23,31). HSF1 specifically binds to heat shock elements (HSE), inverted repeats of nGAAn where "n" is any nucleotide, in the upstream regulatory regions of its target genes (32,33). Among the best-studied target genes of HSF1 are those encoding protein chaperones including Hsp70 and Hsp90 that restore proteostasis by regulating folding, activity, and degradation of proteins (34,35). The heat shock response is attenuated when HSF1 is released from the promoters of its target genes, and either degraded or re-engaged into the HSF1-repressive multichaperone complex by a negative feedback mechanism (21,36).

Here, we report that the isothiocyanate compound sulforaphane (SFN) induces NEAT1 expression and paraspeckle formation in MCF7 cells. This is not dependent on the Keap1-NRF2 pathway, but on binding and transcriptional activation of the NEAT1 promoter by HSF1. We have identified a HSE site in the NEAT1 promoter that is highly conserved among vertebrates. Moreover, we show that NEAT1 is upregulated in response to heat shock demonstrating that upregulation of NEAT1 is a general event in the heat shock response. Finally, we demonstrate that the expression of HSP70, HSP90, and HSP27 is enhanced and sustained in the heat shock response in NEAT1 knockdown cells, compared to control cells.

RESULTS

SFN induces NEAT1 expression and paraspeckle formation

Several lines of evidence clearly point towards NEAT1 being a stress-induced lncRNA that is involved in cytoprotection (11,13,15). NEAT1 expression has recently been shown to be induced by hypoxia and confers protection to hypoxia-induced cell death in breast cancer cells (15). To further determine the role of NEAT1 in oxidative stress, MCF7 cells were treated with the isothiocyanate sulforaphane (SFN), which triggers an antioxidative response in cells by modifying thiol groups in several proteins, including Keap1 in the Keap1-NRF2 pathway (37,38). NEAT1 expression was assessed by RT-qPCR using two different primer sets; one recognizing both isoforms and one solely recognizing the long NEAT1_2 isoform (Fig. 1*A*). SFN potently and

rapidly induced the expression of NEAT1 in MCF7 cells (Fig. 1*A*). Pretreatment of cells with N-acetylcysteine, a strong antioxidant and precursor of cellular glutathione, counteracted the effect of SFN on NEAT1 expression (Fig. 1*B*).

Paraspeckles are dynamic ribonucleoprotein complexes that form around the NEAT1_2 isoform in the nucleus (4). To determine if SFN-induced NEAT1 expression is associated with increased paraspeckle formation, we performed RNA-fluorescence in-situ hybridization (RNA-FISH) on untreated and SFN-treated MCF7 cells using probes recognizing the long NEAT1_2 isoform. Whereas NEAT1_2-containing punctas appeared small and scarcely distributed in the nucleus of untreated MCF7 cells, SFN treatment potently increased the numbers and the overall signal intensity of the paraspeckles (Fig., 1*C* and *D*).

SFN-induced NEAT1 expression is not dependent on NRF2

SFN stimulates several stress signaling pathways in cells, of which the Keap1-NRF2 pathway is the most prominent. To determine if NRF2 is involved in SFN-induced NEAT1 expression, MCF7 cells were transfected with an siRNA towards NRF2 and stimulated with SFN for 6 hours. The NRF2 protein accumulated after 6h SFN treatment, but its depletion did not interfere with the induction of NEAT1 (Fig. 2*A*). We also assessed the NEAT1 expression in control and NRF2-depleted cells after a prolonged treatment with SFN for 24 hours. Elevated levels of NEAT1 were observed in both control and siNRF2-transfected cells (Fig. 2*B*). In contrast, SFN-mediated induction of NQO1 mRNA, a well-established target of NRF2, was severely reduced in NRF2-depleted cells (Fig. 2*C*). We conclude that SFN-induced NEAT1 expression is not dependent on the Keap1-NRF2 pathway.

SFN-induced NEAT1 expression and paraspeckle formation are dependent on HSF1

SFN, as well as other oxidants, have recently been shown to stimulate HSF1, the key transcription factor conferring cellular protection to agents causing protein misfolding (39,40). We therefore sought to determine if SFN-induced NEAT1 expression is dependent on a mechanism involving HSF1. SFN treatment indeed induced a mobility shift of HSF1, which is associated with its activation, and nuclear accumulation of the protein (Fig. 3, *A* and *B*). Consistent with the observed shift and nuclear translocation of HSF1, SFN potently induced the expression of the HSP70 mRNA, a prominent target gene of HSF1 (Fig. 3*C*). We next transfected MCF7 cells with two different siRNAs specifically silencing HSF1 expression, and determined the effect on SFN-induced NEAT1 expression. Both siRNAs significantly reduced the increase in NEAT1 levels observed after SFN treatment (Fig. 3*D*). The same was observed when HSF1 expression was silenced in SFN-treated HeLa cells (Fig. 3*E*). To determine if SFN-induced paraspeckle formation is dependent on HSF1, we performed co-immuno-FISH analyses on control and HSF1-depleted cells using an HSF1 antibody and probes specifically binding to NEAT1_2. In line with the observations described above, SFN enhanced the nuclear staining of HSF1 (Fig. 4, *A* and *B*) and the formation of NEAT1_2 containing paraspeckles (Fig. 4, *A* and *C*). Importantly, SFN-induced paraspeckle formation was severely compromised in HSF1-depleted cells (Fig. 4, *A* and *C*). Taken together, our data clearly demonstrate that HSF1 is essential for increased NEAT1 expression and paraspeckle formation as response to SFN-treatment in MCF7 cells.

NEAT1 is transcriptionally regulated by HSF1

Having established that SFN induces NEAT1 expression by an HSF1-dependent mechanism, we next asked if SFN treatment leads to transcriptional activation of the NEAT1 gene. A luciferase reporter vector containing nucleotides -4040 to +144 of the NEAT1 upstream regulatory region was generated and transfected into MCF7 cells. Reporter gene assays were performed in extracts from untreated and SFN-treated cells. SFN significantly stimulated the NEAT1 promoter-driven luciferase activity (Fig. 5*A*). This stimulation was severely compromised upon co-transfection with an HSF1-directed siRNA, demonstrating that SFN-induced activation of the NEAT1 promoter is dependent on HSF1 (Fig. 5*B*). HSF1 binds to heat shock elements (HSE) within its target genes that are composed of alternating inverted repeats of 5 base pairs, nGAAn where "n" is any nucleotide (32,33). We carefully inspected the NEAT1 promoter, and identified three putative HSEs. One of these, located between nucleotides -

445 and -431 specifically caught our attention as it is highly conserved between species (Fig. 5*C*). To determine if this region is involved in SFN-activated NEAT1 transcription, a truncated construct of the NEAT1 promoter reporter vector was made containing nucleotides -470 to +144. We also made a mutated version where we introduced four point mutations in the predicted HSE core, and both constructs were transfected into MCF7 cells. SFN potently stimulated transcription from the truncated NEAT1 promoter (Fig. 5*D*). This stimulation was absolutely dependent on an intact HSE core, as point mutations in this region totally abolished the SFN-induced increase in NEAT1 promoter driven luciferase activation. To analyze if HSF1 can bind to the NEAT1 promoter in vivo, ChIP experiments were conducted on untreated and SFN treated MCF7 cells using an antibody against HSF1 and RT-qPCR primers amplifying a 100 base pair fragment of the NEAT1 promoter encompassing the HSE site. HSE-containing NEAT1 promoter fragments co-precipitated with the HSF1 antibody (Fig. 5*E*). Importantly, SFN robustly increased HSF1 binding to NEAT1 HSE fragments. Primers amplifying a GAPDH fragment and a region of the NEAT1 promoter upstream of the HSE site ("upstr") were used as controls. Control ChIPs with IgG gave very high Ct values compared to that of the HSF1 antibody and, importantly, showed no differences upon SFN stimulation.

NEAT1 is induced by heat shock

Having established that NEAT1 levels are enhanced by an HSF1-dependent mechanism upon SFN treatment, we next sought to determine if NEAT1 is induced as response to heat shock (HS). MCF7 cells were incubated at 43°C for 30 min, and either harvested directly, or after recovery at 37°C for the indicated periods. HSF1 was rapidly activated during HS as assessed by a mobility shift in western blot (Fig. 6*A*). This was accompanied by increased expression of the HSP70 mRNA (Fig. 6*B*). Importantly, HS rapidly and transiently stimulated the expression of NEAT1 (Fig. 6*C*). This indicates that elevated NEAT1 expression is a general mechanism in the heat shock response pathway.

Proliferation is compromised and expression of HSF1 target genes is amplified in NEAT1-depleted cells

Elevated NEAT1 levels and paraspeckle formation in response to cellular stress are widely observed, and believed to play a pro-survival role by regulating the expression of specific genes. To start unravelling the function of NEAT1 in the heat shock response, we measured the sensitivity of control and NEAT1-depleted cells to heat shock by cell confluence proliferation assays. MCF7 cells were transfected with NEAT1-specific gapmeR antisense oligonucleotides (ASOs), which generally reduced the NEAT1 expression by 70-80 % for up to 120 hours, or a control gapmeR. Cell confluence was then monitored for 96 hours using the IncuCyte® live cell analysis system. After the first 48 hours, half of the cells were subjected to heat shock for 30 min, and then returned to IncuCyte system for another 48 hours. Strikingly, NEAT1-depletion severely decreased the confluency of MCF7 cells, indicating that NEAT1 is necessary for their proliferation or survival (Fig. 7*A*). The proliferation rate was not further decreased after heat shock compared to cells kept at 37°C over the whole monitoring period (Fig. 7*A* and *B*). Taken together, this suggests that NEAT1 is generally required for the proliferation or survival of MCF7 cells, and that an additional stress such as heat shock, does not further affect the already growth-inhibited cells. Control-transfected cells generally recovered well after heat shock with only a slight reduction in confluency (Fig 7*A* and *B*).

To further analyze the role of NEAT1 in the heat shock response, we assayed the expression of the HSF1 target genes HSP70, HSP90, and HSP27 in control and NEAT1-depleted cells. MCF7 cells were transfected with two different gapmeR ASOs, which either targeted both isoforms of NEAT1, or solely the long NEAT1_2 isoform. Transfected cells were exposed to heat shock and HSP70, HSP90, and HSP27 expression was assessed by RT-qPCR. Interestingly, the expression of all target genes was repeatedly amplified and sustained in cells where NEAT1 was silenced, compared to cells transfected with a control gapmeR (Fig. 8). Moreover, the background expression in unstressed cells was slightly enhanced. Of note, a stronger effect on the HSF1

target genes was observed for cells transfected with the gapmeR targeting both isoforms of NEAT1, compared to those transfected with the gapmeR only silencing the NEAT1_2 isoform. Taken together, our data suggest that NEAT1-depletion, by some mechanism, potentiates the HSF1 activity by either creating additional proteotoxic stress in the cells, or by regulating the turnover or the activity of the HSF1 protein.

DISCUSSION

High-throughput RNA-sequencing has demonstrated that most cells express a plethora of long non-coding transcripts (41,42). During the last few years, huge efforts have been made to reveal their biological function, and many of them now appear as important contributors to gene regulation at different levels. NEAT1 is the architectural component of nuclear ribonucleoprotein complexes called paraspeckles, and has recently gained considerable attention as several reports have shown that the transcript is abnormally expressed in human diseases including cancer (13,15,20). The function of NEAT1 remains elusive, but emerging evidences suggest that NEAT1 and paraspeckles have a role in cytoprotection. Here, we show that NEAT1 is induced at the transcriptional level by the isothiocyanate compound sulforaphane (SFN). This is accompanied with increased paraspeckle formation. SFN mimics oxidative stress in cells by modifying thiol groups in cellular proteins, and induces antioxidative response pathways of which Keap1-NRF2 is the most prominent (37,38). We demonstrate that SFN-induced NEAT1 expression is not dependent on NRF2. In contrast, depletion of HSF1 severely abrogates SFN-induced NEAT1 expression and paraspeckle formation. Several reports have shown that SFN and other sulfhydryl-reactive compounds can stimulate the heat shock response pathway in cells by activating HSF1 (39,40,43,44). The mechanism for how SFN activates HSF1 is somewhat obscure, but previous studies have shown that oxidative compounds might promote the DNA-binding activity of HSF1 by modifying cysteine residues in the DNA-binding domain (45,46). SFN has also been shown to modify Hsp90 and thereby disrupt complex formation between Hsp90 and its protein partners (47,48). Recently, Naidu et al. reported that phenethyl isothiocyanate (PEITC) indeed modified cysteine residues within Hsp90 leading to dissociation and activation of HSF1 (44).

Our results show that HSF1 accumulates in the nucleus upon SFN treatment and binds to the NEAT1 promoter in vivo. We have identified a conserved HSE in the NEAT1 promoter that is critical for SFN-induced transcriptional activation of the NEAT1 gene. Intriguingly, this site overlaps with a recently reported NF-κB binding site, which is necessary for LPS-induced NEAT1 expression in lung cancer cells (49). An overlapping NF-κB and HSF1 binding site has been identified previously in the promotor of the gene encoding MHC Class I Chain-Related Protein A (MICA) (50). Here, HSF1 and NF-κB bind mutually exclusive to the site, and overexpression of a truncated version of HSF1 containing only the DNA-binding domain outcompetes NF-κB binding and abolishes TNFα-induced MICA expression. If the overlapping HSF1/NF-κB site in the NEAT1 promoter represents a regulatory hub, coordinating outputs from different signaling pathways, remains to be resolved.

In the present study we show that NEAT1, as well as being induced by SFN, is also induced upon heat shock. This clearly suggests that NEAT1 upregulation is a general phenomenon in the heat shock response. This is supported by a study by Hirose et al., demonstrating that NEAT1 expression and paraspeckle formation are induced by inhibition of the 26S proteasome by MG132 or Bortezomib (11). Proteasome inhibition causes a proteotoxic stress in the cells as proteins that are destined for degradation form aggregates in both the cytoplasm and the nucleus (11,51). Activation of HSF1 to induce expression of molecular chaperones, is a general cellular response mechanisms to proteasome inhibition (52-54). Thus, we envision that NEAT1 induction upon proteasome inhibition might be mediated by HSF1-mediated transcriptional activation of the NEAT1 promoter.

Several reports have shown that NEAT1-depletion sensitizes cells to a variety of stressors. Thus, we hypothesized that knock down of NEAT1 expression would make cells more susceptible to heat shock. However, we repeatedly observed that transient transfection with NEAT1 antisense oligos by itself, dramatically reduced the proliferation of MCF7 cells, and that this tendency was not

reinforced by heat shock. This shows that MCF7 cells cultivated *in vitro*, are highly dependent on NEAT1. To further dissect the function of NEAT1 in the heat shock response, we knocked down NEAT1 expression by antisense oligos and assessed the effect on the expression of three HSF1 target genes including HSP70, HSP90, and HSP27. Interestingly, knockdown of NEAT1 amplified and prolonged the expression of these target genes. The mechanism for this is still obscure. NEAT1-depletion abrogates the formation of paraspeckles (4). This might lead to mislocalization of paraspeckle-associated proteins that disturbs proteostasis in the cells, and thereby contribute to the activation of HSF1. Alternatively, NEAT1 might regulate the turnover of the HSF1 protein or activity by a negative feedback mechanism. Interestingly, the effect of NEAT1-depletion on HSF1 target genes, was significantly stronger when cells were transfected with a gapmeR targeting both isoforms compared to one only reducing NEAT1_2 expression. This indicates that the short NEAT1_1 isoform has an important function in the regulation of the heat shock response.

HSF1 plays a critical role in the cellular defense to proteotoxic stress. Many neurodegenerative diseases including amyotrophic lateral sclerosis (ALS), Huntington's disease, and Alzheimer are associated with the formation of protein aggregates (31,55). Loss of HSF1 expression or activity is frequently observed in these diseases (55-58). Our results demonstrate that HSF1 activates the expression of NEAT1 during the heat shock response. Interestingly, several reports have shown that NEAT1 is abnormally expressed in ALS and Huntinton's disease (59-61). Moreover, mislocalization of two paraspeckle proteins, FUS (Fused in sarcoma) and TDP-43 (TAR DNA-binding protein-43) is well-known to be associated with ALS (62). It has been speculated that NEAT1 expression and paraspeckle formation might have a protective role in neuronal cells in early stages of ALS and Hungtinton's disease (60,61,63). In line with this, Hirose et al. showed that mouse embryonic fibroblasts from NEAT1 knockout cells displayed an increased sensitivity to proteasome inhibitors causing formation of protein aggregates, compared to wild-type cells (11). The crosstalk between NEAT1, paraspeckle formation, sub-cellular localization of FUS and TDP-43, and HSF1 in these devastating diseases should be a focus of future research.

Constitutive activation of HSF1 and abnormal expression of NEAT1 are both frequently observed in human cancers (13,15,20,64-66). There are clear evidences that both HSF1 and NEAT1 have cytoprotective roles in tumors and are associated with poor prognosis. In the present study, we demonstrate that NEAT1 is a novel target gene of HSF1. It remains to be determined if there is any correlation between HSF1 activation and NEAT1 expression in cancer.

EXPERIMENTAL PROCEDURES

Cell culture and treatments

MCF7 (ATCC® HTB-22™) and HeLa (ATCC® CCL-2™) cells were purchased from American Type Culture Collection and maintained in minimal essential medium (MEM, Sigma-Aldrich) supplemented with 10% fetal bovine serum (Biochrom) and 1% penicillin-streptomycin (Sigma-Aldrich). MCF7 cells were cultured in the presence of 0.01 mg /ml insulin (Sigma-Aldrich). All Cells were grown at 37°C in humidified condition containing 5% CO_2. Sulforaphane (SFN, cat# S4441) and N-acetyl cysteine (NAC, cat# A9165) were purchased from Sigma-Aldrich. SFN was added to the cells at a final concentration of 20 μM for short-term treatments up to 8 hours, and at a final concentration of 10 μM for long-term treatment (24 hours). When included, NAC (5 mM) was added to the media 1 hour before SFN treatment. To induce a cellular heat shock response, cells were incubated at 43°C for 30 minutes, and then either harvested directly or returned to 37° for recovery.

Plasmid constructions

The human NEAT1 promoter (-4040/+144) was cloned from genomic DNA by performing two PCR amplification reactions using PrimeSTAR®GXL DNA Polymerase (Takara Bio Inc, R050Q) generating fragments of 1756 bp (primers NP1.1F/NP2.1R) and 2414 bp (nested PCR, outer primer set NP2.1F/NP3.1R; inner primer set NP2.2F/NP3.2R). The 1756 bp fragment was digested with NheI (provided in primer) and HindIII (internal) and cloned into corresponding sites in pGL3-Basic (Promega). This was followed by insertion of the 2414 bp fragment into the

HindIII site using internal HindIII sites. The resulting pNEAT1(-4040/+144)-Luc plasmid was verified by sequencing. pNEAT1(-470/+144)-luc was generated from a promoter construct containing the 2414 PCR-product (pNEAT1(-2384bp/+144)-luc) by cutting with KpnI and PstI followed by religation. pNEAT1(-470/+144)-HSEmut-luc was made by site-directed mutagenesis according to the QuickChange II Site-Directed Mutagenesis kit protocol (Agilent Technologies). All primer sequences are provided in Table 1.

RNA interference

siNRF2 (siGENOME SMART pool Human NFE2L2, DM-003-755-02) was purchased from Dharmacon, and siHSF1_#1 (Silencer® Select, s6950), siHSF1_#2 (Silencer® Select, s6952), and Silencer® Select Negative Control No.2 were obtained from Thermo Fisher Scientific. Locked nucleic acid (LNA)-GapmeR NEAT1 antisense oligos and control GapmeRs were purchased from Exiqon. All sequences are provided in Table 1. Cells were transfected using Lipofectamine 2000 according to the reverse transfection protocol provided by the manufacturer (Thermo Fisher Scientific). Successful knock down was verified by RT-qPCR or Western blot analyses.

Reverse transcription and quantitative PCR

Cells were lysed in 300 µl Tri Reagent, and total RNA was isolated with Direct-zol RNA MiniPrep (Zymo Research) according to the manufacturer. RNA concentration was measured by NanoDrop 2000 (Thermo Fisher Scientific), and cDNA synthesis of total RNA was performed with SuperScript™ IV Reverse Transcriptase (Thermo Fisher Scientific). 2.5 µM of random hexamer primer (Thermo Fisher Scientific) and approximately 250 ng of template was used for the reaction. Total RNA was denaturated at 65ºC for 5 min, and cDNA was synthesized at 50 ºC for 10 minutes. Quantitative PCR was run on a LightCycler 96 (Roche Life Science) with the SYBR green reaction mix FastStart Essential DNA Green Master (Roche Life Science) and 0.25 µM forward and reverse primer. (Thermal cycle conditions; 95°C 10 minutes and 40 cycles of 95°C 10 seconds, 60°C 10 seconds and 72°C for 10 seconds). All primers sequences are provided in Table 1. Experiments were done in triplicates, and the ΔΔCq method was used for fold change calculations. GAPDH was used as reference gene.

Immunoblotting

Whole-cell extracts (WCE) were made by lysing cells directly in 2 x NuPAGE LDS Sample Buffer (Thermo Fisher Scientific). Nuclear extracts (NE) were isolated using the NE-PER™ Nuclear and Cytoplasmic Extraction kit (Thermo Fisher Scientific) according to manufacturer's instruction. In brief, cells were resuspended in Cytoplasmic Extraction reagent I and II and nuclei were pelleted by centrifugation at 16 000 g. The pellet was resuspended in ice-cold Nuclear Extraction Reagent, vortexed for 1 minute and incubated on ice for 10 minutes. This step was repeated 3 more times before centrifugation at 16 000 g for 10 minutes. Proteins were resolved on SDS-PAGE gels and transferred to nitrocellulose membranes. Equal loading of proteins was verified by probing the membranes with an antibody recognizing actin (WCE) or lamin B (NE). The following primary antibodies were used, all at 1:000 dilution: Rabbit anti-NRF2 (Abcam, cat# ab62359), rabbit anti-HSF1 (Cell Signaling, cat# 4356), rabbit anti-Lamin B (Proteintech, ca# 12987-1-AP), mouse anti-Actin (Millipore, MAB1501). The blots were detected with IRDye®-conjugated secondary antibodies (LI-COR Biosciences) at a 1:10 000 dilution (800CW goat anti-rabbit, cat# 926-32211; 680LT goat anti-mouse, cat# 926-68020), and the Odyssey® CLx Infrared Imaging System.

RNA-fluorescence in situ hybridization and immunofluorescence staining

Stellaris® NEAT1 RNA FISH probes recognizing the NEAT1_2 isoform (VSMF-2251-5, Quasar® 670-conjugated) were purchased from LGC Biosearch Technologies. Preparation of cells, hybridization, and mounting were performed according to the Stellaris® RNA FISH Probes manuals. In brief, cells were seeded onto circular coverslips in 12-well dishes and allowed to attach for 2-3 days. They were fixed with 4% freshly made formaldehyde at room temperature, and permeabilized with 70% ethanol. Hybridization was done at 37ºC in a humidifying chamber overnight. For co-immuno-FISH experiments, the hybridization was performed as described above

and cells were subsequently incubated in 1% RNAse-free BSA for 30 minutes, and then stained with anti-HSF1 antibody for 1 hour (1:50, Cell Signaling, cat# 4356A). Cells were incubated with goat anti-rabbit Alexa 488-conjugated secondary antibody (1:500, Thermo Fisher Scientific, cat# A11070), and mounted using Vectashield® Antifade Mounting Medium containing DAPI (Vector Laboratories, H-1200). Images were generated using a Zeiss LSM780 confocal microscope (Carl Zeiss Microscopy GmbH, Jena, Germany). In all samples, Z-stacks (5 slices, 2.5 µm total height) images were taken at 40x magnification. For all images, the middle Z slice was positioned at DAPI's best focus. The same treatment and setting were applied to all replicates, and for each slide at least ten pictures were taken for volocity analysis. The Volocity software (PerkinElmer, version 6.3) was used to measure signals intensity for both NEAT 1_2 and HSF1 signals. At least 250 cells in each group of treatment were analyzed by volocity software. The mean intensity of NEAT 1_2 or nuclear HSF1 signals in the SFN-treated group were normalized against CTRL.

Reporter gene assays

Sub-confluent MCF7 cells in 12-well plates were transfected with 150 ng of luciferase reporter plasmids using Lipofectamine®2000 reagent (Thermo Fisher Scientific) according to the manual provided by the manufacturer. After 24 hours, cells were either left untreated or treated with SFN (20 µM) for 8 hours. Cells were harvested and luciferase assays were performed using the Dual-Light® Luciferase & β-Galactosidase Reporter Gene Assay System (Thermo Fisher Scientific). Of note, cells were initially co-transfected with luciferase reporter plasmids and an expression vector for β-galactosidase, but as SFN repeatedly interfered with the β-galactosidase activity in the cells, the expression vector was omitted from the transfections and only the luciferase activity was included in the analyses. Co-transfections with siRNA and plasmid DNA were performed in two steps using Lipofectamine®2000. First, siRNAs were introduced into the cells by reverse transfection. After 48 hours, plated cells were re-transfected with plasmid DNA and left for another 24 hours.

Chromatin immuoprecipitation (ChIP) assays

MCF7 cells were seeded at a density of 6 million cells per 10 cm dish the day before use. The cells were left untreated or treated with SFN (20 µM) for 6 hours before harvesting. Two 10 cm dishes were used per condition. The "iDeal ChIP-seq kit for Transcription Factors" (Diagenode, C01010055) was used for harvest and ChIP according to the manufacturers instruction. The two dishes for each treatment were combined, and the approximate cell number was estimated to be 15 mill of cells. Volumes of buffers used in the kit was adjusted to this. Cells were fixed for 15 minutes. Sonication was performed in ice cold water on a Bioruptor UCD-200 (Diagenode), 30 sec pulses on/off for 3 x 10 min. Samples run on an agarose gel showed majority of DNA with size from 100-400 bp after shearing. For immunoprecipitation, 10 µl of anti HSF1 antibody (Cell Signaling, 4356) or 1 µl of IgG (provided with the kit) was used with 200 µl sheared chromatin. Two µl (1%) of input chromatin was set aside. The eluate had a volume of 25 µl, which was diluted 1/10 before 5 µl was used in a qPCR reaction. qPCR was performed in triplicates on a LightCycler 96 (Roche Life Science). The relative amount of immunoprecipitated (IP) DNA compared to input DNA was calculated using the "percent input method" as follows: Since the input chromatin was 1%, a dilution factor of 100 (6,644 cycles, log2 of 100) was subtracted to adjust input Ct value to 100%. To calculate the percentage of specific chromatin co-immunoprecipitated with the HSF1 antibody or the IgG control, the triplicate average Ct values, Ct(IP), for the specific qPCR primers (HSE, "upstream", and GAPDH) were used in the equation 100*2^(Adjusted input - Ct(IP)). Primer sequences are given in Table 1.

Cell confluence proliferation assay

MCF7 cells were transfected in solution with indicated LNA-GapmeR antisense oligoes and seeded in 96 well plates at an initial confluency of approximately 30% (20 000 cells per well) and immediately placed in an IncuCyte® S3 live-cell analysis system, which is equipped a fully automated microscope for cell confluence monitoring. Three phase contrast images were acquired from each well at 120 minute intervals over a period of 96 hours, using a 20x objective. For each condition, five wells were monitored.

Data was analyzed using the IncuCyte® S3 Software.

Statistics

GraphPad software (Prism version 7, Mac OS X) was used to analyze quantitative data. Statistical significance was evaluated with unpair student t-Test or one-way ANOVA followed by the Dunnett multiple comparison test. The data were considered statistically significant when $p \leq 0.05$. For all experiments significance is expressed as ***, $p \leq 0.001$, **, $p \leq 0.01$, and *, $p \leq 0.05$. The error bars indicate ± S.D. in all figures. All the experiments were performed at least three times.

Acknowledgements: Thanks to Kenneth Bowitz Larsen for help with the image analyses and to Hanne Britt Brenne for technical advices.

Conflict of interest: The authors declare that they have no conflicts of interest with the contents of this article.

REFERENCES

1. Clemson, C. M., Hutchinson, J. N., Sara, S. A., Ensminger, A. W., Fox, A. H., Chess, A., and Lawrence, J. B. (2009) An architectural role for a nuclear noncoding RNA: NEAT1 RNA is essential for the structure of paraspeckles. *Mol Cell* **33**, 717-726
2. Hutchinson, J. N., Ensminger, A. W., Clemson, C. M., Lynch, C. R., Lawrence, J. B., and Chess, A. (2007) A screen for nuclear transcripts identifies two linked noncoding RNAs associated with SC35 splicing domains. *BMC Genomics* **8**, 39
3. Sunwoo, H., Dinger, M. E., Wilusz, J. E., Amaral, P. P., Mattick, J. S., and Spector, D. L. (2009) MEN epsilon/beta nuclear-retained non-coding RNAs are up-regulated upon muscle differentiation and are essential components of paraspeckles. *Genome Res* **19**, 347-359
4. Naganuma, T., Nakagawa, S., Tanigawa, A., Sasaki, Y. F., Goshima, N., and Hirose, T. (2012) Alternative 3'-end processing of long noncoding RNA initiates construction of nuclear paraspeckles. *EMBO J* **31**, 4020-4034
5. Brown, J. A., Valenstein, M. L., Yario, T. A., Tycowski, K. T., and Steitz, J. A. (2012) Formation of triple-helical structures by the 3'-end sequences of MALAT1 and MENbeta noncoding RNAs. *Proc Natl Acad Sci U S A* **109**, 19202-19207
6. Wilusz, J. E., Freier, S. M., and Spector, D. L. (2008) 3' end processing of a long nuclear-retained noncoding RNA yields a tRNA-like cytoplasmic RNA. *Cell* **135**, 919-932
7. Nakagawa, S., Naganuma, T., Shioi, G., and Hirose, T. (2011) Paraspeckles are subpopulation-specific nuclear bodies that are not essential in mice. *J Cell Biol* **193**, 31-39
8. Standaert, L., Adriaens, C., Radaelli, E., Van Keymeulen, A., Blanpain, C., Hirose, T., Nakagawa, S., and Marine, J. C. (2014) The long noncoding RNA Neat1 is required for mammary gland development and lactation. *RNA* **20**, 1844-1849
9. Nakagawa, S., Shimada, M., Yanaka, K., Mito, M., Arai, T., Takahashi, E., Fujita, Y., Fujimori, T., Standaert, L., Marine, J. C., and Hirose, T. (2014) The lncRNA Neat1 is required for corpus luteum formation and the establishment of pregnancy in a subpopulation of mice. *Development* **141**, 4618-4627
10. Chen, L. L., and Carmichael, G. G. (2009) Altered nuclear retention of mRNAs containing inverted repeats in human embryonic stem cells: functional role of a nuclear noncoding RNA. *Mol Cell* **35**, 467-478
11. Hirose, T., Virnicchi, G., Tanigawa, A., Naganuma, T., Li, R., Kimura, H., Yokoi, T., Nakagawa, S., Benard, M., Fox, A. H., and Pierron, G. (2014) NEAT1 long noncoding RNA regulates transcription via protein sequestration within subnuclear bodies. *Mol Biol Cell* **25**, 169-183

12. Imamura, K., Imamachi, N., Akizuki, G., Kumakura, M., Kawaguchi, A., Nagata, K., Kato, A., Kawaguchi, Y., Sato, H., Yoneda, M., Kai, C., Yada, T., Suzuki, Y., Yamada, T., Ozawa, T., Kaneki, K., Inoue, T., Kobayashi, M., Kodama, T., Wada, Y., Sekimizu, K., and Akimitsu, N. (2014) Long noncoding RNA NEAT1-dependent SFPQ relocation from promoter region to paraspeckle mediates IL8 expression upon immune stimuli. *Mol Cell* **53**, 393-406
13. Adriaens, C., Standaert, L., Barra, J., Latil, M., Verfaillie, A., Kalev, P., Boeckx, B., Wijnhoven, P. W., Radaelli, E., Vermi, W., Leucci, E., Lapouge, G., Beck, B., van den Oord, J., Nakagawa, S., Hirose, T., Sablina, A. A., Lambrechts, D., Aerts, S., Blanpain, C., and Marine, J. C. (2016) p53 induces formation of NEAT1 lncRNA-containing paraspeckles that modulate replication stress response and chemosensitivity. *Nat Med* **22**, 861-868
14. Beeharry, Y., Goodrum, G., Imperiale, C. J., and Pelchat, M. (2018) The Hepatitis Delta Virus accumulation requires paraspeckle components and affects NEAT1 level and PSP1 localization. *Sci Rep* **8**, 6031
15. Choudhry, H., Albukhari, A., Morotti, M., Haider, S., Moralli, D., Smythies, J., Schodel, J., Green, C. M., Camps, C., Buffa, F., Ratcliffe, P., Ragoussis, J., Harris, A. L., and Mole, D. R. (2015) Tumor hypoxia induces nuclear paraspeckle formation through HIF-2alpha dependent transcriptional activation of NEAT1 leading to cancer cell survival. *Oncogene* **34**, 4482-4490
16. Ma, H., Han, P., Ye, W., Chen, H., Zheng, X., Cheng, L., Zhang, L., Yu, L., Wu, X., Xu, Z., Lei, Y., and Zhang, F. (2017) The Long Noncoding RNA NEAT1 Exerts Antihantaviral Effects by Acting as Positive Feedback for RIG-I Signaling. *J Virol* **91**
17. Zhang, Q., Chen, C. Y., Yedavalli, V. S., and Jeang, K. T. (2013) NEAT1 long noncoding RNA and paraspeckle bodies modulate HIV-1 posttranscriptional expression. *MBio* **4**, e00596-00512
18. Idogawa, M., Ohashi, T., Sasaki, Y., Nakase, H., and Tokino, T. (2017) Long non-coding RNA NEAT1 is a transcriptional target of p53 and modulates p53-induced transactivation and tumor-suppressor function. *Int J Cancer* **140**, 2785-2791
19. Mello, S. S., Sinow, C., Raj, N., Mazur, P. K., Bieging-Rolett, K., Broz, D. K., Imam, J. F. C., Vogel, H., Wood, L. D., Sage, J., Hirose, T., Nakagawa, S., Rinn, J., and Attardi, L. D. (2017) Neat1 is a p53-inducible lincRNA essential for transformation suppression. *Genes Dev* **31**, 1095-1108
20. Chakravarty, D., Sboner, A., Nair, S. S., Giannopoulou, E., Li, R., Hennig, S., Mosquera, J. M., Pauwels, J., Park, K., Kossai, M., MacDonald, T. Y., Fontugne, J., Erho, N., Vergara, I. A., Ghadessi, M., Davicioni, E., Jenkins, R. B., Palanisamy, N., Chen, Z., Nakagawa, S., Hirose, T., Bander, N. H., Beltran, H., Fox, A. H., Elemento, O., and Rubin, M. A. (2014) The oestrogen receptor alpha-regulated lncRNA NEAT1 is a critical modulator of prostate cancer. *Nat Commun* **5**, 5383
21. Gomez-Pastor, R., Burchfiel, E. T., and Thiele, D. J. (2018) Regulation of heat shock transcription factors and their roles in physiology and disease. *Nat Rev Mol Cell Biol* **19**, 4-19
22. Li, J., Labbadia, J., and Morimoto, R. I. (2017) Rethinking HSF1 in Stress, Development, and Organismal Health. *Trends Cell Biol* **27**, 895-905
23. Anckar, J., and Sistonen, L. (2011) Regulation of HSF1 function in the heat stress response: implications in aging and disease. *Annu Rev Biochem* **80**, 1089-1115
24. Dayalan Naidu, S., and Dinkova-Kostova, A. T. (2017) Regulation of the mammalian heat shock factor 1. *FEBS J* **284**, 1606-1627
25. Abravaya, K., Myers, M. P., Murphy, S. P., and Morimoto, R. I. (1992) The human heat shock protein hsp70 interacts with HSF, the transcription factor that regulates heat shock gene expression. *Genes Dev* **6**, 1153-1164
26. Ali, A., Bharadwaj, S., O'Carroll, R., and Ovsenek, N. (1998) HSP90 interacts with and regulates the activity of heat shock factor 1 in Xenopus oocytes. *Mol Cell Biol* **18**, 4949-4960
27. Neef, D. W., Jaeger, A. M., Gomez-Pastor, R., Willmund, F., Frydman, J., and Thiele, D. J. (2014) A direct regulatory interaction between chaperonin TRiC and stress-responsive transcription factor HSF1. *Cell Rep* **9**, 955-966

28. Shi, Y., Mosser, D. D., and Morimoto, R. I. (1998) Molecular chaperones as HSF1-specific transcriptional repressors. *Genes Dev* **12**, 654-666
29. Zou, J., Guo, Y., Guettouche, T., Smith, D. F., and Voellmy, R. (1998) Repression of heat shock transcription factor HSF1 activation by HSP90 (HSP90 complex) that forms a stress-sensitive complex with HSF1. *Cell* **94**, 471-480
30. Vujanac, M., Fenaroli, A., and Zimarino, V. (2005) Constitutive nuclear import and stress-regulated nucleocytoplasmic shuttling of mammalian heat-shock factor 1. *Traffic* **6**, 214-229
31. Labbadia, J., and Morimoto, R. I. (2015) The biology of proteostasis in aging and disease. *Annu Rev Biochem* **84**, 435-464
32. Kroeger, P. E., and Morimoto, R. I. (1994) Selection of new HSF1 and HSF2 DNA-binding sites reveals difference in trimer cooperativity. *Mol Cell Biol* **14**, 7592-7603
33. Trinklein, N. D., Chen, W. C., Kingston, R. E., and Myers, R. M. (2004) Transcriptional regulation and binding of heat shock factor 1 and heat shock factor 2 to 32 human heat shock genes during thermal stress and differentiation. *Cell Stress Chaperones* **9**, 21-28
34. Radons, J. (2016) The human HSP70 family of chaperones: where do we stand? *Cell Stress Chaperones* **21**, 379-404
35. Schopf, F. H., Biebl, M. M., and Buchner, J. (2017) The HSP90 chaperone machinery. *Nat Rev Mol Cell Biol* **18**, 345-360
36. Huang, C., Wu, J., Xu, L., Wang, J., Chen, Z., and Yang, R. (2018) Regulation of HSF1 protein stabilization: An updated review. *Eur J Pharmacol* **822**, 69-77
37. Dinkova-Kostova, A. T., Holtzclaw, W. D., Cole, R. N., Itoh, K., Wakabayashi, N., Katoh, Y., Yamamoto, M., and Talalay, P. (2002) Direct evidence that sulfhydryl groups of Keap1 are the sensors regulating induction of phase 2 enzymes that protect against carcinogens and oxidants. *Proc Natl Acad Sci U S A* **99**, 11908-11913
38. Kensler, T. W., Egner, P. A., Agyeman, A. S., Visvanathan, K., Groopman, J. D., Chen, J. G., Chen, T. Y., Fahey, J. W., and Talalay, P. (2013) Keap1-nrf2 signaling: a target for cancer prevention by sulforaphane. *Top Curr Chem* **329**, 163-177
39. Gan, N., Wu, Y. C., Brunet, M., Garrido, C., Chung, F. L., Dai, C., and Mi, L. (2010) Sulforaphane activates heat shock response and enhances proteasome activity through up-regulation of Hsp27. *J Biol Chem* **285**, 35528-35536
40. Zhang, Y., Ahn, Y. H., Benjamin, I. J., Honda, T., Hicks, R. J., Calabrese, V., Cole, P. A., and Dinkova-Kostova, A. T. (2011) HSF1-dependent upregulation of Hsp70 by sulfhydryl-reactive inducers of the KEAP1/NRF2/ARE pathway. *Chem Biol* **18**, 1355-1361
41. Rinn, J. L., and Chang, H. Y. (2012) Genome regulation by long noncoding RNAs. *Annu Rev Biochem* **81**, 145-166
42. Schonrock, N., Jonkhout, N., and Mattick, J. S. (2016) Seq and You Will Find. *Curr Gene Ther* **16**, 220-229
43. Dayalan Naidu, S., Kostov, R. V., and Dinkova-Kostova, A. T. (2015) Transcription factors Hsf1 and Nrf2 engage in crosstalk for cytoprotection. *Trends Pharmacol Sci* **36**, 6-14
44. Naidu, S. D., Suzuki, T., Yamamoto, M., Fahey, J. W., and Dinkova-Kostova, A. T. (2018) Phenethyl Isothiocyanate, a Dual Activator of Transcription Factors NRF2 and HSF1. *Mol Nutr Food Res*, e1700908
45. Ahn, S. G., and Thiele, D. J. (2003) Redox regulation of mammalian heat shock factor 1 is essential for Hsp gene activation and protection from stress. *Genes Dev* **17**, 516-528
46. Lu, M., Kim, H. E., Li, C. R., Kim, S., Kwak, I. J., Lee, Y. J., Kim, S. S., Moon, J. Y., Kim, C. H., Kim, D. K., Kang, H. S., and Park, J. S. (2008) Two distinct disulfide bonds formed in human heat shock transcription factor 1 act in opposition to regulate its DNA binding activity. *Biochemistry* **47**, 6007-6015

47. Gibbs, A., Schwartzman, J., Deng, V., and Alumkal, J. (2009) Sulforaphane destabilizes the androgen receptor in prostate cancer cells by inactivating histone deacetylase 6. *Proc Natl Acad Sci U S A* **106**, 16663-16668
48. Li, Y., Karagoz, G. E., Seo, Y. H., Zhang, T., Jiang, Y., Yu, Y., Duarte, A. M., Schwartz, S. J., Boelens, R., Carroll, K., Rudiger, S. G., and Sun, D. (2012) Sulforaphane inhibits pancreatic cancer through disrupting Hsp90-p50(Cdc37) complex and direct interactions with amino acids residues of Hsp90. *J Nutr Biochem* **23**, 1617-1626
49. Zhou, W., Chen, X., Hu, Q., Chen, X., Chen, Y., and Huang, L. (2018) Galectin-3 activates TLR4/NF-kappaB signaling to promote lung adenocarcinoma cell proliferation through activating lncRNA-NEAT1 expression. *BMC Cancer* **18**, 580
50. Lin, D., Lavender, H., Soilleux, E. J., and O'Callaghan, C. A. (2012) NF-kappaB regulates MICA gene transcription in endothelial cell through a genetically inhibitable control site. *J Biol Chem* **287**, 4299-4310
51. Goldberg, A. L. (2003) Protein degradation and protection against misfolded or damaged proteins. *Nature* **426**, 895-899
52. Holmberg, C. I., Illman, S. A., Kallio, M., Mikhailov, A., and Sistonen, L. (2000) Formation of nuclear HSF1 granules varies depending on stress stimuli. *Cell Stress Chaperones* **5**, 219-228
53. Kim, D., Kim, S. H., and Li, G. C. (1999) Proteasome inhibitors MG132 and lactacystin hyperphosphorylate HSF1 and induce hsp70 and hsp27 expression. *Biochem Biophys Res Commun* **254**, 264-268
54. Zhou, M., Wu, X., and Ginsberg, H. N. (1996) Evidence that a rapidly turning over protein, normally degraded by proteasomes, regulates hsp72 gene transcription in HepG2 cells. J Biol Chem 271, 24769-24775
55. Neef, D. W., Jaeger, A. M., and Thiele, D. J. (2011) Heat shock transcription factor 1 as a therapeutic target in neurodegenerative diseases. *Nat Rev Drug Discov* **10**, 930-944
56. Chen, H. J., Mitchell, J. C., Novoselov, S., Miller, J., Nishimura, A. L., Scotter, E. L., Vance, C. A., Cheetham, M. E., and Shaw, C. E. (2016) The heat shock response plays an important role in TDP-43 clearance: evidence for dysfunction in amyotrophic lateral sclerosis. *Brain* **139**, 1417-1432
57. Gomez-Pastor, R., Burchfiel, E. T., Neef, D. W., Jaeger, A. M., Cabiscol, E., McKinstry, S. U., Doss, A., Aballay, A., Lo, D. C., Akimov, S. S., Ross, C. A., Eroglu, C., and Thiele, D. J. (2017) Abnormal degradation of the neuronal stress-protective transcription factor HSF1 in Huntington's disease. *Nat Commun* **8**, 14405
58. Wang, P., Wander, C. M., Yuan, C. X., Bereman, M. S., and Cohen, T. J. (2017) Acetylation-induced TDP-43 pathology is suppressed by an HSF1-dependent chaperone program. *Nat Commun* **8**, 82
59. Nishimoto, Y., Nakagawa, S., Hirose, T., Okano, H. J., Takao, M., Shibata, S., Suyama, S., Kuwako, K., Imai, T., Murayama, S., Suzuki, N., and Okano, H. (2013) The long non-coding RNA nuclear-enriched abundant transcript 1_2 induces paraspeckle formation in the motor neuron during the early phase of amyotrophic lateral sclerosis. *Mol Brain* **6**, 31
60. Shelkovnikova, T. A., Robinson, H. K., Troakes, C., Ninkina, N., and Buchman, V. L. (2014) Compromised paraspeckle formation as a pathogenic factor in FUSopathies. *Hum Mol Genet* **23**, 2298-2312
61. Sunwoo, J. S., Lee, S. T., Im, W., Lee, M., Byun, J. I., Jung, K. H., Park, K. I., Jung, K. Y., Lee, S. K., Chu, K., and Kim, M. (2017) Altered Expression of the Long Noncoding RNA NEAT1 in Huntington's Disease. *Mol Neurobiol* **54**, 1577-1586
62. Gao, F. B., Almeida, S., and Lopez-Gonzalez, R. (2017) Dysregulated molecular pathways in amyotrophic lateral sclerosis-frontotemporal dementia spectrum disorder. *EMBO J* **36**, 2931-2950
63. Shelkovnikova, T. A., Kukharsky, M. S., An, H., Dimasi, P., Alexeeva, S., Shabir, O., Heath, P. R., and Buchman, V. L. (2018) Protective paraspeckle hyper-assembly downstream of TDP-43 loss of function in amyotrophic lateral sclerosis. *Mol Neurodegener* **13**, 30

64. Dai, C., and Sampson, S. B. (2016) HSF1: Guardian of Proteostasis in Cancer. *Trends Cell Biol* **26**, 17-28
65. Mendillo, M. L., Santagata, S., Koeva, M., Bell, G. W., Hu, R., Tamimi, R. M., Fraenkel, E., Ince, T. A., Whitesell, L., and Lindquist, S. (2012) HSF1 drives a transcriptional program distinct from heat shock to support highly malignant human cancers. *Cell* **150**, 549-562
66. Santagata, S., Hu, R., Lin, N. U., Mendillo, M. L., Collins, L. C., Hankinson, S. E., Schnitt, S. J., Whitesell, L., Tamimi, R. M., Lindquist, S., and Ince, T. A. (2011) High levels of nuclear heat-shock factor 1 (HSF1) are associated with poor prognosis in breast cancer. *Proc Natl Acad Sci U S A* **108**, 18378-18383

Table 1. Primer and siRNA/ASO sequences

Name	Primer sequences (5'→3')
RT-qPCR	
GAPDH	F- GAGCGAGATCCCTCCAAAAT
	R- AAATGAGCCCCAGCCTTCT
***HSP90AA1* (HSP90)**	F- GAGCTTGACCAATGACTGGGA
	R- AGCACGTCGTGGGACAAATA
***HSPA1A* (HSP70)**	F- GGGCCTTTCCAAGATTGCTG
	R- TGCAAACACAGGAAATTGAGAACT
***HSPB1* (HSP27)**	F- TTCACGCGGAAATACACGCT
	R- TTGGACTGCGTGGCTAGCTT
NEAT1	F- TCGGGTATGCTGTTGTGAAA
	R- TGACGTAACAGAATTAGTTCTTACCA
NEAT1_2	F- CGGAGGGTCTTGTAACACCAG
	R- AGTCCGGGCAACACAGAAAG
NQO1	F- GTTGCCTGAAAAATGGGAGA
	R- AAAAACCACCAGTGCCAGTC
Cloning	
NP1.1F	F- GGACGCTAGCCTCCCTTCCTCAGTCAGTCCACAA
NP2.1R	R- CCAAGTCTCCTTTGTGCCCTTGTAT
NP2.1F	F- GTAGAGGAAGAGAGCAGAACCCAG
NP3.1R	R- CTGACTCCTCCACCCCTTCTACCT
NP2.2F	F- AACGAGCTGTGTGGAACTTGGAGG
NP3.2R	R- CTAGACCTAGTCTCCTTGCCAAGCT
Site-directed mutagenesis	
HSEmut	F- CTCCGCCGCCGCCTGCGTTTGTCCAGATGTCCTGCCGG
	R- CCGGCAGGACATCTGGACAAACGCAGGCGGCGGCGGAG
RT-qPCR/ChIP	
HSE	F- GAACCACCGCCCGAAAGT
	R- CCGGCAGGACATCTGGAAA
GAPDH	F- GACTCACCCTCGCCCTCAATA
	R- AAAGGCACTCCTGGAAACCT
«upstr»	F- GGAACTCCCTTCCTCAGTCAG
	R- TAAAGCGCCGCCCCAACTT
Name	**siRNA and ASO sequences**
siRNA	
siNRF2 (sense strand)	CCAAAGAGCAGUUCAAUGA
siHSF1_#1 (sense strand)	GGACAAGAAUGAGCUCAGUtt
siHSF1_#2 (sense strand)	CUGGUGCAGUCAAACCGGAtt
siCtrl	Silencer Select Negative Control No.2 siRNA (ThermoFisher Scientific, 4390847)
Antisense LNA GapmeR Standard	
NEAT1 (described in ref 13)	TAAGCACTTTGGAAAG
NEAT1_2 (described in ref 13)	CTCACACGTCCATCT
Negative Control	AACACGTCTATACGC

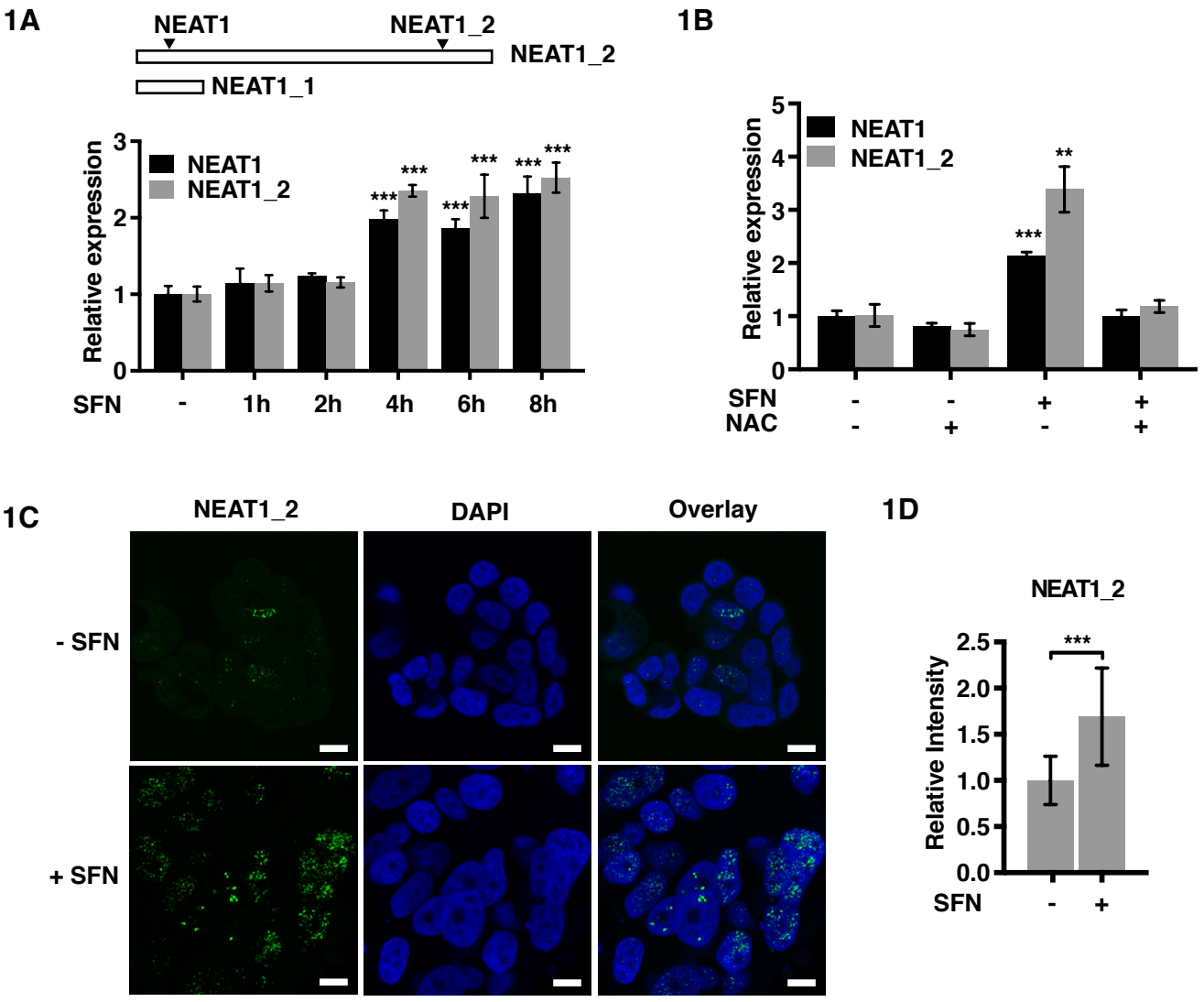

FIGURE 1. **NEAT1 expression and paraspeckle formation are induced by SFN.** *A,* MCF7 cells were treated with SFN (20 μM) for the indicated time points. RNA was isolated and the expression of NEAT1 (both isoforms) and NEAT1_2 was determined by RT-qPCR. The mean value ± SD of three biological replicates in one experiment is presented as fold change relative to untreated cells. The results are representative of three independent experiments. *B,* MCF7 cells were pre-incubated with N-acetylcysteine (NAC, 5 mM) and then treated with SFN for 6 h. NEAT1 expression was determined as described in A. *C,* MCF7 cells were left untreated or treated with SFN for 6 h, fixed and subjected to RNA-fluorescent in situ hybridization (RNA-FISH) using probes recognizing the NEAT1_2 isoform. DAPI was used to visualize the nuclei. *Bars,* 10 μm. *D.* The overall intensity of the dots in at least 250 cells were quantitated using the Volocity software. Mean values ± SD of three biological replicates are shown and presented as fold change relative to untreated cells. P values were calculated using ANOVA (*A*) or student's T-test (*B, D*) with $p < 0.05$ considered statistically significant. (***, $p \leq 0.001$, **, $p \leq 0.01$, *p, ≤ 0.05).

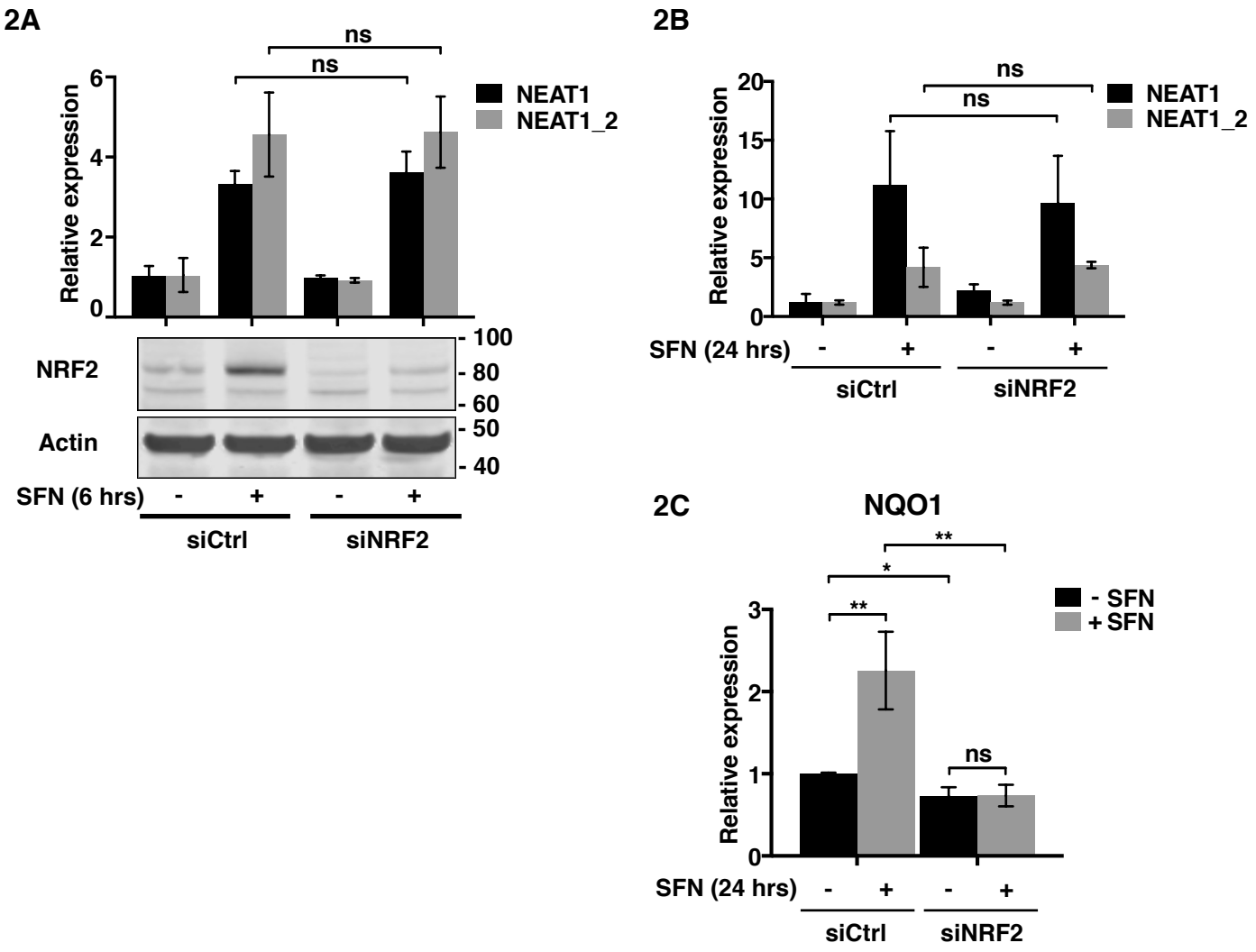

FIGURE 2**. NEAT1 induction by SFN is not dependent on NRF2.** *A,* MCF7 cells were transfected with an siRNA specifically targeting NRF2 (siNRF2) or control siRNA (siCtrl). Twenty-four h post-transfection, cells were either left untreated or treated with SFN (20 μM) for 6 h. NEAT1 expression was determined by RT-qPCR as described in Fig 1. Depletion of NRF2 expression in whole cell extracts was verified by western blot analyses using an NRF2 antibody. The membrane was re-probed with an anti-actin antibody to ensure equal loading. *B, C,* MCF7 cells were transfected as described in *A,* and subjected to a long-term treatment with SFN (10 μM) for 24 h. The expression of NEAT1 and NEAT1_2 (*B*), and NQO1 (*C*) was determined by RT-qPCR. Experiments were performed in triplicates and the graph is representative of three independent experiments. (**, $p \leq 0.01$, *p, ≤ 0.05).

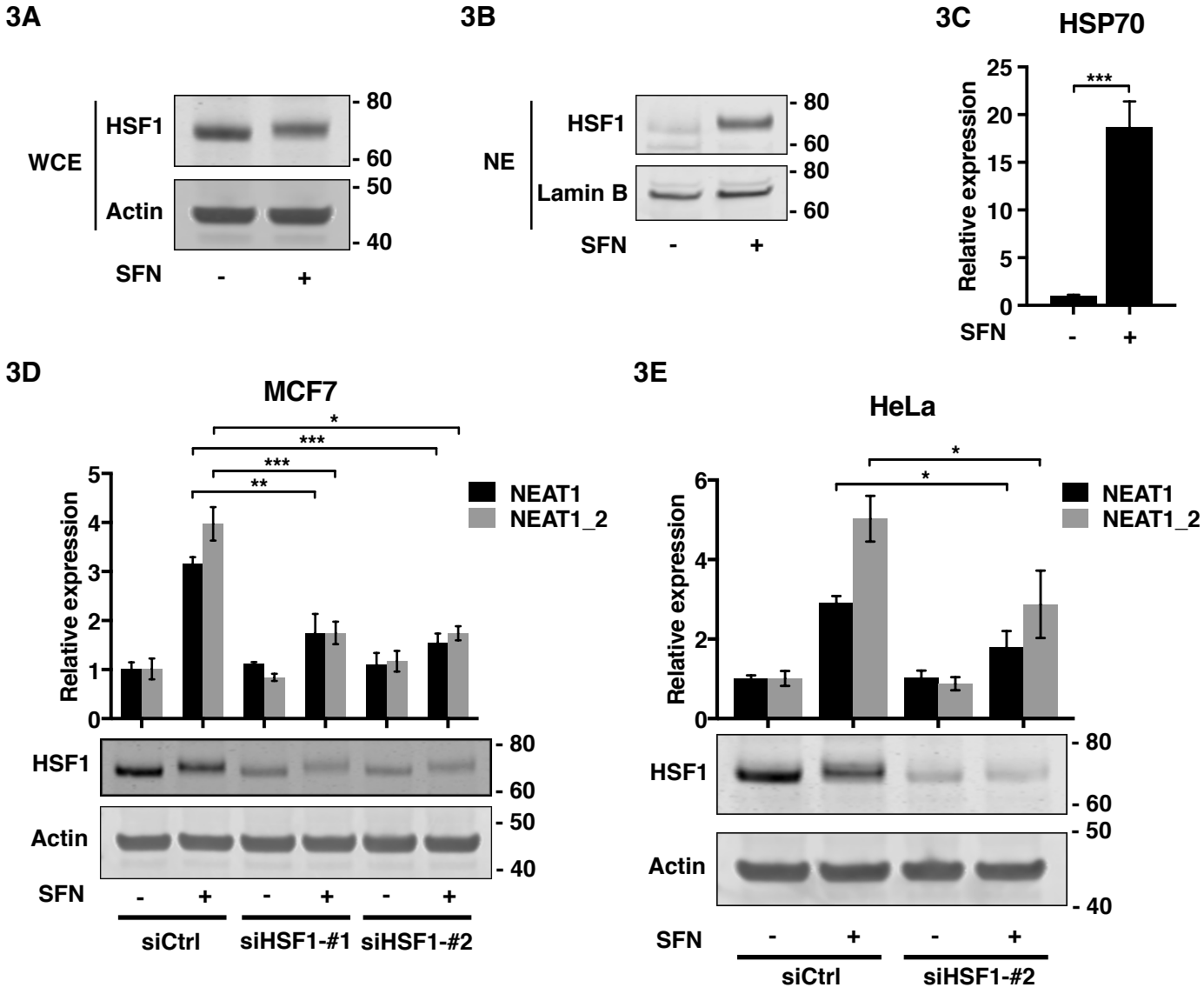

FIGURE 3**. SFN-induced NEAT1 expression is dependent on HSF1.** *A, B,* MCF7 cells were left untreated or treated with SFN (20 uM) for 6 h. HSF1 expression in whole cell extracts (WCE) (*A*) and nuclear extracts (NE) (*B*) was determined by immunoblot analyses. Equal loading was verified by re-probing the membranes with actin (*A*) or lamin B (*B*) antibodies. *C,* Cells were treated with SFN as described above, and HSP70 expression was determined by RT-qPCR. *D,* MCF7 cells were transfected with two different siRNAs targeting HSF1, siHSF1_#1 and siHSF1_#2, or a control siRNA. Forty-eight hours post-transfection, cells were left untreated or treated with SFN for 6 h. NEAT1 expression was assessed by RT-qPCR. SiRNA-mediated HSF1 depletion was verified by immunoblot analyses. *E,* HeLa cells were transfected with siHSF1_#2 or control siRNA and after 48 h SFN-induced NEAT1 expression was determined by RT-qPCR. HSF1 expression was determined by immunoblot analyses using actin as loading control. (*p ≤ 0.05, ***p ≤ 0.001).

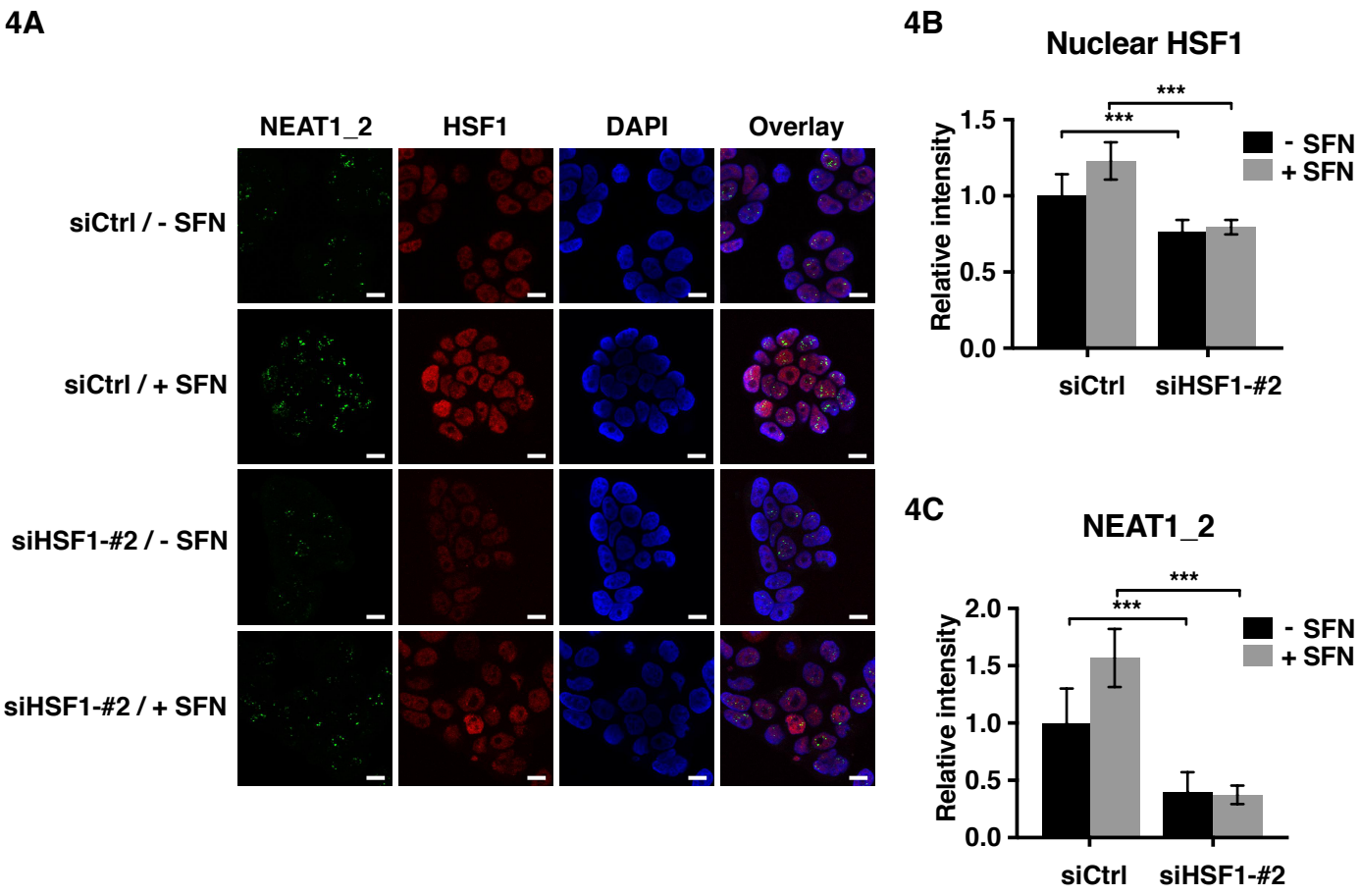

FIGURE 4. **HSF1-depletion abrogates SFN-induced paraspeckle formation.** *A,* MCF7 cells were transfected with an HSF1-specific siRNA or a control siRNA. After 48 h, cells were left untreated or treated with SFN for 6 h, fixed and subjected to coimmuno-FISH analyses by confocal microscopy using an antibody recognizing HSF1 (red) and fluorescent probes binding to NEAT1_2 (green). Nuclei were visualized with DAPI (blue). All experiments were performed in triplicates. *Bars,* 10 μm. *B, C,* The intensities of NEAT1_2 containing paraspeckles and nuclear HSF1 staining in at least 250 cells were quantitated using Volocity software. (***$p \leq 0.001$, **$p \leq 0.01$).

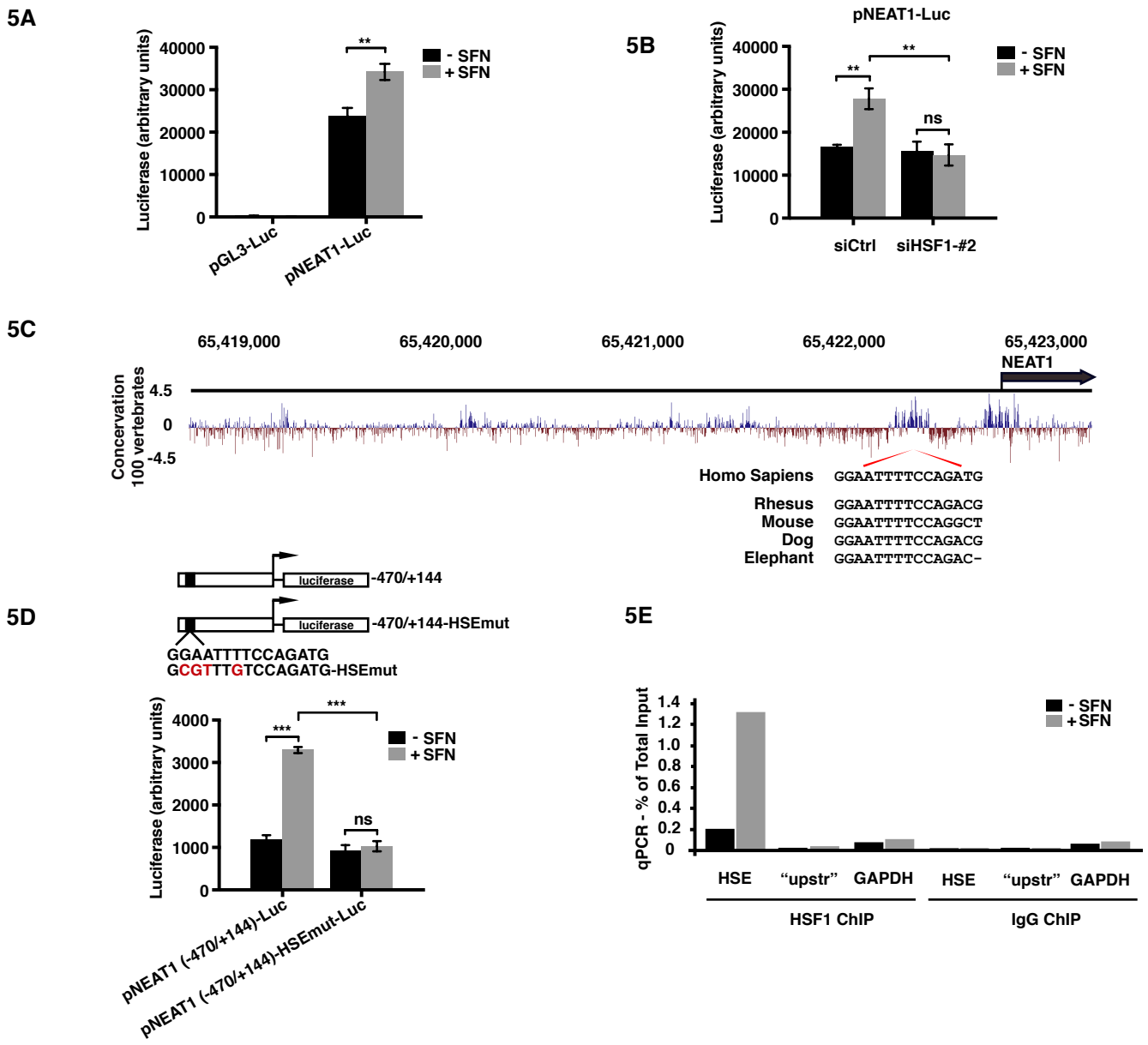

FIGURE 5**. HSF1 binds to and transcriptionally activates the NEAT1 promoter.** *A,* MCF7 cells were transfected with a luciferase reporter vector containing 4040 bp of the NEAT1 upstream region (pNEAT1-luc) or empty control vector. After 24 h, cells were left untreated or treated with SFN (20 μM) for 8 h and luciferase assays were performed. The experiments were performed in triplicates and mean values ± SD are shown. The result is representative of three independent experiments. *B,* MCF7 cells were co-transfected with pNEAT1-luc and siHSF1_#2 as described in experimental procedures. Cells were left untreated or treated with SFN for 8 h and luciferase assays were performed. *C,* sequence conservation within NEAT1 upstream regions is illustrated by PhyloP Basewise Conservation scores from 100 vertebrates (USCS Genome Browser). An alignment of conserved HSE core sequences from human, rhesus, mouse, dog, and elephant is shown. *D,* A truncated mutant of the NEAT1 promoter luciferase reporter construct encompassing the putative HSE site was generated and transfected into MCF7 cells along with a version harboring 4 point mutations within the HSE consensus sequence. SFN-induced luciferase activity was measured 24 h post-transfection. *E,* MCF7 cells were left untreated or treated with SFN (20 uM) for 6 h and ChIP assays were performed using an anti-HSF1 antibody. RT-qPCR was performed with primers flanking the HSE site. Primers flanking a region further upstream in the NEAT1 promoter ("upstr"), as well as primers amplifying a region of the GAPDH promoter, were used as negative controls. The relative amount of immunoprecipitated DNA compared to input DNA for each primer set is shown for the HSF1 ChIP. The values obtained by the IgG ChIP was less than 0.003% for the HSF1 and control primers. The result is representative of three independent ChIP experiments, where qPCR reactions were done as triplicates. (***$p \leq 0.001$, **$p \leq 0.01$).

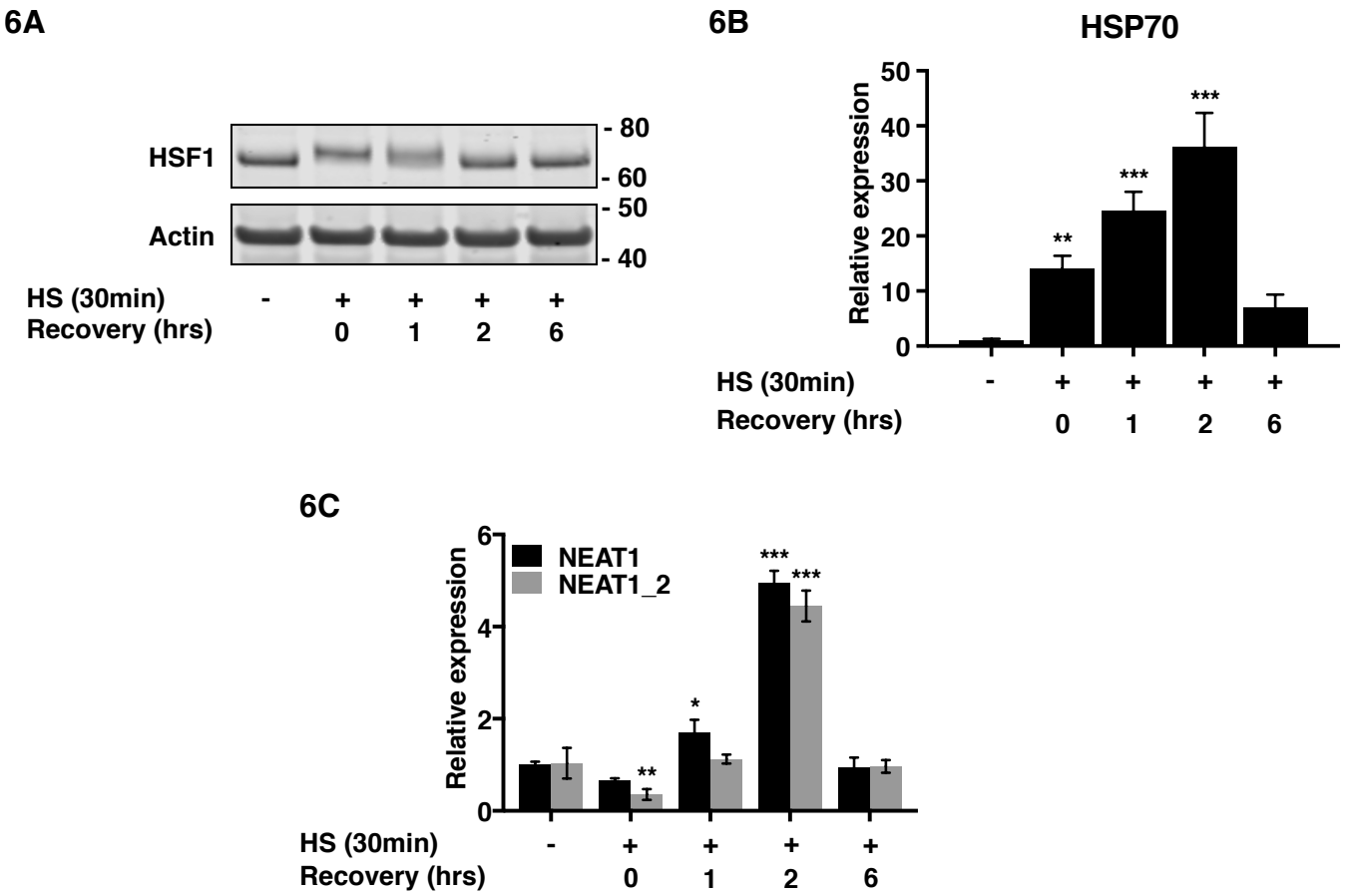

FIGURE 6**. NEAT1 is induced by heat shock.** *A* and *B,* MCF7 cells were subjected to heat shock by incubation at 43° for 30 minutes, and then returned to 37° to recover for the indicated time periods. Activation of HSF1 was verified by shifted migration in western blot analyses (*A*) and by induction of HSP70 mRNA expression (*B*). *C,* Cells were treated as above and expression of NEAT1 and NEAT1_2 were assessed by RT-qPCR. (***p ≤ 0.001, **p ≤ 0.01, *p ≤ 0.05).

7A

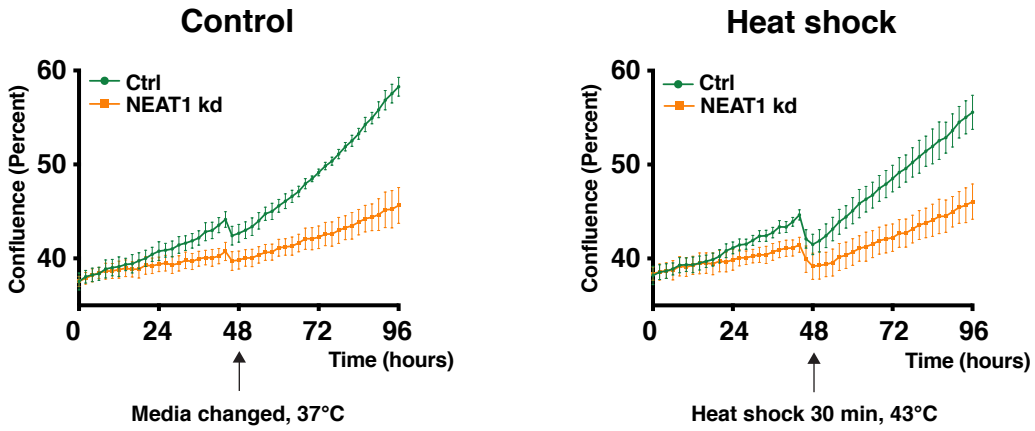

7B

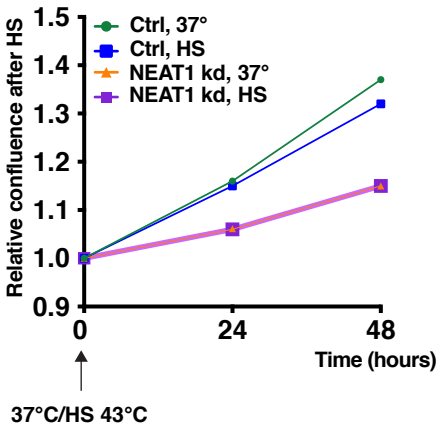

FIGURE 7. **Proliferation is compromised in NEAT1-depleted cells.** *A,* MCF7 cells were transfected with two LNA-gapmeR antisense oligos targeting NEAT1, or a negative control oligo, and immediately placed in a IncuCyte® live cell analysis system for cell confluence monitoring. After 48 h, cells were removed from the incubator, and for half of the cells the media was changed at 37°C, whereas the other half was subjected to heat shock at 43°C for 30 minutes. All the cells were then returned to the IncuCyte® live cell analysis system and monitored for another 48 hours. Confluency (%) was calculated using the IncuCyte® S3 software. Mean values ± SD of 15 images (3 images from each well of 5 wells in total) are shown. The results are representative for three independent experiments. *B,* The relative confluency of cells over the last 48 hours of the experiment described in *A,* is shown.

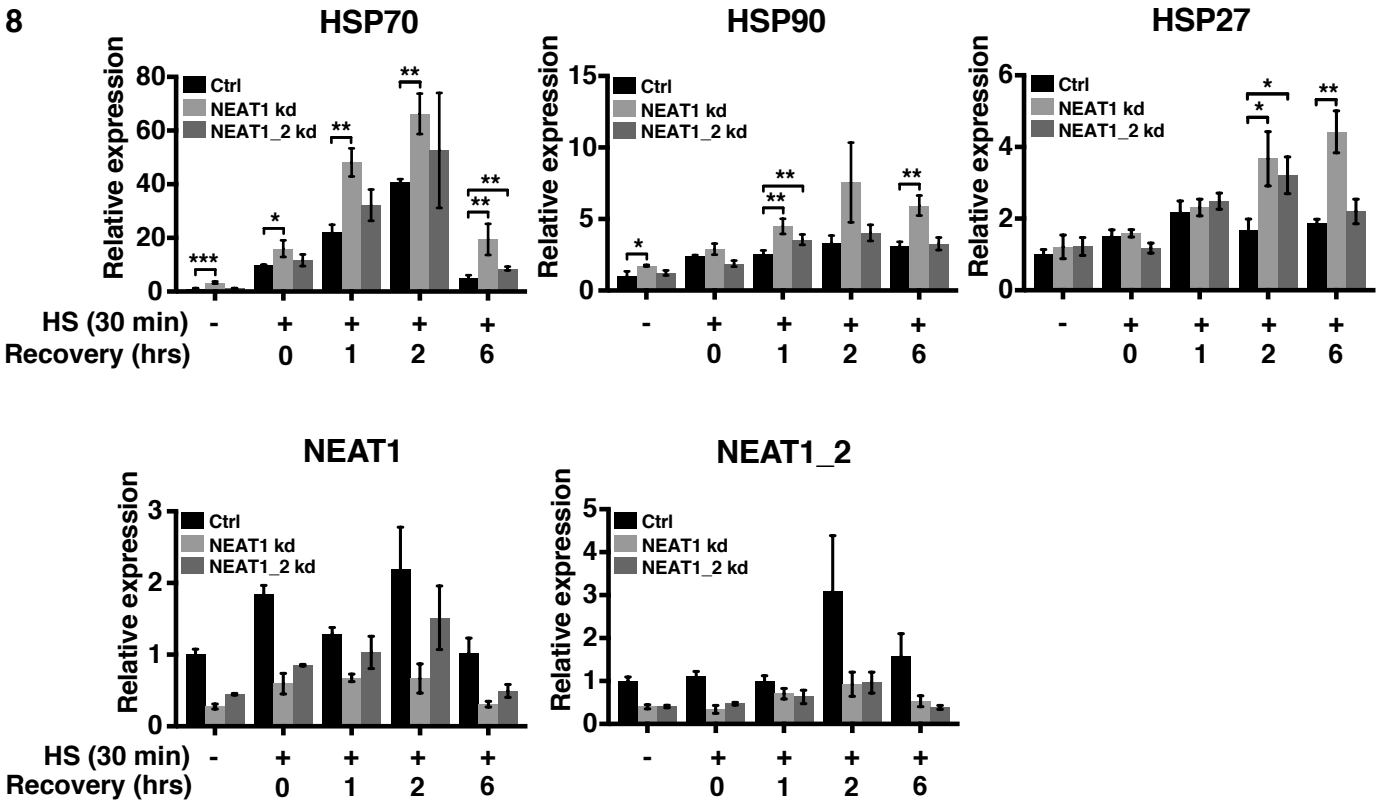

FIGURE 8**. NEAT1 knockdown amplifies the expression of HSF1 target genes upon heat shock.** MCF7 cells were transfected with two different LNA-gapmeR NEAT1 antisense oligos either targeting both isoforms of NEAT1 or solely the long NEAT1_2 isoform, and a negative control oligo. After 48 hours, cells were subjected to heat shock and recovered for the indicated time periods. The expression of HSP70, HSP90, and HSP27 was determined by RT-qPCR. Knockdown of NEAT1 and NEAT1_2 was verified by RT-qPCR. (***p ≤ 0.001, **p ≤ 0.01, *p ≤ 0.05).

The long non-coding RNA NEAT1 and nuclear paraspeckles are upregulated by the transcription factor HSF1 in the heat shock response

S.Mohammad Lellahi, Ingrid Arctander Rosenlund, Annica Hedberg, Liv Torill Kiær, Ingvild Mikkola, Erik Knutsen and Maria Perander

J. Biol. Chem. published online October 10, 2018

Access the most updated version of this article at doi: 10.1074/jbc.RA118.004473

PAPER II

The expression of the long *NEAT1_2* isoform is associated with human epidermal growth factor receptor 2-positive breast cancers

Erik Knutsen[1], Mohammad Seyed Lellahi[1], Silje Nord[2], Silje Fismen[3], Kenneth Bowitz Larsen[1], Marta Tellez Gabriel[1], Annica Hedberg[1], Anna Bofin[4], Therese Sørlie[2], Elin Synnøve Mortensen[1,3], Maria Perander[1*].

[1]Department of Medical Biology, Faculty of Health Sciences, UiT – The Arctic University of Norway, Tromsø, Norway

[2]Department of Cancer Genetics, Institute for Cancer Research, the Norwegian Radium Hospital, Oslo, Norway

[3]Department of Pathology, University Hospital of North Norway, Tromsø, Norway

[4]Department of Clinical and Molecular Medicine, Norwegian University of Science and Technology, Trondheim, Norway

* Corresponding author: *maria.perander@uit.no* Address: RNA and molecular pathology research group, Department of Medical Biology, Faculty of Health Sciences, UiT – the Arctic University of Norway, N-9037 Tromsø, Norway.

ABSTRACT

The long non-coding RNA *NEAT1* locus is transcribed into two overlapping isoforms, *NEAT1_1* and *NEAT1_2*, of which the latter is essential for the assembly of nuclear paraspeckles. *NEAT1* is abnormally expressed in a wide variety of human cancers. Emerging evidence suggests that the two isoforms have distinct functions in gene expression regulation, and recently it was shown that *NEAT1_2*, but not *NEAT1_1*, expression predicts poor clinical outcome in cancer. Here, we report that *NEAT1_2* expression correlates with HER2-positive breast cancer and high-grade disease. HER2-positive breast cancer cell lines are highly dependent on *NEAT1* expression, and *NEAT1*-depletion slightly enhances their sensitivity to lapatinib treatment. We provide evidence that *NEAT1_1* and *NEAT1_2* have distinct expression pattern among different intrinsic breast cancer subtypes. Finally, we show that *NEAT1_2* expression and paraspeckle formation increase upon lactation in humans, confirming what has previously been demonstrated in mice.

INTRODUCTION

The long non-coding RNA (lncRNA) *NEAT1* (Nuclear Paraspeckle Assembly Transcript 1) has recently gained considerable attention as it is abnormally expressed in human diseases, including cancer and neurodegenerative disorders. The *NEAT1* gene is transcribed into two isoforms, *NEAT1_1* of 3.7 kb and *NEAT1_2* of 22.3 kb, where *NEAT1_1* completely overlaps with the 5' end of *NEAT1_2* [1-3]. *NEAT1_2* is essential for the assembly of paraspeckles, dynamic ribonucleoprotein complexes that phase-separate from the nucleoplasm to form liquid drop-like structures [4-7]. In contrast, *NEAT1_1* expression is not sufficient to induce paraspeckle formation and recent reports suggest that *NEAT1_1* can localize to structures that are distinct from paraspeckles [7, 8]. *NEAT1* expression and paraspeckle formation are upregulated in response to a variety of cellular stressors including mitochondrial stress, proteasome inhibition, oncogene-induced replication stress, hypoxia, heat shock, and viral infections [2, 9-17]. It is today generally accepted that *NEAT1* and paraspeckles regulate gene expression at both transcriptional and post-transcriptional levels by acting as hubs that sequester specific gene-regulatory proteins and mRNAs [15-19]. Several lines of evidence suggests that *NEAT1* and paraspeckles play critical roles in stress response pathways in general, and at specific developmental stages. *NEAT1* knockout mice display compromised mammary gland development and corpus luteum formation [20, 21]. Moreover, it was recently shown that maternal and zygotic *NEAT1*-depletion frequently led to early developmental arrest at the 16- or 32-cell stage in mouse embryonic cells [22].

Cancer cells are exposed to a variety of extrinsic and intrinsic stressors like hypoxia, proteotoxicity, DNA damage, and reactive metabolic intermediates [23]. Such malignancy-associated stress has been shown to induce *NEAT1* expression in vivo [14-16]. *NEAT1* levels are elevated in hypoxic regions of breast cancer cell line xenografts, and genotoxic stress induces formation of *NEAT1*-expressing skin tumors in mice [14, 16]. In consistence with these

observations, *NEAT1* is overexpressed in many cancers [16, 24-35]. In most cases, *NEAT1* expression is associated with aggressive disease and poor clinical outcomes.

Breast cancer is the most common type of cancer in women, and covers a broad spectrum of different malignant neoplasms with clinical and genomic heterogeneity [36]. In clinical diagnosis, breast cancer is classified according to histological grade, Ki-67 proliferative index, and to the expression of hormone and growth factor receptors including estrogen receptor (ER), progesterone receptor (PR), and human epidermal growth factor receptor 2 (HER2). The classification of breast cancer has been stratified by gene expression profiling leading to the identification of a 50-gene signature (PAM50) that groups breast cancer into luminal A, luminal B, HER2-enriched, basal-like, and normal-like intrinsic subtypes [37, 38]. Several studies have demonstrated that *NEAT1* is required for proliferation and survival of breast cancer cell lines [9, 16, 20, 39-41]. Moreover, *NEAT1* is frequently overexpressed in breast tumor samples compared to adjacent normal tissue and associated with poor overall survival [16, 40-42]. Recently, genomic analyses of 360 primary breast tumors showed that the core promoter of the *NEAT1* gene is frequently mutated in cancer and most of these mutations are associated with loss of expression in vitro assays [43]. Moreover, focal deletions within the *NEAT1* gene was found in 8% of breast cancer and mutations are frequently found in the exonic region [43, 44]. This suggests that *NEAT1* expression might either protect or enhance cancer initiation and progression dependent on tumor stage.

Most studies on *NEAT1* and breast cancer have not addressed the relative contribution of the short and the long isoform, as they are, with a few exceptions, based on RT-qPCR analyses using primers recognizing both *NEAT1_1* and *NEAT1_2*. Moreover, refined studies systematically analyzing *NEAT1* expression in intrinsic breast cancer subtypes are still scarce. Here, we have examined the relationship between *NEAT1_2* expression and breast cancer subtypes by performing RNA-FISH analyses on core needle biopsies using probes solely

recognizing the *NEAT1_2* isoform. We report that *NEAT1_2* expression associates with HER2-positive breast cancers, and independently, with high tumor grade. This is verified by *in silico* analyses of microarray data from three independent breast cancer cohorts showing that *NEAT1_2* is most highly expressed in luminal B and HER2-enriched cancers. HER2-positive cell lines are highly dependent on *NEAT1* expression as *NEAT1*-depletion induces apoptosis and enhances their sensitivity to lapatinib. Interestingly, we find that total *NEAT1* expression shows a distinct distribution among breast cancer subtypes compared to *NEAT1_2*, being highest in ER-positive luminal A cancers. This indicates that the relative expression of *NEAT1_1* and *NEAT1_2* varies in the different breast cancer subclasses. Finally, we report that *NEAT1_2* and paraspeckle formation are induced in human luminal epithelial cells during lactation.

RESULTS

NEAT1_2 expression is associated with high tumor grade and HER2 positive breast cancers

The *NEAT1_2* isoform is essential for the assembly of paraspeckles that regulate the expression of specific genes at certain cellular circumstances [1-3, 15-19]. Recently, it was shown that the expression of *NEAT1_2*, but not *NEAT1_1*, predicts progression-free survival of ovarian cancer treated with platinum-based chemotherapy [14]. This prompted us to specifically investigate the expression of *NEAT1_2* in breast cancer. To determining the relationship between breast cancer subtypes and both *NEAT1_2* expression and associated paraspeckle formation, we performed *NEAT1_2*-specifc RNA-FISH analyses on 74 formalin-fixed paraffin-embedded needle biopsies taken from females at the time of diagnosis of breast cancer. The samples were selected to represent cancers clinically diagnosed as luminal A (n=23), luminal B (n=27), triple negative/basal-like (n=15) and HER2-positive (n=9). We also included 27 non-cancerous breast samples in the study (23 fibroadenomas, 3 mammary reduction, and 1 *BRCA1* prophylactic mastectomy). Cancer cells were identified by trained pathologists, and *NEAT1_2* expression was manually scored from "0" to "3" based on the presence and morphology of punctuated nuclear signals corresponding to paraspeckles (Figure 1A). Samples in which *NEAT1_2* was detected in more than 50% of the cells (scored as "2" and "3"), were defined as *NEAT1_2*-positive. Twenty-nine patients (39%) were positive for *NEAT1_2* expression (Table 1). In all cases, the expression was strictly restricted to cancer cells, with no detectable *NEAT1_2* signals in surrounding stromal tissue, infiltrating immune cells, or in unaffected breast tissue. In sharp contrast, none of the benign breast tissue samples were *NEAT1_2*-positive, with no detection in 25 of the samples, and detection in less than 50% of luminal epithelial cells in 2 samples (scored as "0" and "1", respectively) (Table 1). Clinicopathological characteristics were acquired from each sample and correlated with *NEAT1_2* expression (Table 2). *NEAT1_2* levels significantly associated with higher tumor grade ($p<0.05$) (Figure

1B, Table 2), confirming what has previously been reported by others on total *NEAT1*. Importantly, *NEAT1_2* expression also correlated with HER2 expression ($p<0.05$) (Figure 1C, Table 2). To verify these results, we analyzed microarray expression data from 390 breast cancer patients (Oslo-2), using data generated by a *NEAT1_2*-specific probe. We confirmed that high *NEAT1_2* expression associated with high-grade tumors ($p<0.001$) and HER2 expression ($p<0.001$) (Figure 2, A and B). Intriguingly, we also found that *NEAT1_2* expression negatively correlated with ER-positive tumors in this cohort ($p<0.01$) (Supplementary figure 1). Finally, we assessed the expression of *NEAT1_2* by RNA-FISH and RT-qPCR in nine breast cancer cell lines classified according to the expression of hormone- and growth factor receptors into ER/PR-positive HER2-negative cells (MCF7, T-47D), HER2-positive cells (BT474, HCC1569, SK-BR-3), and triple negative cells (BT549, Hs 578T, MDA-MB-231, MDA-MB-468). In consistence with previous reports, the morphology, as well as the number and size of *NEAT1_2*-containing paraspeckles, varied substantially between the different cell lines (Supplementary figure 2) [45]. We also observed cell-to-cell variations within each cell line. In general, both the number and size of *NEAT1_2*-containing punctas were hard to determine as they frequently formed clusters. We therefore measured the average intensities of NEAT_2 signals per cell in all cell lines (Figure 2C). Interestingly, HER2-positive BT474 and HCC1569 clearly expressed the highest levels of *NEAT1_2*. Moreover, *NEAT1_2* expression levels in HER2-positive SK-BR-3 cells were only exceeded by those in MCF7 cells. This was confirmed by RT-qPCR analyses using primers specifically amplifying the *NEAT1_2* isoform (Figure 2D). Generally, results obtained by imaging and RT-qPCR were concordant, only showing deviations for the BT549 cell line. We conclude that *NEAT1_2* expression correlates with HER2-positive breast cancer, and independently, with high-stage disease. Moreover, the presence of *NEAT1_2* and paraspeckles are highly specific for cancer cells as neither surrounding normal tissue nor non-cancerous samples contain *NEAT1_2* signals.

NEAT1_2 expression is associated with the HER2-enriched and luminal B breast cancer subtypes

We demonstrated above that *NEAT1_2* expression correlates with HER2-positive breast cancer. HER2 overexpressing cancers are classified as HER2-enriched or luminal B using the PAM50 gene expression signature identifier. To assess the correlation between *NEAT1_2* expression and intrinsic breast cancer subtypes, we analyzed microarray gene expression data derived from the Oslo-2 cohort described above, and two publicly available breast cancer patient cohorts, METABRIC [46] and The Cancer Genome Atlas (TCGA) [47]. Patients were subclassified according to the PAM50 expression signature and only data generated from probes solely recognizing the *NEAT1_2* isoform were considered. In all three cohorts, *NEAT1_2* was most highly expressed in HER2-enriched and luminal B breast cancers, but with different intrinsic distributions (HER2-enriched > luminal B in METABRIC and Oslo-2; Luminal B > HER2-enriched in TCGA) (Figure 3, A-C). Luminal A breast cancers had the lowest expression of *NEAT1_2* in all three cohorts. Taken together, these results are in accordance with the observed correlation between *NEAT1_2* expression and HER2-positive cancers.

Knock down of NEAT1_2 induces apoptosis and increases sensitivity of HER2-positive cells to lapatinib

NEAT1 has previously been associated with chemotherapy resistance and poor overall prognosis [14, 16, 24, 48]. This prompted us to compare the sensitivity of control and *NEAT1*-depleted SK-BR-3 cells to lapatinib, a HER2 and epidermal growth factor receptor (EGFR) inhibitor that is used in second-line treatment of advanced HER2-positive breast cancers. SK-BR-3 cells were transfected with a control GapmeR oligonucleotide or GapmeR antisense oligonucleotides (ASOs) targeting both isoforms of *NEAT1* that generally reduced the

expression by 70-80% (Supplementary figure 3). Forty-eight hours post-transfection, cells were left untreated or treated with 0.05 μM lapatinib for 24 h and apoptosis was assessed by Annexin V-staining and flow cytometry. Importantly, *NEAT1*-depletion was sufficient to potently induce apoptosis in SK-BR-3 cells (Figure 4A). Moreover, although not significant ($p<0.096$), *NEAT1*-depletion slightly increased the sensitivity of the cells to lapatinib (Figure 4A).

Total NEAT1 expression is highest in luminal A breast cancers

Previous reports have demonstrated that the *NEAT1* gene is transcriptionally activated by ERα in both prostate and breast cancer, and the transcript participates in a gene repressor complex that induces EMT in a mouse model of ER-positive breast cancer [24, 42]. Here, we have found that the expression of the long *NEAT1_2* isoform negatively correlates with ER-expression in the Oslo-2 breast cancer cohort (Supplementary figure 1). This potential discrepancy made us analyze the expression of total *NEAT1* using microarray data derived from probes binding to both *NEAT1_1* and *NEAT1_2* from the TCGA cohort. Interestingly, total *NEAT1* expression showed a different distribution among the PAM50 subtypes compared to *NEAT1_2*, being most highly expressed in luminal A cancers (Figure 5, A-D). This indicates that the relative expression of *NEAT1_1* and *NEAT1_2* varies in the different breast cancer subclasses, and that *NEAT1_1* is highly expressed in luminal A cancers.

NEAT1_2 expression is upregulated in human breast tissue during lactation

We have demonstrated that *NEAT1_2* is not, or infrequently expressed, in normal human breast tissue. *NEAT1* female knock-out mice display compromised mammary gland development during puberty and pregnancy, and fail to lactate due to impaired proliferation of luminal alveolar cells [21]. This suggests an important function for *NEAT1* in mammary gland development and during pregnancy and lactation. In order to investigate if *NEAT1_2* is

expressed during lactation in humans, we analyzed eight needle biopsies taken from females with lactation-related benign changes in the mammary gland. Importantly, 50% (n=4) of the lactating breast tissue samples were positive for *NEAT1_2* using the same scoring scheme as above (Figure 1A and 6A). Of note, we also had access to one sample from a pregnant woman, which was scored as *NEAT1_2* positive. In both the lactating tissue and the breast tissue from the pregnant female, the expression of *NEAT1_2* was restricted to the luminal breast epithelial cells (Figure 6B).

DISCUSSION

The lncRNA *NEAT1* locus is conserved in mammalian species and encodes two overlapping transcripts, *NEAT1_1* and *NEAT1_2*, of which the latter is essential for the assembly of paraspeckles [1-3]. Early analyses in mice indicated that whereas *NEAT1_1* is ubiquitously expressed, the expression pattern of *NEAT1_2*, and thus the presence of paraspeckles, are more restricted [6]. Emerging evidence now suggests that *NEAT1_2* and paraspeckles play critical roles in orchestrating specific gene expression upon cellular stress and at specific developmental stages [2, 9-17, 20-22]. Importantly, it was recently shown that the expression of *NEAT1_2*, but not total *NEAT1*, was associated with aggressive cancers [14]. Here, we have specifically analyzed the expression of *NEAT1_2* in breast cancer. By performing RNA-FISH on 74 breast cancer needle biopsies, we found that *NEAT1_2* expression and paraspeckle formation associated with HER2-positive cancers. We verified this by inspecting microarray data generated by a *NEAT1_2*-specific probe from a cohort of 390 patients. Moreover, we found that *NEAT1_2* is highly expressed in HER2-positive compared to HER2-negative breast cancer cell lines. Finally, in three different breast cancer cohorts, *NEAT1_2* expression associated with HER2-enriched and luminal B PAM50 intrinsic subtypes. Around 20% of all breast cancers overexpress the HER2 receptor due to the amplification of the *ERBB2* gene on chromosome 17, and HER2-driven cancers are generally aggressive [49, 50]. The HER2 receptor is an orphan member of the epidermal growth factor receptor family that upon overexpression forms homodimers or heterodimers with either EGFR, HER3, or HER4, which elicit signaling pathways, including the MEK-ERK and PI3-kinase-Akt pathways, that drive tumorigenesis [49, 50]. *NEAT1* expression is generally regulated at the transcriptional level, and it is reasonable to assume that HER2-signaling leads to the activation of the *NEAT1* promoter. Indeed, *NEAT1* transcription is activated by a series of stress-induced transcription factors including HIF2α, HSF1, and NF-κB, which have been shown to be constitutively upregulated or activated in

HER2 overexpressing cells [51-54]. However, as discussed below, transcriptional upregulation is most likely not the only mechanism accounting for the high levels of *NEAT1_2* in HER2-positive cancer cells. *NEAT1_2* is produced when the polyadenylation signal required for the formation of *NEAT1_1*, is suppressed by a hnRNPK-dependent mechanism [7, 55]. Moreover, key paraspeckle-associated proteins including NONO and SFPQ bind to and stabilize *NEAT1_2* [56] . Further experiments should be undertaken to determine their expression and subcellular localization in HER2-positive cell lines.

As *NEAT1_1* and *NEAT1_2* is transcribed from the same promoter, it is logical to hypothesize that the expression pattern of *NEAT1_1* mirrors that of *NEAT1_2*. Importantly, by analyzing microarray data derived from probes binding to both isoforms, we found that total *NEAT1* expression showed an entirely different distribution among the PAM50 subtypes, being highest in ER-positive luminal A cancers. This is in agreement with previous reports showing that *NEAT1* is transcriptionally activated by ERα in both prostate and breast cancer cell lines [24, 42]. Contradictory to this, we find a negative correlation between *NEAT1_2* and ERα expression levels in breast cancer patients. Thus, our analyses strongly suggest that the relative levels of *NEAT1_1* and *NEAT1_2* vary in different breast cancer subtypes. Recently, Li et al. found that *NEAT1* participates in a transcriptional repressor complex with FOXN3 and SIN3A in ER-positive breast cancer cells [42]. The complex induces epithelial-mesenchymal transition *in vitro* by downregulating GATA3 expression and promotes metastasis in mouse models of ER-positive breast cancer. The FOXN3-*NEAT1*-SIN3A complex also binds to and represses the promoter of the *ESR1* gene indicating the presence of a negative feed-back regulatory mechanism. Importantly, the authors suggest that the FOXN3-*NEAT1*-SIN3A complex functions independently of paraspeckles and that it is the *NEAT1_1* isoform that participates in this complex. In line with this, Chakravarty et al demonstrated that *NEAT1_1*, but not *NEAT1_2*, binds directly to histone H3 and recruits ERα to the *PSMA* promoter in

prostate cancer cell lines [24]. We hypothesize that in ER-positive cancers, *NEAT1_1* contributes to the tumorigenic phenotype by directly participating in transcriptional regulation at the chromatin level. This mechanism might be less important in HER2-positive cancers where increased *NEAT1_2* levels and paraspeckle formation is required for their adaptation to malignancy-associated stress and survival. We have indeed shown that *NEAT1*-depletion is sufficient to induce apoptosis in HER2-positive SK-BR-3 cells, and slightly increased their sensitivity to the HER2- and EGFR-inhibitor lapatinib. Furthermore, it was recently shown that the expression of *NEAT1_2*, predicted progression-free survival of ovarian cancer treated with platinum-based chemotherapy [14]. Our *NEAT1_2* RNA-FISH analyses were done on needle biopsies taken at the time of diagnosis of breast cancer. In the future, it will be important to monitor if *NEAT1_2* expression changes in the course of treatment of HER2-positive cancers, and if it is a predictor of therapy response. Relevant to this, unpublished data from our group show that *NEAT1_2* levels increase in HER2-positive cell lines upon lapatinib treatment. It should be noted that RNA stability is a technical challenge when analyzing *NEAT1_2* expression in patient samples by RNA-FISH. We performed RNA-FISH on tissue micro arrays of 409 breast cancer patient samples diagnosed between 1961 and 2008. Here, only 12 samples (2.9%) were positive for *NEAT1*_2 (data not shown) as opposed to 39% of the needle biopsies.

We find that *NEAT1_2* is not expressed in normal tissue surrounding breast cancer cells at levels that can be detected by RNA-FISH. Furthermore, none of the analyzed benign breast tissue samples were *NEAT1_2* positive using detection in >50% of cells as a cut-off. Murine *Neat1* is critical for normal development of the mammary gland, and *Neat1_2* and paraspeckles were detected in 30-50% of K8/K18-positive luminal cells in adult mice [21]. The number of *Neat1_2* positive cells increased upon pregnancy and lactation. To further inspect *NEAT1* expression pattern in human mammary gland development, we performed RNA-FISH on 8 benign breast tissue samples taken from lactating women. We detected *NEAT1_2* and

paraspekles in more than 50% of the cells in 4 samples (50%). Our data strongly supports the observations done in mice and suggests that *NEAT1_2* and paraspeckle formation are upregulated during lactation also in humans. The mechanisms behind this upregulation should be further studied as they also can give important hints about abnormal *NEAT1* expression in breast cancer, as well as the normal function of *NEAT1*.

We provide evidence that *NEAT1_2* expression associates with HER2-positive cancers and suggest that the relative expression of *NEAT1_1* and *NEAT1_2* varies in breast cancer subtypes. The overlapping nature of the *NEAT1_1* and *NEAT1_2* hampers isoform-specific analyses and might affect the interpretation of expression data. *NEAT1_2* is not polyadenylated, which needs to be taken into account when analyzing poly(A)-enriched RNA-sequencing data. Nevertheless, both *NEAT1_1* and *NEAT1_2* are likely to contribute to breast cancers tumorigenesis and the cancer-specific expression of *NEAT1_2* makes it a promising target for therapeutic intervention in the future.

EXPERIMENTAL PROCEDURES

Cell Culture and Treatments

BT474 (ATCC® HTB-20™), BT549 (ATCC® HTB-122™), HCC1569 (ATCC® CRL-2330™), Hs 578T (ATCC® HTB-126™), MDA-MB-231 (ATCC® HTB-26™), MDA-MB-468 (ATCC® HTB-132™), MCF7 (ATCC® HTB-22™), SK-BR-3 (ATCC® HTB-30™), and T-47D (ATCC® HTB-133™) cells were all purchased from the American Type Culture Collection (ATCC). BT474, BT549, HCC1569, MDA-MB-231, MDA-MB-468, SK-BR-3, and T-47D were cultured in RPMI 1640 (Sigma-Aldrich) supplemented with 10% Fetal bovine serum (FBS) (Biochrom) and 1% penicillin-streptomycin (Sigma-Aldrich). BT549 cells were grown in the presence of 0.001 mg/ml insulin (Sigma-Aldrich) and T-47D were grown in the presence of 0.006 mg/ml insulin. Hs 578T were cultured in Dulbecco's Modified Eagle's Medium (DMEM; Sigma-Aldrich) supplemented with 10% FBS, 1% penicillin-streptomycin, and 0.01 mg/ml insulin. MCF7 were cultured in Minimum Essential Medium Eagle (MEM; Sigma-Aldrich) supplemented with 10% FBS, 1% penicillin-streptomycin, and 0.01 mg/ml insulin. All cell lines were incubated in a 5% CO2 humidified incubator at 37°C.

Lapatinib (L-4899) was purchased from LC Laboratories and diluted in DMSO to a final concentration of 1 M. For apoptosis assay, a final concentration of 0,05 uM lapatinib in full media was added to the cells 24H before assessed by Annexin V-staining and flow cytometry. An equal volume of DMSO was used as control.

RNA Isolation, cDNA Synthesis, and RT-qPCR

Cells were lysed in 300 µl Tri Reagent, heated for 10 min at 55 degree Celsius, and total RNA was isolated with Direct-zol RNA MiniPrep (Zymo Research) according to the manufacturer’s recommendation. RNA concentration was measured by NanoDrop 2000 (Thermo Fisher

Scientific). cDNA synthesis of total RNA was performed with SuperScript™ IV Reverse Transcriptase (ThermoFisher Scientific). 2.5 μM of random hexamer primer (ThermoFisher Scientific) and approximately 400 ng of template were used for the reaction. Total RNA was denaturated at 65ºC for 5 min, and cDNA was synthesized at 50 ºC for 10 min.

For RT-qPCR of cDNA from total RNA, 12,5 ng cDNA was mixed with FastStart Essential DNA Green Master (Roche Life Science) and 0.25 μM forward and reverse primer. All primers sequences are provided in Supplementary Table 1. The LightCycler® 96 was used for quantification, and the ΔΔCq-method was used to calculate fold change using GAPDH, B2M, and/or RPLPO as internal reference.

RNA Interference

Antisense locked nucleic acid (LNA)-GapmeR were purchased from Exiqon. For transfection, Lipofectamine® 2000 were used according to the protocols provided by the manufacturer. 30 μM *NEAT1* antisense oligos (TAAGCACTTTGGAAAG and CTCACACGTCCATCT) or control GapmeR (AACACGTCTATACGC) were used in the knock down experiments.

Annexing Apoptosis Assay

The percentage of apoptotic cells was measured using the FITC Annexin V apoptosis detection kit (BD Biosciences). Single-cell suspensions were prepared for each group. Cells were washed with PBS and suspended in 1× binding buffer before stained with FITC-labeled Annexin V and PI for 15 min at room temperature in the dark. Apoptosis was analyzed immediately using the FACS LRS fortessa.

RNA-FISH of Cells and FFPE Tissue

Stellaris® *NEAT1* RNA FISH probes either recognizing both *NEAT1_1* and *NEAT1_2* isoforms (SMF-2036-1 conjugated with Quasar® 570), or only the *NEAT1_2* isoform (SMF-2037-1 conjugated with Quasar® 670), were purchased from LGC Biosearch Technologies. Preparation of cells and FFPE sections, hybridization, and mounting was performed according to the Stellaris® RNA FISH Probes manuals. In brief, cells were seeded onto circular coverslips in 12-well dishes and allowed to attach for 2-3 days, before fixed with 4% formaldehyde, and permeabilized with 70% EtOH. Hybridization was done at 37ºC in a humidifying chamber for at least 4 hours. FFPE tissue sections were cut fresh and placed at 60 degree Celsius for 45 min before deparaffinised with xylene. Here, hybridization was performed overnight. Vectashield® Mounting Medium containing DAPI was used for mounting of both cells and FFPE sections. Images were generated using a Zeiss LSM780 confocal microscope. For cells, 3-dimensial Z-stack images were taken at 40x magnification (seven pictures, with 0.600 μm distance between each picture). Images of FFPE sections were taken at 20x magnification with no Z-stacking. All images were processed using ZEN 2012 (black edition) v8.0. NEAT1_2 fluorescence was quantified from maximum intensity projections of confocal z-stacks using Fiji [57] running ImageJ [58] version 1.52n. An automatic threshold was set in the DAPI channel in order to segment individual nuclei using the wand tool. In some cases, nuclear outlines were manually traced. The average intensity in the NEAT1_2 channel was then measured for each nucleus.

Clinical Samples

Archived FFPE needle biopsies were obtained from the Department of Pathology, University Hospital of North Norway (UNN) with corresponding hematoxylin and eosin (HE) slides from all patients. Samples from 74 patients diagnosed with breast cancer (2012-2018), 27 normal

samples, 8 samples from lactating females, and 1 sample from a pregnant female were included in the study. The samples were handled in accordance with the regulations of the Regional Ethics Committee. Histological tumor grade was assessed by the Nottingham Grading System [59]. Correlation of *NEAT1_2* expression and clinicopathological characteristics were analyzed by the Chi square test (χ2-value) using SPSS version 25 (SPSS Inc., Chicago, IL, USA). P-values < 0.05 (two-tailed) were considered statistically significant.

Gene Expression Analyses in Breast Cancer Cohorts

NEAT1 gene expression was assessed in three independent breast cancer cohorts; Oslo-2, METABRIC [46], and TCGA [47]. The Oslo-2 cohort is an ongoing consecutive study in the Oslo region. Matched patient samples are being collected from primary tumor, sentinel lymph nodes, peripheral blood, bone marrow, and metastatic lesions. More than 1000 patients have been enrolled. To date, gene expression analysis has been completed from about 400 samples. Gene expression was measured using SurePrint G3 Human GE 8x60K one-color microarrays from Agilent (Agilent Technologies). The data was log2 transformed after normalization. The probe A_33_P3263538, covered part of the unique 3' end of *NEAT1_2*. The METABRIC cohort is composed of 1980 breast cancer patients collected at five different hospitals in the UK and Canada. Gene expression was assessed using the Illumina HT-12 v3 microarray and downloaded from the European Genome-phenome Archive (EGA) data portal. The data was log2 transformed, and unexpressed genes were excluded prior to analysis. The probe, ILMN_1675354, covered part of the unique 3' end of *NEAT1_2*. Gene expression levels for the Caucasian fraction of the TCGA cohort (n= 526) were assayed by Agilent 244K Custom Gene Expression G4502A-07-3. The data was log2 transformed after normalization. The probe, A_32_P206561, covered parts of the unique 3' end of *NEAT1_2*, while the probes A_32_P1036, A_32_P1037, A_24_P566917, and A_24_P566916 covered parts of the common region of

NEAT1_1 and *NEAT1_2*. The significant differences in gene expression between the five molecular subtypes of breast cancer were examined in all three cohorts using the none-parametric Kruskal-Wallis rank test. A significant Kruskal-Wallis test indicates that at least one subtype stochastically dominates one other subgroup.

REFERENCE

1. Guru, S.C., et al., *A transcript map for the 2.8-Mb region containing the multiple endocrine neoplasia type 1 locus.* Genome Res, 1997. **7**(7): p. 725-35.
2. Saha, S., S. Murthy, and P.N. Rangarajan, *Identification and characterization of a virus-inducible non-coding RNA in mouse brain.* J Gen Virol, 2006. **87**(Pt 7): p. 1991-5.
3. Hutchinson, J.N., et al., *A screen for nuclear transcripts identifies two linked noncoding RNAs associated with SC35 splicing domains.* BMC Genomics, 2007. **8**: p. 39.
4. Sasaki, Y.T., et al., *MENepsilon/beta noncoding RNAs are essential for structural integrity of nuclear paraspeckles.* Proc Natl Acad Sci U S A, 2009. **106**(8): p. 2525-30.
5. Sunwoo, H., et al., *MEN epsilon/beta nuclear-retained non-coding RNAs are up-regulated upon muscle differentiation and are essential components of paraspeckles.* Genome Res, 2009. **19**(3): p. 347-59.
6. Nakagawa, S., et al., *Paraspeckles are subpopulation-specific nuclear bodies that are not essential in mice.* J Cell Biol, 2011. **193**(1): p. 31-9.
7. Naganuma, T., et al., *Alternative 3'-end processing of long noncoding RNA initiates construction of nuclear paraspeckles.* EMBO J, 2012. **31**(20): p. 4020-34.
8. Li, R., et al., *Functional dissection of NEAT1 using genome editing reveals substantial localization of the NEAT1_1 isoform outside paraspeckles.* RNA, 2017. **23**(6): p. 872-881.
9. Lellahi, S.M., et al., *The long noncoding RNA NEAT1 and nuclear paraspeckles are up-regulated by the transcription factor HSF1 in the heat shock response.* J Biol Chem, 2018. **293**(49): p. 18965-18976.
10. Michelhaugh, S.K., et al., *Mining Affymetrix microarray data for long non-coding RNAs: altered expression in the nucleus accumbens of heroin abusers.* J Neurochem, 2011. **116**(3): p. 459-66.
11. Zhang, Q., et al., *NEAT1 long noncoding RNA and paraspeckle bodies modulate HIV-1 posttranscriptional expression.* MBio, 2013. **4**(1): p. e00596-12.
12. Ma, H., et al., *The Long Noncoding RNA NEAT1 Exerts Antihantaviral Effects by Acting as Positive Feedback for RIG-I Signaling.* J Virol, 2017. **91**(9).
13. Wang, Y., et al., *Genome-wide screening of NEAT1 regulators reveals cross-regulation between paraspeckles and mitochondria.* Nat Cell Biol, 2018. **20**(10): p. 1145-1158.
14. Adriaens, C., et al., *p53 induces formation of NEAT1 lncRNA-containing paraspeckles that modulate replication stress response and chemosensitivity.* Nat Med, 2016. **22**(8): p. 861-8.
15. Hirose, T., et al., *NEAT1 long noncoding RNA regulates transcription via protein sequestration within subnuclear bodies.* Mol Biol Cell, 2014. **25**(1): p. 169-83.
16. Choudhry, H., et al., *Tumor hypoxia induces nuclear paraspeckle formation through HIF-2alpha dependent transcriptional activation of NEAT1 leading to cancer cell survival.* Oncogene, 2015. **34**(34): p. 4546.
17. Imamura, K., et al., *Long noncoding RNA NEAT1-dependent SFPQ relocation from promoter region to paraspeckle mediates IL8 expression upon immune stimuli.* Mol Cell, 2014. **53**(3): p. 393-406.
18. Chen, L.L. and G.G. Carmichael, *Altered nuclear retention of mRNAs containing inverted repeats in human embryonic stem cells: functional role of a nuclear noncoding RNA.* Mol Cell, 2009. **35**(4): p. 467-78.
19. Prasanth, K.V., et al., *Regulating gene expression through RNA nuclear retention.* Cell, 2005. **123**(2): p. 249-63.

20. Nakagawa, S., et al., *The lncRNA Neat1 is required for corpus luteum formation and the establishment of pregnancy in a subpopulation of mice.* Development, 2014. **141**(23): p. 4618-27.
21. Standaert, L., et al., *The long noncoding RNA Neat1 is required for mammary gland development and lactation.* RNA, 2014. **20**(12): p. 1844-9.
22. Hupalowska, A., et al., *CARM1 and Paraspeckles Regulate Pre-implantation Mouse Embryo Development.* Cell, 2018. **175**(7): p. 1902-1916 e13.
23. Hanahan, D. and R.A. Weinberg, *Hallmarks of cancer: the next generation.* Cell, 2011. **144**(5): p. 646-74.
24. Chakravarty, D., et al., *The oestrogen receptor alpha-regulated lncRNA NEAT1 is a critical modulator of prostate cancer.* Nat Commun, 2014. **5**: p. 5383.
25. Guo, S., et al., *Clinical implication of long non-coding RNA NEAT1 expression in hepatocellular carcinoma patients.* Int J Clin Exp Pathol, 2015. **8**(5): p. 5395-402.
26. Ma, Y., et al., *Enhanced expression of long non-coding RNA NEAT1 is associated with the progression of gastric adenocarcinomas.* World J Surg Oncol, 2016. **14**(1): p. 41.
27. Kim, Y.S., et al., *Identification of differentially expressed genes using an annealing control primer system in stage III serous ovarian carcinoma.* BMC Cancer, 2010. **10**: p. 576.
28. Wang, H., et al., *Knockdown of Long Non-Coding RNA NEAT1 Inhibits Proliferation and Invasion and Induces Apoptosis of Osteosarcoma by Inhibiting miR-194 Expression.* Yonsei Med J, 2017. **58**(6): p. 1092-1100.
29. Han, D., J. Wang, and G. Cheng, *LncRNA NEAT1 enhances the radio-resistance of cervical cancer via miR-193b-3p/CCND1 axis.* Oncotarget, 2018. **9**(2): p. 2395-2409.
30. Huang, G., X. He, and X.L. Wei, *lncRNA NEAT1 promotes cell proliferation and invasion by regulating miR365/RGS20 in oral squamous cell carcinoma.* Oncol Rep, 2018. **39**(4): p. 1948-1956.
31. Cheng, N. and Y. Guo, *Long noncoding RNA NEAT1 promotes nasopharyngeal carcinoma progression through regulation of miR-124/NF-kappaB pathway.* Onco Targets Ther, 2017. **10**: p. 5843-5853.
32. Zhen, L., et al., *Long noncoding RNA NEAT1 promotes glioma pathogenesis by regulating miR-449b-5p/c-Met axis.* Tumour Biol, 2016. **37**(1): p. 673-83.
33. Liu, F., et al., *The long non-coding RNA NEAT1 enhances epithelial-to-mesenchymal transition and chemoresistance via the miR-34a/c-Met axis in renal cell carcinoma.* Oncotarget, 2017. **8**(38): p. 62927-62938.
34. Pan, L.J., et al., *Upregulation and clinicopathological significance of long non-coding NEAT1 RNA in NSCLC tissues.* Asian Pac J Cancer Prev, 2015. **16**(7): p. 2851-5.
35. Wedge, D.C., et al., *Sequencing of prostate cancers identifies new cancer genes, routes of progression and drug targets.* Nat Genet, 2018. **50**(5): p. 682-692.
36. Koren, S. and M. Bentires-Alj, *Breast Tumor Heterogeneity: Source of Fitness, Hurdle for Therapy.* Mol Cell, 2015. **60**(4): p. 537-46.
37. Perou, C.M., et al., *Molecular portraits of human breast tumours.* Nature, 2000. **406**(6797): p. 747-52.
38. Sorlie, T., et al., *Gene expression patterns of breast carcinomas distinguish tumor subclasses with clinical implications.* Proc Natl Acad Sci U S A, 2001. **98**(19): p. 10869-74.
39. Ke, H., et al., *NEAT1 is Required for Survival of Breast Cancer Cells Through FUS and miR-548.* Gene Regul Syst Bio, 2016. **10**(Suppl 1): p. 11-7.
40. Qian, K., et al., *The long non-coding RNA NEAT1 interacted with miR-101 modulates breast cancer growth by targeting EZH2.* Arch Biochem Biophys, 2017. **615**: p. 1-9.

41. Zhao, D., et al., *NEAT1 negatively regulates miR-218 expression and promotes breast cancer progression.* Cancer Biomark, 2017. **20**(3): p. 247-254.
42. Li, W., et al., *The FOXN3-NEAT1-SIN3A repressor complex promotes progression of hormonally responsive breast cancer.* J Clin Invest, 2017. **127**(9): p. 3421-3440.
43. Rheinbay, E., et al., *Recurrent and functional regulatory mutations in breast cancer.* Nature, 2017. **547**(7661): p. 55-60.
44. Nik-Zainal, S., et al., *Landscape of somatic mutations in 560 breast cancer whole-genome sequences.* Nature, 2016. **534**(7605): p. 47-54.
45. Chujo, T., et al., *Unusual semi-extractability as a hallmark of nuclear body-associated architectural noncoding RNAs.* EMBO J, 2017. **36**(10): p. 1447-1462.
46. Curtis, C., et al., *The genomic and transcriptomic architecture of 2,000 breast tumours reveals novel subgroups.* Nature, 2012. **486**(7403): p. 346-52.
47. Cancer Genome Atlas, N., *Comprehensive molecular portraits of human breast tumours.* Nature, 2012. **490**(7418): p. 61-70.
48. Shin, V.Y., et al., *Long non-coding RNA NEAT1 confers oncogenic role in triple-negative breast cancer through modulating chemoresistance and cancer stemness.* Cell Death Dis, 2019. **10**(4): p. 270.
49. Gutierrez, C. and R. Schiff, *HER2: biology, detection, and clinical implications.* Arch Pathol Lab Med, 2011. **135**(1): p. 55-62.
50. Moasser, M.M., *The oncogene HER2: its signaling and transforming functions and its role in human cancer pathogenesis.* Oncogene, 2007. **26**(45): p. 6469-87.
51. Jarman, E.J., et al., *HER2 regulates HIF-2alpha and drives an increased hypoxic response in breast cancer.* Breast Cancer Res, 2019. **21**(1): p. 10.
52. Schulz, R., et al., *HER2/ErbB2 activates HSF1 and thereby controls HSP90 clients including MIF in HER2-overexpressing breast cancer.* Cell Death Dis, 2014. **5**: p. e980.
53. Xi, C., et al., *Heat shock factor Hsf1 cooperates with ErbB2 (Her2/Neu) protein to promote mammary tumorigenesis and metastasis.* J Biol Chem, 2012. **287**(42): p. 35646-57.
54. Cogswell, P.C., et al., *Selective activation of NF-kappa B subunits in human breast cancer: potential roles for NF-kappa B2/p52 and for Bcl-3.* Oncogene, 2000. **19**(9): p. 1123-31.
55. Naganuma, T. and T. Hirose, *Paraspeckle formation during the biogenesis of long non-coding RNAs.* RNA Biol, 2013. **10**(3): p. 456-61.
56. Yamazaki, T., et al., *Functional Domains of NEAT1 Architectural lncRNA Induce Paraspeckle Assembly through Phase Separation.* Mol Cell, 2018. **70**(6): p. 1038-1053 e7.
57. Schindelin, J., et al., *Fiji: an open-source platform for biological-image analysis.* Nat Methods, 2012. **9**(7): p. 676-82.
58. Schneider, C.A., W.S. Rasband, and K.W. Eliceiri, *NIH Image to ImageJ: 25 years of image analysis.* Nat Methods, 2012. **9**(7): p. 671-5.
59. Elston, C.W. and I.O. Ellis, *Pathological prognostic factors in breast cancer. I. The value of histological grade in breast cancer: experience from a large study with long-term follow-up.* Histopathology, 1991. **19**(5): p. 403-10.

Table 1: *NEAT1_2* expression in breast cancer screening cohort and normal breast tissue.

NEAT1_2	**Tumor**	**Normal**
0, n(%)	25 (33.8)	25 (92.6)
1, n(%)	20 (27.0)	2 (7.4)
2, n(%)	23 (31.1)	0 (0.0)
3, n(%)	6 (8.1)	0 (0.0)
Total, n(%)	74 (100.0)	27(100.0)

Table 2. Clinicopathological variables and *NEAT1_2* expression in breast cancer screening cohort (n = 74).

Variable, n(%)		*NEAT1_2* expression				*p*	
		0 (n=25)	1 (n=20)	2 (n=23)	3 (n=6)		Total (n=74)
Age at diagnosis	<55	10 (34.5)	8 (27.6)	8 (27.6)	3 (10.3)	0.920	29 (39.2)
	>55	15 (33.3)	12 (26.7)	15 (33.3)	3 (6.7)		45 (60.8)
Histologic grade	1	10 (55.6)	5 (27.8)	3 (16.7)	0 (0.0)	**0.027***	18 (24.3)
	2	8 (34.8)	9 (39.1)	5 (21.7)	1 (4.3)		23 (31.1)
	3	7 (22.2)	6 (18.2)	15 (45.5)	5 (15.2)		33 (44.6)
Tumor type	NST	20 (29.9)	20 (29.9)	22 (32.8)	5 (7.5)	0.156	67 (90.5)
	ILC	3 (100.0)	0 (0.0)	0 (0.0)	0 (0.0)		3 (4.1)
	Other invasive carsinoma[a]	2 (50.0)	0 (0.0)	1 (25.0)	1 (25.0)		4 (5.4)
Tumor diameter[b]	<20 mm	14 (37.8)	12 (32.4)	7 (18.9)	4 (10.8)	0.213	37 (53.6)
	>20 mm	11 (34.4)	6 (18.8)	13 (40.6)	2 (6.3)		32 (46.4)
Lymph node metastasis[b]	Negative	17 (35.5)	14 (29.2)	13 (27.1)	4 (8.3)	0.990	48 (67.6)
	Positive	8 (34.8)	6 (26.1)	7 (30.4)	2 (8.7)		23 (32.4)
ER	Negative (<1%)	4 (16.7)	7 (29.2)	11 (45.8)	2 (8.3)	0.131	24 (32.4)
	Positive (>1%)	21 (42.0)	13 (26.0)	12 (24.0)	4 (8.0)		50 (67.6)
PGR	Negative (<10%)	6 (18.2)	10 (30.3)	13 (39.4)	4 (12.1)	0.071	33 (44.6)
	Positive (>10%)	19 (46.3)	10 (24.4)	10 (24.4)	2 (4.9)		41 (55.4)
HER2	Negative (0,+1)	22 (42.3)	13 (25.0)	15 (28.8)	2 (3.8)	**0.042***	52 (70.3)
	Positive (2+,3+)	3 (13.6)	7 (31.8)	8 (36.4)	4 (18.2)		22 (29.7)

[a]Tubulolobular carcinoma (n=1), Metaplastic squamous cell carcinoma (n=1), Mucinous carcinoma (n=1), Apocrine carcinoma (n=1)
[b]Patient(s) data missing

FIGURE LEGENDS

FIGURE 1: *NEAT1_2* expression and paraspeckle formation correlate with tumor grade and HER2 positive breast cancer. (**a**) RNA-FISH analyses of *NEAT1_2* in breast formalin-fixed paraffin-embedded needle biopsies. *NEAT1_2* expression is scored from "0" to "3" based on punctuated nuclear *NEAT1_2* signals according to the indicated criteria. (**b**) *NEAT1_2* expression correlates to tumor grade. Data are given as mean (thick black line) ± standard deviation (thin black lines). Circles represent single patient scores. P value was calculated by the Chi square test ($\chi 2$-value). (**c**) *NEAT1_2* expression correlates to HER2. Data are shown as mean (thick black line) ± standard deviation (thin black lines). Circles represent single patient scores. P value was calculated by the Chi square test ($\chi 2$-value).

FIGURE 2: *NEAT1_2* expression was verified in an independent breast cancer cohort and in breast cancer cell lines. *NEAT1_2*-specific expression was analyzed in microarray expression data from 390 breast cancer patients (Oslo-2). (**a**) *NEAT1_2* expression correlates to HER2 and (**b**) tumor grade. (**c**) Cells were subjected to RNA-fluorescent in situ hybridization (RNA-FISH) using probes recognizing the *NEAT1_2* isoform. DAPI was used to visualize the nuclei. The overall intensity of the dots per nucleus in at least 250 cells were quantitated. Data are given as mean (thick black line) ± standard deviation (thin black lines). Circles represent single cell intensities. (**d**) RNA was isolated and the expression of *NEAT1_2* was determined by RT-qPCR. The geometric mean of B2M, GAPDH, and RPLP0 was used for normalization. The mean value ± SD of three biological independent experiments is presented as fold change relative to MCF7 *NEAT1_2* expression.

FIGURE 3: *NEAT1_2* expression correlates with the HER2-enriched and Luminal B subtype of breast cancer. Gene expression of *NEAT1_2* in breast cancer in (**a**) Oslo-2, (**b**) METABRIC, and in (**c**) TCGA classified according to the PAM50 signature.

FIGURE 4: Apoptosis is induced in *NEAT1*-depleted cells treated with lapatinib. (**a**) SK-BR-3 cells were transfected with two LNA-GapmeR antisense oligos targeting *NEAT1*, or a negative control oligo. After 48h, cells were treated with 0.05 µM lapatinib or DMSO as control for 24h. The percentage of apoptotic cells was measured by annexin V staining and flow cytometry. The mean value ± SD of three independent biological experiments is presented. P value was calculated using student's T-test.

FIGURE 5: *NEAT1* expression correlates with luminal A subtype of breast cancer in the TCGA cohort. Expression of total *NEAT1* in PAM50 intrinsic breast cancer subtypes was determined using data generated from four independent probes in the TCGA cohort.

FIGURE 6: *NEAT1_2* is expressed in lactating breast tissue. (a) RNA-fluorescent in situ hybridization (RNA-FISH) analyses of *NEAT1_2* in breast tissue from lactating female (n=8) and normal tissue (n=27). *NEAT1_2* expression is scored from "0" to "3" based on punctuated nuclear *NEAT1_2* signals according to the indicated criteria in Figure 1A. Data are shown as mean (thick black line) ± standard deviation (thin black lines). Circles represent single patient scores. P value was calculated using student's T-test. (b) RNA-FISH images from three lactating females. DAPI was used to visualize the nuclei.

Supplementary Table 1. RT-qPCR primers.

Gene	Sequence
NEAT1_2	F: CGGAGGGTCTTGTAACACCAG
	R: AGTCCGGGCAACACAGAAAG
GAPDH	F: GAGCGAGATCCCTCCAAAAT
	R: AAATGAGCCCCAGCCTTCT
RPLP0	F: GCTGCTGCCCGTGCTGGTG
	R: TGGTGCCCCTGGAGATTTTAGTGG
B2M	F: TCATCCAGCAGAGAATGGAA
	R: TCTGAATGCTCCACTTTTTCAA

SUPPLEMENTARY FIGURE LEGENDS

SUPPLEMENTARY FIGURE 1: *NEAT1_2* is negatively correlated with ER. *NEAT1_2*-specific expression was analyzed in microarray expression data from 390 breast cancer patients (Oslo-2).

SUPPLEMENTARY FIGURE 2: *NEAT1_2* expression and paraspeckle formation in a panel of nine breast cancer cell lines. Cells were subjected to RNA-fluorescent in situ hybridization (RNA-FISH) using probes recognizing the *NEAT1_2* isoform (green signal). DAPI was used to visualize the nuclei.

SUPPLEMENTARY FIGURE 3: Knock down efficiency in SK-BR3 cells. Cells were transfected with two LNA-gapmeR antisense oligos targeting *NEAT1*, or a negative control oligo. After 48H RNA was isolated and the expression of *NEAT1_2* was determined by RT-qPCR. GAPDH was used for normalization. The mean value ± SD of three biological replicates in one experiment is presented as fold change relative to negative control cells. P value was calculated using student's T-test.

Figure 1

A

Score 0, Negative

No detection of *NEAT1_2*, or detection in less than 10% of tumor cells.

Score 1, Negative

Detection of *NEAT1_2* in less than 50% of tumor cells.

Score 2, Positive

Detection of *NEAT1_2* in more than 50% of tumor cells. Punctuated single structures.

Score 3, Positive

Detection of *NEAT1_2* in more than 50% of tumor cells. Overlapping large structures.

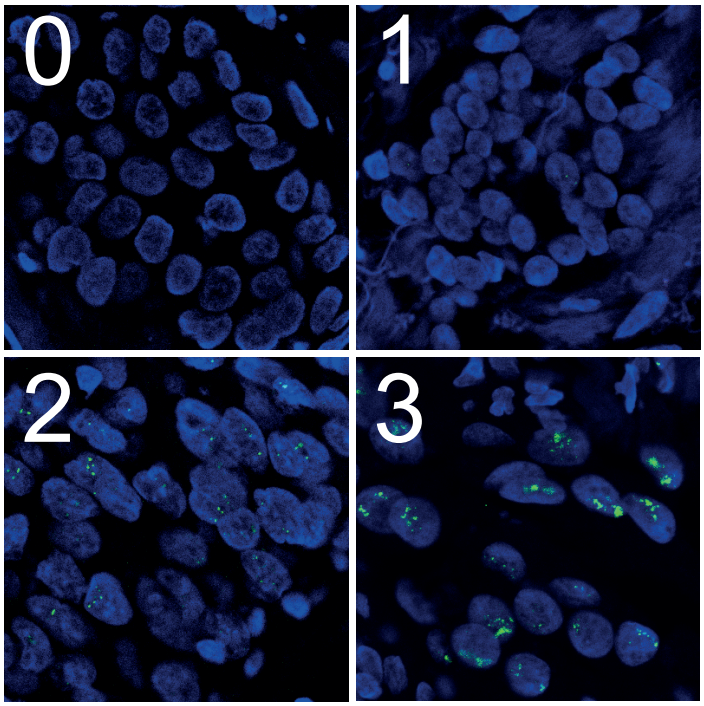

B

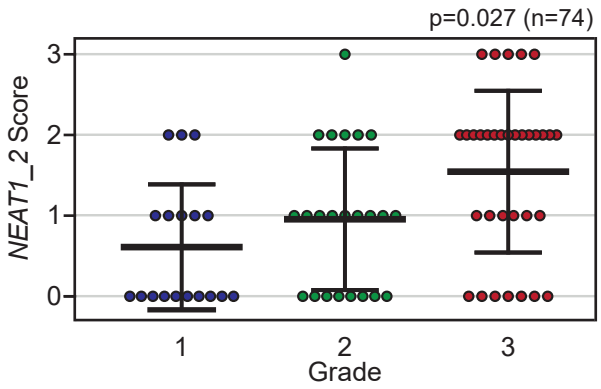

C

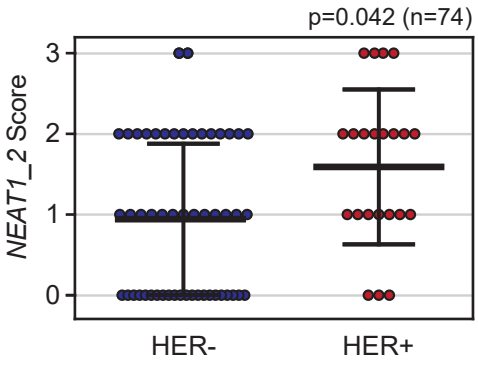

Figure 2

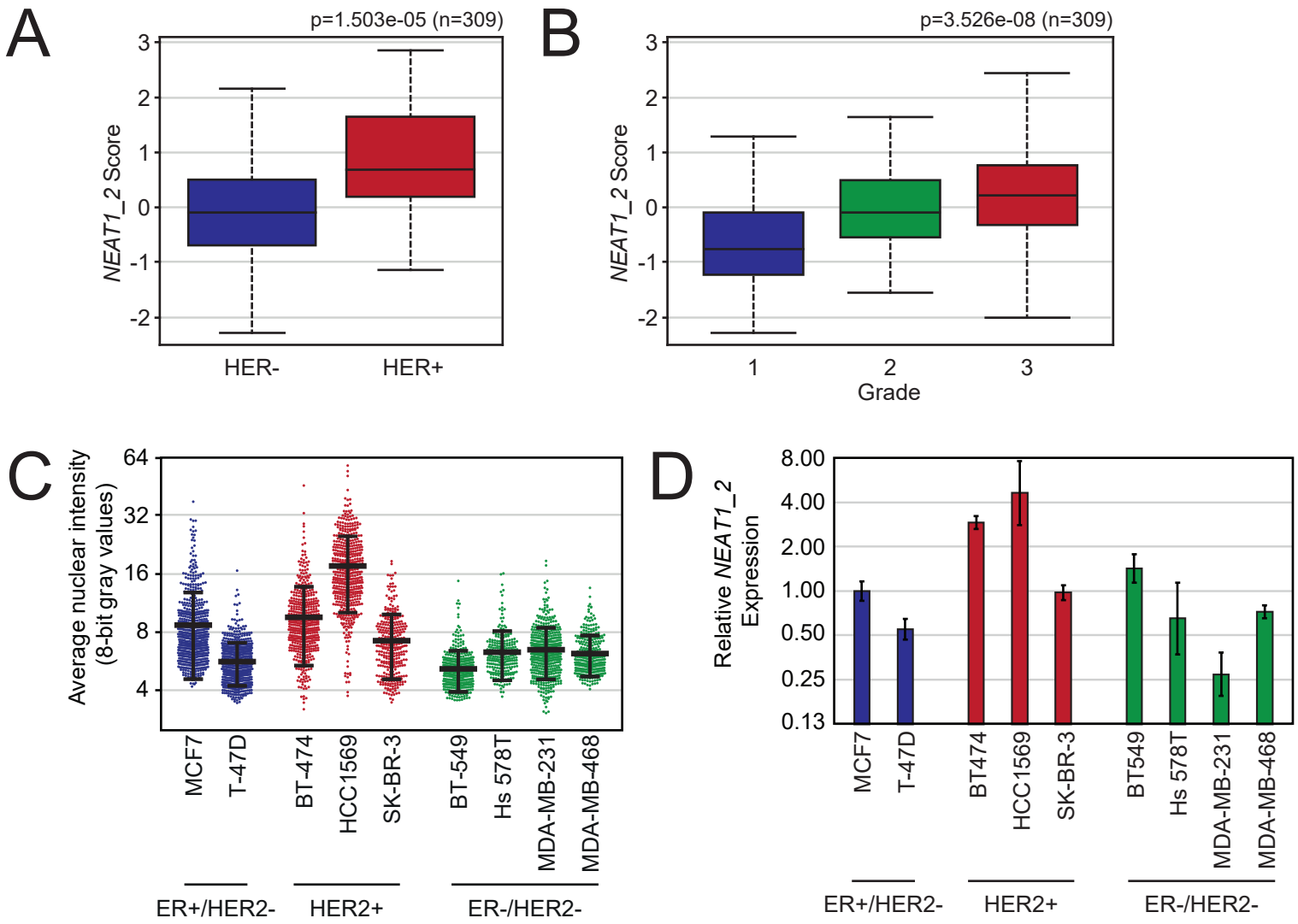
A
p=1.503e-05 (n=309)
NEAT1_2 Score
HER-
HER+
B
p=3.526e-08 (n=309)
NEAT1_2 Score
Grade
C
Average nuclear intensity (8-bit gray values)
MCF7
T-47D
BT-474
HCC1569
SK-BR-3
BT-549
Hs 578T
MDA-MB-231
MDA-MB-468
ER+/HER2-
HER2+
ER-/HER2-
D
Relative NEAT1_2 Expression
MCF7
T-47D
BT474
HCC1569
SK-BR-3
BT549
Hs 578T
MDA-MB-231
MDA-MB-468
ER+/HER2-
HER2+
ER-/HER2-

Figure 3

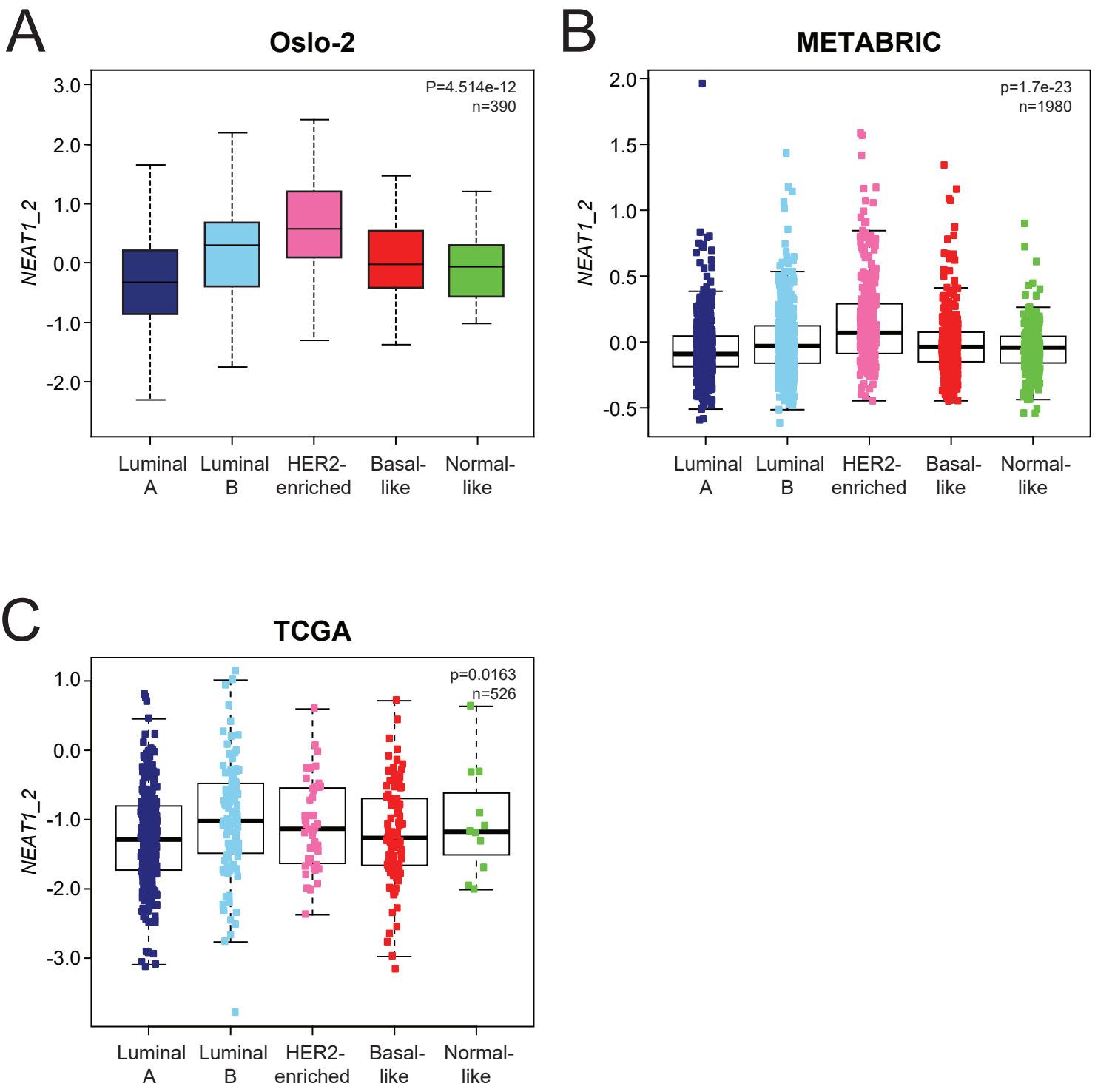
A
Oslo-2
P=4.514e-12
n=390
NEAT1_2
3.0
2.0
1.0
0.0
-1.0
-2.0
Luminal A
Luminal B
HER2-enriched
Basal-like
Normal-like
B
METABRIC
p=1.7e-23
n=1980
NEAT1_2
2.0
1.5
1.0
0.5
0.0
-0.5
Luminal A
Luminal B
HER2-enriched
Basal-like
Normal-like
C
TCGA
p=0.0163
n=526
NEAT1_2
1.0
0.0
-1.0
-2.0
-3.0
Luminal A
Luminal B
HER2-enriched
Basal-like
Normal-like

Figure 4

A

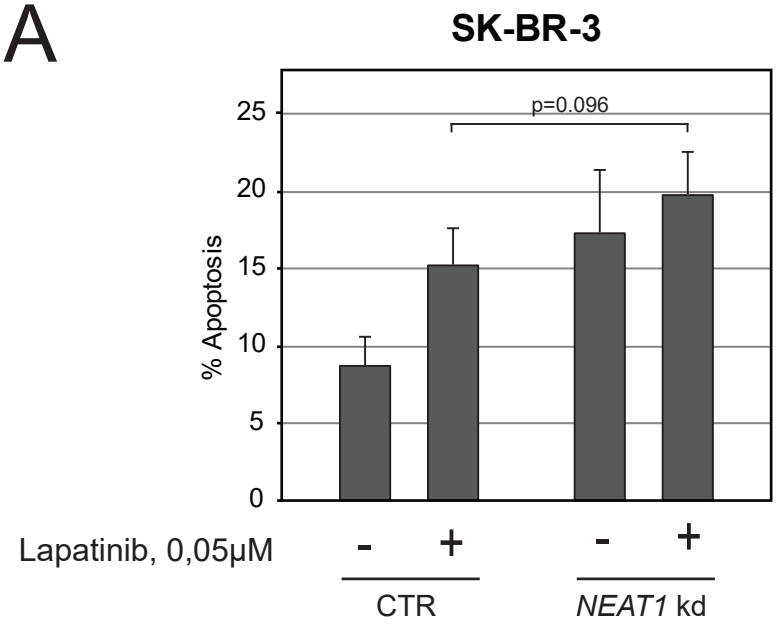
SK-BR-3
p=0.096
% Apoptosis
25
20
15
10
5
0
Lapatinib, 0,05μM
-
+
-
+
CTR
NEAT1 kd

Figure 5

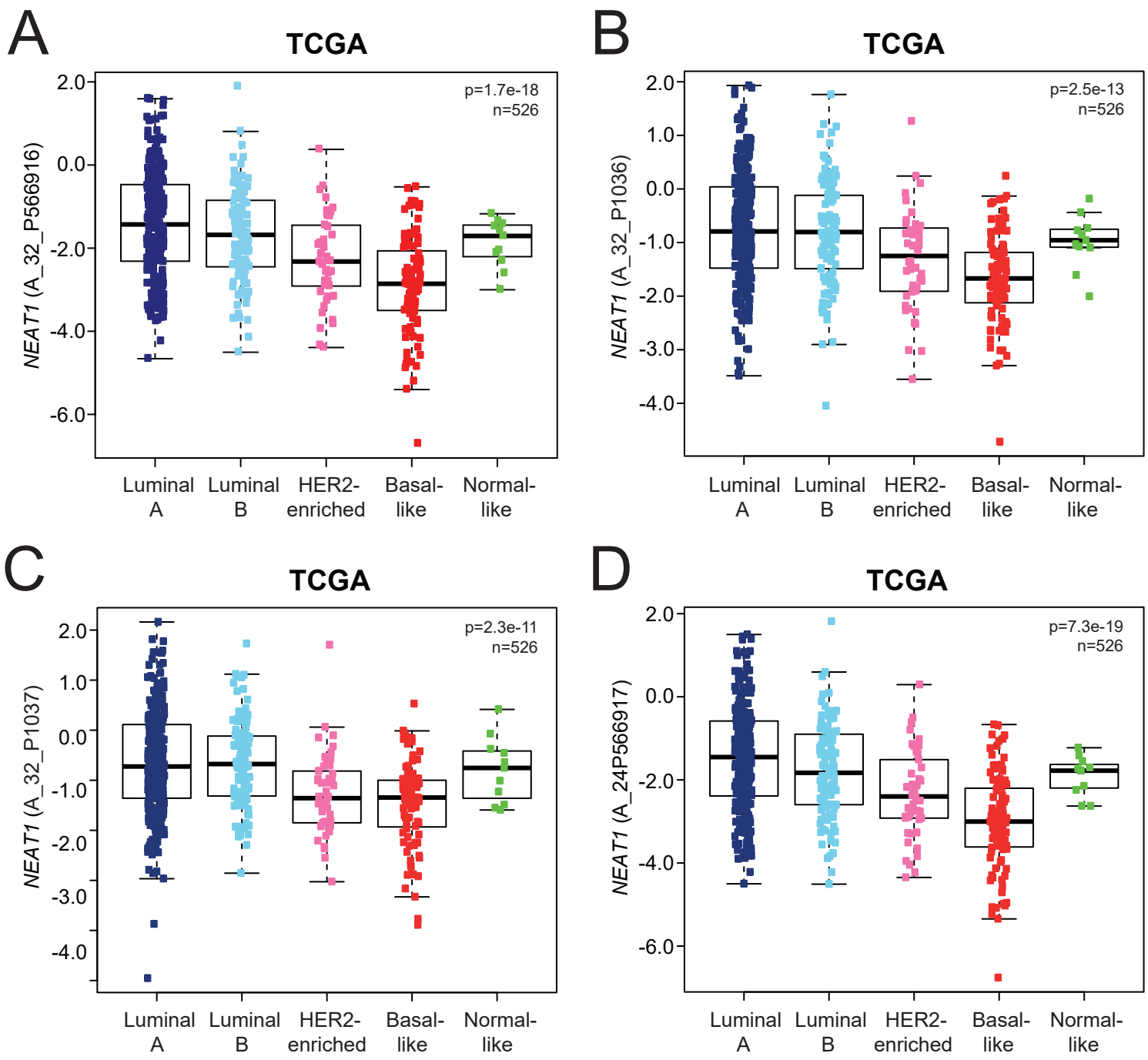
A
TCGA
p=1.7e-18
n=526
NEAT1 (A_32_P566916)
2.0
0.0
-2.0
-4.0
-6.0
Luminal A
Luminal B
HER2-enriched
Basal-like
Normal-like
B
TCGA
p=2.5e-13
n=526
NEAT1 (A_32_P1036)
2.0
1.0
0.0
-1.0
-2.0
-3.0
-4.0
Luminal A
Luminal B
HER2-enriched
Basal-like
Normal-like
C
TCGA
p=2.3e-11
n=526
NEAT1 (A_32_P1037)
2.0
1.0
0.0
-1.0
-2.0
-3.0
-4.0
Luminal A
Luminal B
HER2-enriched
Basal-like
Normal-like
D
TCGA
p=7.3e-19
n=526
NEAT1 (A_24P566917)
2.0
0.0
-2.0
-4.0
-6.0
Luminal A
Luminal B
HER2-enriched
Basal-like
Normal-like

Figure 6

A

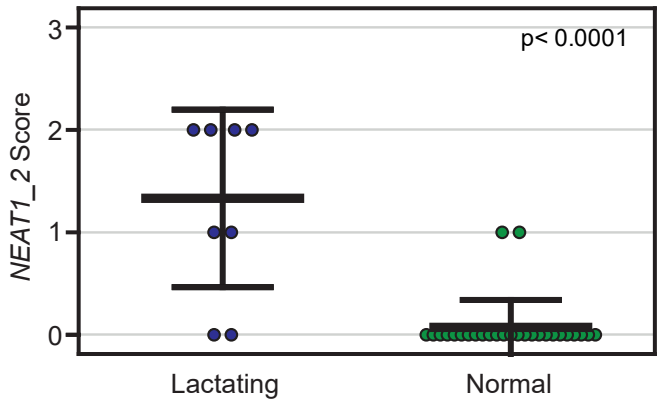

B

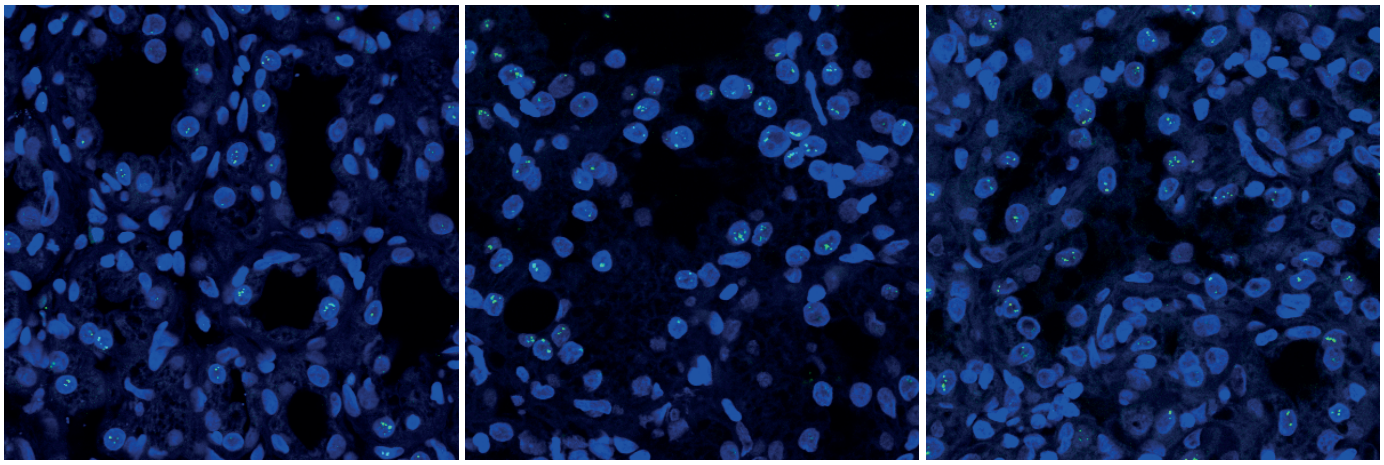

Supp Fig 1

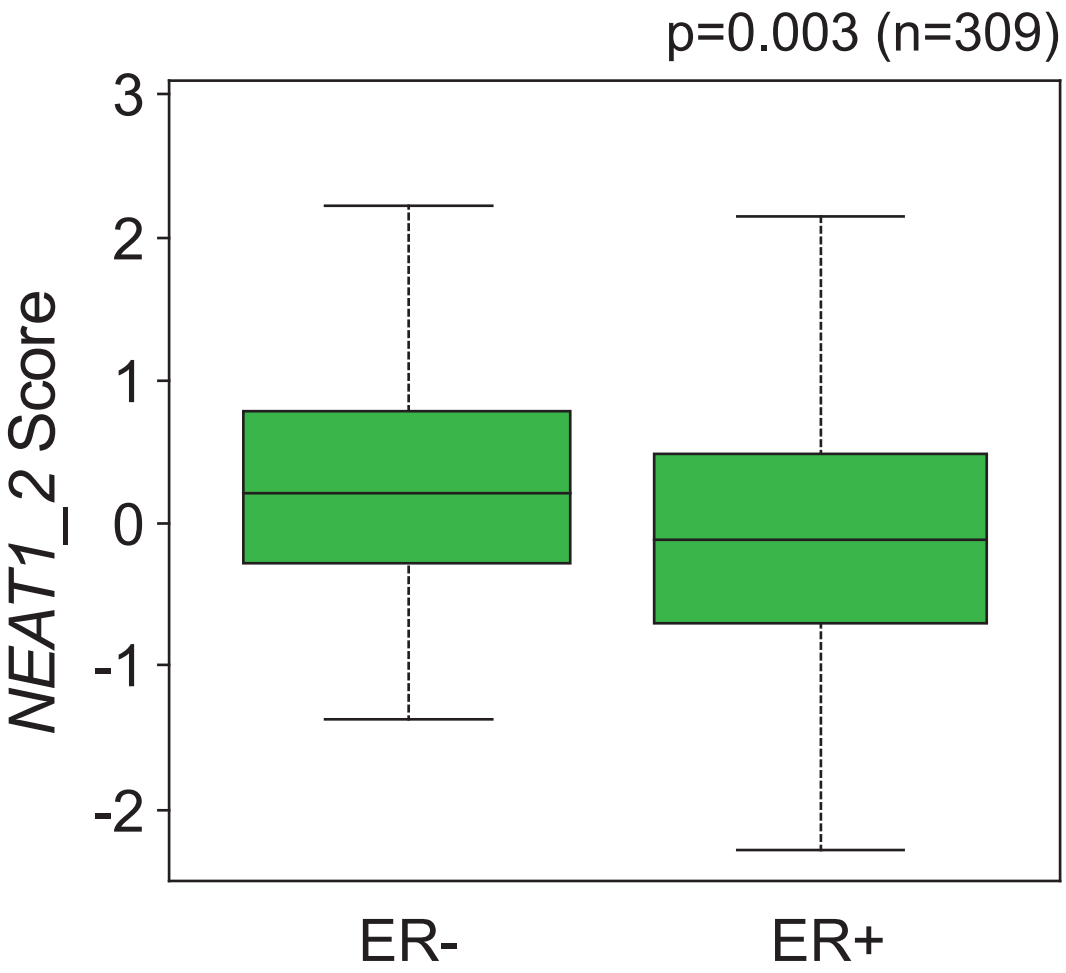

Supp Fig 2

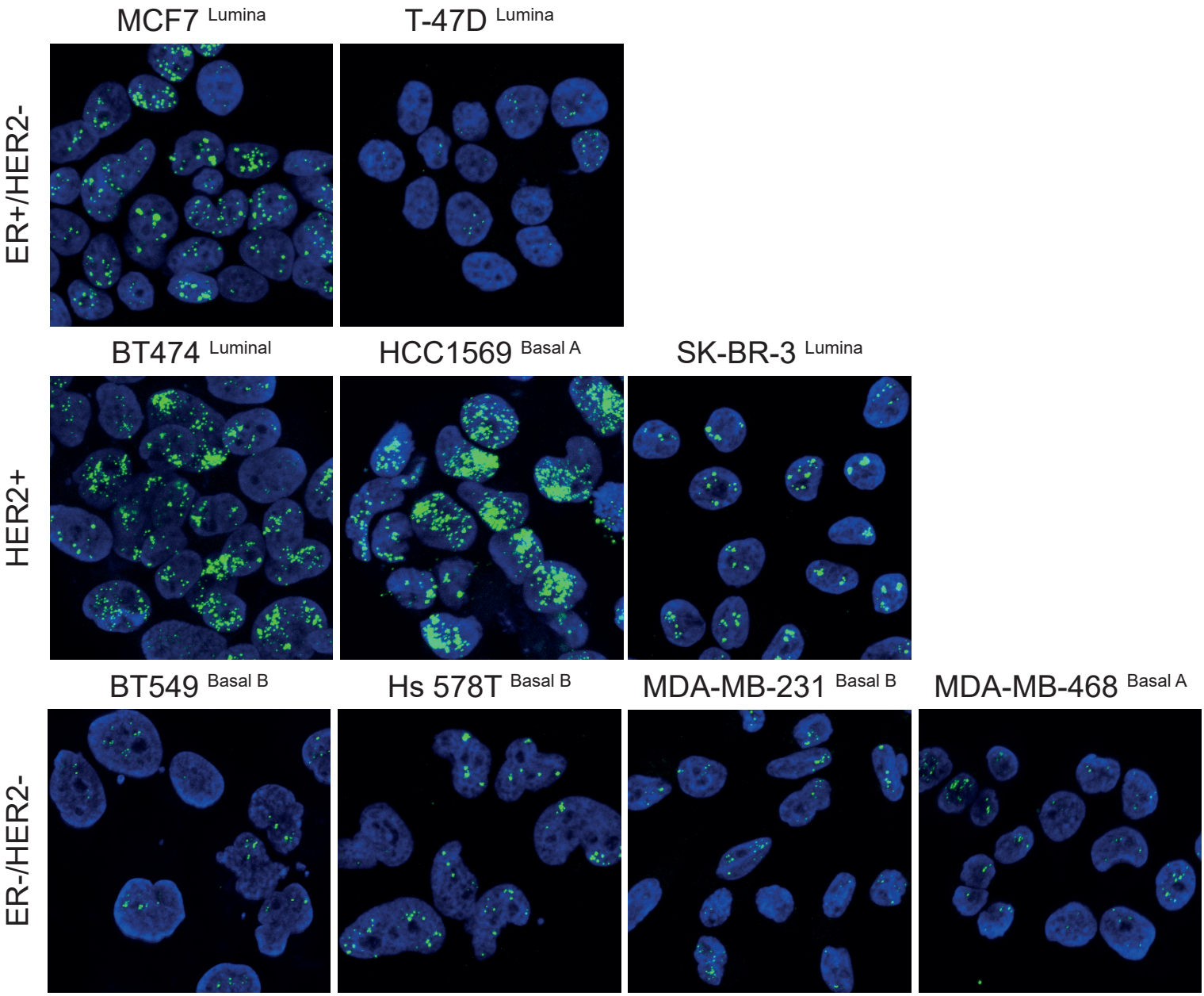
MCF7 Lumina
T-47D Lumina
ER+/HER2-
BT474 Luminal
HCC1569 Basal A
SK-BR-3 Lumina
HER2+
BT549 Basal B
Hs 578T Basal B
MDA-MB-231 Basal B
MDA-MB-468 Basal A
ER-/HER2-

Supp Fig 3

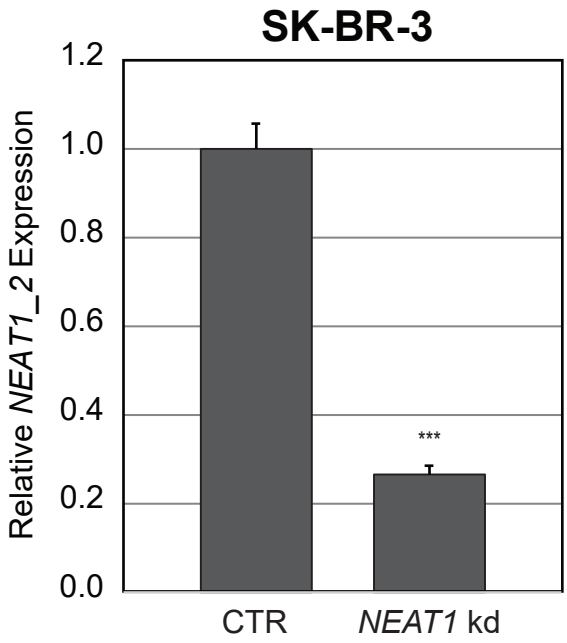
SK-BR-3
Relative NEAT1_2 Expression
1.2
1.0
0.8
0.6
0.4
0.2
0.0
***
CTR
NEAT1 kd

PAPER III

Knockdown of the long non-coding RNA *NEAT1* induces basal autophagy in breast cancer cell lines

Mohammad Seyed Lellahi, Annica Hedberg, Hallvard Olsvik, Erik Knutsen, Maria Perander*.

[1]Department of Medical Biology, Faculty of Health Sciences, UiT – The Arctic University of Norway, Tromsø, Norway

* Corresponding author: *maria.perander@uit.no* Address: RNA and molecular pathology research group, Department of Medical Biology, Faculty of Health Sciences, UiT – the Arctic University of Norway, N-9037 Tromsø, Norway.

ABSTRACT

The long non-coding RNA *NEAT1* is the structural RNA component of nuclear paraspeckles and has been implicated in a wide variety of cellular stress response pathways. Emerging evidence suggests that *NEAT1* plays a role in cytoprotection and cell survival. Abnormal *NEAT1* expression is associated with cancer and neurodegenerative diseases. Here, we report that cells depleted of *NEAT1* expression has altered basic autophagy as measured by increased number of LC3B-containing punctas in the nucleus and accumulation of the lipidated LC3B-II form. Moreover, *NEAT1*-depeltion enhances the effect of sulforaphane on autophagy. We provide evidence that *NEAT1* deficiency leads to induction of autophagy through increasing the activity of AMP-regulated protein kinase (AMPK) towards ULK1. Our results support the notion that *NEAT1* plays a role in protecting organelles and macromolecules from damages upon cellular stress.

INTRODUCTION

Nuclear paraspeckle assembly transcript 1 (*NEAT1*) is a long non-coding RNA that is highly conserved in mammalian cells[1–3]. The *NEAT1* locus is transcribed into two overlapping isoforms, *NEAT1_1* of 3.7 kb and *NEAT1_2* of 22.3 kb[4]. *NEAT1* is the structural RNA component and critical for the assembly of a class of highly dynamic nuclear ribonucleoprotein complexes called paraspeckles[5,6]. More than 40 proteins have been reported to localize to paraspeckles in a manner depending on the cellular context and extracellular cues[6–8]. The paraspeckles change morphology and increase in numbers when *NEAT1_2* expression is elevated[9]. *NEAT1* levels are upregulated in response to cellular stress including hypoxia, heat shock, proteasome inhibitors, DNA damaging reagents, and mitochondrial stress, and *NEAT1*-depleted cells have in many cases been shown to be more sensitive to such stressors[10–17]. *Neat1* knock out mice are viable and healthy, but emerging evidence suggests that *NEAT1* expression is critical at specific developmental stages[18–20]. Female mice display compromised mammary gland development during puberty and pregnancy, and fail to lactate due to impaired proliferation of luminal alveolar cells[18]. They are also less fertile due to defect corpus luteum formation[19]. Importantly, it was recently shown that maternal and zygotic *Neat1*-depletion frequently led to early developmental arrest at the 16- or 32-cell stage in mouse embryonic cells[20]. Generally, it is now accepted that in certain cellular circumstances and developmental stages, *NEAT1* and paraspeckles act as hubs that regulate gene expression by sequestering certain mRNAs and gene regulatory proteins[13,20–27]. *NEAT1* is abnormally expressed in human diseases including cancer and neurodegenerative disorders[14,17,28–32]. In most cancers, high *NEAT1* levels are associated with poor clinical outcome. Importantly, it has been shown that *NEAT1* expression increases in cancer cells treated with chemotherapeutic agents, and *NEAT1* silencing sensitizes cancer cells to drug treatment[14,31,33–40]. Several studies have demonstrated that *NEAT1* is overexpressed in devastating neurodegenerative disorders including amyotrophic

lateral sclerosis (ALS), Huntington's disease, and Alzheimer[28–30,32,41]. Moreover, mislocalization and dysfunction of two paraspeklce-proteins, TAR DNA-binding protein 43 (TDP-43) and fused in sarcoma (FUS), are frequently observed in ALS[42].

Autophagy is a catabolic process where damaged proteins and organelles are degraded by the lysosome and recycled[43]. In macroautophagy, hereafter just referred to as autophagy, the cellular content to be degraded is engulfed into a double-membrane vesicle called the autophagosome, which fuses with the lysosome forming an autolysosome[44]. A variety of cellular stressors that perturb proteostasis, organelle functions and metabolism, induce autophagy[45]. Both basal and induced autophagy are essential for maintenance of cellular homeostasis. Autophagy initiation is orchestrated by the Unc-51-like kinase 1 (ULK1) complex that together with the VPS34-Beclin1 complex, is critical for the formation of the phagophore that subsequently elongates into the autophagosome[46,47]. ULK1 activity and autophagy initiation are negatively regulated by mammalian target of rapamycin, mTOR, that plays an instrumental role in coordinating the balance between cell growth and autophagy in response to growth factors, nutrients and stress[48–50]. In contrast, ULK1 activity is stimulated by AMP-activated protein kinase (AMPK) that is a critical sensor of ATP levels in cells and is activated when the levels of AMP relative to ATP increase[51]. Autophagy is frequently altered in human diseases[52]. In many neurodegenerative disorders, compromised autophagy is associated with formation of pathological protein aggregates[53]. In line with this, genes encoding key components of the autophagic pathway, are frequently mutated in ALS, Huntington’s disease, and Alzheimer. Even though autophagy protects an organisms from developing cancer, elevated autophagy is associated with survival of tumor cells and therapy resistance[54]. This makes autophagy proteins attractive targets in cancer treatment.

We have previously shown that the isocyanate sulforaphane (SFN), which is known to elicit autophagy, induces *NEAT1* expression by activating the heat shock response pathway. Here,

we report that *NEAT1*-depletion affects basal autophagy that results in accumulation of the lipidated form of microtubule-associated protein 1 light chain 3 beta (LC3B), a marker of increased formation of autophagosomes and autolysosomes. This is accompanied by increased formation of punctuated structures containing LC3B. *NEAT1* silencing also leads to the accumulation of the selective autophagy receptor p62, which indicates that lysosomal activity is impaired. Finally, we present evidence that knock down of *NEAT1* activates AMPK kinase, which then phosphorylates ULK1 at Serine-555 that is critical for induction of autophagy. Taken together, our data indicate that *NEAT1*-depletion induces autophagy and also suggest that *NEAT1* might be required for normal lysosomal activity.

RESULTS

NEAT1 depletion leads to the accumulation of autophagosomes

NEAT1 is a stress-induced transcript that is abnormally expressed in human diseases like cancer and neurodegenerative disorders, which are also associated with defective autophagy. We recently showed that *NEAT1* is induced at the transcriptional level by the isocyanate sulforaphane (SFN), a compound that is known to induce autophagy in cells. This prompted us to analyse if *NEAT1* is involved cellular autophagy. A hallmark in autophagy is the formation of double membrane vesicles called the autophagosomes that engulf the cargo to be delivered and degraded by the lysosomes[55]. The ATG8 family protein member Microtubule-associated protein 1 light chain 3 beta (LC3B), is important for autophagosome formation and its conjugation to phosphatidylethanolamine forming the lipidated LC3B-II isoform, is a marker of autophagy in cells. To determine if *NEAT1* has a role in SFN-mediated autophagy, we measured by immunoblot analyses the formation of the lipidated LC3B-II form in control cells and in cells where *NEAT1* was silenced by specific antisense oligonucleotides, which were subsequently either left untreated or treated with SFN for 24 hours. Efficient knock down of

NEAT1 was confirmed by RT-qPCR analyses (supplementary figure 1). We verified what has been shown by others, that SFN indeed induces the formation of the LC3B-II (FIG. 1A). Interestingly, knockdown of *NEAT1* in control cells led to accumulation of LC3B-II, indicating that *NEAT1*-depletion affects basal autophagy. Moreover, *NEAT1*-depletion enhanced SFN-mediated lipidation of LC3B. In autophagy, LC3B-II localizes to autophagosomes and autolysosomes[55]. To further study the effect of *NEAT1* silencing on LC3B, MCF7 cells were transfected with control or *NEAT1* antisense oligonucleotides and endogenous LC3B was analyzed by immunofluorescence staining and confocal microscopy. *NEAT1*-depletion induced the formation of LC3B containing punctas that displayed a perinuclear localization in the majority of the cells (FIG. 1B). Quantitative analyses verified that of the number and volume of LC3B-containing punctas increased upon *NEAT1* silencing. Finally, we verified that *NEAT1*-depletion led to the accumulation of LC3B-II by transfecting cells with a second set of *NEAT1*-specific antisense oligonucleotides (FIG. 1C). Autophagy is a dynamic process, and accumulation of LC3B-II/autophagosomes at a specific time point could be due to either increased in autophagosome formation, or inhibition of their maturation into autolysosomes or lysosomal activity (autophagic flux). Consequently, our data so far suggest that *NEAT1*-depletion either induces autophagy or interferes with the autophagic flux in MCF7 cells. To start delineating the role of *NEAT1* in autophagy more precisely, we treated control and *NEAT1*-depleted MCF7 cells with the lysosomal inhibitor bafilomycin A1 (BafA1) for 4 hours, and assessed its effect on LC3B lipidation compared to untreated cells. As expected, BafA1 caused accumulation of LC3B-II in control cells (FIG. 2A). Importantly, LC3B-II continued to accumulate in *NEAT1*-depleted cells after lysosomal inhibition (FIG. 2A, lane 3 and lane 6). This was clearly verified by immunofluorescence analyses showing increased number of LC3B-contaning punctas in *NEAT1*-depleted cells treated with BafA1 compared to those left untreated (FIG. 2B). Also, the number of punctuated LC3B signals was significantly higher in

BafA1-treated *NEAT1* knock down cells compared to control cells. Even though we can't rule out that lysosomal activity is partially inhibited in *NEAT1* knock down cells, our results indicate that the on-rate of autophagosome formation is elevated upon *NEAT1* depletion.

p62 is a key selective autophagy receptor that binds to ubiquitinated cargo and mediates its association to the inner membrane of the developing phagophore via binding to LC3B and other ATG8 members[56]. Eventually, p62 is degraded with the cargo in the autolysosome. Thus, measuring p62 levels in cells can provide important clues about autophagic degradation. We therefore performed another western blot analyses of the extracts described in FIG. 2A using an antibody that specifically binds to p62. As expected, lysosomal inhibition by 4 hours BafA1 treatment led to a slight, but consistent, accumulation of the p62 protein (FIG. 2C). Intriguingly, p62 protein levels were slightly elevated in untreated *NEAT1*-depleted cells, and this was further enhanced by BafA1. To rule out any cell-specific effect of *NEAT1*-depletion on LC3B and p62 in MCF7 cells, we repeated the immunoblot experiments in control and *NEAT1*-silenced BT474 cells. We confirmed that knock down of *NEAT1* led to accumulation of both LC3B and p62 that was further enhanced by BafA1 treatment also in BT474 (FIG. 2D).

mTOR activity is not affected by NEAT1 depletion.

The mTOR kinase is a master regulator of autophagy[48–50]. In normal physiological conditions, mTOR complex 1 (mTORC1), which in addition to mTOR also consists of Raptor and mLST8, actively suppresses autophagy by phosphorylating and inhibiting the activity of ULK1. To analyse if *NEAT1*-depletion interferes with mTOR activity, we determined the phosphorylation status of Threonine 389 (Thr389) of p70 ribosomal S6 kinase (p70S6K), one of the best characterized substrates of mTOR, by immunoblot analyses. We first confirmed that amino acid starvation (HBSS) that potently inactivates mTOR, abolished the phosphorylation of Thr389 of p70S6K in MCF7 cells (FIG. 3A). In contrast, knock down of *NEAT1* in neither MCF7 nor

BT474 cells, changed the activity of mTOR as assessed by Thr389 p70S6K phosphorylation (FIG. 3B).

AMPK is activated in NEAT1-depleted cells

AMPK is a central kinase in the regulation of cellular metabolism. Upon nutrient starvation and different cellular stressors that interfere with ATP production, AMPK is activated which in turn elicits autophagy by both inactivating mTORC1 and by directly activating ULK1 through phosphorylation of Serine 317 (Ser317) and Serine 555 (Ser555)[51,57]. To investigate the activation of AMPK in *NEAT1*-silenced cells, we first determined the phosphorylation status of Threonine 172 (Thr72) that is critical for AMPK catalytic activity. *NEAT1*-depletion indeed increased the phosphorylation of Thr172 in MCF7 cells (FIG. 4A). We next analysed if the increased phosphorylation of AMPK is accompanied by increased phosphorylation of Ser317 and Ser555 of ULK1. Importantly, *NEAT1* knock down enhanced both ULK1 Ser317 and ULK1 555 phosphorylation (FIG4B). Taken together, our data suggest that AMPK activity is increased in cells as a consequence of reduced *NEAT1* expression and that this leads to the activation of ULK1 and autophagy.

DISCUSSION

The long non-coding RNA *NEAT1* has emerged as an important regulator of gene expression in cellular stress and at certain developmental stages[13,17,20–27]. *NEAT1* expression is activated by a wide variety of cellular stressors including hypoxia, heat shock, genotoxic and mitochondrial stress[10–17]. Such stressors can cause serious damage on proteins, DNA, and organelles[45]. To counteract this, the autophagic machinery will be activated in cells to degrade dysfunctional macromolecules and organelles, and recycle their components. This prompted us

to investigate whether *NEAT1* is involved in the regulation of autophagy. Here, we have shown that *NEAT1*-depletion leads to increased formation of LC3B-containing punctas and accumulation of the lipidated LC3B-II form in in two different breast cancer cell lines. LC3B-II continues to accumulate in *NEAT1* knockdown cells after inhibiting lysosomal acidification and degradation with bafilomycin A1. This indicates that on-rate of autophagy is increased. In line with this, we report that the AMPK is activated in *NEAT1*-depleted cells as measured by increased phosphorylation of Serine 172. This is accompanied by increased phosphorylation of Serine 555 and Serine 317 of ULK1, which is required for its activation and induction of autophagy.

NEAT1 and paraspeckles have recently been shown to be essential for mitochondrial homeostasis[27]. Wang et al. showed that *NEAT1*-depletion led to formation of elongated mitochondria through a mechanism where the expression and activity of dynamin-related protein 1 (DRP1), a protein required for mitochondrial fission, were inhibited. Increased autophagy is in many cases known to be followed by mitochondrial elongation[58,59]. Therefore, the formation of elongated mitochondria upon NEAT1 knockout could be a direct consequence of increased basal autophagy in the cells. Elongated mitochondria are less prone to be degraded by autophagy (mitophagy) and are more efficient in producing ATP, implicating that this is an immediate cellular defence mechanism to preserve the mitochondrial functions and avoid cell death[58,59]. However, in the study mentioned above, Wang et al demonstrated that *NEAT1*-depletion resulted in reduced respiration and ATP production in the cells, indicating that even though the mitochondria had elongated, they were highly dysfunctional. As the AMP-activated protein kinase (AMPK) is directly activated when the ATP to AMP ratio drops, it is reasonable to assume that dysfunctional mitochondria in *NEAT1*-depleted cells will lead to AMPK activation and induction of autophagy. Generally, AMPK has a central role in regulating mitochondrial dynamics and biogenesis, and is activated by agents interfering with

mitochondrial functions[60]. In the future, it will indeed be important to analyse if reduced *NEAT1* expression is accompanied by induced mitophagy and further experiments should be undertaken to dissect the intricate crosstalk between *NEAT1*, mitochondrial functions, AMPK and autophagy.

Recently, it was reported that *NEAT1*-depleted MCF7 cells undergo replication stress and display increased levels of γ-H2A.X, a histone marker of DNA damage[14]. Moreover, compared to wild type mice, *Neat1* knockout mice displayed prolonged accumulation of DNA damages upon exposure to the carcinogenic compound DMBA. This was accompanied by enhanced stabilization of p53. Accumulation of p53 is known to induce autophagy at least partially by activating AMPK[61,62]. This indicates that *NEAT1*-depletion could result in accumulation of wild type (MCF7) or mutant (BT474) p53 that subsequently induces autophagy.

We show that LC3B-II in *NEAT1* knockdown cells continues to accumulate after inhibiting lysosomal activity with bafilomycin B. This made us hypothesize that the on-rate of autophagy is increased in *NEAT1*-depleted cells, which is further supported by AMPK activity being enhanced in *NEAT1* silenced cells. Upon induction of autophagy, selective autophagy receptors including p62, will bind to ubiquitinated cargo and bring it to the developing phagophore by binding to LC3B and other ATG8 members via a LC3-interacting region (LIR)[56]. As p62 is degraded with the cargo in the autolysosome, enhanced autophagy is often accompanied with a reduction in p62 protein levels. Here, we show that *NEAT1*-depletion does not lead to reduction, but rather slight accumulation, of p62 protein levels. This might indicate that *NEAT1* expression is required for normal lysosomal activity. Alternatively, *NEAT1* knock down might upregulate the expression of the gene encoding p62, *SQSTM1*. The transcription of the *SQSTM*1 gene has been shown to activated by the transcription factor Nrf2[63]. Nrf2 has a key role in eliciting a cytoprotective response to oxidative stress caused by excess formation of reactive oxygen species[64]. As *NEAT1*-depletion is known to seriously interfere with

mitochondrial functions, it is reasonable to assume that ROS levels are increased in *NEAT1* knockdown cells. Whether Nrf2 activity and *SQSTM1* transcription are elevated in *NEAT1*-deficient cells, remain to be determined.

The long *NEAT1_2* isoform is essential for the assembly of paraspeckles. More than 40 proteins have been demonstrated to localize to paraspeckles[5–8]. It is therefore logical to envision that *NEAT1*-depletion will lead to mislocalization of paraspeckle proteins. Importantly, mislocalization of two paraspeckle-associated proteins, TAR DNA-binding protein 43 (TDP-43) and fused in sarcoma (FUS), is associated with serious neurodegenerative diseases[30,41,42]. Both proteins are prone to form aggregates in the cytoplasm, which will elicit autophagy in order to get them removed[65]. Thus, it is likely that protein mislocalization upon *NEAT1* deficiency can trigger the autophagic machinery.

NEAT1 expression is induced by a wide variety of stressors. Emerging evidence suggests that *NEAT1* and paraspeckle are required to preserve and protect macromolecules and organelles, including DNA, proteins and mitochondria, upon stress. We hypothesize that when *NEAT1* expression is repressed under such conditions, accumulation of damaged macromolecules and organelles will trigger autophagy. The link between *NEAT1* and autophagy should be further studied in human diseases like cancer and neurodegenerative disorders.

EXPERIMENTAL PROCEDURES

Cell culture and treatment

MCF7 (ATCC® HTB-22™) and BT-474 (ATCC® HTB-20™) were obtained from the American Type Culture Collection (ATCC) and maintained in the humidified atmosphere at 37°C with 5% CO_2. MCF7 cells were cultured in minimal essential medium (MEM, Sigma-Aldrich), and BT474 cells were cultured in Roswell Park Memorial Institute 1640 (RPMI1640, Sigma-Aldrich). Both media were supplemented with 10% fetal bovine serum (Biochrom, Merck) and 1% penicillin-streptomycin (Sigma-Aldrich). Insulin (0.01mg/ml, Sigma-Aldrich) was added to MCF7 culture media. Bafilomycin A1 (BafA1) was purchased from Santa Cruz Biotechnology and was added to the cells at a final concentration of 200nM. Hank's Balanced Salt Solution (HBSS) was purchased from Sigma, and were used for the starvation of cells. To remove all the supplementary nutrition, cells were washed two times with HBSS and then incubated in HBSS for specific time points. Experiments on MCF7 were performed when cells were between passage 10-30. Cells were tested regularly for mycoplasma.

RNA interference

Locked nucleic acid (LNA)-GapmeR *NEAT1* antisense oligos and control GapmeRs were purchased from Qiagene (Table 1). Cells were transfected using Lipofectamine 2000 according to the reverse transfection protocol provided by the manufacturer (ThermoFisher Scientific) and generally left for 48 hours. Successful knockdown was verified by RT-qPCR.

Reverse transcription and quantitative PCR

Total RNA was extracted using Direct-zol RNA Miniprep (Zymo Research) according to the manufacturer's instruction, and RNA concentration was measured by NanoDrop 2000 (Thermo Fisher Scientific). The reverse Transcription (RT) was carried out with the SuperScript™ IV

Reverse Transcriptase (Thermo Fisher Scientific), following the manufacturer recommendations. The quantitative polymerase chain reaction was performed with SYBR green reaction mix FastStart Essential DNA Green Master (Roche Life Science) using LightCycler 96 (Roche Life Science). 2.5ul of 10 times diluted cDNA was mixed by 0.25uM of forward and reverse primer in combination with 5ul of SYBR green with the following thermal cycle conditions: 95°C 10 minutes and 40 cycles of 95°C 10 seconds, 60°C 10 seconds and 72°C for 10 seconds. All the primer sequences are provided in Table 1. All the experiments were done at least in triplicates. GAPDH was used as reference gene for normalization. Data are shown in fold change using ΔΔCq method.

Immunoblotting

Cells were lysed in 2% SDS, 10% glycerol, and 50mM Tris-HCl, pH 6.8. Protein concentration was measured using Pierce™ BCA Protein Assay Kit (Thermo Fisher Scientific) according to manufacturer's recommendation. Equal amount of proteins was loaded (20 ug or 30 ug depending on the antibody), and proteins were resolved on SDS-PAGE gels and transferred to nitrocellulose membranes. Nitrocellulose membranes were blocked with Odyssey® Blocking Buffer (PBS) or Odyssey® Blocking Buffer (TBS) (ULK1 antibodies). Both blocking buffers were purchased from LI-COR Biosciences. The following primary antibodies were used at 1:1000 dilution and purchased from Cell Signaling Technology: Rabbit mAb anti-phospho-AMPKα (Thr172)(40H9) (cat# 2535), Rabbit mAb anti-AMPKα (D63G4) (cat# 5832), Rabbit mAb anti-p70 S6 kinase (cat# 9202), Rabbit mAb anti-phospho-p70S6 kinase (Thr 389)(cat# 9205), Rabbit mAb anti-phospho-ULK1 (Ser555) (D1H4) (cat# 5869). The following antibodies were diluted 1:400: Rabbit mAb anti-phospho-ULK1 (Ser 317) (cat# 6887), and Rabbit mAb anti-ULK1 (D8H5) (cat# 8054). Rabbit mAb anti-LC3B was purchased from Sigma (1:1000, cat# L7543). Mouse monoclonal anti-p62-LCK was obtained from BD-

bioscience (1:1000, cat# 610833), and Mouse monoclonal anti-Actin was from Millipore (1:1000, cat# MAB1501). IRDye®-conjugated secondary antibodies (LI-COR Biosciences) was used in a dilution of 1: 10 000 for both goat anti-Rabbit (800CW, cat# 926-32211) and goat anti-mouse (680LT, cat# 926-68020). The images were taken using the Odyssey® CLx Infrared Imaging System.

Fluorescence immunostaining

Cells were seeded on coverslips and fixed and permeabilized in cold (-20) methanol for 10 minutes. Cells were washed with cold PBS three times and blocked with 2% bovine serum (BSA, prepared in PBS-Tween (0.1%)) for 10 minutes at room temperature. Next, cells were incubated with anti-LC3-B antibody for 90 minutes (1:400, Sigma, cat# L7543), and then incubated with goat anti-rabbit Alexa 488-conjugated secondary antibody (1:1000, Thermo Fisher Scientific, cat# A11070) for 45 minutes. Both primary and secondary antibodies were diluted in PBST containing 2% BSA. Following extensive washing, coverslips were mounted using Vectashield® Antifade Mounting Medium containing DAPI (Vector Laboratories, H-1200). All images were acquired by Zeiss LSM780 confocal microscope (Carl Zeiss Microscopy GmbH, Jena, Germany) using 63x magnification. To take the picture, middle Z slice was positioned at DAPI's best focus, and in total, five slices were imaged with a total high of 2.5μm. All the samples were treated similarly, and the same settings were used for all of the study groups. At least ten random positions were chosen from each coverslip, and pictures were analyzed by the Volocity software (PerkinElmer, version 6.3). Each experiment was performed in triplicates. At least 160 cells in each group of treatment were analyzed by volocity software.

Statistics

Statistical analyses were done using unpaired Student's t-Test using the GraphPad software (Prism version 7, Mac OS X). *P*-values <0.05 were defined as statistically significant, and for all experiment's significance is expressed as ***, $p \leq 0.001$, **, $p \leq 0.01$, and *, $p \leq 0.05$. All the experiments were performed in triplicates and data were presented as mean ± SD.

REFERENCE

1. Hutchinson, J. N. *et al.* A screen for nuclear transcripts identifies two linked noncoding RNAs associated with SC35 splicing domains. *BMC Genomics* **8,** 39 (2007).
2. Saha, S. Identification and characterization of a virus-inducible non-coding RNA in mouse brain. *J. Gen. Virol.* **87,** 1991–1995 (2006).
3. Guru, S. C. *et al.* A transcript map for the 2.8-Mb region containing the multiple endocrine neoplasia type 1 locus. *Genome Res.* **7,** 725–35 (1997).
4. Bond, C. S. & Fox, A. H. Paraspeckles: nuclear bodies built on long noncoding RNA. *J. Cell Biol.* **186,** 637–644 (2009).
5. Nakagawa, S., Naganuma, T., Shioi, G. & Hirose, T. Paraspeckles are subpopulation-specific nuclear bodies that are not essential in mice. *J. Cell Biol.* **193,** 31–39 (2011).
6. Naganuma, T. *et al.* Alternative 3′-end processing of long noncoding RNA initiates construction of nuclear paraspeckles. *EMBO J.* **31,** 4020–4034 (2012).
7. Yamazaki, T. & Hirose, T. The building process of the functional paraspeckle with long non-coding RNAs. *Front. Biosci. (Elite Ed).* **7,** 1–41 (2015).
8. Fox, A. H., Nakagawa, S., Hirose, T. & Bond, C. S. Paraspeckles: Where Long Noncoding RNA Meets Phase Separation. *Trends Biochem. Sci.* **43,** 124–135 (2018).
9. Naganuma, T. & Hirose, T. Paraspeckle formation during the biogenesis of long non-coding RNAs. *RNA Biol.* **10,** 456–461 (2013).
10. Imamura, K. *et al.* Long Noncoding RNA NEAT1-Dependent SFPQ Relocation from Promoter Region to Paraspeckle Mediates IL8 Expression upon Immune Stimuli. *Mol. Cell* **53,** 393–406 (2014).
11. Michelhaugh, S. K. *et al.* Mining Affymetrix microarray data for long non-coding RNAs: altered expression in the nucleus accumbens of heroin abusers. *J. Neurochem.* **116,** 459–466 (2011).
12. Zhang, Q., Chen, C.-Y., Yedavalli, V. S. R. K. & Jeang, K.-T. NEAT1 Long Noncoding RNA and Paraspeckle Bodies Modulate HIV-1 Posttranscriptional Expression. *MBio* **4,** e00596-12 (2013).
13. Hirose, T. *et al.* NEAT1 long noncoding RNA regulates transcription via protein sequestration within subnuclear bodies. *Mol. Biol. Cell* **25,** 169–183 (2014).
14. Adriaens, C. *et al.* p53 induces formation of NEAT1 lncRNA-containing paraspeckles that modulate replication stress response and chemosensitivity. *Nat. Med.* **22,** 861–868 (2016).
15. Beeharry, Y., Goodrum, G., Imperiale, C. J. & Pelchat, M. The Hepatitis Delta Virus accumulation requires paraspeckle components and affects NEAT1 level and PSP1 localization. *Sci. Rep.* **8,** 6031 (2018).
16. Ma, H. *et al.* The Long Noncoding RNA NEAT1 Exerts Antihantaviral Effects by Acting as Positive Feedback for RIG-I Signaling. *J. Virol.* **91,** 1–20 (2017).

17. Choudhry, H. *et al.* Tumor hypoxia induces nuclear paraspeckle formation through HIF-2α dependent transcriptional activation of NEAT1 leading to cancer cell survival. *Oncogene* **34,** 4482–4490 (2015).
18. Standaert, L. *et al.* development and lactation The long noncoding RNA Neat1 is required for mammary gland development and lactation. 1–6 (2014). doi:10.1261/rna.047332.114.
19. Nakagawa, S. *et al.* The lncRNA Neat1 is required for corpus luteum formation and the establishment of pregnancy in a subpopulation of mice. *Development* **141,** 4618–4627 (2014).
20. Hupalowska, A. *et al.* CARM1 and Paraspeckles Regulate Pre-implantation Mouse Embryo Development. *Cell* **175,** 1902–1916.e13 (2018).
21. Imamura, K. *et al.* Long Noncoding RNA NEAT1-Dependent SFPQ Relocation from Promoter Region to Paraspeckle Mediates IL8 Expression upon Immune Stimuli. *Mol. Cell* **53,** 393–406 (2014).
22. Chen, L.-L. & Carmichael, G. G. Altered Nuclear Retention of mRNAs Containing Inverted Repeats in Human Embryonic Stem Cells: Functional Role of a Nuclear Noncoding RNA. *Mol. Cell* **35,** 467–478 (2009).
23. Prasanth, K. V. *et al.* Regulating Gene Expression through RNA Nuclear Retention. *Cell* **123,** 249–263 (2005).
24. Torres, M. *et al.* Circadian RNA expression elicited by 3'-UTR IRAlu-paraspeckle associated elements. *Elife* **5,** 1–23 (2016).
25. Hu, S.-B. *et al.* Protein arginine methyltransferase CARM1 attenuates the paraspeckle-mediated nuclear retention of mRNAs containing IR Alu s. *Genes Dev.* **29,** 630–645 (2015).
26. West, J. A. *et al.* The Long Noncoding RNAs NEAT1 and MALAT1 Bind Active Chromatin Sites. *Mol. Cell* **55,** 791–802 (2014).
27. Wang, Y. *et al.* Genome-wide screening of NEAT1 regulators reveals cross-regulation between paraspeckles and mitochondria. *Nat. Cell Biol.* **20,** 1145–1158 (2018).
28. Liu, Y. & Lu, Z. Long non-coding RNA NEAT1 mediates the toxic of Parkinson's disease induced by MPTP/MPP+ via regulation of gene expression. *Clin. Exp. Pharmacol. Physiol.* **45,** 841–848 (2018).
29. Cheng, C. *et al.* The long non-coding RNA NEAT1 is elevated in polyglutamine repeat expansion diseases and protects from disease gene-dependent toxicities. *Hum. Mol. Genet.* **27,** 4303–4314 (2018).
30. Česnik, A. B. *et al.* Nuclear RNA foci from C9ORF72 expansion mutation form paraspeckle-like bodies. *J. Cell Sci.* jcs.224303 (2019). doi:10.1242/jcs.224303
31. Chakravarty, D. *et al.* The oestrogen receptor alpha-regulated lncRNA NEAT1 is a critical modulator of prostate cancer. *Nat. Commun.* **5,** 5383 (2014).
32. Annese, A. *et al.* Whole transcriptome profiling of Late-Onset Alzheimer's Disease patients provides insights into the molecular changes involved in the disease. *Sci. Rep.* **8,** 4282 (2018).
33. Wu, Y. & Wang, H. LncRNA NEAT1 promotes dexamethasone resistance in multiple myeloma by targeting miR-193a/MCL1 pathway. *J. Biochem. Mol. Toxicol.* **32,** 1–6 (2018).
34. Lo, P.-K. *et al.* Dysregulation of the BRCA1/long non-coding RNA NEAT1 signaling axis contributes to breast tumorigenesis. *Oncotarget* **7,** (2016).
35. Gong, W. *et al.* Knockdown of NEAT1 restrained the malignant progression of glioma stem cells by activating microRNA *let-7e*. *Oncotarget* **7,** 62208–62223 (2016).
36. Li, B., Gu, W. & Zhu, X. NEAT1 mediates paclitaxel-resistance of non-small cell of lung cancer through activation of Akt/mTOR signaling pathway. *J. Drug Target.* **0,** 1–

23 (2019).
37. Jiang, P. *et al.* NEAT1 acts as an inducer of cancer stem cell-like phenotypes in NSCLC by inhibiting EGCG-upregulated CTR1. *J. Cell. Physiol.* **233,** 4852–4863 (2018).
38. Tian, X., Zhang, G., Zhao, H., Li, Y. & Zhu, C. Long non-coding RNA NEAT1 contributes to docetaxel resistance of prostate cancer through inducing RET expression by sponging miR-34a. *RSC Adv.* **7,** 42986–42996 (2017).
39. Zhang, J. *et al.* Silence of Long Noncoding RNA NEAT1 Inhibits Malignant Biological Behaviors and Chemotherapy Resistance in Gastric Cancer. *Pathol. Oncol. Res.* **24,** 109–113 (2018).
40. Shin, V. Y. *et al.* Long non-coding RNA NEAT1 confers oncogenic role in triple-negative breast cancer through modulating chemoresistance and cancer stemness. *Cell Death Dis.* **10,** 270 (2019).
41. Shelkovnikova, T. A., Robinson, H. K., Troakes, C., Ninkina, N. & Buchman, V. L. Compromised paraspeckle formation as a pathogenic factor in FUSopathies. *Hum. Mol. Genet.* **23,** 2298–2312 (2014).
42. Pokrishevsky, E. *et al.* Aberrant Localization of FUS and TDP43 Is Associated with Misfolding of SOD1 in Amyotrophic Lateral Sclerosis. *PLoS One* **7,** e35050 (2012).
43. Dikic, I. & Elazar, Z. Mechanism and medical implications of mammalian autophagy. *Nat. Rev. Mol. Cell Biol.* **19,** 349–364 (2018).
44. Eskelinen, E.-L. Maturation of Autophagic Vacuoles in Mammalian Cells. *Autophagy* **1,** 1–10 (2005).
45. Levine, B. & Kroemer, G. Autophagy in the Pathogenesis of Disease. *Cell* **132,** 27–42 (2008).
46. Hosokawa, N. *et al.* Nutrient-dependent mTORC1 Association with the ULK1–Atg13–FIP200 Complex Required for Autophagy. *Mol. Biol. Cell* **20,** 1981–1991 (2009).
47. Itakura, E., Kishi, C., Inoue, K. & Mizushima, N. Beclin 1 Forms Two Distinct Phosphatidylinositol 3-Kinase Complexes with Mammalian Atg14 and UVRAG. *Mol. Biol. Cell* **19,** 5360–5372 (2008).
48. He, C. & Klionsky, D. J. Regulation Mechanisms and Signaling Pathways of Autophagy. *Annu. Rev. Genet.* **43,** 67–93 (2009).
49. Kamada, Y. *et al.* Tor Directly Controls the Atg1 Kinase Complex To Regulate Autophagy. *Mol. Cell. Biol.* **30,** 1049–1058 (2010).
50. Kamada, Y. *et al.* Tor-Mediated Induction of Autophagy via an Apg1 Protein Kinase Complex. *J. Cell Biol.* **150,** 1507–1513 (2000).
51. Kim, J., Kundu, M., Viollet, B. & Guan, K.-L. AMPK and mTOR regulate autophagy through direct phosphorylation of Ulk1. *Nat. Cell Biol.* **13,** 132–141 (2011).
52. Schneider, J. L. & Cuervo, A. M. Autophagy and human disease: Emerging themes. *Curr. Opin. Genet. Dev.* **26,** 16–23 (2014).
53. Nixon, R. A. The role of autophagy in neurodegenerative disease. *Nat. Med.* **19,** 983–997 (2013).
54. Kondo, Y., Kanzawa, T., Sawaya, R. & Kondo, S. The role of autophagy in cancer development and response to therapy. *Nat. Rev. Cancer* **5,** 726–734 (2005).
55. Klionsky, D. J. *et al.* Guidelines for the use and interpretation of assays for monitoring autophagy (3rd edition). *Autophagy* **12,** 1–222 (2016).
56. Pankiv, S. *et al.* p62/SQSTM1 Binds Directly to Atg8/LC3 to Facilitate Degradation of Ubiquitinated Protein Aggregates by Autophagy. *J. Biol. Chem.* **282,** 24131–24145 (2007).
57. Egan, D. F. *et al.* Energy Sensing to Mitophagy. *Science (80-.).* **331,** 456–461 (2010).
58. Gomes, L. C., Benedetto, G. Di & Scorrano, L. During autophagy mitochondria elongate, are spared from degradation and sustain cell viability. *Nat. Cell Biol.* **13,** 589–598

(2011).
59. Rambold, A. S., Kostelecky, B., Elia, N. & Lippincott-Schwartz, J. Tubular network formation protects mitochondria from autophagosomal degradation during nutrient starvation. *Proc. Natl. Acad. Sci.* **108,** 10190–10195 (2011).
60. Herzig, S. & Shaw, R. J. AMPK: guardian of metabolism and mitochondrial homeostasis. *Nat. Rev. Mol. Cell Biol.* **19,** 121–135 (2017).
61. Levine, B. & Abrams, J. p53: The Janus of autophagy? *Nat. Cell Biol.* **10,** 637–639 (2008).
62. Feng, Z., Zhang, H., Levine, A. J. & Jin, S. The coordinate regulation of the p53 and mTOR pathways in cells. *Proc. Natl. Acad. Sci.* **102,** 8204–8209 (2005).
63. Jain, A. *et al.* p62/SQSTM1 Is a Target Gene for Transcription Factor NRF2 and Creates a Positive Feedback Loop by Inducing Antioxidant Response Element-driven Gene Transcription. *J. Biol. Chem.* **285,** 22576–22591 (2010).
64. Ma, Q. Role of Nrf2 in Oxidative Stress and Toxicity. *Annu. Rev. Pharmacol. Toxicol.* **53,** 401–426 (2013).
65. Ramesh, N. & Pandey, U. B. Autophagy Dysregulation in ALS: When Protein Aggregates Get Out of Hand. *Front. Mol. Neurosci.* **10,** 1–18 (2017).

FIGURE 1. ***NEAT1*-depletion leads to accumulation of lipidated LC3B and formation of autophagosomes.** *A,* MCF7 cells were transfected with *NEAT1* antisense oligos targeting both isoforms of *NEAT1*, or a negative control oligo. Twenty-four h post-transfection, cells were either left untreated or treated with SFN (10μM) for 24 h. LC3B-I and II expression was determined by immunoblot analyses. The intensities of the specific signals/bands were measured by the Odyssey® Infrared Imaging System and relative values to non-transfected cells are shown. Equal loading was verified by re-probing the membranes with an anti-actin antibody. *B,* MCF7 cells were transfected with *NEAT1* antisense oligos or a negative control oligo. After 48 h, cells were fixed and stained with an anti-LC3B antibody. DAPI was used to visualize the nuclei. The number of LC3B-punctas per cell and volume of each puncta/volume of the cell were measured in at least 160 cells by the Volocity software. Scale bar, 10 μM. P values were calculated using student's T-test with $p < 0.05$ considered statistically significant. (***, $p \leq 0.001$). *C,* MCF7 cells were transfected with two different sets of *NEAT1* antisense oligoes (*NEAT1* kd #1 and *NEAT1* kd #2) and the expression of LC3B-I and II was determined by immunoblot analyses. Membranes were re-probed with an anti-actin antibody.

FIGURE 2. ***NEAT1*-depletion induces autophagy.** *A,* MCF7 cells were transfected with *NEAT1* antisense oligos or control oligos. After 48 h, cells were left untreated or treated with 200 nM bafilomycin A1 (BafA1) for 4 h. LC3B-I and II expression were measured by immunoblot analyses. Membranes were re-probed with an anti-actin antibody to verify equal loading. *B,* MCF7 cells were transfected and treated as in *A* and stained with an anti-LC3B antibody. The number of LC3B-punctas and volume of each dot/volume of the cell were measured by the Volocity software in at least 160 cells. Scale bar, 10 μM. P values were calculated using student's T-test with $p < 0.05$ considered statistically significant (**, $p \leq 0.01$,

*p, ≤ 0.05). *C*, p62 expression in the same samples as described in *A*, was determined by immunoblot analyses. *D*, The experiments described in *A*, and *C*, were repeated in BT474 cells.

FIGURE 3. **mTOR activity is not affected by *NEAT1* depletion.** *A*, MCF7 cells were grown in full media or starved in HBSS for 4 hours. The phosphorylation status of Threonine 389 of p70S6K and total p70S6K expression were determined by immunoblotting. Membranes were re-probed with an anti-actin antibody to verify equal loading. *B*, BT474 and MCF7 cells were transfected with *NEAT1* antisense oligos or control oligos. Phosphorylation of Thr389 and total p70S6K levels were determined by immunoblot analyses.

FIGURE 4. **AMPK is activated in *NEAT1*-depleted** *A*, *NEAT1* was knocked down in MCF7 and the phosphorylation status of Threonine 172 within AMPK and total AMPK expression, were analysed by immunoblotting. ***B*,** The phosphorylation status of Serine 317 and Serine 555 in ULK1, as well as total ULK1 expression, were determined by immunoblot analyses using anti-phospho-Ser317 ULK1, anti-phospho-Ser555 ULK1, and anti-ULK1 antibodies, respectively. Equal loading was verified by re-probing the membranes with an anti-actin antibody.

Supplementary 1. *NEAT1* knockdown efficiency in MCF7 cells. MCF7 cells were transfected with LNA-gapmeR *NEAT1* antisense oligos for 24 hours. *NEAT1* and *NEAT1_2* expression was determined by RT-qPCR. The mean value ± SD of three biological replicates are shown and presented as fold change relative to Ctrl cells.

Table 1. Primer and ASO sequences

Name	**RT-qPCR (5'→3')**
GAPDH	F- GAGCGAGATCCCTCCAAAAT
	R- AAATGAGCCCCAGCCTTCT
NEAT1	F- TCGGGTATGCTGTTGTGAAA
	R- TGACGTAACAGAATTAGTTCTTACCA
NEAT1_2	F- CGGAGGGTCTTGTAACACCAG
	R- AGTCCGGGCAACACAGAAAG
Name	**Antisense LNA GapmeR Standard**
***NEAT1*- #1 (described in ref 13)**	TAAGCACTTTGGAAAG
***NEAT1_2*- #1 (described in ref 13)**	CTCACACGTCCATCT
***NEAT1*- #2**	TGTGGCATCAACGTTA
***NEAT1_2*- #2**	GAAAGTCATCGCAAGT
Negative Control	AACACGTCTATACGC

Figure 1

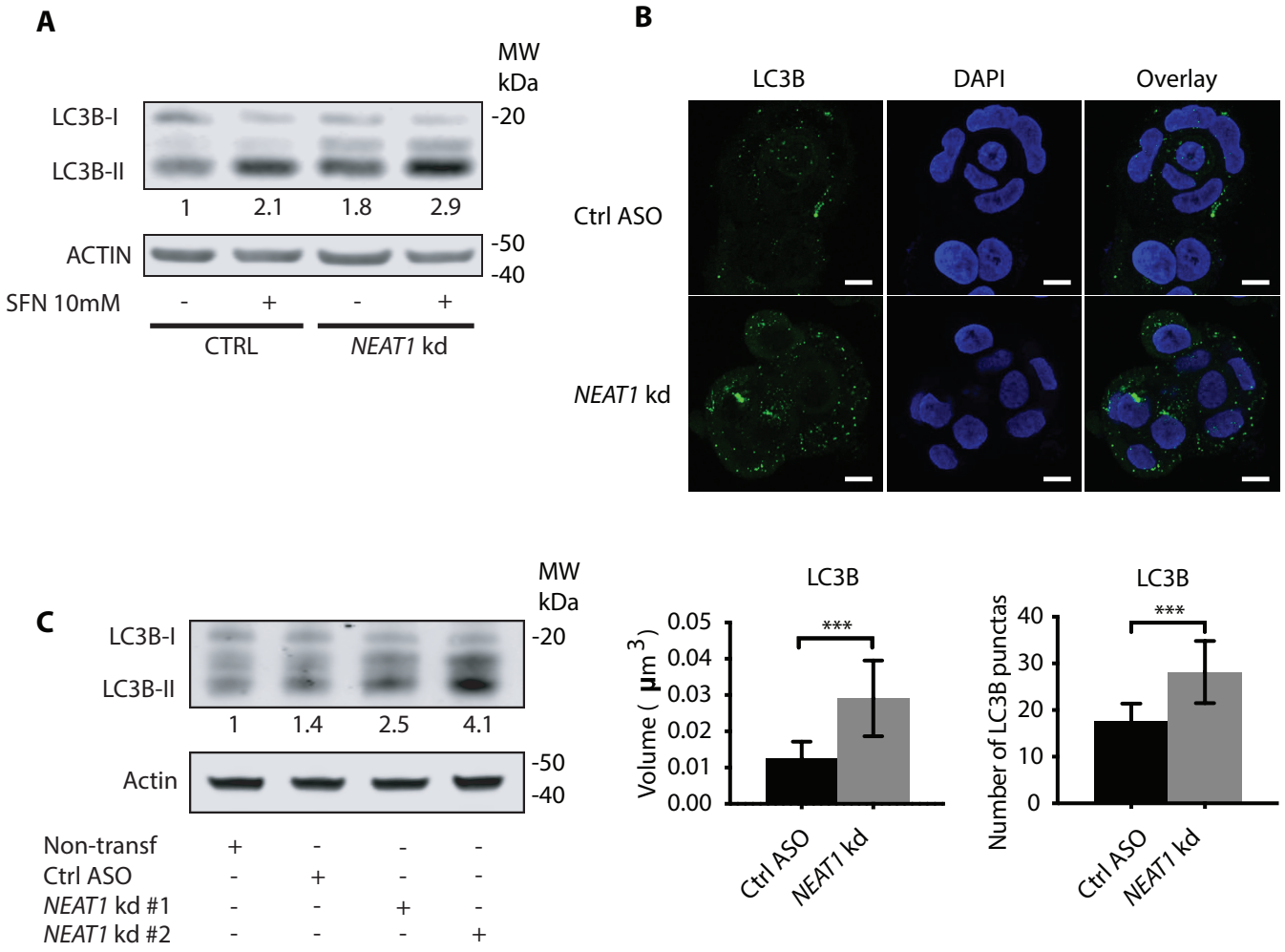
A
MW kDa
LC3B-I
LC3B-II
-20
1
2.1
1.8
2.9
ACTIN
-50
-40
SFN 10mM
- + - +
CTRL
NEAT1 kd
B
LC3B
DAPI
Overlay
Ctrl ASO
NEAT1 kd
C
MW kDa
LC3B-I
LC3B-II
-20
1
1.4
2.5
4.1
Actin
-50
-40
Non-transf + - - -
Ctrl ASO - + - -
NEAT1 kd #1 - - + -
NEAT1 kd #2 - - - +
LC3B
***
Volume (µm3)
0.05
0.04
0.03
0.02
0.01
0.00
Ctrl ASO
NEAT1 kd
LC3B
***
Number of LC3B punctas
40
30
20
10
0
Ctrl ASO
NEAT1 kd

Figure 2

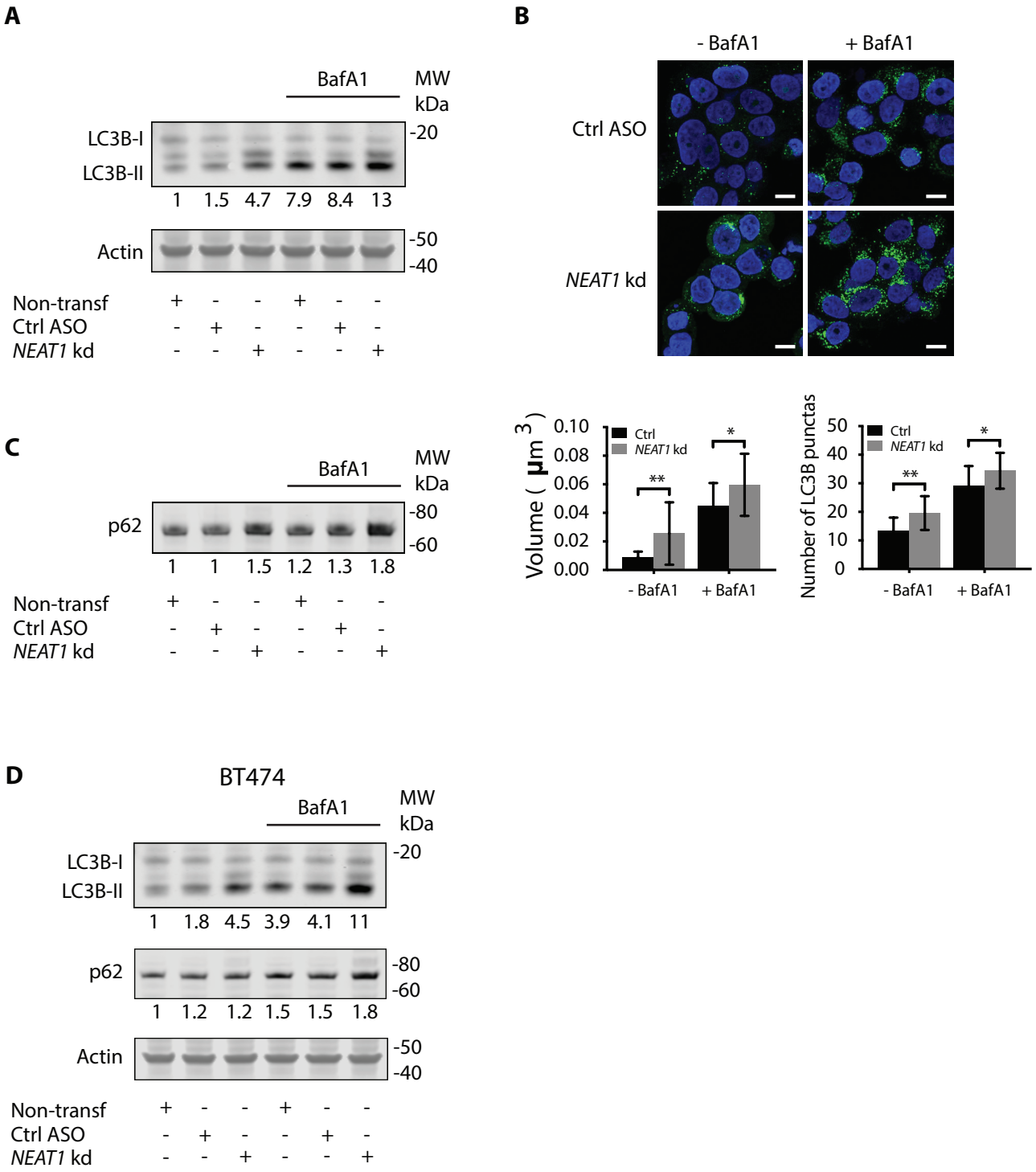
A
BafA1
MW kDa
LC3B-I
LC3B-II
-20
1 1.5 4.7 7.9 8.4 13
Actin
-50
-40
Non-transf + - - + - -
Ctrl ASO - + - - + -
NEAT1 kd - - + - - +
B
- BafA1
+ BafA1
Ctrl ASO
NEAT1 kd
Volume (µm 3)
0.10
0.08
0.06
0.04
0.02
0.00
Ctrl
NEAT1 kd
**
*
- BafA1
+ BafA1
Number of LC3B punctas
50
40
30
20
10
0
C
BafA1
MW kDa
p62
-80
-60
1 1 1.5 1.2 1.3 1.8
Non-transf + - - + - -
Ctrl ASO - + - - + -
NEAT1 kd - - + - - +
D
BT474
BafA1
MW kDa
LC3B-I
LC3B-II
-20
1 1.8 4.5 3.9 4.1 11
p62
-80
-60
1 1.2 1.2 1.5 1.5 1.8
Actin
-50
-40
Non-transf + - - + - -
Ctrl ASO - + - - + -
NEAT1 kd - - + - - +

Figure 3

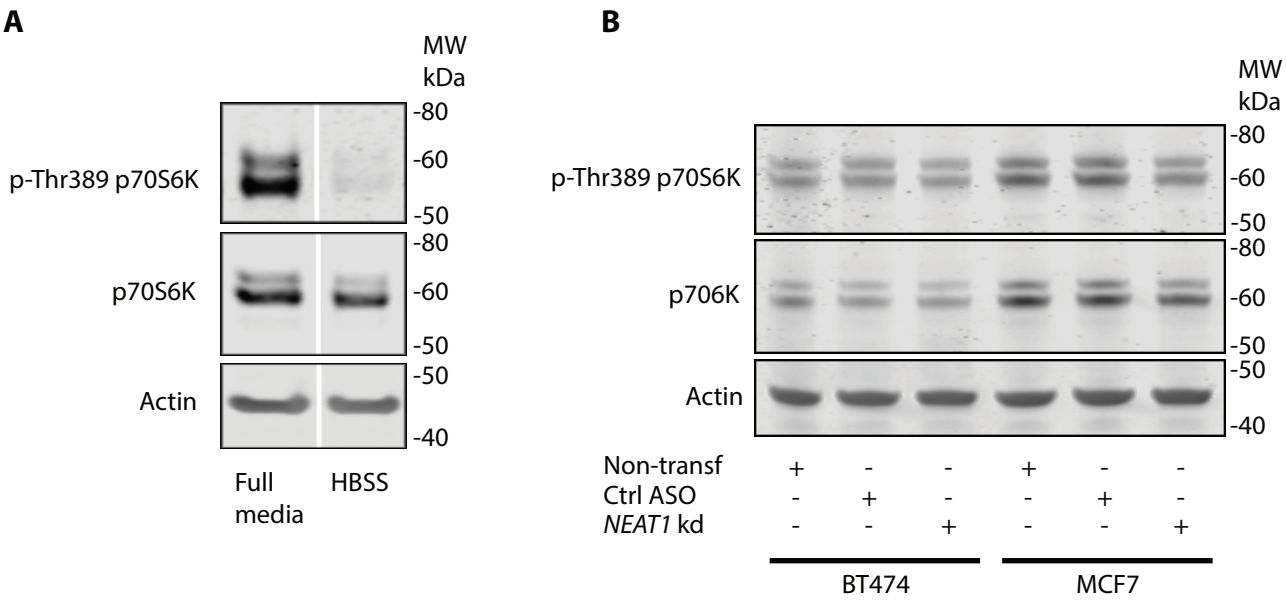
A
MW
kDa
p-Thr389 p70S6K
-80
-60
-50
p70S6K
-80
-60
-50
Actin
-50
-40
Full media
HBSS
B
MW
kDa
p-Thr389 p70S6K
-80
-60
-50
p706K
-80
-60
-50
Actin
-50
-40
Non-transf + - - + - -
Ctrl ASO - + - - + -
NEAT1 kd - - + - - +
BT474
MCF7

Figure 4

A

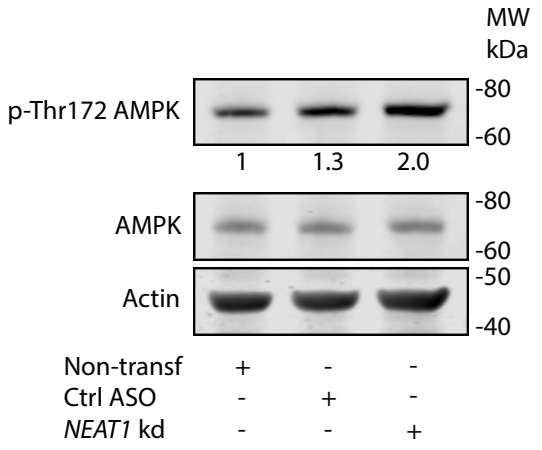
MW
kDa
p-Thr172 AMPK
-80
-60
1
1.3
2.0
AMPK
-80
-60
Actin
-50
-40
Non-transf + - -
Ctrl ASO - + -
NEAT1 kd - - +

B

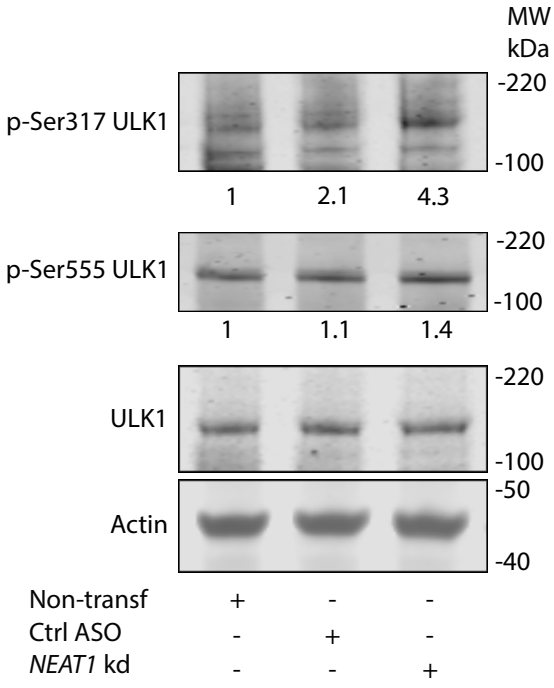
MW
kDa
p-Ser317 ULK1
-220
-100
1
2.1
4.3
p-Ser555 ULK1
-220
-100
1
1.1
1.4
ULK1
-220
-100
Actin
-50
-40
Non-transf + - -
Ctrl ASO - + -
NEAT1 kd - - +

Supplementary figure 1